Studying and manipulating chromatin motion in mammalian cells

Inga Thomson

Thesis presented for the degree of Doctor of Philisophy,
University of Edinburgh
2006

DECLARATION

I declare that this thesis has been composed by me, and that all of the work is my own unless otherwise stated.

Inga Thomson
January 2006

ACKNOWLEDGEMENTS

First and most importantly I have to thank Wendy, as without her this thesis would not be here. Wendy's door has always been open and she is always full of optimism, advice and enthusiasm for my work, as well as having lots of interesting ideas of where to go next.

Next I need to thank both Jon and Nick. Jon originally supervised me in the lab when I first began my PhD and even now when I need to ask a silly question he is only an email away. Nick has also been really helpful and always makes the time to help me out. Nick is full of suggestions and ideas for my work and knows what to do when things have gone horribly wrong. Shelagh also deserves a special mention, for unrivalled problem shooting skills when it comes to FISH, her maths abilities, and her cake baking. I would also like to thank Paul Perry, as he is someone else who always goes out of his way to help me out.

Next I have to thank the other lab members past and present including, Anne, (who I still have to see juggling, biscuits don't count!), Steph, Heidi, Severine, (never one to mince her words), Duncan (who is forever tired!), Clemence, Celine, Annenette, Liz, Catherine and Elodie. Although not in the lab, I would also like to thank Andy and Joel for their daily entertainment, and despite what Andy thinks, I don't break *everything!* The lab really has been a good place to work, and I will miss everyone when I finally leave.

I also have to say a big thank you to my mum and dad. Without their support I would never have started my PhD and throughout the last three years, they have been a continuous source of encouragement and always listen to me, even when no one else does! Finally, I also have to say a big thank you to Scott. The last few months have not been easy, but without his encouragement, support and belief in me, I would not have got this far. I still cannot quite believe it myself!

ABSTRACT

Histone modifications such as methylation and acetylation are known to be key determinants in the regulation of gene expression, but little is known about how higher order chromatin structures, and their spatial organisation in the nucleus, can control gene expression. This remains a key question in addressing the role of spatial organisation in genomic function.

If changes in nuclear position have a role in gene expression, chromatin within the cell must be able to move distances that would accommodate this. In the first part of my PhD I investigated the range of chromatin motion in living human cells. *E.coli* Lac operator arrays inserted into the human genome and visualised using Lac repressor protein fused to GFP, are able to move up to 2-3 μm over the period of two hours, distances greater than previously reported and similar to motion observed in yeast. I have also determined whether the position of a locus is conserved from one cell cycle to the next by following cells through mitosis. From this analysis it was concluded that although some aspects of positioning were conserved, loci position was established anew each cell cycle.

Although I have shown that chromatin mobility is quite constrained within the nucleus, proteins associated with chromatin have been shown to be highly mobile. I have investigated the effect of different factors that might affect the mobility of linker histones using fluorescence recovery after photobleaching. I have shown that while Su(Var)3-9, responsible for tri-methylation of Lysine 9 on histone 3, and MeCP2, a DNA methylation binding protein, have no effect on linker histone mobility, the methylation of DNA does. In the absence of DNA methylation, linker histones are more tightly bound to the chromatin fibre.

In humans it is well established that chromosomes have a gene-density related radial organisation within the cell nucleus. I have mapped the radial position of mouse chromosomes in ES cells to determine if a similar pattern of organisation exists. My results suggest there may be a loose correlation between chromosome size and position within the mouse genome, but not gene density. Furthermore differentiation

of mouse ES cells, induced changes in the position of some chromosomes, suggesting that gene expression may have a role in chromosome position.

Although correlations in nuclear position and expression have been seen in many model organisms, only in budding yeast has there been direct experimental confirmation that position can control gene expression. To determine directly if nuclear position can regulate gene expression in the mouse I aimed to artificially tether a gene to the edge of the mouse nucleus. Arrays of Lac operator sequences were inserted into or near genes. To tether genes to the nuclear periphery, Lac repressor was fused to the integral membrane proteins emerin or LAP2β. I have shown that these fusion proteins can transiently anchor transfected Lac-operator containing plasmids to the nuclear periphery of mouse cells and that this silences gene expression from these plasmids. Anchoring of endogenous mouse genes was also investigated.

CONTENTS **PAGE**

LIST OF FIGURES PAGE

CHAPTER 1

CHAPTER 3

CHAPTER 4

CHAPTER 5

CHAPTER 6

APPENDIX 1

LIST OF TABLES PAGE

LIST OF BOXES PAGE

ABBREVIATIONS

2D	two-dimensional
3D	three-dimensional
A	Adenine
Ac	Acetylated
Arabidopsis	*Arabidopsis thaliana*
ATP	adenosine triphosphate
BrdU	5-bromo-2-deoxyuridine
BSA	bovine serum albumin
C	cytosine
CCD	charged coupled device camera
CENP	centromere protein
Chromodomain	chromatin organiser motif
CpG	cytosine and guanine
CT	chromosome territory
C-terminal	carboxyl-terminal
DAPI	4,6-diamidino-2-phenylindole
dATP	deoxyadenosine triphosphate
dCTP	deoxycytosine triphosphate
dGTP	deoxyguanine triphosphate
DMEM	dulbecco's modified Eagles medium
DNMT	DNA methyltransferase
DMSO	dimethyl sulphoxide
DNA	deoxyribonucleic acid
DNase	deoxyribonuclease
dNTP	deoxythymine triphosphate

Drosophilia	*Drosophila melanogaster*
DSB	Double strand breaks
dTTP	deoxythymine triphosphate
dUTP	deoxyuridine triphosphate
E.coli	*Escherichia coli*
ES cells	Embryonic stem cells
e.m	electron microscopy
ER	endoplasmic reticulum
FCS	fetal calf serum
FISH	fluorescence in situ hybridisation
FITC	fluorescein isothiocyanate fluorochrome
FLIP	fluorescence loss in phobleaching
FRAP	fluorescence recovery after photobleaching
G	guanine
g	gravities
G1	growth phase 1 of the cell cycle
G2	growth phase 2 of the cell cycle
GC	guanine and cytosine
GFP	green fluorescent protein
GMEM	glasgows modified Eagles medium
HAT	histone acetyltransferase
HCl	hydrochloric acid
HDAC	histone deacetyltransferase
HMT	histone methyltransferase
HP1	heterochromatin protein 1
HRP	horseradish peroxidase conjugate
HSA	Homo sapiens autosome

HSV-TK	herpes simplex virus thymidine kinase
ICD	interchromatin domain
IF	immunofluorescence
INM	inner nuclear membrane
ISWI	imitation switch
K	lysine
kb	kilobases of DNA
KCl	potassium chloride
kDa	kilo Daltons (molecular weight/$10^{3)}$
LacI	lactose inducer
LacO	lactose operator
LAP2β	lamina associated polypeptide 2β
LBR	lamin B receptor
LEM	LAP,emerin, MAN
LIF	leukaemia inhibitory factor
LM	light microscopy
M	molar
MAA	methanol, acetic acid
Mb	megabase pairs of DNA
MBD	methyl binding domain
me1	monomethylated
me2	dimethylated
me3	trimethylated
MeCP	methyl binding protein
mRNA	messenger RNA
MMU	mouse autosomal

NaCl	sodium chloride
NOR	nuclear organising region
NPC	nuclear pore complex
N-terminal	amino-terminal
OD	optical density
ONM	outer nuclear membrane
p	chromosome short arm
PAGE	polyacrylamide gel electrophoresis
PBS	phosphate buffered saline
PcG	polycomb group protein
PCR	polymerase chain reaction
pcv	packed cell volume
PEV	position effect variation
pFa	Paraformaldehyde
PML	Promyelocytic leukaemia
q	chromosome long arm
R	arginine
RA	retinoic acid
rDNA	rRNA encoding DNA
RNA	ribonucleic acid
RNase	ribonuclease
ROI	region of interest
rRNA	ribosomal RNA
S	serine
S.cerevisiae	*Saccharomyces cerevisiae*
S.pombe	*Schizosaccharomyces pombe*

S/MAR	scaffold/matrix attachment region
SAGA	spt-Ada-Gcn5 acetyltransferase
SDS	sodium dodecyl sulphate
SEM	standard error of mean
S-phase	synthesis phase of cell cycle
SSC	standard saline citrate (1x 150mM NaCl, 15mM tri-Na citrate,pH7.4)
SWI/SNF	mating type switching/sucrose non-fermenting
T	thymine
t ½	recovery half time
TAE	Tris,EDTA acetic acid buffer (1x 90mM Tris-HCl, 90mM glacial acetic acid, 2mM EDTA,pH8.0)
TE	Tris, EDTA buffer (10mM Tris, 1mM EDTA,pH8.0)
TSA	trichostatin A
Xenopus	*Xenopus laevis*
Xi	inactive X

CHAPTER 1

INTRODUCTION

Although the human genome has been sequenced, and we have some knowledge about the primary structure of genes and sequence elements, we still know very little about the higher order organisation of DNA in the cell and how this can control gene expression. There are over 2m of DNA in each mammalian cell and so this requires many different levels of folding, and compaction with different proteins, to organise it into chromatin able to reside within a nucleus of only 5-15μm in diameter. Chromatin must also be packaged in a way that will allow the many factors required in the control of gene regulation to access it.

In addition to chromatin, the nucleus also contains many dynamic membrane free compartments enriched with high concentrations of specific proteins (figure 1.1, Spector, 2003). Maintaining the spatial and temporal organisation of these nuclear compartments is essential to the correct functioning of a cell. For example PML bodies have been implicated in gene regulation, DNA repair, proteolysis and apoptosis (Borden et al., 2002; Dellaire and Bazett-Jones, 2004). In patients with acute promyelocytic leukaemia, PML bodies are fragmented (Weis et al., 1994), but treatment with trans-retinoic acid can result in the reformation of PML bodies and the regression of the disease (Weis et al., 1994). In addition the spatial organisation of DNA relative to nuclear structures is also thought to a have a role in regulating gene expression. The disruption of position of both nuclear organelles and chromatin has been implicated in many different genetic diseases, cancers, and viral infections and has been observed in extreme physiological or environmental stresses (reviewed by Zimber et al., 2004).

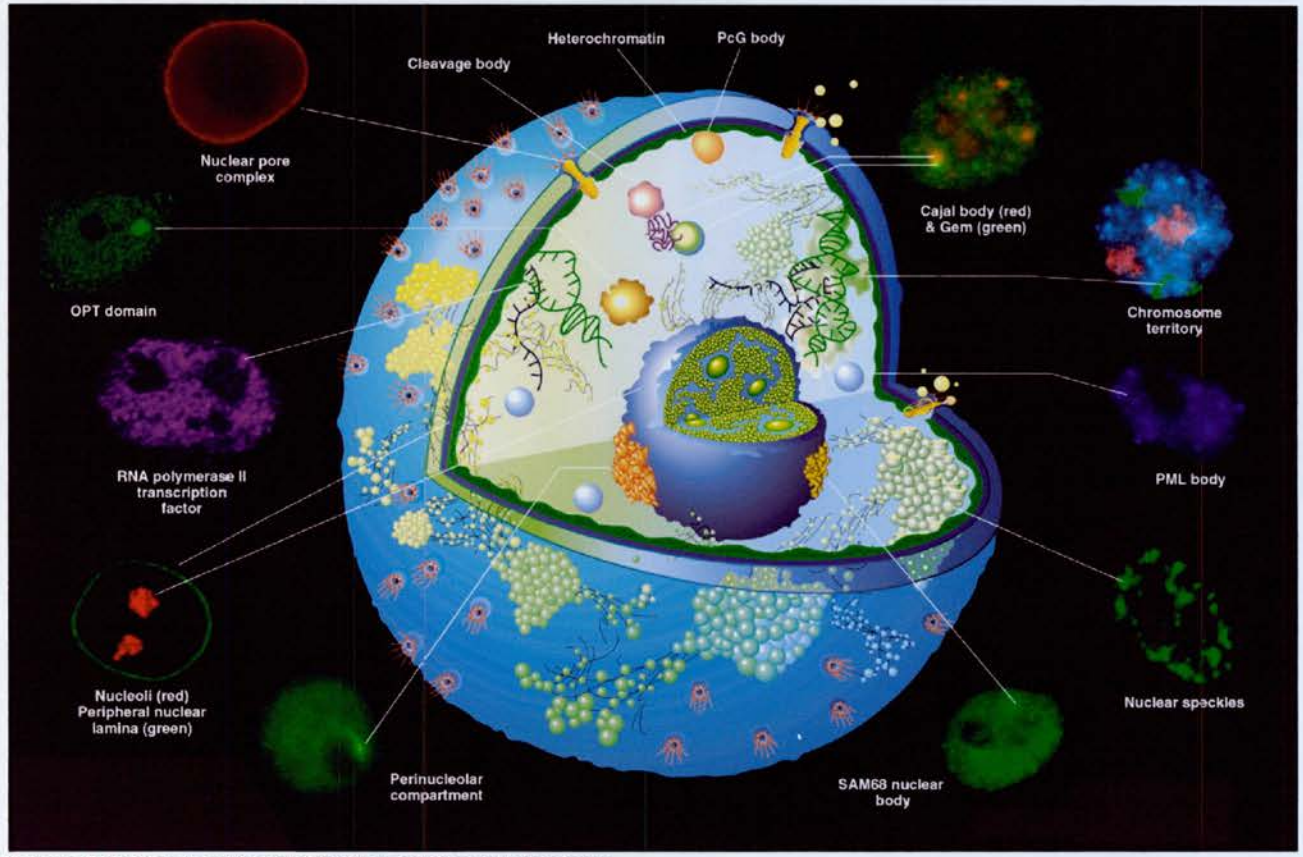

Figure 1.1: Compartmentalisation of the cell nucleus.
The nucleus of a cell is a dynamic organelle full of many domains enriched in nuclear proteins able to be seen by light microscopy.The spatial and tempcral organisation of each domain,plays a role in the correct functioning of the cell. Figure adapted from Spector 2001.

1.1 CHROMATIN COMPOSITION

The packaging of DNA within the nucleus takes place in a number of distinct stages, the first of which is the assembly of DNA into nucleosomes. Each core nucleosome particle contains approximately 146 bp of negatively charged DNA wound twice around a positively charged histone octamer. The histone octamer is composed of dimers of the four core histones H2A, H2B, H3 and H4 (Luger et al., 1997). These are small highly conserved lysine (K) and arginine (R) rich proteins (11-16kDa), which have a central globular domain, and C- and N- terminal domains. Both the C and N terminal domains lack secondary structure and whilst the C termini is found on the inside of the nucleosome, the N termini protrudes from the nucleosome and forms contacts with DNA, other nucleosomes and non-histone proteins. The N terminal histone tail also has roles in folding nucleosome arrays into higher order chromatin fibres as well as mediating fibre-fibre associations (Carruthers and Hansen, 2000; Gordon et al., 2005). Specific amino acids in the N terminal domain of each histone can be modified by acetylation, methylation, phosphorylation, ADP-ribosylation or ubiquitination (figure 1.2). These modifications are able to establish and maintain distinct chromatin states that correlate with transcriptional activity and create binding sites for other chromatin-associated proteins. Such modifications have been proposed to act as a "code" for downstream events (Strahl and Allis, 2000). However in order to function as a code, modifications must consistently have the same role and be able to act in combination (Kurdistani and Grunstein, 2003; Fischle et al., 2003). An alternative hypothesis to "the histone code" is that histone modifications are simply part of protein signalling pathways (Schreiber and Bernstein, 2002).

1.1.1 Histone acetylation

Reversible acetylation of specific K residues on the N terminal tails of histones H3 and H4 is correlated with transcriptionally active chromatin. Conserved sites of acetylation include K5, K8, K12, K16 and K20 upon H4, K9, K14, K18, K23 and

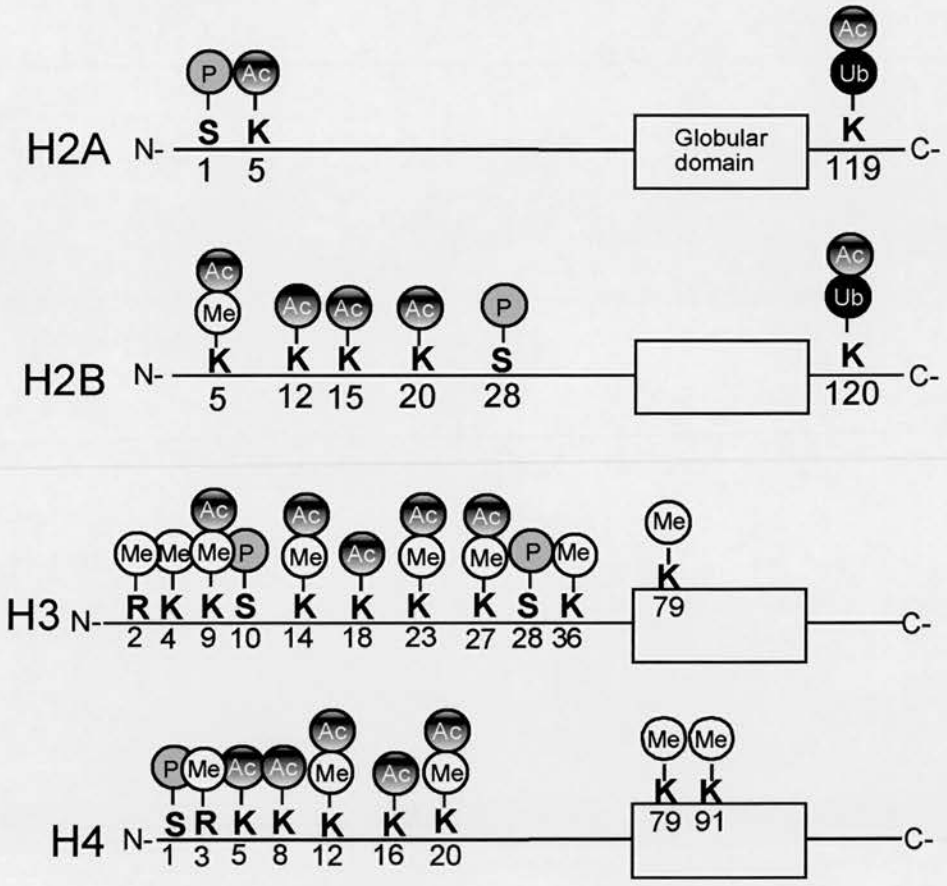

Figure 1.2: Histone modifications.
Specific residues at the N- and C- terminal tails of the four core histones can be chemically modified by methylation (Me), acetylation (Ac), phosphorylation (P) and ubiquitination (Ub). A sub-set of these marks are illustrated.(K=Lysine; S=Serine; R=Arginine).

K27 upon H3 and less well-conserved sites on H2A and H2B (figure 1.2). Unique patterns of acetylation at given genes or their promoters have been proposed to specify protein-binding surfaces (Kurdistani and Grunstein, 2003). In mammalian cells, peaks of histone acetylation are found at the promoters of active genes (Bernstein et al., 2005; Roh et al., 2004).

Many histone acetyltransferases (HATs) and histone deacetylases (HDACs) with specific site specificities are known and these mediate the fine balance between acetylation and deacetylation and hence the transcriptional competency of target genes. HATs were first identified in yeast as transcriptional activators. Confirmed and putative HAT proteins conserved in various organisms from yeast to humans include; the Gcn5-related N-acetyltransferase (GNAT) super family members; the MYST family; p300; the nuclear receptor co activators SRC-1, ACTR, and TIF2; the TATA-binding protein-associated factor $TAF_{II}250$ and its homologs; and subunits of RNA polymerase III general factor TFIIIC (Sterner and Berger, 2000; Borrow et al., 1996; Kawasaki et al., 2000; Takami and Nakayama, 2000). Although these HAT families have distinct activities and different preferred histone substrates, they often contain two conserved domains: the acetyltransferase domain and the bromodomain. In turn, the bromodomain has been shown to bind to acetylated lysine residues (for a review of HATs see Yang 2004). Mutations in the HATs, p300 and CBP have been linked to the Rubinstein-Taybi syndrome (Roelsema et al., 2005). Patients with this syndrome have short stature, developmental delay and abnormal facial features.

HDACs were first identified as transcriptional repressors and can generally be split into three classes: Rpd3 and Hos2 like (class I) enzymes, Hda-1 like (class II enzymes) and Sir-2 like (class III) enzymes (reviewed by Kurdistani and Grunstein, 2003). Class I and II HDACS share a conserved central enzymatic domain and, whilst class I HDACs are ubiquitously expressed and found in the nucleus, class II HDACs are tissue specific and can be found both in the cytoplasm and the nucleus. Class III HDACs share no homology to classes I and II, are nicotinamid adenine dinucleotide (NAD) dependent and found in both the cytoplasm and the nucleus. Recently it has been shown that Hos2-like HDACs bind to residues in the open

reading frames of active genes in both budding and fission yeast (Wang et al., 2002; Wiren et al., 2005).

In fission yeast, Sir2 functions both to deacetylate heterochromatin and euchromatin and can bind to the open reading frames of highly expressed genes to act primarily upon H3K9 acetylation (Wiren et al., 2005). Sir2 also has also been implicated in the silencing of telomeric regions at the nuclear periphery of budding yeast (Gotta et al., 1996; Maillet et al.,1996).

In humans, HDACs 1, 2, 3, 8 and 11 are members of class I, whilst HDACs 4, 5, 6, 7, 9 and 10 are class II members and Sirt1-Sirt7 are class III HDACs. HDACs 1 and 2 can be found in at least three repressive complexes which include, the major chromatin remodelling complexes, NuRD (also known as Mi-2, section 1.4.3) SIN3 (Bird and Wolffe, 1999; Knoepfler and Eisenman, 1999) and CoREST. In addition to HDAC activity, NuRD also contains ATP-dependent nucleosomal remodelling activity, MBD3 (section 1.1.3), and the histone binding proteins RbAp46 and RbAp48, which are also found in the SIN3 complex (Ng and Bird, 2000; Humphery et al., 2001).

Class I and II, HDACs can be inhibited by the fungal toxins, trichostatin A (TSA) and traponin, and treating cells with these inhibitors causes global hyperacetylation. Cancer cells frequently have alterations in the structure and expression of HATs and HDACs and HDAC inhibitors are currently being investigated as potential treatments for specific types of cancers (Taddei et al., 2005). Furthermore, it has been suggested that HDAC inhibitors such as TSA, can cause gross remodelling of nuclear structures (Taddei et al., 2001). However more recent evidence suggests this is not the case (Gilchrist et al., 2004).

1.1.2 Histone methylation

Core histones can also be methylated at conserved K and R residues (figure 1.2). Each residue can accept up to three methyl groups and different degrees of methylation are associated with different types of gene regulation. Histone methylation has been associated with both active and inactive chromatin, dependent on the residue methylated and the number of methyl groups it contains. For example,

methylation of H3K9 is associated with transcriptionally inactive chromatin and H3K4 methylation is associated with transcriptionally active sites of the genome (Peters et al., 2003, Bernstein et al., 2002; Schubeler et al., 2004).

Different histone methylation marks are also associated with different locations within the genome. For example trimethylation of H3K9 (me3), H4K27 monomethylation (me1) and H4K20me3 are found concentrated at sites of pericentric constitutive heterochromatin within mouse cells (Peters et al., 2003; Schotta et al., 2004; Martens et al., 2005). The localisation of both H3K27me1 and H4K20me3 to these sites is dependent on the trimethylation of H3K9 by the Suv39h histone methyltransferases (Peters et al., 2003; Schotta et al., 2004). In the mouse, centromeric heterochromatin can be further defined into two different classes of repetitive sequence, each associated with a different histone methylation mark: H3K20me2 at the minor satellite sequences and H3K9me3 at major satellite sequences (Lehnertz et al., 2003). Recently it was also predicted that any genomic region containing tandem repeat sequences will accumulate both H3K9me3 and H4K20me3 (Martens et al., 2005). Although usually associated with inactive chromatin, both H3K9 me2 and me3 can also occur in the transcribed region of active genes in mammals (Vakoc et al., 2005). H3K9me3 is thought to mediate gene repression by providing binding sites for the heterochromatic protein 1 (HP1) (section 1.1.7) (Jacobs et al., 2001) Distinctive histone modification marks also occur at facultative heterochromatin and H3K27me3 is found on the inactive X chromosome (Plath et al., 2003; Silva et al., 2003; Kohlmaier et al., 2004).

H3K4me3 is a mark of active chromatin and has been reported to be present at the start sites of mammalian genes, whereas H3K4me2 can be found throughout the coding region (Miao et al., 2005; Bernstein et al., 2005). Both modifications correlate with regions of histone hyperacetylation (Miao et al., 2005). In contrast, H3K4me3 and H3K4me2 are both enriched at the 5' end of genes in *Drosophila* (Wirbelauer et al., 2005).

The first proteins shown to have lysine histone methyltransferase activity (HMTase) activity were the mammalian homologues of the *Drosophila* position-effect variegation (PEV) modifier Su(Var)3-9. In mammals both Suv39h1 and Suv39h2, have been shown to trimethylate H3K9 (Peters et al., 2003; Rice et al.,

2003). Similarly Suv4-20h1 and Suv 4-20h2 catalyse H4K20me3 (Schotta et al., 2004). The majority of HMTases contain SET domains, essential for their catalytic activity (Jenuwein, 2001).

A second HMTase with site specificity for H3K9 is SETDB1/ESET, however in contrast to the Suv39h genes, SETDB1 converts H3K9me2 to H3K9me3 and acts at euchromatin (Schultz et al., 2002; Wang et al., 2003). A third HMTase, G9a is responsible for most of the dimethylated and monomethlyated H3K9 in mouse embryonic stem (ES) cells (Tachibana et al., 2002), and a fourth HMTase able to methylate H3K9, Glp1, also functions at euchromatin. Glp1 is found in a complex with E2F-6, Mga and Max, and is able to bind to E2F, Myc- and Brachyury-binding sites, implicating a role of Eu-HMTase in regulating E2F and myc- responsive genes (Ogawa et al., 2002).

Knockout mouse models show different phenotypes for three of the H3K9 HMTases. Mice lacking Suv39h1/Suv39h2 are viable but show massive chromosomal mis-segregation consistent with a defect in heterochromatin structure (Peters et al., 2001). Mice lacking G9a show embryonic lethality around 8.5 days postcoitum (dpc) due to severe differentiation defects (Zhang et al., 2002). G9a is also required to maintain DNA methylation in the Prader-Willi imprinted region and G9a null ES cells show the ectopic expression of imprinted genes (Xin et al., 2003). Homozygous mutations of SetDB1/Eset result in an even more severe phenotype with peri-implantation lethality between 3.5 and 5.5 dpc and ES cells null for SetDB1 could not be isolated (Dodge et al., 2005).

The mammalian EED-EZH2 proteins catalyse H3-K27 mono-, di- and trimethylation (Montgomery 2005; Cao and Zhang 2002) and are components of the polycomb complex 2 (PRC2, section 1.1.7). This also contains the HDACs 1 and 2 (Van der Vlag 1999) and EZH2 has been shown to be essential for early development (O'Carroll et al., 2001).

Mutations in the HMTase NSD1, which is able to methylate H3K36 and H4K20, are associated with Sotos syndrome, also known as cerebral gigantism (Faravelli et al., 2005). Children with Sotos Syndrome are often taller, heavier, and have larger heads than their peers.

In *Saccharomyces cerevisiae*, Set1 has been identified as the sole histone methyltransferase required for histone H3K4 methylation and mediates silencing of rDNA genes in Sir2 independent manner (Bryk et al., 2002). In humans, Set7 and Set9 have H3K4 specific activity and methylation of H3K4 by these enzymes can inhibit H3K9 methylation by SuVar 39h1 (Wang et al., 2001; Nishioka et al., 2002).

HMTases also act on arginine residues. For example, the nuclear receptor co-activator CARM1, specifically methylates H3R17 and H3R26 in response to transcriptional activation. Furthermore CARM1 can also methylate non-histone proteins such as p300/CBP (Chen et al., 1999). The intrinsic methyltransferase activity of CARM1, and its interaction with the SRC is able to activate nuclear hormone receptor activities in reporter gene assays in mammalian cells (Chen et al., 1999, Wang et al., 2001).

For a long time it was thought that histone methylation, in contrast to acetylation may be irreversible. However, PAD4 was the first enzyme identified which could remove the methylation mark from a histone. PAD4 functions by converting R to the amino acid, citrulline. Deimination by PAD4 prevents R methylation by CARM1, and PAD4 is recruited to the *ps2* promoter following the down regulation of the gene (Cuthbert et al., 2004, Wang et al., 2004). Dimethylation of arginines prevents deimination from occurring, but monomethylation does not.
The transcriptional co-repressor LSD1 has also been shown to function as a histone demethylase and is able to demethylate H3K4 (Shi et al., 2004). LSD1 is found in co-repressor complexes and associates with other HDACs and HMTases. The loss of LSD1 results in the deregulation of genes regulated by the CoREST complex. Recently LSD1 has been shown to also have roles in androgen receptor activation where it can demethylate H3K9me1 and H3K9me2 (Metzger et al., 2005). In contrast to PAD4 demethylation, K demethylation by LSD1 occurs via an oxidation reaction that generates formaldehyde (Shi et al., 2004).

1.1.3 DNA methylation

Modifications of histones are not the only epigenetic marks capable of conferring information about the transcriptional status of chromatin. The major consequence of DNA methylation is gene silencing and DNA methylation is essential to development with roles in X-chromosome inactivation and genomic imprinting (Lee and Jaenisch 1997). Furthermore, defects in DNA methylation have been linked to human disease and cancer (reviewed by Ballestar and Esteller 2005). Methylation in mammals takes place primarily upon the cytosine residue at CpG dinucleotides (CpGs), of which 60-90% are methylated. CpG islands are regions of the genome enriched in unmethylated CpGs and are often found at the 5' ends of genes (Bird, 1986, Larsen et al., 1992; Jones and Takai, 2001).

So far three DNA methyltransferases (DNMT) capable of transferring a methyl group to cytosine have been identified. These can be classed into two groups: *de novo* methyltransferases DNMT3a and DNMT3b and a maintenance methyltransferase DNMT1 (Bestor 2000; Okano et al., 1998). DNMTs share a highly conserved C-terminal catalytic domain, but have their own distinct N-terminal domains, thought to control nuclear positioning and interactions with other proteins.

DNMT1 has a binding preference for hemimethylated DNA. This collectively with the knowledge that it localises to replication foci, is ubiquitously expressed, and interacts with the methyl binding protein MeCP2, suggest that it has maintenance activity and is responsible for copying the DNA methylation pattern onto newly replicated DNA (Pradhan et al., 1999; Leonhardt et al., 1992; Kimura and Schiota, 2003). Mutations in *Dnmt1* result in global hypomethylation, embryo lethality, and demethylation of a subset of imprinted genes (Li et al., 1999; Okano et al., 1999). The lethality of *Dnmt1 -/-* mice is thought to primarily be due to cell death. Mouse ES cells carrying a homozygous mutation of *dnmt1* show micro satellite instability (MSI) and a reduced efficiency of mismatch repair (Guo et al., 2004; Kim et al., 2004). Despite this, *Dnmt1 -/-* ES cells with only 20% of normal methylation are able to begin, but not complete, differentiation (Jackson et al., 2004). Human cancer cells with mutations in *DNMT1* show instability of pericentric heterochromatin sequences (Espada et al., 2004).

Unlike DNMT1 both DNMT3a and DNMT3b have no preference for either hemimethylated or unmethylated DNA and are concentrated at regions of pericentric heterochromatin (Okano et al., 1999, Bachmann et al., 2001).*Dnmt3a -/-* mice have no significant changes to levels of DNA methylation at birth and appear normal. However within a few weeks they become runted and die due to multiple organ defects (Okano et al., 1999). In contrast, no live born *Dnmt3b -/-* mice have been obtained (Okano et al., 1999). *Dnmt3b -/-* embryos die at around 13.5 dpc and have multiple developmental defects that include growth retardation and neural tube abnormalities. Hypomethylation of centromeric minor satellite sequences was observed in such embryos. *Dnmt3b -/-* MEF cells isolated from these embryos show global hypomethylation, premature senescence, spontaneous immortalisation and chromosome instability. However MEFS from *Dnmt3a-/-* mice do not (Dodge et al., 2005). Despite the apparent lack of phenotype in *Dnmt3a -/-* MEFs, *Dnmt 3a/3b* double knock out embryos, have a similar phenotype to *Dnmt1 -/-* embryos and die around 9.5 dpc (Okano et al., 1999).

Dnmt3a and 3b are highly expressed in undifferentiated ES cells, but become down regulated upon differentiation, and are only expressed at low levels in adult tissues (Okano et al., 1999). DNMT3a has also been shown to methylate non-CpGs dinucleotides and can function as a co-repressor (Gowher et al., 2001; Fuks et al., 2001; Rountree et al., 2001).*Dnmt3a*$^{-/-}$*/3b*$^{-/-}$ ES cells are well methylated at early passages and can differentiate, but over time methylation levels fall progressively, presumably due to the inability of DNMT 1 to efficiency maintain methylation. At low levels of DNA methylation, *Dnmt3a*$^{-/-}$*/3b*$^{-/-}$ ES cells are unable to differentiate upon LIF withdrawal and retain markers that are characteristic of undifferentiated cells (Jackson et al., 2004). The rescue of either *Dnmt3a* or *Dnmt3b* in high passage *Dnmt3a*$^{-/-}$*/3b*$^{-/-}$ cells can restore the ability to differentiate (Jackson et al., 2004).
Mutations in *DNMT3b* cause the syndrome ICF, characterised by immunodeficiency, chromosomal instabilities, and facial abnormalities (Ehrlich et al., 2003). Although global patterns of methylation are within the normal range in these patients, regions of heterochromatin such as centromeric αsatellite repeats, and the inactive X, are decondensed and hypomethylated.

1.1.3.2 Methyl CpG binding proteins

It is thought that DNA methylation inhibits transcription by either directly preventing transcription machinery from binding to the major grove of the double helix or by creating a binding site for repressor proteins. MeCp2 is the founder member of the methyl CpG binding protein family (Lewis et al., 1992; Hendrich and Bird 1998) and in addition to its methyl-binding domain (MBD), contains a transcriptional repressor domain (TRD), and can interact with Sin3A, which in turn interacts with HDACs (Nan et al., 1998; Knoepfler and Eisenman 1999;Boeke et al., 2000). Immunofluorescence with antibodies against MeCP2 have shown that it is localised to pericentromeric heterochromatin in mouse cells. This region of the genome also contains a large fraction of the total methylated CpGs (Lewis et al., 1992). MeCP2 has recently been shown to have roles in chromatin compaction. During myogenic differentiation, pericentric heterochromatin aggregates are formed which coinside with the increased expression of MeCP2 and increased DNA methylation. Ectopic expression of MeCP2 can mimic this effect and requires only the presence of the methyl CpG-binding domain (MBD) (Broers et al., 2005).

Rett syndrome is an X-linked neurodevelopmental disorder caused by mutations in MeCP2 and is the most common cause of mental retardation in females. MeCP2 mutations in the mouse create a phenotype that is very similar to Rett syndrome (Guy et al., 2001). Female mice heterozygous for a deletion of *Mecp2* are normal for the first few months of life, however, at around ~6 months the mice begin to develop Rett-like symptoms, which include irregular gait, breathing abnormalities and decreased movement (Guy et al., 2001).

Closely related to MeCP2 are four other proteins known as, MBDs 1-4. MeCP2 and MBDs1-3 are all transcriptional repressors, whilst MBD4 functions as a thymine DNA glycosylase able to repair G:T mismatches at CpG sites (Hendrich et al., 1999). Both MBD1 and MBD2, like MeCP2 recruit co-repressor complexes with HDAC activities to repress transcription (Bird and Wolffe 1999). MBD1 is also enriched at centromeric heterochromatin (Ng et al., 2000) and has a role in base pair excision repair alongside methyl-purine DNA glycosylase (Watanabe et al., 2003). Moreover, MBD1 can recruit SETDB1 to the large subunit of the chromatin

assembly factor, CAF1 during S phase (Sarraf and Stancheva, 2004). In the absence of such complexes HP1 enriched heterochromatin is depleted (Ichimura et al., 2005; section 1.1.6). MBDs act at different sites within the genome and cannot functionally substitute for one another (Klose et al., 2005).

In contrast to MBD1 and MBD2, MBD3 is part of the chromatin remodelling complex Mi-2/NURD and can disrupt DNA-histone interactions (Wade et al., 1999; Zhang et al., 1999; section 1.4.3).

Given the link between HDACs and DNA methyl binding proteins (Fuks et al., 2003; Nan et al., 1998), it might be expected that reduced DNA methylation causes increased histone acetylation. This is indeed the case for H4K5 acetylation in *Dnmt3a*$^{-/-}$/*3b*$^{-/-}$ ES cells, although a similar increase of hyperacetylation could not be detected in *Dnmt1* -/- ES cells (Jackson et al., 2004). However, *DNMT1* mutations in human cancer cells also cause increased hyperacetylation (Espada et al., 2004).

1.1.4 Other histone variants

As well as the four core histones, there are several core histone variants thought to confer more specialised functions to chromatin. The best studied are the H3 variants, CENPA and H3.3. CENPA localises exclusively to active centromeres (Sullivan et al., 1994) and differs from H3 extensively in its N-terminal region. However, H3.3 differs from H3 by only 4 amino acids, and is incorporated into nucleosomes surrounding the promoters of transcriptionally active mammalian genes by chromatin remodelling independent of DNA replication (Chow et al., 2005). In contrast to mammals, H3.3 is present throughout the transcribed region of active genes in *Drosophila* and is not enriched at gene promoters (Wirebelauer et al., 2005).

The stability of chromatin-bound H3.3 differs between loci. For example, in active rDNA genes, H3.3 is continually replaced but is stable in induced HSP70 genes that have become repressed, suggesting that H3.3 deposition only takes place whilst a gene is active (Schwartz and Ahmad 2005). Moreover H3.3 has been implicated as a potential mediator of the epigenetic memory of active transcriptional states.

Four variants of H2A have also been reported: H2AZ, H2AX, macroH2A and H2A-bar-body-deficient (H2ABBD). H2AZ is an essential histone variant with a role in gene activation (Faast et al., 2001) and is concentrated at sites of pericentric heterochromatin. The direct replacement of H2A with H2A.Z causes alterations at the interface between the histone H2A-H2B dimer and the histone $(H3\text{-}H4)_2$ tetramer which then alter nucleosome stability or packaging. This then leads to localized chromatin structures and genes packaged into H2A.Z-containing nucleosomes are more transcriptionally permissive (Park et al., 2004). Recent knock down studies in mammalian cells highlighted potential roles of H2AZ in chromosome segregation and HP1 localisation (Rangasamy et al., 2003; Rangasamy et al., 2004). Since then, further studies have shown that H2AZ mediates these effects by altering the surface of the nucleosome to enhance condensation and the folding of higher chromatin structures by HP1α (Fan et al., 2004).

H2AX represents between 2-25% of H2A within a cell and contains an extension of the C-terminus. In response to double stranded DNA breaks (DSB) the C terminus is phosphorylated around the site of DNA strand breakage. This is thought to act as a signal to recruit repair factors to DSBs (Bassing et al., 2003; Celeste et al., 2003).

MacroH2A is a vertebrate specific isoform of H2A, and is found enriched on the inactive X chromosome (Angelov et al., 2003). Loss of MacroH2A from the inactive X results can cause its reactivation (Hernandez- Munoz et al., 2005). The crystal structure of human macroH2A1.1 has also revealed that it interacts with the Sir2 homolog, SirT1 through its macro domain (Kustatcher et al., 2005). In addition, *Dnmt1-/-* ES cells, which have severely hypomethylated pericentric heterochromatin have an enrichment of macroH2A at these sites (Ma et al., 2005).

Finally H2ABBD is the most recently discovered H2A variant and little is known of its function, although it is excluded from the inactive chromosome X and co-localises with H4 acetylated at lysine 12, suggesting a possible role in gene activation (Chadwick et al., 2001).

1.1.5 Other histones modifications and the interplay between epigenetic modifications

Besides acetylation and methylation, other post-translational modifications of histones take place. These include phosphorylation, ADP-ribosylation, glycosylation and ubiquitination. The phosphorylation of histones has important roles in transcriptional regulation (Berger et al., 2002), mitosis (Smith et al., 2002) and DSB (Redon et al., 2002). Rapid decondensation of chromatin is associated with polyADP-ribosylation and could be important for long-term memory (Cohen-Armon et al., 2004). PolyADP-ribosylation may also have a role in DNA repair (Wielckens et al., 1982).

Histone H2B and histone H2A can be modified by the addition of ubiquitin (West and Bonner, 1980). Polyubiquitylation has a role in protein turnover, however histones are generally monoubiquitylated, and this form of ubiquitination is not associated with protein degradation (reviewed by Osley, 2004). Instead, ubiquitination of H2B may have an important role in the mediating H4K4me and ubiquitination of H2A is found on the inactive X chromosome (Dover et al., 2002; Moore et al., 2002).

There is considerable interplay between histone modifications. *In vitro,* acetylation of H3K14 is increased 5-10 fold when phosphorylation is already present at serine (S) 10 on the same histone tail (Cheung et al.,2000), dependent on the HAT involved (Lo et al., 2000). Phosphorylation of H3S10 has also been shown to block the binding of the HP1 to adjacent methylated H3K9 residues (Rea et al., 2000). These interactions between phosphorylation, acetylation and methylation promote the idea of a "binary switch" for the regulation of histone modification states (Fischle et al., 2003).

A further example of the interplay between histone marks comes from the estrogen stimulation of gene promoters. Within 15 minutes of stimulation of a responsive promoter, acetylation of H3K18 takes place, closely followed by K23 acetylation. CARM1 then associates with the chromatin and R17 methylation occurs (Daujat et al., 2002).

Interplay also takes place between H3K4 and H3K9 methylation and these modifications are believed to be mutually exclusive (Heard et al., 2001; Boggs et al., 2002). H3K4 methylation has little affect on the SETDB1 methylation of H3K9, but SUV39H1 is significantly reduced in its ability to methylate H3K9 if K4 on the same histone tail is already methylated (Schultz et al.,2002).

The interplay between epigenetic modifications is not restricted to histones. Interactions between DNA methylation and histone modifications, and the enzymes that control them, are believed to act together to bring out the long term silencing of genes. DNMT3b interacts directly with HDACs 1 and 2, HP1, Suv39h1 and the ATP dependent chromatin remodelling enzyme hSNF2H. Furthermore several of these proteins co-localise to heterochromatin (Geiman et al., 2004). Moreover, in ES cells, Suv39h1 mediated H3K9me3 can direct Dnmt3b to the major satellite regions in pericentric heterochromatin and both Dnmts3a and 3b interact directly with HP1α and HP1β (Lehnertz et al., 2003). These interactions may also be conserved in humans, as patients with ICF syndrome have unstable type 2 and 3 satellites, sequences known to be heavily trimethylated at H3K9.

Besides the co-localisation of components involved in histone and DNA methylation, recent studies have provided a more conclusive link between DNA methylation, H3K9 methylation and heterochromatin formation (Goll and Bestor 2002; Tariq et al., 2003). In *Neurospora crassa*, mutations in *DIM5,* which encodes a H3K9 specific HMTase, result in the complete loss of methylated cytosines from DNA (Tamura and Selker 2001). Likewise mutations in the H3K9 HMTase *KRYPTONITE* (*KYP*) in *Arabidopsis* affect both histone and DNA methylation (Jackson et al., 2002, Malagnac et al., 2002). This situation is also reflected in mammals, where the loss of Suv39h activity causes reduced DNA methylation of major satellite sequences (Lehnertz et al., 2003). Furthermore, MBD1 has been linked to HDACs through Suv39h1 (Fujita et al., 2003).

Further examples of the link between DNA and histone methylation also come from plants. In *Arabidopsis,* LH1, which is a homolog of HP1, is able to bind with high affinity to methylated H3K9 and can interact with CMT3, a DNMT. Hence it was proposed that LH1 is able to recruit CMT3 to inactive chromatin (Jackson et al., 2002). This has led to a model in which methylated histones provide a binding

site for HP1 which then recruits DNMTs, through an interaction with Suv39h1. DNMTs would only then be able to methylate DNA already wrapped around H3K9me and chromatin may have to be remodelled to allow this (section 1.4.3). The recruitment of Dnmt3b to major satellite sequences by Suvar39h supports this model.

However the opposite scenario should also be considered, i.e. that DNA methylation may recruit histone methylation. In plants, mutations in *MET1*(*DECREASED METHYLATION 2DNA*), the homolog of *DNMT1*, do not affect H3K9 methylation at silent centromeric repeat regions, but do affect it at loci which have become active due to hypomethylation. In mammals MeCP2 is associated with H3K9 HMTase activity and can deliver this chromatin modification to genes already methylated on their DNA sequence (Fuks et al., 2003). Furthermore, human cancer cells with *DNMT1* mutations, have decreased di- and trimethylation of H3K9, loss of histone deacetylases (HDACs) and loss of HP1 at pericentromeric repetitive sequences (Esapda et al., 2004).

1.1.6 Linker histones and chromatin compaction

Each nucleosome of core histones is connected to the next via the interaction of H2A with a linker histone, such as H1. This creates the basis of the 10nm chromatin fibre which can be visualised as "beads on a string" when chromatin is prepared under low salt conditions (Woodcock, 1973; Olins and Olins, 1974). Each octamer of core histones is connected to a linker histone in a structure called the chromatosome. Linker histones also function in part to stabilise condensed states of the 30 nm chromatin fibre (Thoma et al., 1979; Allan et al., 1981). Recently the crystal structure of a tetranucleosome was resolved and showed that the two stacks of nucleosome pairs form a truncated two-start helix upon which the linker DNA associated with the linker histones zigzagged back and forth between the two stacks (Schalch et al., 2005).

Linker histones are more variable in their structure than the core histones, and can be tissue or species specific and developmentally regulated. In mice there are

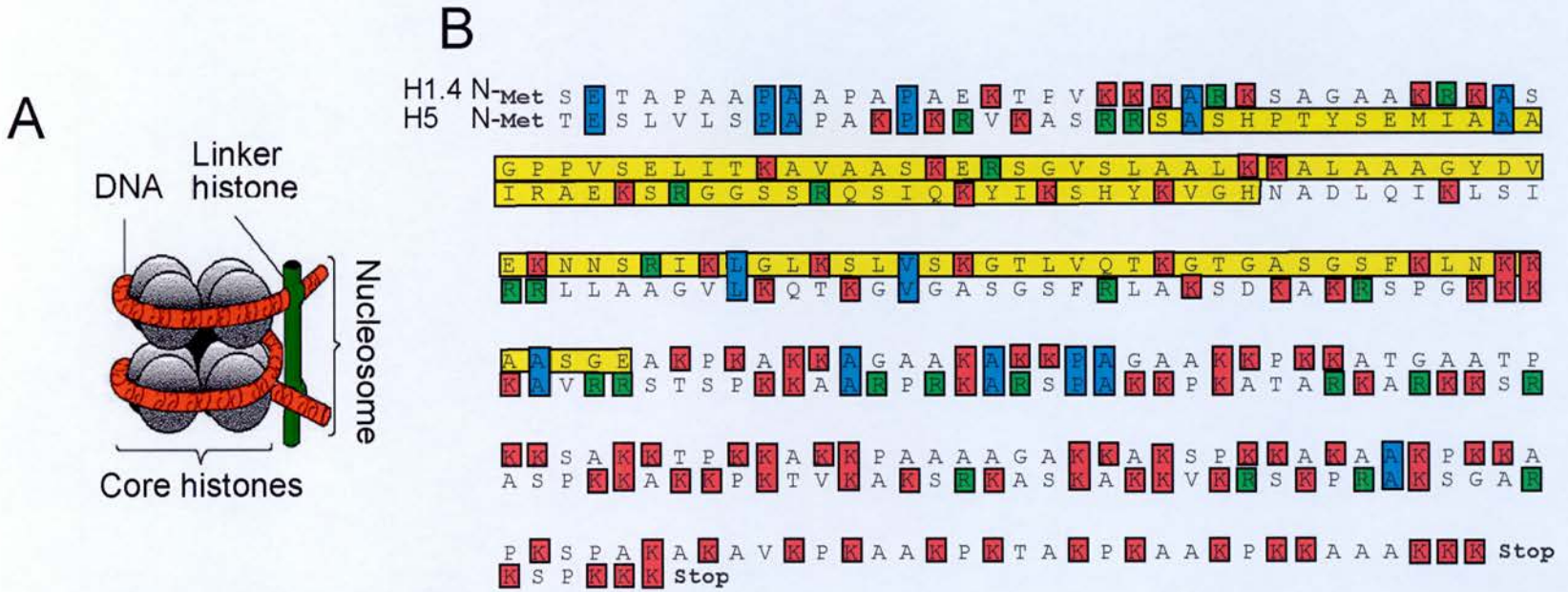

Figure 1.3: Linker histones connect nucleosomes together to create higher order chromatin structures and can be highly divergent. A) Schematic showing the position of linker histones relative to the core histone octamer and the structure of the nucleosome. B)Linker histones despite having common functions can share little sequence similarity.The protein sequences of H1.4, the most commonly expressed H1 variant and H5, a specialized variant found in chicken erythrocytes share few conserved residues(blue). Furthermore H1.4 is rich in Lysine residues (red) whilst H5 is rich in Arginine(green).The globular domain of each protein is shown by the yellow box.

at least eight H1 variants expressed in different tissues, and at different times in development (Wang et al., 1997). Each linker histone shares a common basic organization consisting of a globular core flanked by two "unorganized" tails (figure 1.3). Both the globular domain and the tails can exhibit significant differences among mammalian linker histones (Wang et al., 1997).

Functional studies have indicated roles of linker histones in regulatory processes such as: chromatin accessibility, homologous recombination, and apoptosis (Alami et al., 2003; reviewed by Harvey and Downs, 2004). Mice lacking multiple subtypes of H1 die mid-gestation, and have altered nucleosome spacing (Fan et al., 2003). Linker histone knockouts also disrupt chromosome compaction in *Tetrahymena thermophilia* (Shen et al., 1995) and have been proposed to have further roles in mitosis (Maresca et al., 2005).

Other linker histone variants with roles in chromatin compaction have been described. During chicken erythrocyte development, the cell nucleus becomes largely heterochromatised in a manner that coinsides with the expression of the linker histone variant H5 and a serpin like protein called MENT (Weintraub et al., 1994; Bergman et al., 1988; Grigoryev et al., 1999). Both of these are required to compact the chromatin fibre and when H5 is injected into mammalian cells it is able to block both transcription and DNA replication (Bergman et al., 1988). H5 has two DNA binding sites within its globular domain which are essential for its binding to the nucleosome (Duggan and Thomas 2000). Moreover the globular domains of H5 show a high degree of sequence similarity with the DNA binding proteins CAP (McKay and Steitz 1981; Schultz et al., 1991) and RAP30 (Groft et al., 1998). This suggests that linker histones and transcription factors could occupy similar positions on chromatin fibres. The expression of HP1 has also been shown to decrease during chicken embryonic erythrocyte differentiation as levels of H5 increase, suggesting that H5 may replace the role of HP1 in the formation of facultative heterochromatin (Gilbert et al., 2003; section 1.1.6).

Xenopus erythrocytes express the linker histone variant H1°. The expression of this, like H5, co-insides with the cessation of proliferation and the compaction of chromatin (Koutzamani et al., 2002).

Linker histones can be phosphorylated at conserved serine motifs along the N terminal tail. This neutralises the positive charge of the linker histone and disrupts the chromatin structure to allow transcription (Wolffe and Hayes 1999, Dou et al., 2002). In the absence of phosphorylation, linker histones can inhibit the actions of SWI/SNF remodelling complexes (Horn et al., 2002) and hyperphosphorylation of H1 is associated with mitosis in many cell types (Boggs et al., 2000, Hansen et al., 2002).

Histone 1.4, the most abundant subtype of H1, is dimethylated at K26 by the PRC2 complex (Kuzmichev et al., 2004). H1.4K26me2 can recruit the heterochromatic protein, HP1 and this stimulates the phosphorylation of adjacent serine residues (Daujat et al., 2005).

1.1.7 Heterochromatin

Heterochromatin was first defined as chromatin that did not decondense at the end of telophase (Heitz 1928). Since then many microscope studies on interphase and mitotic chromosomes have revealed two distinct chromatin populations within the cell. By electron microscopy (e.m), heterochromatin is more electron dense than euchromatin and is often seen enriched at the nuclear periphery (figure 1.4.a). DNA dyes such as DAPI (4',6-Diamidino-2-phenylindole) show bright distinct patches of staining in both human and mouse nuclei, which correspond to the heterochromatic portion of the genome (figure 1.4.b). DAPI stains this portion of the genome brightly, not only because it is condensed but also because it is enriched in AT satellite repeats. In the mouse, these bright patches correspond to minor and major satellite sequences, and in humans to α–satellite and satellites 2 and 3.

Heterochromatin can be further defined into two classes: facultative and constitutive. Constitutive heterochromatin is composed of tandem repeats and can be identified by several epigenetic marks including; DNA methylation, H3K9me3, H3-K27me1, H4-K20me3 and the hypoacetylation of histones (sections 1.1.2 and 1.1.1).

Facultative heterochromatin is euchromatin able to adopt heterochromatic properties in a developmentally controlled manner. The classic example of this is the inactive X chromosome in females which is rich in H3K27me3, H3K9me2 and

histone hypoacetylation (Peters et al., 2002; Rougeulle et al., 2004). In contrast chicken erythrocytes which have undergone heterochromatinization contain only very low levels of H3K27me3 (Gilbert et al., 2003), suggesting this is not a general mark of facultative heterochromatin and different pathways may exist to establish the formation of facultative heterochromatin.

The distinct functional and structural differences between heterochromatin and euchromatin are revealed, when euchromatic transgenes integrate next to heterochromatin. Such genes can become compacted and have heterochromatic proteins recruited to them resulting in their repression. This is stochastic and happens only in a subset of cells but is mitotically heritable, causing a phenomenon called position effect variegation (PEV) (Csink and Henikoff, 1996; Fesenstein et al., 1999; Wakimoto, 1998). Transgenes inserted close to centromeric heterochromatin can recruit HP1 and induce gene repression. Moreover, when transgenes are inserted away from heterochromatin in mutiple copies, repression in a HP1 dependent manner still takes place (Festenstein et al., 1999).Two models to explain PEV have been proposed. The first suggests that the repressed structure of the heterochromatin is able to "spread" into adjacent chromatin. This occurs as HP1 binds to H3K9me3, leading to Suvar39h recruitment which in turn causes further recruitment of HP1, and thus heterochromatin spreads down the chromatin fibre (Ahmad and Heinkoff, 2001). The second model suggests that PEV is achieved by protein components of heterochromatin that bind to multiple sites along the chromatin fibre. Silencing is then caused by the physical contact of euchromatic genes with heterochromatin through chromatin loops (Henikoff et al., 1996; Talbert and Henikoff, 2000; Harmon and Sedat, 2005). Recently, Sedat and colleagues developed a system to look at the relationship between the expression of a variegated gene and its co-localisation with centromeric heterochromatin several Mbp away, on a cell-to-cell basis in *Drosophila*. Cells containing a silent variegated gene, showed a strong association with heterochromatin, and cells expressing a variegated gene did not (Harmon and Sedat, 2005). These findings imply that contacts with heterochromatin, rather than heterochromatin spreading may mediate PEV in *Drosophila.*

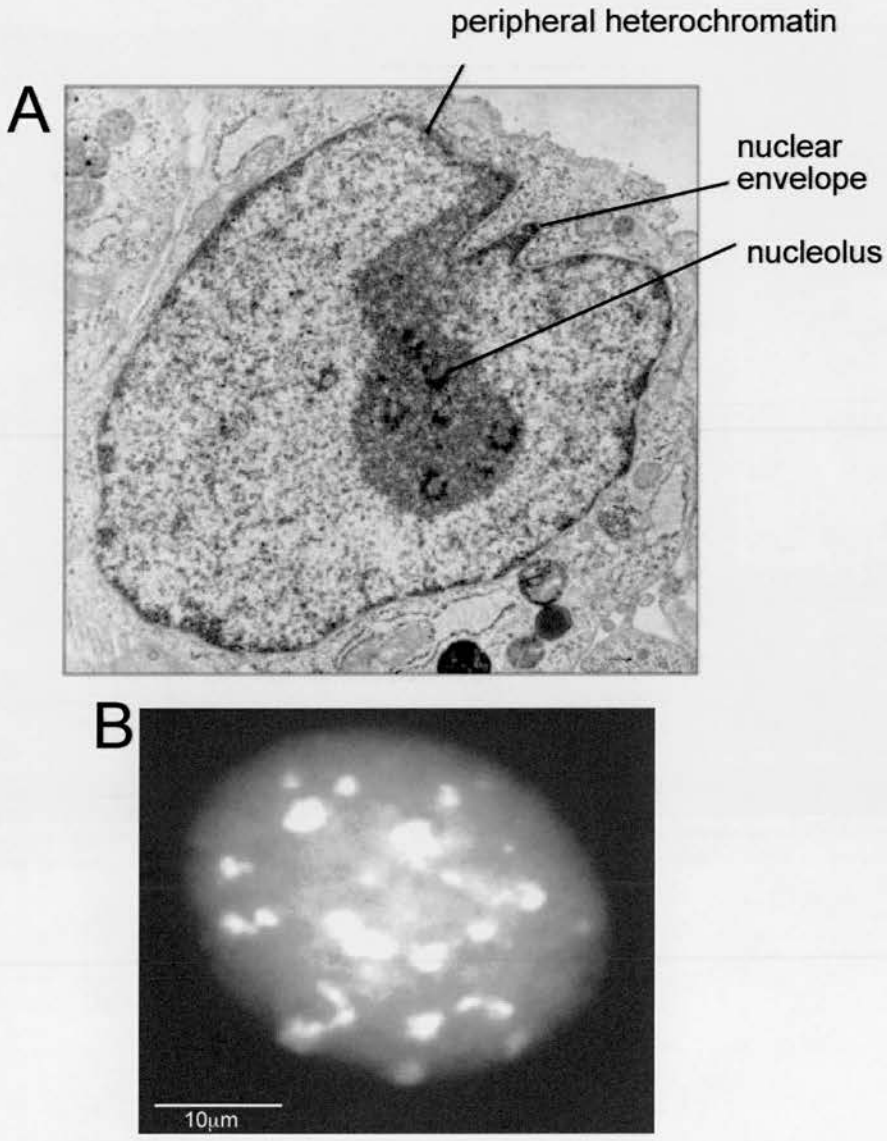

Figure 1.4: The cellular chromatin environment.
A) Electron micrographs of the nucleus of a human fibroblast.Areas of dark condensed heterochromatin can be seen adjacent to the to the nuclear envelope. Taken from Alberts *et al,*Molecular biology of the Cell, third edition. z
B) DAPI stained mouse ES cells, show heterochromatin clearly visible as DAPI bright spots,typically these represent the location of centromeres.Euchromatin is diffusely stained.

1.1.8 Heterochromatic protein-1 and Polycomb complexes

Many proteins which localise at heterochromatin, and that have roles in establishing repressive chromatin structures were originally identified as modifiers of PEV in *Drosophila.* Homologues of several PEV modifiers have since been identified in mammals and include Suv39h and the HP1. In mammals there are three isoforms of HP1(α,β and γ) . The α and β isoforms are predominantly found at pericentric heterochromatin whilst the HP1γ isoform is found at euchromatin (Minc et al., 2000, Nielsen et al., 2001; Vakoc et al., 2005). Each HP1 isoform contains a chromodomain connected via a hinge region to a chromosome shadow domain (Eissenberg and Elgin, 2000). The chromodomain is essential for H3K9 mediated gene silencing and is able to bind to H3K9me3 (Bannister et al., 2001; Lachner et al., 2001). The chromoshadow domain, mediates homo and heterodimerisation and interactions with the lamin B receptor (LBR) and Suv39h (Ye et al., 1997, Aagaard et al., 2000, Nielson et al., 2001) and the hinge region mediates binding to linker histones, DNA and RNA (Nielsen et al., 2001; Muchardt et al., 2003; Maison et al., 2002).

Once bound to chromatin, the ability of HP1 to self-dimerise enables it to recruit HDACs and Suv39h to adjacent nucleosomes and so induces the spreading of histone hypoacetylation and H3K9me3. HP1 may also have roles in silencing euchromatic genes as H3K9 methylation and HP1 can be found at the promoters of some repressed genes (Ayyanathan et al., 2003; Dillon and Fesenstein, 2002).

There is no evidence for HP1 localisation on the inactive X chromosome (Heard et al., 2005; Boggs et al., 2002; Peters et al., 2002). Rather H3K27me3 recruits Polycomb complexes to the chromosome, which bring about gene repression. These bind via a chromodomain to H3K27me3 (Fischle et al., 2003). Similarly, H3K27me3 in *Drosophila* is implicated in the long term silencing of the homeotic genes, and is again dependent on Polycomb complexes (Ringrose and Paro, 2004).

Two PcG complexes are characterized in mammals: Polycomb Repressive Complex 1 (PRC1), and Polycomb Repressive complex 2 (PRC2). The PRC2

complex contains the HMTase Ezh2, the WD-repeat protein Eed, and the Zn-finger protein Suz12 and is able to methylate H3K27 to allow binding of the PRC1 complex through its chromodomain. This may provide a stable mark for PcG repressed chromatin (Fischle et al., 2003). The PRC1 complex includes the proteins Edr2 and RING1a and RING1b amongst others (Shao et al., 1999; Saurin et al., 2001). Recently RING proteins 1A and 1B were shown to be responsible for ubiquitylation of H2A on the inactive X chromosome (de Napoles et al., 2004).

1.1.9 Histone modifications during ES cell differentiation

During mammalian development cells become committed to restricted lineages and this requires the epigenetic regulation of chromatin structures. In mouse ES cells, global levels of histone acetylation decline dramatically within a day of inducing differentiation. This is then followed by a partial recovery at day 2. As acetylation declines, histone H3K9me increases. H3K4me, another mark of active chromatin, decreases transiently upon differentiation followed by in an increase back to levels found in undifferentiated cells by day 4. This is then followed by second decrease by day 6 (Lee et al., 2004). Importantly, preventing global histone deacetylation by TSA treatment can inhibit ES cell differentiation (Lee et al., 2004, Hattori et al., 2004).

During female ES cell differentiation, a number of step-wise chromatin remodelling events also take place to stably inactivate one copy of the X chromosome (Xi) to ensure gene dosage compensation between males and females. The earliest recognisable event identifying the chromosome which is to become inactive is the appearance of a coat of untranslated RNA called *Xist* on the prospective inactive chromosome X (Xi) (Lee et al., 1999). This is closely followed by the transient association of the PRC2 complex, and thus the subsequent methylation of H3K27 (Plath et al., 2003; Silva et al., 2003, section 1.1.8). PRC1 proteins then co-localize to the inactive X chromosome probably partly due to the binding of the PRC1 chromodomain to H3K27me3 . One role of the PRC1 proteins is to induce H2A ubiquitylation (de Napoles et al., 2004). The Xi accumulation of PRC1 proteins requires Xist RNA and is not solely regulated by H3K27me3 (Plath et al., 2004). Subsequently, histones become hypoacetylated (Keohane et al., 1998; Keohane et al., 1996) and H3K9me2 levels increase. Later, the histone variant

macroH2A is incorporated into the inactive Xi (Costanzi et al., 1998;Csankovszki et al., 2001).

The final Xi is characterised by hypoacetylated histones H2A, H2B, H3 and H4, H3K9me2 and H3K27me3 with hypomethylation of H3K4 (reviewed by Heard,2005). Interestingly, these modifications can all be reversed during the mammalian nuclear transfer cloning process which reprograms X chromosome inactivation.

Recently histone modifications associated with different repetitive elements across the genome were mapped in mouse ES cells, fibroblasts and trophoblasts. For all repeat-associated methylation marks there was significant differences between the variability and combination of marks in different cell lines and only H3K9me3 and H4K20me3 upon tandem repeats were present in each cell line analysed (Martens et al., 2005). In wildtype ES cells, tandem satellite repeats and DNA transposons were observed to accumulate the repressive histone modifications, H3K9me3, H3K27me1, and H4K20me3 or H4K20me2. In contrast, interspersed long terminal repeat (LTR) repeat sequences found integrated all over the genome as singular repetitive elements, are characterised by H4K20me3 as their sole signature mark. However, these marks are not stably maintained in other cell types and are often significantly reduced or lost (e.g. H3K9me3 in mouse embryonic fibroblasts and trophoblasts for the DNA transposon Charlie, and H4K20me3 for LTR interspersed repeats in RA induced ES cells) or greatly increased (e.g. H4K20me2 for Charlie and H4K20me3 for LTRs in RA induced ES cells). Other repeats such as SINEs and LINEs which comprise >21 % of the mouse genome surprising do not contain informative histone modifications. In *Suv39h* dn ES cells, H3K9me3 and H4K20me3 is greatly reduced across major and minor satellite repeats but only at a subset of DNA transposons (Marten et al.,2005).

1.2: THE CELLULAR CHROMATIN ENVIRONMENT

1.2.1 Chromosome territories

In the nucleus of many higher eukaryotes chromosomes are found in discrete patches known as chromosome territories (CTs). The early cytologists Theodor Boveri and Carl Rabl, in 1885, were the first to propose such territories existed. Rabl proposed that plant chromosomes maintained a position during interphase, which was a reflection of their mitotic orientation and both proposed that telomeres were attached to one side of the nucleus and centromeres to the other. This orientation is now known as the Rabl configuration and has been shown to exist in yeast (Jin et al., 1998; Loidl 1999; Guacci et al., 1997), *Drosophila* (Marshall et al., 1996), trypanosomes (Chung et al., 1993), and some plant species (Aragon-Alcaide et al., 1997; Schwarzacher and Heslop-Harrison 1994; Comings 1980). In the late 1970s and early 80s the territorial organisation of interphase chromosomes in mammalian cells was indirectly visualised for the first time through experiments in which damaged regions of micro-irradiated cell nuclei formed as clusters in subsequent metaphase chromosomes (Zorn et al., 1979, Cremer et al., 1982). Distinct CTs were then confirmed in the mid 1980s using *in situ* hybridisation in interspecies somatic cell hybrids (Manuelidis 1985; Schardin et al., 1985) and subsequently confirmed in many cell types by fluorescence *in situ* hybridisation (FISH)(reviewed by Cremer and Cremer, 2001).

1.2.2 The radial distribution of chromosome territories

The idea that different chromosomes may have preferred locations within the nucleus came about with the discovery that the rDNA containing chromosomes of the human genome associated with the nucleolus (Bobrow and Heritage; 1980; Sullivan et al., 2001). Human chromosomes 19 and 18 then showed the most striking example of preferred radial positions. Both are similar in size and DNA content, but chromosome 19 is very gene-rich and found in the centre of the nucleus, while chromosome 18 is gene-poor is found at the periphery (Croft et al., 1999; figure

1.5.a). Since then an extensive study which has looked at the radial position of each chromosome in diploid lymphoblasts and tumour cell lines has proposed chromosome position is dependent upon the gene content of a chromosome as gene-rich chromosomes were found towards the nuclear interior and gene-poor chromosomes towards the nuclear periphery (Boyle et al.,2001). This localisation is present in human ES cells, suggesting that position is established early in development (Wiblin et al., 2005). A parallel study has quantified the 3D arrangement of chromosomes in flat-ellipsoid nuclei of human amniotic cells, fibroblasts and in the nuclei of spherical T and B lymphoblasts. In lymphoblasts, small-gene dense chromosomes were observed in the nuclear interior and small gene-poor chromosomes at the periphery, but the territories of the larger chromosomes (1-5) were found predominantly towards the nuclear edge regardless of gene content. In addition size correlated radial distributions were observed for amniotic and fibroblast cells (Cremer et al., 2001).

A recent study may have provided the answers to these earlier and often conflicting results. Bolzer and colleagues have reported that nuclear shape has a large impact upon the radial positioning of CTs. In flat, ellipsoidal nuclei of fibroblasts, quiescent and cycling human amniotic fluid cells, radial positioning of CTs was size related with large chromosomes towards the nuclear edge, and smaller chromosomes in internal locations, however in spherical nuclei such as T and B lymphocytes, a gene density related radial positioning was found (Bolzer et al., 2005).

The distinct differences in radial distribution of human chromosomes 18 and 19 are conserved in the equivalent chromosomes in New and Old World monkeys, despite extensive chromosome re-arrangement (Tanabe et al., 2002, Tanabe et al., 2005). Furthermore, these studies support the hypothesis that radial distribution of CTs is dependent upon gene density. Chromosome 14 in the squirrel monkey consists of a gene-poor segment syntenic to human (HSA) chromosome 1 and a gene-rich segment homologous to HSA 19. This chromosome was found to have a specific orientation such that the gene poor segment was orientated towards the periphery. The radial distribution of chromosomes has also been examined in the chicken (Habermann et al., 2001). The chicken genome contains two distinct groups

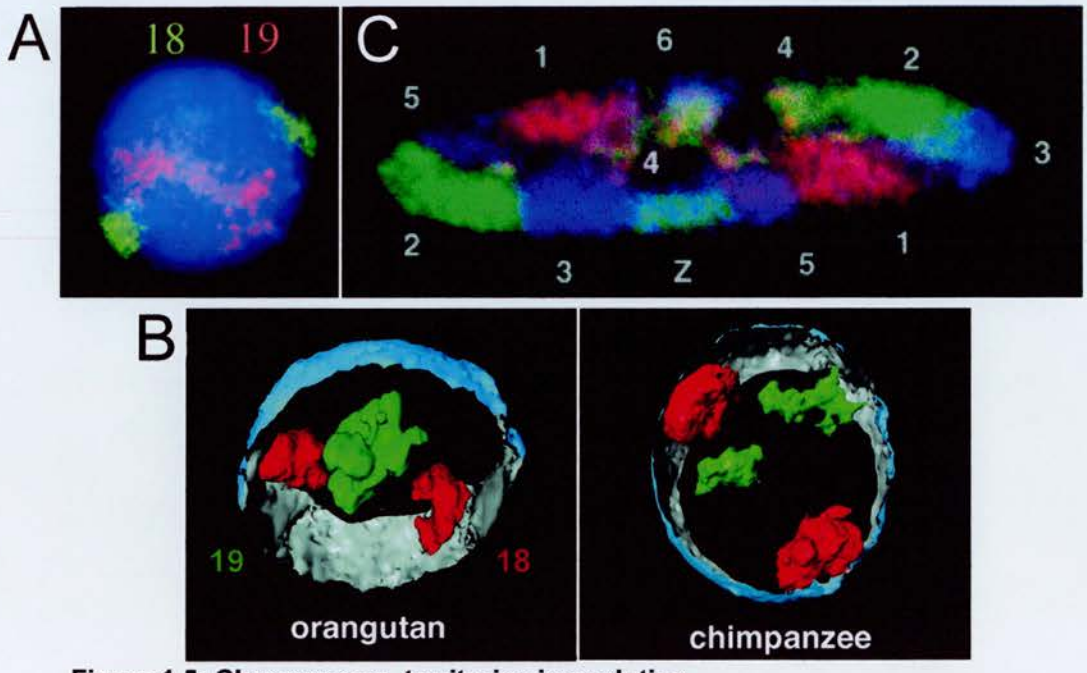

Figure 1.5: Chromosome territories in evolution.
A) In humans, despite similar sizes the gene poor chromosome 18 is found at the nuclear edge and the gene rich chromosome 19 in the interior of the nucleus. Image adapted from Croft et al.,1999. B) Positioning of chromosomes 18 and 19 is conserved in Old world monkeys. Image adapted from Tanabe,2002. C) In the chicken, multicolour FISH can detect exclusive chromosome territories. Homologuous chromosomes are found in different locations.Image adapted from Cremer and Cremer, 2001.

of chromosomes, early replicating gene -rich micro-chromosomes and late replicating gene-poor macro-chromosomes (figure 1.5.c). Gene rich micro-chromosomes are predominantly found in the nuclear interior and macro-chromosomes in the nuclear periphery. This suggests that the radial distribution of chromatin is evolutionary conserved from the chicken to human, spanning over 300 million years of evolution (Tanabe et al., 2002).

1.2.3 Functions of chromosome positioning

Conservation of CT radial positioning implies some sort of functional relevance. Recent studies have suggested CT position can alter during differentiation and in some cancer cell lines (Kuroda et al., 2004; Kim et al., 2004; Wiblin et al., 2005; Cremer et al., 2003). In the mouse, where there are no particularly gene-rich and gene-poor chromosomes, Parada and colleagues investigated the nuclear position of several chromosomes in a range of primary cells from different mouse tissues and concluded that there is tissue specificity in chromosome positioning. For example, chromosome 5 (MMU5) was preferentially found towards the centre of the nucleus in liver cells, was predominantly peripheral in small and large lung cells, but located in an intermediate position in lymphocytes (Parada et al., 2004). In a similar type of analysis Kim et al, have systematically analysed the spatial genome organization in differentiating mouse T-cells and found significant global reorganization of centromeres, chromosomes and gene loci during differentiation. Centromeres were repositioned from a preferentially internal distribution in undifferentiated cells to a preferentially peripheral position in differentiated CD4+ and CD8+ cells and MMU6, containing the differentially expressed T-cell markers CD4 and CD8, underwent differential changes in position depending on whether cells differentiated into CD4+ or CD8+ thymocytes (Kim et al., 2004). The relative and radial positions of human chromosomes 12 and 16 during the differentiation of pre-adipocytes into adipocytes is also altered (Kuroda et al., 2004). These studies show that chromatin and nuclear compartments are dynamic during cell differentiation, and that these changes may play a role in the regulation of transcriptional activity in chromatin.

Different ideas to why gene -rich CTs may be localised to the nuclear interior have been proposed. Firstly it has been suggested that the interior of the nucleus may be enriched in factors required for transcription. However there is little evidence for this as, sites of transcription and labelled nascent RNAs are located throughout the entire nucleus (Szentirmay and Swadogo, 2000, Verschure et al.,1999). Furthermore antibodies against hyperphosphorylated forms of RNA polymerase II (Zeng et al., 1997), and detection of BrdUTP incorporation (Jackson et al., 1993) show transcription foci are randomly positioned.

A second hypothesis is that the nuclear periphery is a zone of gene repression. In yeast the nuclear periphery contains high concentrations of factors essential for gene repression (section 1.3.1) and several studies in mammalian cells report the repositioning of genes to the nuclear periphery upon gene inactivation (see section 1.3.3.2.). Moreover a layer of heterochromatin is associated with the nuclear envelope and histone acetylation is depleted in this nuclear compartment (Taddei et al., 2001; Gilchrist et al., 2004).

Another "bodyguard" hypothesis proposed by Hsu in 1975 (Hsu 1975) and discussed by Tanabe et al., (2002b), suggests that gene-rich chromatin is located towards the interior of the nucleus to help protect it from mutagens, clastogens and viruses as chromatin at the nuclear periphery would soak up most of the DNA damage. Evidence arguing against this hypothesis was recently published by Gazave et al., 2005, who showed that DNA damage induced by oxidation or UV does not occur preferentially at the nuclear periphery but rather, occurs in excess in the nuclear interior. Consistent with this they also showed that the synonymous mutation rate of genes on HSA19 was greater than HSA18 (Gazave et al.,2005).

The treatment of cells with the transcription inhibitors actinomycin D and 5,6-dichloro-β–D-ribofuranosylbenzimidazole (DRB) has no effect on the positioning of chromosome territories in human lymphoblasts (Croft et al., 1999). Therefore transcription itself is not recruiting HSA19 to the centre of the nucleus. However, there is some evidence that genomic regions are tethered to different nuclear compartments such as the nuclear periphery and the nucleolus. This may be a means by which chromosome territories maintain their radial positions (Chubb et al., 2002). In addition, several integral membrane proteins have the ability to bind to

chromatin (section 1.2.8) and could provide a mechanism by which chromosomes are located at the nuclear edge.

1.2.4 Organisation within Chromosome territories

Early studies looking at the position of genes within a CT using 3D FISH suggested there was a preferential localisation of genes to the CT periphery independent of their expression status (Kurz et al., 1996; Verschure et al., 1999; Dietzel, 1999). This then led to the suggestion that there is a chromatin-free space between CTs, continuous with the nuclear pores and able to weave between CTs to end between chromatin branches 1Mb-100kb in length (Cremer et al., 1993; Zirbel et al., 1993; Verschure et al., 1999; Cremer et al., 1995). This hypothetical space, along with its contents and boundaries, was named the Interchromatin domain compartment (ICD). (Zirbel et al., 1999; Kurz et al., 1996), and the channels of this compartment were thought to contain the macromolecular machinery required for transcription, RNA splicing and transport. Thus, it was proposed that transcription could only take place within the ICD (Zirbel et al., 1996,Kurz et al., 1996; Cremer and Cremer, 2001) and that chromatin was arranged so that transcriptionally active loci were at the surface of large-scale chromatin fibres (Verschuhe et al., 1999; Falkan and Nobis, 1978; Wansink et al., 1996; Cmarko et al., 1999).

In conflict with this model, several studies which have since looked at the spatial arrangement of early-replicating, GC-rich, transcriptionally-active chromatin and compared it to late replicating, AT-rich, transcriptionally silent chromatin, have shown that transcriptionally active genes can be found in the interior of a CT (Abranches et al., 1998; Tajbakhsh et al., 2000; Verschure et al., 1999; Visser et al., 1998; Mahy et al., 2002). Furthermore the results of many recent fluorescence recovery after photobleaching (FRAP) studies show that the nucleus is highly dynamic (section 1.4.1) and many proteins including RNA polymerase II, and several transcription factors are highly mobile (Heida et al., 2005, Misteli et al., 2000). If the IC-CT model held true, then CTs would present a barrier to the diffusion of such proteins and their mobility would be impaired.

Despite evidence that genes can be transcribed from within CTs, large regions of the major histocompatibility (MHC) locus on human chromosome 6 have been reported to extend out from the chromosome territory. The frequency of this "looping" is dependent on the cell type and the number of genes within the region which are active (Volpi et al., 2000). Similarly, the epidermal differentiation complex (EDC) on chromosome 1, and the gene-dense regions 11p15.5 and 11q13 act in a similar manner (Williams et al., 2002; Mahy et al., 2002). Both the MHC and EDC, are co-ordinately regulated and looping out is only observed in cell types which express the genes they contain. Furthermore looping of the MHC class II genes can be greatly enhanced by Interferon-gamma in MRC5 fibroblasts. In contrast 11q13 and 11p15 are not co-ordinately regulated but generally contain high levels of gene expression. The inhibition of transcription can decrease but not eliminate the looping out of the 11p15.5 region (Mahy et al., 2002).

Looping out of a gene from its CT has been shown to occur during differentiation. Differentiation of mouse ES cells induces the transcriptional activation of the *HoxB* cluster in a time dependent manner. *Hoxb1* was observed to loop out of its CT as it beomes expressed at day 4 of differentiation, this is followed by *Hoxb9* at the opposite end of the cluster at day 10 of differentiation, once it too is transcriptionally active (Chamberyon and Bickmore, 2004). Looping out from the CT for both of these genes when expressed, has also been seen in the mouse embryo (Chamberyon et al., 2005). The looping of active genomic regions could be a mechanism conserved between mammals and *Drosophila*, as actively transcribed regions of *Drosophila* polytene chromosomes are known to "puff" up.

Together these studies indicate that the propagation of chromatin out with the CT, although not essential, may aid the expression of a gene. Looping out may relocate a gene to a more permissive environment for transcription. Support for this hypothesis comes from a recent study by Osborne and colleagues (Osborne et al., 2004). They reported the co-localisation of genes from a range of different genomic locations to shared RNA polymerase II factories. Even though RNA polymerase II has been shown by FRAP experiments to be highly mobile, transcription is thought to take place at fixed points in the nucleus. The idea of RNA polymerase factories was proposed after transcription sites within mammalian cells were mapped using

Brd-UTP incorporation (Pombe et al., 2000; Iborra et al., 1996). This revealed approxiamately 10,000 sites of non-nucleolar transcription of which 8,000 were estimated to be due to RNA polymerase II. From this, it was proposed that RNA polymerases at each site of transcription are associated with a nuclear skeleton forming factory. Transcripts are then extruded from factories upon the passage of templates through positionally fixed polymerases (Jackson et al., 1998). Osbourne and colleagues have provided evidence to suggest that genes move in and out of replication "factories" as they are activated and repressed. Spilianakis et al., have also recently shown that genes from different chromosomes are brought together upon repression to common sites within the nucleus (Spilianakis et al., 2005).

1.2.5 The role of the nuclear matrix in chromatin organisation

Fixed cells treated with DNaseI, and then permeabilised to remove soluble proteins, show a fibrogranular non-chromatin structure when examined by e.m. This structure is composed of an RNA-protein complex (RNP) and has been termed the nuclear matrix. The attachment of chromatin domains to such a matrix has been proposed to regulate nuclear compartmentalisation of the genome and provide the structural basis of nuclear order (Nickerson, 2001; Pederson, 2000). However, the molecular basis of such a matrix remains unclear as attempts to isolate it biochemically have been unsuccessful.

Despite the uncertainty over the molecular basis of the matrix, many genes have been identified to contain scaffold and matrix attachment regions (SARs and MARS) within them. These are A-T rich DNA sequences able to bind to the nuclear scaffold (Mirkovitch et al., 1984; Cockerill et al., 1986) and located near the promoters and enhancers of genes. SMAR sequences can also stimulate the expression of a reporter gene when integrated into the genome (Stief et al., 1989), and can regulate chromatin accessibility (Jeunwien et al., 1997). The best-characterised MAR binding protein is SATB1. In human thymocytes, SATB1 forms a cage like network of protein filaments to which genes can attach via SMAR regions (Cai et al., 2003). Another protein with a potential role in the nuclear matrix is actin (Bettinger et al., 2004).

Human lymphocytes extracted with high salt concentrations show striking differences in the behavior of HSA18 and 19. In high salt concentrations HSA18 DNA is released up to 3 μm away from the nuclear remnants, whereas the detectable HSA19 DNA remains in the center of the nucleus, suggesting that HSA19 but not HSA18 is attached to the nuclear matrices (Croft et al.,1999).

1.2.6 The role of the nuclear periphery in chromatin organisation

The nuclear and cytoplasmic compartments of eukaryotic cells are separated by the outer (ONM) and the inner (INM) nuclear membranes. Nuclear pore complexes (NPCs) which mediate the bi-directional transport of macromolecules between the cytoplasm and the nucleus, bridge the lumen space between both membranes and interconnect the two (figure 1.6). Underlying the INM in mammalian cells is the nuclear lamina consisting of lamin polymers. Lamins are also found throughout the nucleoplasm, often within dense patches of chromatin, and have been implicated in the structure of the nuclear matrix (Neri et al., 1999).

The lamins are type V intermediate filament proteins with a short N terminal head domain, a long α helical coiled-coil "rod" domain and a globular tail. The rod domain mediates lamin dimerisation and polymer assembly whilst the globular and head domains contribute towards polymer assembly only (Heitlinger et al.,1992, Strelkov et al., 2004, Stuurman et al., 1998).

In vertebrates there are two types of lamins, A and B. Vertebrates have three lamin genes encoding lamin B1, lamin B2 and lamins A and C. Lamins A and C are splice variants of *LMNA* and are only expressed in differentiated cells, whilst type B lamins are ubiquitous and essential for development (Stick and Hausen 1985; Rober et al.,1989; Lehner et al.,1987). Lamins are able to bind *in vitro* to many INM proteins which include emerin, MAN1, lamin B receptor, lamina-associated polypeptides-1, 2α and 2β □(LAP1, LAP2α, LAP2β)□□ and nesprin (reviewd by Gruenbaum, 2005). Lamins can also bind to chromatin proteins such as H2A and H2B, retinoblastoma protein (RB), and components of the RNA pol II transcription

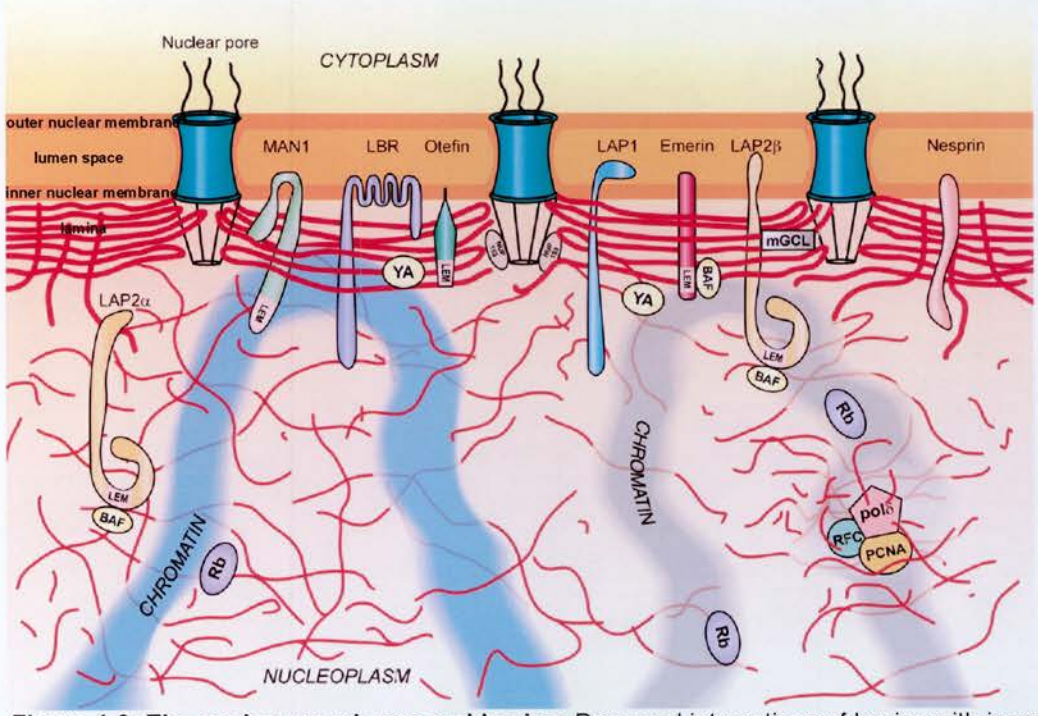

Figure 1.6: The nuclear membrane and lamina. Proposed interactions of lamins with inner membrane proteins, nuclear pores, and other nucleoplasmic factors (see text). Lamins predominantly located at the nuclear edge (thick red lines) are also found throughout the nucleoplasm (thinner red lines). Also shown are LEM domain proteins binding to lamins and chromatin.Other factors thought to interact directly or indirectly with lamins are also depicted, including BAF, Rb,LBR, LAP1,mGCL and nesprin. Image taken from Goldman et al.,2002.

complexes (Gruenbaum et al., 2003, Zastrow et al., 2004). Lamins and their associated proteins are thought to have roles in large-scale chromatin organisation (Liu et al., 2000; Liu et al., 2003); the spacing of NPCs (Schirmer et al., 2001), the positioning of the nucleus within the cell (Starr et al., 2001; 2002), and the reassembly of the nucleus after mitosis (Lopez-Soler et al., 2001).Essential nuclear functions such as RNA pol II dependent gene transcription and DNA replication also dependent on the type B lamins (Ellis et al., 1997, Spann et al., 1997; Spann et al., 2002).

In most cells, there is a large portion of electron dense chromatin localised at the nuclear periphery. However, this is lost in cells with different types of mutations in Lamin A (Sullivan et al., 1999; Nikolova et al., 2004; Goldman et al., 2004), suggesting a further role of lamins in anchoring chromatin to the nuclear periphery.
A wide range of disease phenotypes arise through mutations in the lamins and over 180 disease causing mutations have been mapped to the *LMNA* gene alone (Worman et al., 2004; Mounkes et al., 2003). These disorders include muscular dystrophies, lipodystrophies, bone disorders and the premature aging syndrome Hutchison-Gilford. Many of them affect specific tissues and even different mutations within the same gene can have different disease phenotypes. How such widely expressed proteins cause such specific phenotypes is not clear, although one idea is that gene expression is perturbed through the mis-localisation of chromatin sequences. Another cause of tissue specific phenotypes could be impaired interactions with binding proteins.

Over 300 dystrophies remain, in which the gene responsible is not known. This suggests that there may be other NE proteins with important roles in nuclear architecture that have not been identified (Schirmer and Gerace, 2005). In recent years, attempts to identify further NE proteins have used proteomic analysis and genomic databases to identify a whole range of new NE proteins and their associated diseases (Dreger et al., 2001, Schirmer et al., 2003). However it may still be some time before the full complement of NE proteins is known and the NE proteome may differ in different vertebrates and at different times of development. Furthermore, understanding the complex interactions of NE proteins with their binding partners and how they regulate gene expression will take even longer.

LBR is one of a number of integral membrane proteins embedded within the nuclear membrane. LBR binds type B lamins and *in vitro* can bind double stranded DNA, histone H3-H4 tetramers, and HP1 (Holmer et al., 2001). Pelger-Huet anomaly is an autosomal dominant condition due to mutations in LBR. Patients with this disorder have white blood cells with abnormal chromatin organisation and decreased lobulation. Greenberg skeletal dysplasia is also due to mutations in LBR (Waterham et al., 2003).

LAP2β, emerin and MAN1 are all integral INM proteins that contain a 40 a.a. LEM (LAP, Emerin, MAN1) domain, able to mediate binding to chromatin via barrier-to-auto integration factor (BAF) (Furukawa et al., 1999, Shumaker et al., 2001; Lee et al., 2001; Dechat et al., 2000; Liu et al., 2003; figure 1.8). BAF is an essential protein able to bind non-specifically to DNA *in vitro* (Zheng et al., 2000) and interactions of the LEM domain with BAF may create a means by which endogenous chromatin is anchored to the nuclear edge (figure 1.7). As well as the LEM domains, LAP2β, emerin and MAN1 all contain at transmembrane domains near the C terminus (Manilal et al.,1996).

Emerin is expressed in nearly all tissues, but is absent or mutated in patients with the X-linked condition Emery-Dreifuss muscular dystrophy (Bione et al., 1994). In these patients condensed chromatin underlying the nuclear envelope as detected by e.m, is thin or absent. However the nuclear position of a subset of gene-poor chromosomes is not affected by Emery-Dreifuss muscular dystrophy as these chromosomes are still located preferentially at the nuclear periphery in emerin deficient cells (Boyle et al., 2001). Emerin can also interact with an ubiquitously expressed transcriptional regulator, germ cell-less (GCL). GCL localises at the INM (Nili et al., 2001; Jongens et al., 1994), where it is able to bind and repress the heterodimeric transcriptional repressor E2F-DP3 (Nili et al., 2001; de la Luna et al., 1999). The binding of BAF to emerin can displace GCL *in vitro*, suggesting that emerin is present in two different lamin anchored complexes (Holaska et al., 2003; Bengtsson et al., 2004). The GCL binding region in emerin is also recognised by the transcriptional regulator Btf (Bcl-2-associated transcription factor) (Haraguchi et al., 2004). Both Emerin and lamin A can bind to monomeric globular (G)-actin *in vitro* (Bengtsson et al., 2004; Fairley et al., 1999). Actin is a major component of the cell

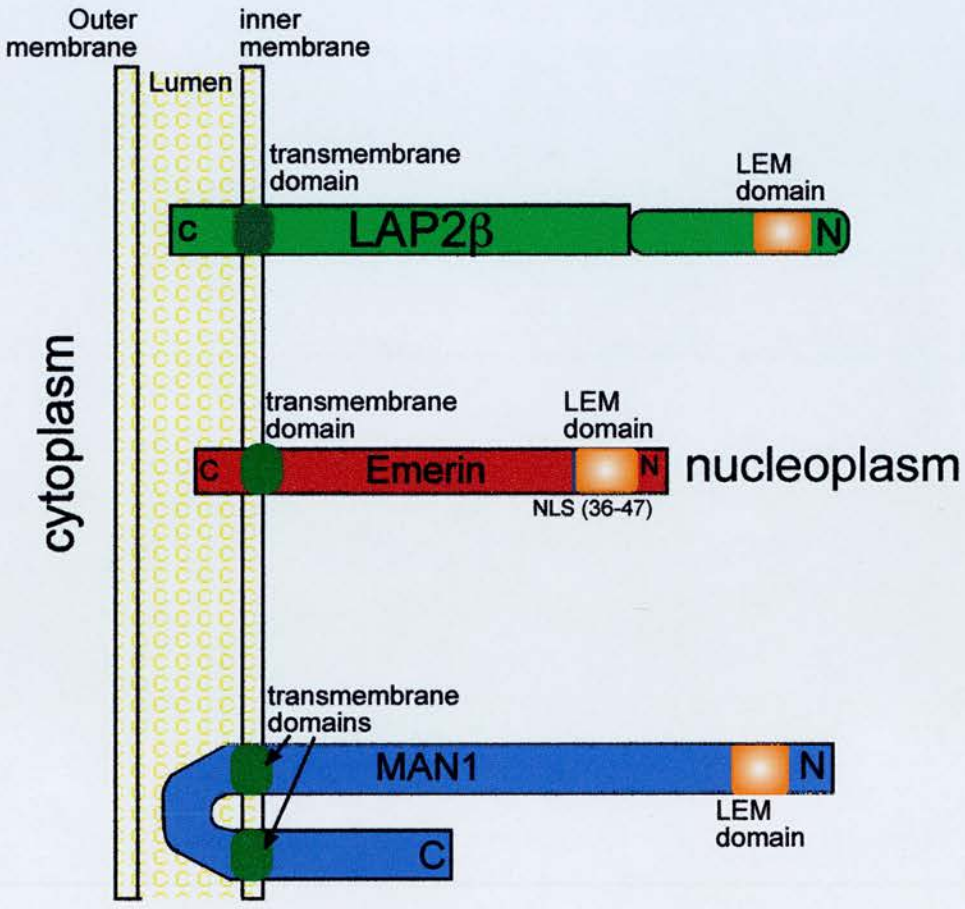

Figure 1.7: LAP2β, emerin and MAN1 share transmembrane and LEM domains. Schematic showing the conserved domains of LAP2β,emerin and MAN1 and the positioning of each protein at the inner nuclear membrane. The transmembrane domain at the C terminus is required to localise the protein to the nuclear membrane whilst the N terminal LEM domain, binds to the DNA binding protein, BAF and has roles in anchoring endogenous chromatin to the nuclear periphery.

cytoskeleton and nuclear actin may have roles in chromatin remodelling, the formation of heterogeneous RNA particles, stress responses, nuclear export and transcription (Pederson and Aebi 2002). The composition or function of lamin-emerin-actin complexes may be regulated by phosphorylation mediated by protein kinase A, which interacts with these complexes (Lattanzi et al., 2003; Mattioli et al., 2005). Emerin can also bind and cap the pointed ends of polymeric-F-actin (Holaska et al., 2004), suggesting that its mis-localisation in *LMNA* mutant cells could disrupt the mechanical integrity of the cell.

A single gene in mammals encodes the several distinct isoforms of LAP2. However the LAP2α and LAP2β isoforms are the most commonly expressed (Furukawa et al., 1995; Berger et al., 1996; Foisner and Gerace 1993; Berger et al., 1996). The β,δ,ε, and γ LAP2 isoforms, are closely related and contain transmembrane domains. In contrast, LAP2α has an unique C-terminus and lacks a transmembrane domain resulting in its localisation to the nucleoplasm. In general, little is known about the different expression patterns and functions of LAP2 isoforms, but LAP2β has recently been shown to repress transcription of a number of different transcription factors including, p53, NF-κB, and members of the E2F-DP family, as part of a repressive complex which also includes HDAC3. Repression by LAP2β was alleviated by TSA, and over expression of LAP2β caused the deacetylation of H4 (Somech et al., 2005). Like emerin, LAP2β can also bind to GCL (Nili et al., 2001). Furthermore LAP2β has also been implicated in nuclear growth (Yang et al., 1997).

MAN1 is mutated in three related bone disorders: osteopoikilosis, Buschke-Ollendorff syndrome and melorheostosis (Hellemans et al., 2004). MAN1 protein crosses the INM twice (Lin et al., 2000, figure 1.7), and can bind directly to SMAD proteins via its C terminus to repress signalling by the TGFβ cytokines (Osada et al., 2003, Pan et al., 2005; Lin et al., 2005). MAN1 is the first INM protein with a role in signal transduction to be identified.

1.3 NUCLEAR ORGANISATION AND GENE REGULATION IN MODEL ORGANISMS

1.3.1 Saccharomyces Cerevisiae

In contrast to higher eukaryotes, the genome of the budding yeast *Saccharomyces cerevisiae* contains very little repetitive DNA and very few constitutively silent genes. In addition, the yeast genome is organised in a Rabl configuration with telomeres anchored to one side of the nucleus periphery and centromeres to the opposite side. The 32 different telomeres cluster together into three to eight foci adjacent to the nuclear periphery (Gotta et al., 1996).

Sub-telomeric regions are subject to gene silencing in yeast and this, together with the localisation of the silent mating type loci (HMR and HML) at the nuclear periphery, provides strong evidence for a role in the yeast nuclear periphery in gene silencing. Furthermore, the silent information regulator (SIR2, SIR3 and SIR4) proteins required for the silencing of the HMR and HML, and telomeres, and are found concentrated at the nuclear periphery (Gotta et al., 1996, Maillet et al., 1996). Silencing of the HML and HMR loci is dependent on DNA silencers which bind to sequence specific factors and recruit the binding of SIR proteins (Rusche et al., 2003). In contrast, silencing at the telomeres depends on Rap1, which binds to the terminal $[TG_{1\text{-}3}]_n$ sequence and co-operates with the yKU70/yKU80 complex to recruit SIR proteins to the telomere ends (Laroche et al., 1998, Mishra and Shore 1999, Roy et al., 2004). Once bound the SIR proteins spread along the adjacent nucleosomes and the HDAC activity of Sir2 propagates histone hypoacetylation. (Renault et al., 1993, Hecht et al., 1997, Rusche et al., 2002).

Telomere anchoring can be separated into two partially redundant pathways, one of which depends on the heterodimeric yKu complex (Gotta et al., 1996; Tham et al., 2001; Hediger et al., 2002, figure 1.8). yKu is part of a heterodimer, with roles in DSB repair by non-homologous end joining, and the recruitment of telomerase (Gravel et al., 1998, Peterson et al., 2001). Deletions of yKu result in the displacement of around 50% of the telomeres from the nuclear periphery alongside severely compromised telomeric and HMR repression (Laroche et al., 1998).

Mutants that are able to restore telomere position in the absence of yKu have shown that there is a SIR4 dependent anchor able to function independently of yKu at the native telomere VI-R. This SIR4 pathway of telomere anchoring is dependent on the protein Esc1 (Andrulis et al., 2002). When tethered to a de-repressed telomere or mutated HMR silencer, Esc1 can restore its repression. In addition when fused to a DNA binding domain, Esc1 has the ability to relocalise non-telomeric chromatin to the nuclear edge (Taddei et al., 2004). Targeting either yKu80 or a subdomain of SIR4, to DNA is sufficient to drag it the nuclear edge (Taddei et al., 2004, figure 1.8).

Recently it has been shown that mating type loci can be silenced without telomeric pools of SIR proteins (Gartenberg et al., 2004). Inducible site-specific recombination uncoupled the HMR locus and its silencers from its normal chromosome position near the telomere 3R. In the absence of yKu and Esc1 the HMR locus was released from the nuclear periphery but remained silent, showing that SIR-mediated silencing can occur outside the periphery. Therefore, not only can telomeres be tethered without repression (Heidger et al., 2002, Taddei et al., 2004, Tham et al., 2001), but silencers can silence without chromatin being anchoring to the nuclear edge. These studies provide evidence that SIR proteins are essential for nucleating repression and suggest telomeres may mediate repression by creating reservoirs of silencing factors. The authors of this paper proposed that sequestering of SIR proteins at telomeres simply acts as an anti-silencing mechanism for the rest of the genome as localising the SIR proteins to the telomeres prevents them binding to other genomic locations (Gartenberg et al., 2004).

A now classic study by the Sternglanz lab has shown the direct role of the nuclear periphery in yeast silencing. Andrulis and colleagues took an HMR locus with a defective silencer and artificially anchored it the nuclear periphery to investigate the effect upon its expression. In yeast, over-expression of Golgi proteins results in their accumulation in the ER and nuclear membrane. Therefore, to tether the defective locus, Gal4-golgi protein fusions were over-expressed and Gal4 binding sites were inserted into the defective locus. The fusion proteins bound the Gal4 binding sites and recruited the HMR to the periphery, where SIR dependent silencing of the HMR locus was restored (Andrulis et al., 1998).

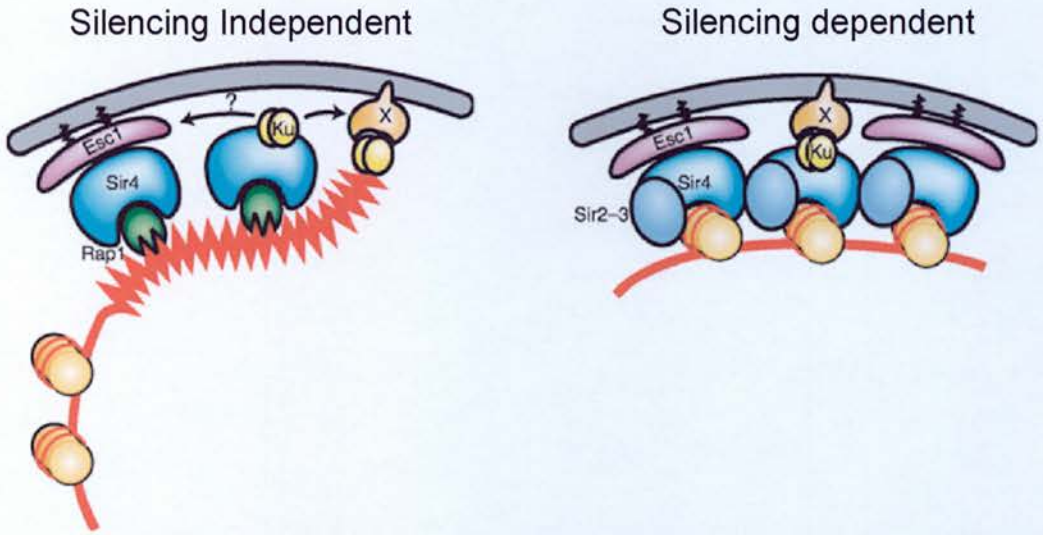

Figure 1.8: Alternative pathways of telomere anchoring in yeast. Dual pathways to tether telomeres to the nuclear periphery exist within *S.cerevisiae.* One path, mediated by Ku and an unknown protein X is silencing independent, whilst the second is mediated by SIR4 and Esc1 and is silencing dependent. Rap1-bound SIR4 can bring a telomere to the nuclear edge through interactions with both Ku or Esc1. Likewise SIR4 can promote the perinuclear anchoring of silent chromatin in either path. Image adapted from Taddei et al.,2004.

Interestingly, a SIR2-like protein has recently been implicated in silencing of *var* genes in the protozoan malaria parasite *P.falciparum*. Similar to the situation in yeast, these genes are found within 20-50kb of telomere ends, which are also anchored to the nuclear periphery (Freitas-Junior et al., 2005, Freitas-Junior et al., 2000). In yeast, nuclear pore complexes (NPCs) have been implicated in both gene activation and gene silencing. The nucleoporins, NUP60 and NUP145, are essential for the complete silencing of the mating type locus (Feuerbach et al., 2002) and the conserved TPR homologues MLP1 and MLP2 proteins are required for silencing of a reporter gene placed at HMR (Galy et al., 2000; Feuerbach et al., 2002). Tpr is a 267-kDa protein located at nucleoplasmic side of the nuclear pore complex in mammals (NPC). However, although the nuclear periphery is generally regarded as a repressive zone, Ishii and colleagues have been able to show that components of the nuclear transport machinery exhibit strong boundary activities, which permit the activation of a reporter gene by shielding it from a silent chromatin environment (Ishii et al., 2002). Genomic location analysis, has since identified all the genes bound by the NPCs, several different karyopherins and the RanGEF protein in *S. cerevisiae* (Casolari et al., 2004). Both karyopherin and RanGEF proteins have roles in nuclear transport and from the genes identified in this study, the authors were able to make several conclusions. Firstly, members of the nuclear transport complexes that had similar functions had similar subsets of genes bound to then, with most genes being highly expressed. The exception to this, were the genes bound to RanGEF as these were mostly transcriptionally inactive. Secondly, NPC-associated genes are greatly enriched with binding sites for Rap1, suggesting it may also have roles in tethering genes to NPCs. Finally, and perhaps most importantly, when the transcription of genes involved in galactose metabolism was induced, genes were seen to move to NPC upon activation, implying relocation is the consequence of changes in gene expression. A similar study by Brickner and Walter has also reported movement of the Inositol 1-phosphate synthetase (*INO1*) gene to the nuclear periphery upon its activation (Brickner and Walter 2004). In a recent extension of their study, Casolari and colleagues analysed the binding pattern of the NPC-associated protein Mlp1, before and after the transcriptional activation of a range of

α-factor-induced genes by the α-factor mating pheromone. These genes became associated with nuclear transport machinery upon activation, indicating a global re-organisation of newly activated genes to the nuclear periphery can take place. High resolution mapping of chromosome III then revealed several α-factor-dependent determinants of nuclear organisation were required for the re-localisation of genes to the NPCs, including DNA replication and intergenic regions. A bias of Mlp1 binding to towards the 3' ends of transcriptionally activate genes was also observed (Casolari et al., 2005).

1.3.2 Drosophila Melanogaster

Like yeast, *Drosophila* chromosomes in both early embryonic and polytene larval tissues are polarised in a Rabl configuration and chromatin is associated with the nuclear envelope (Marshall et al., 1996). However in contrast to the yeast genome, where telomeres account for nearly all the simple repetitive DNA, up to 30% of the *Drosophila* genome is composed of dispersed satellite or centromeric repeat DNA.

Repositioning of loci to sites of constitutive heterochromatin in the nucleus has been associated with gene silencing in *Drosophila*. An insertion of a large block of heterochromatin containing the AAGAG satellite next to the *brown* gene is responsible for the *brown* dominant mutation (Bw^{D}). This has the unique property of being able to induce PEV in the remaining wild-type *brown* locus (Dreesen et al., 1991, Csink and Heinkoff, 1996). An essential requirement of this variegation is the pairing of homologs. Decreased expression of *brown* in eye tissue correlates with the sequestration of the mutated gene, and its homologous wild-type copy, to the heterochromatic compartment of the nucleus. In the new environment, transcription of the normal locus is repressed. The key piece of evidence for this model is that the extent of trans-inactivation of the normal locus is dependent on the chromosomal position of the mutated copy of the brown gene (Talbert et al., 1994).

In *Drosophila*, chromatin insulators are DNA sequences able to buffer the expression of a transgene from PEV and can interfere with the ability of an enhancer to activate a promoter when placed between them (Gerasimova and Corces 1996, Geyer 1997, Bell and Felsenfield 1999). Insulators are thought to mediate these

effects by altering the nuclear position of a gene. The *Drosophila gypsy* insulator was first identified within the *gypsy* retrotransposon (Gdula et al., 1996) and at least two proteins, suppresser of hairy-wing (Su(Hw)) and mod(mdg4) are found bound to sites of the *gypsy* sequence which are dispersed many times throughout the *Drosophila* genome. However immunofluorescence studies show these two proteins localise to only 20-25 sites in each nucleus (Gerasimova and Corces 1998). One explanation for this is that *gypsy* insulators cluster together through chromatin looping to create large protein complexes, in regions of the nucleus with different abilities to support regulation. A later study has since proposed that the *gypsy* insulator regulates gene expression by organising DNA within the nucleus into higher order domains (Gerasimova et al., 2000). In this study, a DNA sequence usually found at random in the nucleus was found to be preferentially located at the nuclear periphery when a copy of the *gypsy* insulator was inserted into it. To test whether the association of *gypsy* to the nuclear periphery is required for its function, the nuclear localization of suHw in multiple transgenic lines containing either a single or tandemly paired suHw insulator was investigated. This showed that genomic loci with full-length *gypsy* insulators are present at higher proportions near the nuclear periphery than loci without the *gypsy* insulator. However, transgenes which contained only the functional 340 bp suHw region of the *gypsy* insulator did not exhibit such a biased distribution towards the nuclear periphery, and antibody staining to look at the distribution of the SuHW protein revealed it was present both at the periphery and the nuclear interior, in foci similar to the distribution of the transgenes containing the suHw DNA (Xu et al., 2004). The function of the *gypsy* insulator is therefore not solely dependent on its localisation to the nuclear periphery. However by changing the position of a transgene within the nucleus, *gypsy* and other insulators may control gene regulation by moving chromatin to regions of the nucleus with an increased or decreased ability to support transcription, highlighting the role of nuclear compartmentalisation in gene expression.

Loop formation such as that induced by insulators usually brings together distant sequences that are linked in *cis,* however in *Drosophila* GAGA factor sequences can also bring together sequences located on different chromosomes (*in trans*), dependent on the btb/poz domain. GAGA can also bind to polycomb-response

elements (PREs) that are part of the cellular memory modules (CMMs) in the bithorax complex (BX-C) (Hagstrom et al., 1997;Cavalli et al., 1998; Horard et al., 2000). In *Drosophila* it is common for chromosomes to pair with their homologous counterpart in somatic cells to mediate gene silencing (Henikoff and Comai 1998). This can involve PREs and PREs interact genetically with one another *in trans* (Sigrist and Pirrotta 1997). The *abdominal –A* and *–B* parts of the BX-C can interact, not only when the alleles are located on homologous chromosomes but also when a translocation has moved one of the alleles to a different chromosome (Gemkow et al., 1998). This interaction depends on the *Fab-7* cellular memory module within the BX-C (Bantignies et al., 2003). Interactions of the endogenous *Fab-7* with other *Fab-7* elements that are located in transgenes at a variety of genomic locations was shown, and were able to mediate transgene silencing (Bantignies et al., 2003). Polycomb proteins are the key candidates thought to be responsible for mediating interactions between *Fab-7* elements as the co-localisation of transgenes with the BX-C is lost in a polycomb mutant (Bantignies et al., 2003). Whether gene silencing is the cause or consequence of these interactions is unclear, although co-localisation is seen in less than half of all nuclei, even in lines with strong repression. This suggests that localisation is dynamic or stochastic, and makes it unlikely that nuclear co-localisation is essential for silencing but may be important for its establishment or maintenance (Gemkov et al., 1998).

1.3.3 Nuclear compartments and gene regulation in mammals

1.3.3.1 Heterochromatin and gene transcription

As in *Drosophila*, the localisation of genes to sites of constitutive heterochromatin is associated with gene silencing in mammalian cells. In cycling but not quiescent mouse B cells transcriptionally active genes are generally positioned away from centromeric heterochromatin whereas many transcriptionally inactive genes are localised adjacent to heterochromatin domains (Brown et al., 1999). This localisation can be induced by the mitogenic stimulation of quiescent cells to enter the cell cycle and a model has been proposed in which an active gene localized in a

transcriptionally permissive environment is sequestered upon transcriptional shutdown to a repressive environment by a hypothetical "recruiter" (Brown et al., 1997). This recruitment may be achieved by the increased binding of local recruiting factors to motifs in the target gene or by centromere-bound recruiters. Ikaros is found at high levels in centromeric clusters alongside transcriptionally repressed genes and thus Ikaros is a candidate recruiter (Brown et al.., 1997). Ikaros is required for normal haematopoiesis and shares homology with the *Drosophila* protein Hunchback that has been implicated in the recruitment of Polycomb proteins and the establishment of silencing complexes (Georgopoulos et al., 1992; Zhang et al., 1992; Poux et al., 1996). Ikaros is also able to mediate the silencing of the λ5 promoter by localising it to pericentric heterochromatin in mature B cells (Sabbattini et al., 2001). Recently a detailed analysis of the positioning of CD4 and CD8 loci at different transitional time points in thymocyte differentiation looked at what came first, the silencing of genes or their re-localisation to pericentromeric heterochromatin. This revealed lineage choice is the consequence of repositioning of co-receptor alleles to centromeric heterochromatin domains. Centromeric repositioning of loci was therefore concluded to be progressive, developmentally regulated, and selective, affecting only co-receptor loci that are subject to stable silencing (Merkenschlager et al., 2004).

Similar studies analysing the relationship between gene recruitment to centromeric heterochromatin and transcriptional shutdown have analysed the V(D)J recombination system during lymphocyte development. To create the diverse range of antigen receptors found in lymphocytes, recombination between variable (V), diversity (D) and joining (J) regions of immunoglobin and T cell receptor genes takes place during B and T cell development (Hesslein et al., 2001;Bassing et al., 2002). This is tightly controlled in a lineage and stage-specific manner and requires the recombination activating gene (RAG) 1 and RAG2 recombinases in addition to DNA repair enzymes (Rolink and Melchers 1999; Rajewsky 1996; Schatz, Oettinger and Baltimore, 1989). V(D)J rearrangement occurs initially at the immunoglobulin heavy chain (IgH) loci of pro-B cells and is followed by recombination of the two immunoglobulin light chain loci (IgL), Igκ and Igλ, in small pre-B cells and early immature B cells (Hesslein et al., 2001;Bassing et al., 2002). Recombination of IgH

induces a feedback mechanism in which the production of a functional IgH protein restricts further rearrangements by inhibiting the expression of RAG proteins, thorough the presence of a protein called μ which is expressed as part of the pre-B cell receptor (Nussenzweig et al., 1987;Manz et al., 1988; Costa et al., 1992; Chang et al., 1999). This feedback process is called "allelic exclusion" (Barreto and Cumano 2000). Upon differentiation into pre-B cells, RAG proteins are re-expressed and until recently it was unclear what changes took place in the IgH locus to prevent it from being rearranged further. However, a recent study by Skok and co-workers has shown that upon the expression of μ , there is rapid locus decontraction of both IgH loci and centromeric recruitment of the non-functional IgH locus. Centromeric positioning of the non-productive IgH locus is retained in small pre-B cells and immature B cells as they undergo IgL rearrangements. Furthermore, in contrast to the IgH alleles, during IgL rearrangements, the Igκ locus, which is rearranged before the Igλ locus, undergoes contraction specifically in small pre-B cells, suggesting that loci are only in a contracted state during their rearrangement (Roldan et al., 2005). The recruitment of non-rearranged IgH loci to centromeric heterochromatin is in line with an earlier study by the same group which reported the expressed alleles of IgH and Igκ to be located in positions away from centromeric heterochromatin whereas non-expressed alleles were not (Skok et al., 2001).

1.3.3.2 The nuclear periphery and gene expression

Localisation of genes to the nuclear periphery has also been implicated in gene regulation in mammals and consistant with this, the nuclear periphery is depleted in histone acetylation (Saddoni et al., 1999, Taddei et al., 2001, Gilchrist et al., 2001).

The first known example of transcriptionally inactive chromatin at the nuclear periphery was the inactive X chromosome. This is frequently found at the nuclear edge in a very compact structure known as a Barr body (Belmont et al., 1986). In more recent years further examples of genes relocating towards the nuclear periphery upon silencing or away from the periphery upon activation have been discovered.

In haematopoietic progenitors and pro-T cells, IgH and Igκ are located at the nuclear periphery but not at centromeric heterochromatin. In pro-B cells

however, both loci have a central location and large-scale compaction is seen, similar to the compaction reported recently by Roldan et al., (Kosak et al., 2002). Kosak proposed a model in which IgH and Igκ in their default state are localised at the nuclear edge through interactions with the nuclear lamina. During early B cell development this interaction is disrupted as IgH and Igκ are rearranged, with compaction of the loci aiding long-range interactions. In agreement with this model, IgH and Igκ in their default silent state are found at the nuclear periphery in mouse ES cells.

In a similar study, Zink and colleagues have looked at the positioning of three adjacent genes, ankyrin repeat SAM and basic leucine zipper domain containing 1 (*GASZ*), cystic fibrosis transmembrane conductance regulator (*CFTR*) and cortactin-binding protein 2 (*CORTBP2*), and have shown that each adjacent gene can locate to a distinct nuclear compartments in accordance with its transcriptional status (Zink et al., 2004). When silent, the genes co-localised with the integral membrane protein LAP2β and when active were found in a more internal position. In contrast to previous studies these genes were not co-localised with centromeric heterochromatin, suggesting different heterochromatin fractions may have different roles in gene silencing.

Also highlighting the role of the nuclear periphery in gene silencing is a study that followed the positioning of a Lac operator (LacO) tagged transgene during the targeting of the transcription factor VP16 to it. Upon transcriptional activation the tagged locus moved from the nuclear edge to the nuclear interior (Tumbar and Belmont 2001). A similar study by Dietzal and co-workers used the ß-globin LCR and promoter to drive a ß-galactosidase reporter gene (*LacZ*), tagged with 64 lac operator repeats. Again transcriptionally active transgenes had a more interior distribution within the cell nucleus than inactive arrays. However, LacO inserted into gene-rich chromosome regions are found in the interior of the nucleus despite changes in transcriptional status of the array (Janicki et al., 2004).

Chamberyon and Bickmore have also shown the movement of an endogenous gene further into the nuclear interior upon its activation (Chamberyon and Bickmore 2004).

1.3.3.3 The role of other nuclear compartments in gene expression

The silencing of genes in mammals has been linked with changes in nuclear position to regions enriched with heterochromatin and to the nuclear periphery. However, active genes can also associate with other distinct nuclear compartments.

Nuclear speckles (enriched with pre-mRNA splicing factors) preferentially localise with active genes in muscle fibres and fibroblasts (Smith et al., 1999, Xing et al., 1995). Large euchromatic regions cluster proximal to particular Sc-35 domains (a pre-mRNA splicing factor) (Shopland et al., 2003), and the histone and U2 small nuclear RNA genes have been shown to co-localise with Cajal bodies, nuclear compartments involved in snRNP biogenesis (Frey et al., 1999, Sheeman et al., 1999). A study by the Sheer lab has since looked at the localisation of genes with another prominent nuclear body, the promyelocytic leukaemia nuclear body (PML). PML bodies recruit a variety of other proteins and have been linked to DNA replication, repair, cell cycle control and apoptosis (Seeler and Dejean 1999, Ruggero et al., 2000) and have previously been shown to co-localise with the MHC complex in human primary fibroblasts (Shiels et al., 2001). Consistent with a role in gene transcription, Sheer and colleagues showed regions of the genome with increased transcription levels localised with PML bodies (Wang et al., 2004). However disrupting PML bodies by RNAi of the PML protein has no affect on the expression of these genes.

The results of all of these studies suggest the eukaryotic nucleus can be divided into heterochromatic regions able to repress transcription of genes, and compartments in which transcription is favoured. The positioning of a gene near heterochromatin is generally associated with silencing and silencing at heterochromatic compartments in the mammalian genome may be comparable to the silencing at telomeres found in yeast. However in mammals, in contrast to yeast, there is no direct evidence that gene location can control expression.

1.4: THE DYNAMIC CELL NUCLEUS

1.4.1 Protein mobility within the nucleus

Immunofluorescence analysis of nuclear proteins paints a rather static picture of the nucleus, however the nucleus is a dynamic organelle with many active processes occurring simultaneously. Information can be gathered on protein dynamics using a number of different techniques, the most common of which are Fluorescence recovery after photobleaching (FRAP) and Fluorescence loss in photobleaching (FLIP). Both these techniques follow the mobility of fluorescently tagged proteins in living cells and the most commonly used tag is the green fluorescent protein (GFP) from the jellyfish *Aequorea Victori* (Chalfie et al., 1994; Cubitt et al., 1995). In FRAP, a cell expressing the fluorescently tagged protein of interest is imaged at low laser intensity, before a small region of interest (ROI) is irreversibly photo bleached using high laser intensity. The whole cell is then imaged over the recovery period and the kinetics of fluorescence recovery calculated. Recovery of fluorescence is due to diffusion of the protein back into the ROI, and not the recovery of fluorescence by the same molecules that were bleached. Highly mobile proteins will rapidly recover to pre-bleach levels, whilst proteins in which a fraction is immobile will only recover to a proportion of the initial fluorescence. The rate of fluorescence recovery of a protein is frequently measured as the recovery halftime ($t_{1/2}$). This is the time it takes for the photobleached ROI to recover half of its final fluorescence (reviewed by Lippincott-Schwartz et al., 2003, figure 1.9.b).

FLIP also uses photobleaching techniques, but concentrates on the movement of proteins from one cell compartment to other. A small region of the cell is repeatedly bleached and the loss of fluorescence in adjacent and remote regions of the cell measured between bleaching rounds (figure 1.9.c).

Rather surprising FRAP studies have shown that the cell nucleus is anything but static (Dundr and Misteli 2001, Spector 2003, table 1.1). Both chromatin and chromatin-associated proteins have been tagged with GFP and their mobility analysed. H3 and H4 have relatively slow dynamics, that may be expected for proteins with a slow turnover, however histones H2A and H2B are more dynamic (Kimura and Cook 2001). In contrast to the core histones, linker histones are highly

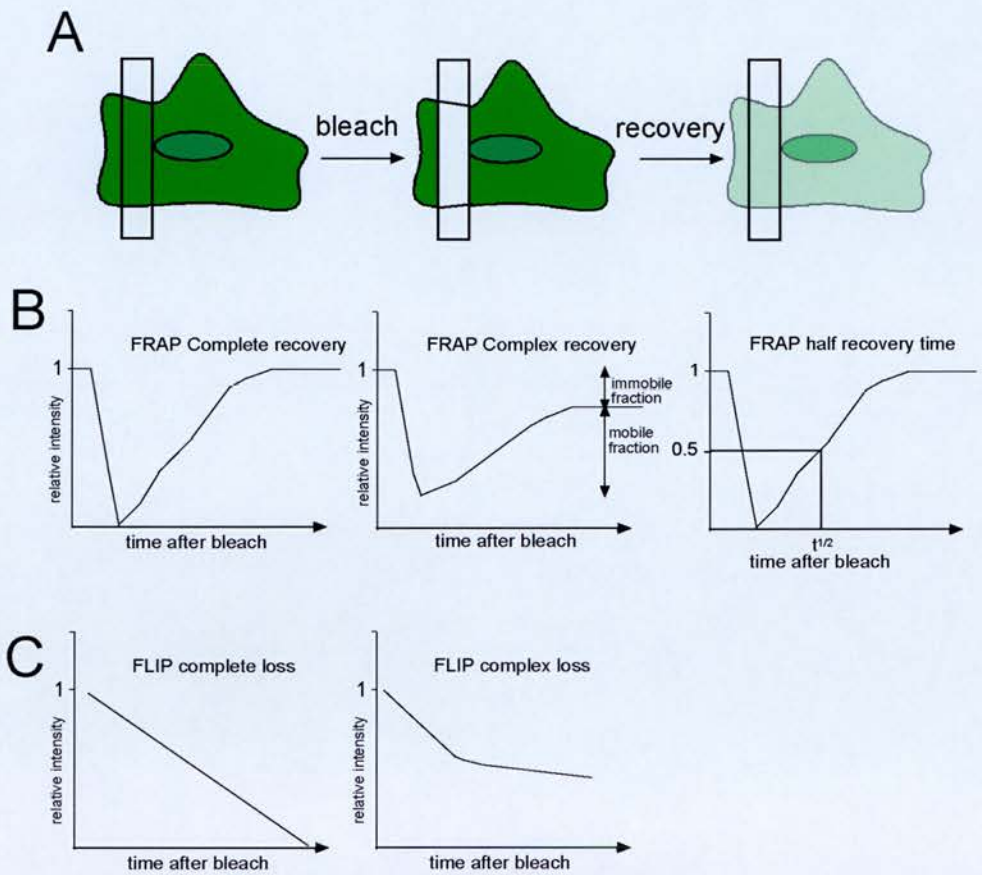

Figure 1.9: Principles of Fluorescence recovery after photobleaching.
A) A cell expressing fluorescent proteins is imaged at low laser power before and after irreversible photobleaching of the region of interest (ROI, rectangle in A). Over time the whole cell will slowly become photobleached.This is corrected for in the subsequent analysis (see text). In fluorescence recovery after photobleaching experiments (FRAP), the relative intensity of the ROI is measured over a period of time following a single bleach event (B). An unbound or highly mobile protein will rapidly recover 100% of the pre-bleach level of fluorescence (left). In the absence of full recovery following FRAP, the % of the protein population that is mobile and immobile can be calculated (middle). The time taken for half the fluorescence to recover within the ROI ($t_{1/2}$) is commonly used as a measure of mobility (right). In fluorescence loss after photobleaching experiments (FLIP) , an ROI is repeatly bleached and the relative intensity of the bleach region decreases over time. Measuring the fluorescent intensity of adjacent regions allows the diffusion constant of the fluorescent protein to be calculated (C). When a protein can freely diffuse between the bleached compartment and other cell compartments a straight line is recorded (left) and when a % of the protein is immobile or there is complex protein dynamics a hyperbola is recorded (right).

dynamic (Lever et al., 2000, Misteli et al., 2000) and the chromatin associated protein HP1 is even more dynamic than the linker histones (Cheutin et al., 2003, Fesenstein et al., 2003). Given the structural role of HP1 in heterochromatin, this result is rather surprising. However more recent studies of HP1 dynamics using a technique called fluorescence correlated spectroscopy (FCS) to calculate the diffusion co-efficient, combined with FRAP, have detected three different populations of HP1, including a fraction of very slow molecules in the constitutive heterochromatin of mammalian cells (Schmiedeberg et al., 2004). The differing dynamics of HP1 suggest that it may have different functions at different chromatin environments. FRAP studies have also shown splicing factors, and transcription factors are all highly dynamic (Verschure et al., 2003; Gorisch et al., 2003; Misteli 2001; Phair and Misteli, 2001). The results of these studies suggest that genes wherever they are positioned throughout the nucleus are able to interact with transcription factors.

In contrast to the nucleoplasmic proteins mentioned so far, lamin A and B1 show very slow recovery times in FRAP experiments and are largely immobile (Broers et al., 1999, Gilchrist et al., 2004, Moir et al., 2000). Small dextran molecules of <600kDa injected into the cell nucleus are also highly dynamic (Vershure et al., 2003, Gorisch et al., 2003), showing that protein complexes within the cell have the ability to diffuse freely throughout the nucleoplasm. The recovery half times of several different transcription factors, nuclear bodies and chromatin-associated proteins are summarised in table 1.1.

Protein	Recovery half time	Reference
Oestrogen receptor	<1 secs	Stenoien et al., 2001
GRIP-1 (transcription factor)	approxiamately 5 secs	Becker et al., 2002
SF2 (pre-mRNA splicing factor)	<3 secs	Phair and Misteli, 2000
Fibrillarin (rDNA processing enzyme)	<3 secs	Phair and Misteli, 2000
H2A	Two populations: 40%- 130 minutes 53%- 510 minutes	Kimura and Cook, 2001
H2B	As H2A	Kimura and Cook ,2001
H3	Two populations: 16%- >130 minutes 68%- immobile	Kimura and Cook, 2001
H4	As H3	Kimura and Cook, 2001
Linker histone H1	19 secs	Lever et al., 2000
Linker histone H1	H1.1gfp- 2-secs gfpH1.1-55secs	Henzdel et al., 2004
HP1	Three populations: 50-80%- 0.9secs 20-40%- 10 secs 5-7%- very slow	Schmieberg et al., 2004
HMG17 (chromatin binding)	<3 secs	Phair and Misteli 2000
RNA polymerase II	Two populations: 75%-< 15secs 25%- 20mins	Kimura et al., 2002
lamin A	> 140 mins	Gilchrist et al., 2004
lamin B1	> 180 mins	Moir et al., 2000
Lamin C	No detectable recovery	Broer s et al., 1999

Table 1.1: Summary of recovery half times for a range of fluorescently tagged nuclear proteins.

1.4.2 ATP dependent chromatin remodelling:

Not only are chromatin-associated proteins dynamic within the cell nucleus, but nucleosomes can also change position. ATP dependent chromatin remodelling complexes activate or repress transcription by altering the position or composition of nucleosomes on the chromatin fibre. Such complexes are well conserved throughout eukaryotes and many have essential roles. Currently, four different classes of remodelling complexes have been recognized: SWI/SNF (mating type switching/sucrose non-fermenting), ISWI (imitation switch), CHD and Ino80/Swr1. Each class is defined by a unique subunit composition and they all use the energy of ATP hydrolysis to alter chromatin structure during gene regulation.

The founding member of the SWI/SNF family is the Swi/Snf2 complex, originally identified in genetic screens in budding yeast (Vignali et al., 2000). This group of remodellers alter nucleosome position at gene promoters to either positively or negatively alter transcription (Narlikar et al., 2002). Chromatin opening of the promoter for the homothallic switching gene (HO) by SWI/SNF proceeds histone modification and is associated with the recruitment of SAGA (the Spt-Ada-Gcn5-acetyltransferase complex) (Krebs et al., 1999). The SWI2 protein is the ATPase subunit of SWI/SNF. Two proteins, BRM and Brg1, closely related to the yeast SWI2 have been identified in mammals (Khavari et al., 1993; Muchardt & Yaniv 1993) and are associated with multi-subunit complexes. SWI/SNF complexes have roles in tumourigenesis, differentiation and development and are thought to function at gene promoters by sliding histone octamers and/or distorting the path of DNA around the nucleosome without nucleosome removal.

The ISWI family is distinguished by the presence of a SANT-like domain at the C terminal (Grüne et al., 2003) and have functions in chromatin assembly and the formation of ordered nucleosome arrays. In mammals there are two forms of ISWI: SNF2H and SNF2L. SNF2H is found in NoRC, WICH and ACF/CHRAC complexes that have roles in chromatin assembly after replication and in silencing of rDNA (Strohner et al., 2004, Li et al., 2001, Collins et al., 2005, Poot et al., 2005). NoRC has been shown to mediate rDNA silencing by associating with the rDNA promoter and altering the position of the promoter-bound nucleosomes

(Strohner et al., 2004). Moreover NoRC can recruit HDAC1 and DNMTs to the ribosomal promoter (Zhou et al., 2002, Santoro et al., 2004) and can establish structural characteristics similar to heterochromatin.

The ACF/CHRAC complex is involved in chromatin assembly after replication (Poot et al., 2000). In humans, SNF2L has so far only been identified in the NURF complex (Barak et al., 2003).

The most prominent member of the CHD family of chromatin remodelling complexes is Mi-2. This family is characterised by the presence of a chromodomain able to bind RNA (Delmas et al., 1993, Kelley et al., 1999). Mi-2 is found in the NuRD complex, which has HDAC activity (Feng and Zhang, 2003), and associates with MBD2 and p66/68 to create the MeCP1 complex (Feng and Zhang, 2001). CHD complexes function by sliding nucleosomes along the chromatin fibre (Brehm et al., 2000).

The Ino80p and Swr1p chromatin remodellers have inserts within their ATPase domains, splitting the domain into two. The SWR complex is unique in that it can exchange H2A for H2A variants and Ino80 exchanges H2A on the inactive X chromosome (Mizuguchi et al., 2004, Li et al., 2005). It is likely that these complexes are responsible for the enhanced mobility of H2A when compared to H3 and H4 as measured by FRAP (Kimura and Cook 2001, table 1.1) Although no equivalent complexes have yet been found in mammals, orthologs to SWR1 exist and it is likely such complexes will be found.

1.4.3 Chromatin movement in living cells

Early studies of chromatin movement in live cells used dihydroethidium to label DNA in Swiss 3T3 and Hela cells and then photobleached areas of heterochromatin and euchromatin spanning over 0.4μm. These studies concluded that chromatin was relatively immobile over the time period of an hour (Abney et al., 1997) and that chromatin movement was constrained by physical attachments to nuclear structures, such as the lamina, nucleolus or the nuclear matrix.

Both Zink et al., 1998 and Bornfleth et al.,1999 then went on to use the incorporation of fluorescently labeled nucleotides into newly replicating DNA to

label individual chromosomes for analysis. Cells injected with fluorescently labeled nucleotides were allowed to undergo several rounds of cell division before image capture, so that there were only a few labeled chromosomal domains per cell. The motion of tagged loci was then followed over time. In some cells, tagged chromatids could move distances of up to several microns during a time period of several hours, whilst in other cells the tagged chromatin maintained a more stable position (Zink et al., 1998). As an extension of this, Bornfleth et al., proposed that human chromatin displayed three different levels of motion: a confined Brownian diffusion component, a small scale movement due to refolding events within sub-chromosomal regions, and a rarer large scale movement of whole or sub regions of chromosome territories.

Two further studies have used histone H2B tagged with GFP to follow chromatin motion during mitosis to determine if its position is maintained from one cell cycle to the next in mammalian cells (Gerlich et al., 2003;Walter et al., 2003). Prior to mitosis both groups bleached areas of chromatin and the bleach pattern was followed through to the daughter nuclei. In the first study by Walter and colleagues, substantial re-organisation of chromosomes was noted as cells progressed from G2 into metaphase. From these observations, Walter et al., concluded that the positioning of chromosome segments in daughter nuclei differ significantly from the positions in the mother cell nuclei, therefore "significant changes of chromosome territory order occur during mitosis". This was confirmed by FISH to analysis CT position in 4 and 8 cell HeLa cell clones and while radial position was seen to be re-established in daughter and grand-daughter cells, CT position next to neighbouring CTs was not. In contrast, Gerlich et al, conclude that the organisation of chromatin in daughter nuclei has a "strong similarity" to that in the mother cell nucleus, and thus "chromosome positions are heritable through the cell cycle", despite their conclusions mixing of bleached and unbleached regions can be seen in their data. Walter and colleagues also reported enhanced chromatin movement of up to several microns in early G1.

All of these studies have measured the movement of relatively large chromosomal domains and it was not until the development of the Lac Operator/Lac Repressor (LacO/LacI) system by Straight and colleagues that chromatin in live cells was studied at high resolution for the first time. This system has greatly increased our

understanding of chromatin dynamics (Robinett et al., 1996, Belmont and Straight 1998) and uses the integration of bacterial *E.Coli* Lac or Tet Operator sequences into sites of interest in the genome. GFP is then fused to the appropriate repressor protein to allow the visualization of specific loci in living cells (figure 1.10). LacO/LacI were initially used for this system as LacI binds to LacO with a K_d of 10^{-13} . This value is six orders of magnitude lower than values obtained for non-specific binding (Miller 1980). LacI also has a high affinity for LacO sequences located within nucleosomes (Chao et al., 1980). LacI was adapted to contain a nuclear localisation signal (NLS), and its C terminus mutated to prevent tetramerisation, which might have allowed binding to two different operator sequences simultaneously (Belmont and Straight 1998). When this modified GFP-LacI is expressed in a cell containing a LacO array, a bright spot corresponding to the integration site can be seen and followed in response to cellular events and environmental stimuli (figure 1.10) Originally the system was used to observe a 90Mb array in Chinese hamster ovary cells, but has since been used to visualize LacO arrays containing only 256 copies of the 36bp LacO sequence (Robinett et al., 1996). Although developed in yeast and mammal cells, use of this system to visualize chromatin has been extended to *Caenorhabditis elegans, Drosophila*, bacteria, viruses and human cells (Li et al., 1998; Marshall et al., 1997; Kato and Lam, 2001; Serrichio and Sternberg, 1998; Vazquez et al., 2001, Belmont, 2001; Chubb et al., 2002). One possible disadvantage of the technique is that large integrations of repetitive sequences may result in the disruption of the higher organization of chromatin and the mislocalisation of chromatin regions. However Chubb et al., used a FISH based approach to show that nuclear position of several loci was not disrupted by the insertion of ~50kb long LacO arrays in human cells (Chubb et al., 2002).

Chromatin movement using this system is typically measured as the mean squared displacement (MSD) of two loci from each other, plotted over a range of time (Δt). From graphs plotting MSD against Δt, the change in time different regimes of motion can be deduced: simple Brownian motion or diffusion gives a straight line; an initial straight line that plateaus represents constrained diffusion usually due to interactions with mobile or immobile barriers; and an upwards curve

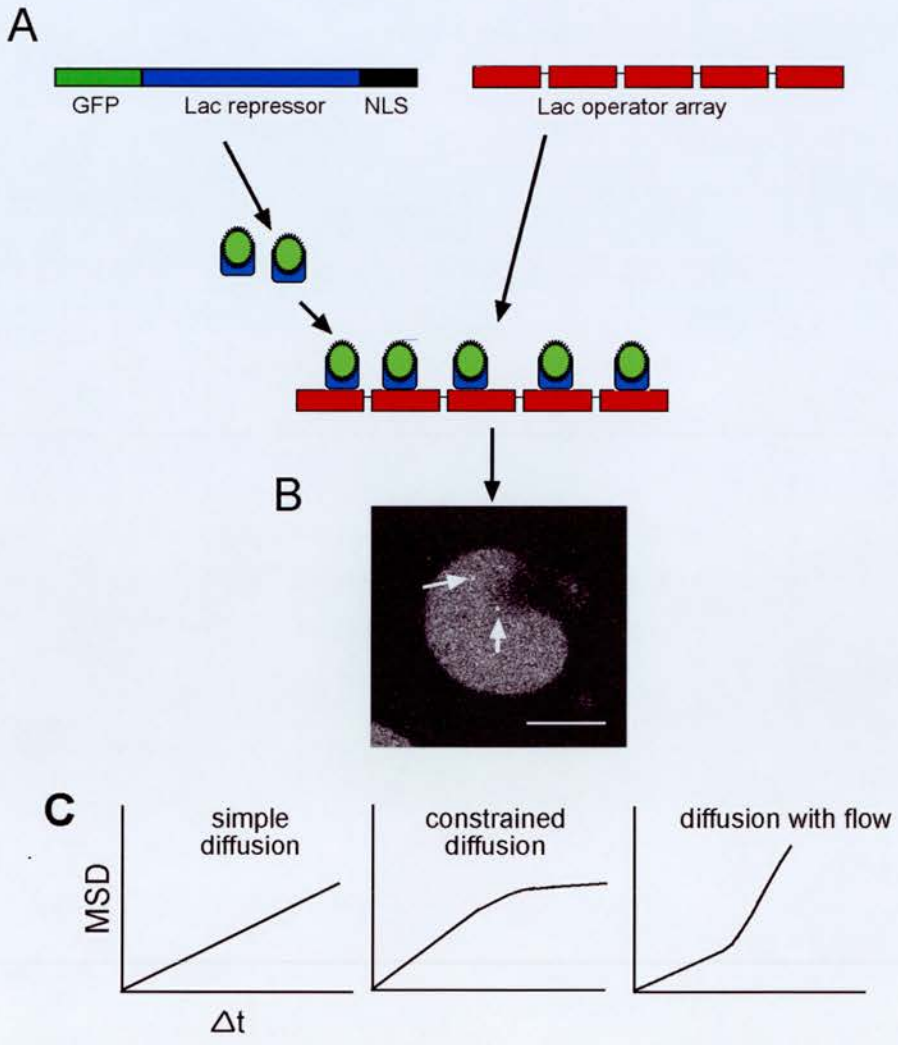

Figure 1.10: Principles of the LacI-LacO system used to tag loci in living cells. A) A fusion protein of GFP-LacI-NLS is used to tag Lac operator arrays inserted into the genome. B) An image taken of a live cell. The arrows point to GFP tagged Lac operator arrays. The scale bar represents 10μm. C)The mean squared displacement of tagged loci plotted against the change in time can reveal three types of movement: simple diffusion,constrained diffusion or diffusion with flow.

shows diffusion with flow or some other exogenous force (figure 1.10 Platani et al., 2002).

Using the GFP-LacI to tag LacO loci, both long and short-range chromatin movements with respect to either the nuclear periphery or the calculated center of the nuclear plane over time have been reported in yeast (Heun et al., 2001). Many large movements of over >0.5μm in under 10 seconds were observed in G1, with smaller salutatory movements of up 0.2μm occurring throughout interphase. GFP-LacI tagged telomeres have also been shown to be highly dynamic in yeast when compared to the movement of integral nuclear envelope components such as the spindle body (Hediger et al., 2002). However in comparison to loci that are distal from the telomere, telomeres move within a relatively small domain of the nuclear volume (Heun et al., 2001). The use of ATPase inhibitors reduces chromatin movement in G1, suggesting that chromatin motion in yeast is energy dependent. From this, the authors proposed that chromatin remodeling events mediated these movements. Furthermore mobility was reduced in S phase and was dependent on active replication origins.

In contrast to yeast, chromatin motion in both *Drosophila* and human cells shows constrained diffusion, thought to be due to Brownian motion (Zink et al., 1998, Bornfleth et al., 1999, Chubb et al., 2002). Like yeast, chromatin in developing *Drosophila* spermocytes has multiple regimes of movement (Vazquez et al., 2001). Short-range movements averaging 0.3μm in 1.2 seconds and long-range movements of up to 4-5 μm/hr have been recorded. The long-range component of chromatin motion was cell cycle regulated and decreased as cells approached meiotic prophase.

The motion of several different GFP tagged LacO loci in human fibrosacroma cells over the time period of a few minutes shows an average chromatin movement in the range of 0.5μm for nucleoplasmic loci (Chubb et al., 2002). In agreement with Abney et al, this paper provides strong experimental evidence that physical attachments of chromatin to nuclear structures exist, as loci found near the nucleolus and nuclear periphery show reduced chromatin movement.

1.5 THESIS RESEARCH

The overall objective of my Ph.D project is to investigate some of the issues raised by studies looking at nuclear positioning and its role in gene regulation. To do this my Ph.D was divided into four interrelated projects that each analyse aspects of chromatin dynamics and chromatin movement.

The first of these was to analysis the motion of human chromatin in more detail. If changes in chromatin position, are a mechanism by which the nucleus controls gene expression, then chromatin must be able to move distances that are compatible with this. Previously chromatin motion in human cells had only been investigated over the time period of a few minutes (section 1.4.3). In addition, to answer questions regarding how nuclear architecture is established, understanding when in the cell cycle chromatin position is determined may provide insights to this. By looking at the positioning of LacO tagged loci in live cells before and after mitosis this question was addressed (Chapter 3).

Not only is chromatin mobile, but many chromatin-associated proteins are highly dynamic. The second part of my Ph.D aimed to address how chromatin modifications may affect the mobility of chromatin components. In order to address this I decided to analysis the mobility of linker histones by photobleaching in mouse ES cell lines. Each cell line contained a different null mutation of a gene involved in maintaining or establishing an epigenetic modification (Chapter 4).

My final two projects both address the functional significance of CT position in the nucleus. CT position is conserved from chicken to humans spanning over 300 M yrs of evolution, yet we still do not understand the functional significance of this. Furthermore the radial position of the whole mouse genome has never been published. The mouse karyotype is very different to that of humans; therefore, any differences in its nuclear position may provide insights in to the mechanisms governing CT position. To test if this hypothesis is true and to determine if CT position can change during differentiation, I have mapped the radial position of the each mouse chromosome in undifferentiated mouse ES cells and the radial position of a subset of the mouse karyotype in differentiated ES cells. Lastly, rather than analysing chromatin motion and changes in chromosome position I tried to

experimentally manipulate the nuclear position of genes in mouse ES cells (Chapter 6). Although many studies have implicated the nuclear periphery in gene repression (section 1.3.3.2), no direct experimental evidence of this exists in mammals. Therefore I wanted to prove directly what role nuclear position has in the regulation of gene expression in mammals by "forcing " a gene to locate to the nuclear periphery. By artificially tethering a gene to the nuclear periphery in mouse ES cells, its expression when tethered and when not tethered can be compared (Chapter 6).

CHAPTER 2

MATERIALS AND METHODS

All reagents used were obtained from Sigma or Roche unless otherwise stated.

2.1 MOLECULAR BIOLOGY

2.1.1 Bacterial strains

Competent commercially produced DH5-α (sub cloning or library efficient, Invitrogen™) *E.Coli* were used for all cloning procedures involving stable inserts. For cloning procedures involving unstable inserts or repeats, the recombination deficient MAX Efficiency ® Stbl2™ Cells (Invitrogen™) were used.

2.1.2 Bacterial Glycerol stocks

Aliquots of bacterial cultures were pelleted at 600g for 2 minutes, and resuspended in 10% glycerol v/v Luria-Bertani (L-Broth) before storage at -80^0 C.

2.1.3 Generating Competent bacteria

1ml of an overnight Stbl2™ culture was added to 100ml of L-Broth and grown in a shaking incubator at 30^{0}C until the absorbance at 600nm (A_{600}) was between 0.5-0.6. Cells were then pelleted at 600g, resuspended in 25ml 0.1M $CaCl_2$ and incubated on ice for 25mins. After repelleting at 4^{0}C, cells were resuspended in 10ml of freezing mix (15% glycerol, 50mM $CaCl_2$ in dH_2o). Aliquots of 200 µl were then snap frozen using dry ice and stored at -80^0 C until required.

2.1.4 Bacterial transformation

Competent cells were incubated on ice with plasmid or ligation DNA for at least 15 minutes. Transformations were then heat shocked at 42^0C for 25 seconds, followed by incubation on ice for a further 2 minutes before the addition of 1ml of SOC (2% tryptone, 0.5% yeast extract, 10 mM NaCl, 2.5 mM KCl, 10 mM $MgCl_2$, 10 mM $MgSO_4$, 20 mM glucose, Invitrogen™) or LB medium. Cells were then incubated in a shaking incubator for 45 minutes at 37^0C (DH5-α) or 90 minutes 30^0C (Stbl2™) before plating out on L-agar plates containing the appropriate antibiotic for selection (Ampicillin or Kanamycin both at 50μg/ml). Plates were then incubated overnight at 37^0C (DH5-α) or 30^0C (Stbl2™).

2.1.5 Isolation of plasmid DNA

2.1.51 Isolation of plasmid DNA from small bacterial cultures

Single bacteria colonies were picked and grown overnight in 5ml of LB medium containing the appropriate antibiotic and at the appropriate temperature. Plasmid preparations were then harvested using commercial mini-prep kits (Qiagen). In brief, bacteria are lysed under alkaline conditions, the lysate neutralised and passed over a silica-gel membrane that selectively absorbs the DNA. The membrane is then washed and DNA eluted by the addition of dH_2O.

2.1.5.2 Alkaline lysis of plasmid DNA from large bacterial cultures

To prepare clean, supercoiled plasmid DNA, for transfections of mammalian cells, plasmid DNA was prepared by alkaline lysis of bacteria and isolation of the DNA on CsCl gradients (Sambrook et al.,2001).

Bacteria cultures were grown from a single colony in 250 ml of LB medium with the appropriate antibiotic and temperature overnight. Cells were then pelleted at 12,000 g, for 20 minutes using a GSA rotor Sorvall RC5, the spent LB medium removed and cells resuspended in 20ml of suspension buffer (50mM glucose, 25mM Tris HCL pH

8.0, 10mM EDTA, RNase A) before lysis under alkaline conditions (0.2M NaOH, and 1% SDS [sodium dodecyl sulfate] [w/v]). Chromosomal DNA was precipitated by the addition of 3M-potassium acetate and 2M acetic acid, pH5.2 and the whole mixture then placed at 4° C for 30 minutes, centrifuged at 4,600g for 15 minutes and filtered through muslin. 0.6 volumes isopropanol was added to the filtered solution and the mixture left for a hour at room temperature. The DNA was precipitated at 20,000g for 30 minutes, the supernatant removed, the pellet washed in 70% ethanol, and air dried for a few minutes to remove residual isopropanol.

The DNA pellet was resuspended in 2.5 ml of TE (Tris-EDTA) buffer, and 1g caesium chloride (CsCl) was added for every ml of solution alongside 0.37 ml of Ethidium Bromide (10mg/ml) (EtBr, 2,7-diamino-10-ethyl-9-phenyl-phenathridium bromide). This was centrifuged at 2.5g for a few minutes to remove any precipitated RNA and protein to create a cleaner gradient. The final solution was added to 3ml Beckmann tubes, sealed, and spun in a Beckman Ti100.3 rotor at 80g overnight at room temperature on acceleration programme 2, deceleration 9 (temperatures below 16-°C result in CsCl precipitation). Supercoiled DNA was removed from the gradient by puncturing the side of the tube with a 21 gauge needle and drawing out the appropriate DNA band (Sambrook et al.,2001). EtBr was removed from the DNA by repetitive extractions with equal volumes of water-saturated butan-1-ol. DNA was precipitated with 2 volumes EtOH and 1/10th volume 5M Sodium Acetate (NaAc) pH5.2 as described 2.1.6.2.

2.1.6. Purification of DNA

2.1.6.1 Phenol/Chloroform extraction

An equal volume of buffered phenol/chloroform (50% buffered phenol pH >7.8/48% chloroform v/v, 0.5% isoamylalcohol) was added to the DNA sample, vortexed, and centrifuged at 12,000 g for 10 minutes. After centrifugation the top aqueous layer was removed, avoiding the white precipitate present at the boundary between the two layers, and added to a fresh tube. An equal volume of buffered phenol was then added, and the vortexing and centrifugation repeated. Again the top

layer was decanted. To concentrate DNA further, ethanol precipitation was performed as described below.

2.1.6.2 Ethanol precipitation

2 volumes ethanol and 1/10th volume 5M Sodium Acetate at pH4.6 were added to the DNA sample. After incubation on ice for 15 minutes, and centrifugation at 12,000 g for 30 minutes, the supernatant was discarded and the pellet washed in 70% ethanol (v/v with dH_2O). Centrifugation was repeated and the supernatant removed. The pellet was then dried at room temperature and resuspended in the appropriate volume of dH_2O.

2.1.6.3 Extraction of genomic DNA from cell lines

Confluent 75cm^2 tissue culture flasks were split and cells washed and subsequently pelleted in 500 µl of PBS (section 2.2). To this 500 µl of lysis buffer (100mM Tris pH 7.5, 100mM NaCl, 10mM EDTA and 1% lauryl sarcosine [v/v dH_2O]) with proteinase K(100µg/ml) was added gently and the suspension incubated overnight at 55°C, before phenol/chloroform extraction and ethanol precipitation of the DNA (2.1.6.1 and 2.1.6.2).

2.1.7 DNA digestion and preparation

All DNA digests were performed in the reaction buffer supplied and in accordance with the manufactors instructions (New England Biolabs) with enzyme concentrations never exceeding 10% of the final digestion mixture to prevent enzyme inhibition by glycerol. Double digests were carried out when enzyme reaction conditions were compatible. When incompatible, they were performed sequentially after a phenol/chloroform extraction and ethanol precipitation. Digestion products were analysed and/or purified by gel electrophoresis or cleaned by ethanol precipitation and used for further cloning steps.

2.1.7.1 Filling in 3' recessed ends of DNA

To create blunt ends or partial fill ins, for subsequent ligations (section 2.1.7.5), the DNA polymerase activity of Klenow fragment was utilised to fill in 3' recessed ends of DNA template with 100 μM of the relevant dNTPs (deoxynucleotide triphosphates) (Abgene) in accordance with the manufactors instructions. Each reaction was incubated for 15 minutes at room temperature.

2.1.7.2 Gel electrophoresis

1-2% horizontal agarose ("Hi-Pure" Low Eeo agarose, BioGene UK) gels in 1 x TAE (90 mM Tris-HCl [pH 8], 90 mM glacial acetic acid, 2 mM EDTA [pH 8]) were used with 1 x TAE electrophoresis buffer to resolve DNA samples, PCR products and plasmid digestion products. Loading buffer (15% Ficoll™ 400 [Amersham Biosciences], 0.25% Orange G [Sigma] both w/v in dH_2O) was added to all samples before gel electrophoresis at a ratio of 1 part buffer to 6 parts sample. Commercial DNA size markers (λ DNA Hind III digest, [Invitrogen™] were diluted to 50ng/μl and 500 ng loaded per well to allow size determination and quantification of DNA fragments.

2.1.7.3 Gel purification of DNA fragments

To purify DNA fragments from agarose, the appropriate fragment was dissected out of gels after EtBr staining using a clean razor blade. The DNA was then extracted using a commercial kit (Qiagen). In brief, gel samples were melted in an equilibration buffer, and the solution passed over a silica-gel membrane to selectively bind the DNA. Washing then removes residual EtBr and agarose before DNA is eluted to the required volume in dH_2O.

2.1.7.4 Measuring quality and quantity of DNA

DNA concentration was measured by resolving DNA alongside samples of known concentration by gel electrophoresis and/or spectrophotometrically. To measure DNA concentrations spectrophotometrically, DNA was diluted 1:100 in TE (10mM Tris-HCl, 1mM EDTA, pH 7) and placed in a quartz curvette. The absorbance or optical density (OD) at 260nm (A_{260}) was measured using an Ultrospec 3000pro, (Amersham Pharmacia Biotech). An OD of 1 equals ≈50μg/ml of DNA. To determine the purity, the A280 was also measured. Pure DNA has a A_{260}/ A_{280} ratio of 1.8. Values lower than this indicate contamination by proteins, RNA or phenol.

2.1.7.5 Ligation of DNA fragments

200ng of DNA were used in each ligation, this usually consisted of a 1:3 vector to insert molar ratio, with cohesive complementary ends of both DNA fragments. 400U(1μl) of T4 DNA ligase enzyme (New England BioLabs) and the appropriate volume of 1x ligation buffer was used per ligation reaction, typically in a volume of 10μl. Reactions were then incubated overnight at 16°C and subsequently half of the reaction used for bacterial transformation (see 2.1.4).

2.1.7.6 Reverse transcription polymerase chain reaction(RT-PCR)

RNA was prepared as described in section 2.1.8. 20μl of this was then treated with DNase I and RNase inhibitor for 1 hour at 37°C, phenol/chloroform extracted and ethanol precipitated as described (section 2.1.5.1 and 2.1.5.2). Reverse transcription to create first strand cDNA was then performed using random hexamers. 2μg of RNA was annealed to 50μM of random hexamers by incubation at 70°C for 10 minutes and transfered to ice. To then create the first strand cDNA, the annealed RNA was incubated with 10 mM DTT (dithiothreitol), 10 mM dNTPs and 200 U of Superscript II reverse transcriptase (Invitrogen™) at 42°C for 1 hr in a total volume of 80 μl. PCR was then performed with 2.5 mM $MgCl_2$, using the first strand cDNA as a template, 1μl of a 25mM stock of each primer and 1U of Taq polymerase.

Primers and PCR programmes used are shown in table 2.1. PCR products were resolved by gel electrophoresis as described in section 2.1.7.2.

Table 2.1 Primers used in RT-PCR

Gene	Primers	Programme
Oct 4	5'-GGCGTTCTCTTTGGAAAGGTGTTC-3' 5'-CTCGAACCACATCCTTCTCT-3'	95°C x 5 minutes, followed by 30 cycles of: 94°C x 30 secs, 55°C x 30 secs, 72°C for 30 secs and a final 10 minute elongation step at 72°C.
Gene trap-sfb1 junction	5'-CGCCCACTTTCTGATGAAGA-3' 5'-GGCGATTAAGTTGGGTAACG-3'	95°C x 5 min, 25-30 cycles of: 94 °C for 30 secs: 60 °C for 30 secs, 72 °C for 30 secs) 72 °C x 10 mins, and a final 10 minute elongation step at 72°C.
GAPDH	5'-CCTTCCACAATGCCAAAGTT-3' 5'-CTCAAGATTGTCAGCAATGCA-3'	95°C x 5 min, 25-30 cycles of: 94 °C for 30 secs: 60 °C for 30 secs, 72 °C for 30 secs) 72 °C x 10 mins, and a final 10 minute elongation step at 72°C.

2.1.7.7 Sequencing of DNA fragments

All cloning and RACE products were sequenced to monitor the integrity of recombinant plasmids and inserts, or to determine the identity of recombinant genes. BigDye Terminator v3.0 (ABI prism) chemistry was used in a protocol similar to Sanger di-deoxy sequencing. In brief, 200ng of plasmid DNA was added to 0.8μM sequencing primer and 4μl of BigDye. This was then diluted to 10μl in accordance with the manufactors instructions. Reactions were run on a DNA Engine Tetrad (MJ Research) for 25 cycles of 96 °C for 30 seconds, 50 °C for 15 seconds, and 60 °C for 4 minutes. To clean reactions 5μl of 125mM EDTA and 2 volumes ethanol were

added and the mixture incubated on ice for 15 minutes before centrifugation at 12,000 g for 30 minutes. The supernatant was subsequently removed, the remaining pellet washed in 70% ethanol (v/v dH_2O) and centrifuged at 12,000g for 15 minutes. Finally the supernatant was removed again and the pellet left to dry at room temperature. Resuspended pellets were run through 50cm capillaries on POP6 polymer gels (3100 Genetic Analyser, Applied Biosystems) and data collection performed using the v3.7 supplied version of software.

2.1.8 Analysis of genomic DNA by Southern blotting and hybridisation

2.1.8.1 Southern Blotting

100μg of genomic DNA were digested with EcoRI in 100μl reactions as per the manufactors instructions for a minimum of two hours at 37°C. DNA was then phenol/chloroform extracted, ethanol precipitated, and resuspended in 50μl of dH_2O. This was quantified spectrophotometrically and 25μg of DNA, re-digested to completion with 10 fold excess EcoRI for 4 hours. DNA was once more phenol/chloroform extracted, and ethanol precipitated before resuspending in a small volume of dH_2O for electrophoresis. 10μg of each digested DNA was then resolved by electrophoresis in 0.8% agarose gels containing EtBr (section 2.2.7). Prior to transfer, gels were washed in 0.1 M HCl for 10 minutes, rinsed in dH_2O and washed 0.4 M NaOH for 20 minutes. Capillary blotting onto Hybond-N^+ membrane (Amersham Biosciences) was performed using 0.4 M NaOH, as the transfer solution (Reed and Mann, 1985). After transfer, the membrane was briefly neutralised at room temperature in 0.5 M Tris-HCl [pH 7.4], and rinsed in 2x SSC (made from a 20 x stock [3 M NaCl, 0.3 M tri-sodium citrate, pH7.4]) for 5 min at RT. To detect the DNA of interest, membranes were firstly prehybridised in 20 ml of hybridisation solution (50% Church phosphate stock [89g Na_2 HPO4.$2H_2O$ dissolved in 1 litre of dH_2O,thus containing 1M of Na^+ ions] 7% 20x SDS, and 0.4 mM EDTA) in cylindrical glass bottles (Amersham Biosciences) at 65 °C with continuous rotation. Membranes were prehybridised for 30 minutes before addition of freshly boiled probe DNA (section 2.1.8.2) to the prehybridisation solution. After an overnight

hybridisation with the probe, membranes were washed three times in Church wash (4% church phosphate, 1% SDS (w/v) in dH_2O) at 65°C for 20 min each time. Membranes were exposed to a storage phosphor screen (BSA cassette, Fuji Film) for 1-3 days and visualised using Fuji Film FLA-5100 v. 2 phosphor imager hardware and Aida Image Analyser v. 3.52 software (both Raytek Scientific Ltd).

2.1.8.2 Probe preparation and radio-labelling of probes

DNA fragments were prepared by restriction enzyme digestion from plasmids. 25 ng of purified DNA was then made up to 11 µl with dH_2O and denatured by boiling for at least 10 min and immediately placing on ice. Denatured DNA was labelled using random priming with High Prime (Roche) and [α-^{32}P]dCTP. Briefly, 4 µl of High Prime reagent was added to the probe along with 5 µl (50 µCi) [α-^{32}P]dCTP and mixed to a total volume of 20 µl. The reaction mix was incubated at 37°C for 1 hour, after which it was placed on a G-50 Sephadex Quick Spin column (Roche) and eluted with 80µl TE (pH 8) to separate the labelled DNA fragments from unincorporated nucleotides (as in section 2.4.4.2). Labelled probe was then denatured once more by boiling for 10 min, and added to prehybridised membranes in hybridisation solution.

2.1.9 Preparation and manipulation of RNA

2.1.9.1 RNA isolation and purification

To isolate and purify total RNA from cells, Bio/RNA-Xcell™ (Bio/Gene) with a single step method was used. In brief, cells were homogenised in the Bio/RNA-Xcell™ solution by passage through a 21 gauge needle followed by passage through a 23 gauge needle. Samples were then left at 4°C for 5 minutes to allow complete dissociation of nucleoprotein complexes. Chloroform was then added and the homogenate centrifuged at 12,000 g to create two phases. The RNA is in the upper aqueous phase. This was removed and mixed vigorously with propan-2-ol and an RNA binding resin provided. The RNA bound resin was pelleted by micro-

centrifugation and washed twice in 75% ethanol before elution into the appropriate volume of dH_20. One last centrifugation was then performed to allow RNA in solution to be eluted from resin. RNA was quantified by measuring the A_{260} and concentration calculated as described in Sambrook et al., 2001.

2.1.9.2 5' Rapid amplification of cDNA ends (5' RACE)

5' RACE products were generated as previously described (Tate et al., 1998, Sutherland et al., 2001) using primers purchased from MWG Biotech and Invitrogen™. RNA was reverse transcribed into first strand cDNA by annealing 10 ng of P456 primer (specific for *LacZ*) to 5 μg total RNA at 70°C. To create the first strand cDNA, the annealed RNA was then incubated with 10mM DTT (dithiothreitol), 10 mM dNTPs and 200 U of Superscript II reverse transcriptase (Invitrogen™) at 37°C for 1 hr in a total volume of 20 μl. RNA was removed from the first strand of cDNA, by hydrolysis at 65°C for 20 min by the addition of freshly prepared NaOH to a concentration of 0.1 M. This was then neutralised by the addition of 0.1 M HCl, and followed by microdialysis of the DNA for 4 hrs at 4°C on 0.025 μm nitrocellulose discs against TE (pH 8). This removes excess dNTPs and exchange buffer from the first strand cDNA. After dialysis the sample volume was made up to 20 μl with ddH_2O and a poly A tail added to first strand cDNA by incubation at 37°C for 10 min with 2 mM dATP and 30U of recombinant terminal deoxynucleotidyl transferase (TdT) (Invitrogen™). TdT is able to catalyse the template-independent addition of dNTPs to the 3' hydroxyl terminus of single stranded (ss) DNA. Newly tailed DNA was used as a template to synthesise the second strand cDNA using primer 56. Two consecutive rounds of PCR (30 cycles consisting each of 94°C 90 seconds, 60°C 90 seconds, 72°C 3 minutes) with nested *LacZ* primers amplified the specific 5' DNA sequences of genes (59, 80, and 79). This was followed by microdialysis on 0.1 μm nitrocellulose disks to size select larger PCR products. These RACE products were directly sequenced with a 40 *LacZ* sequencing primer (section 2.1.6.7).

Table 2.2 Primers used for 5' RACE

Primer no.	*Sequence*
P456	5'-CCGTGCATCTGCCAGTTTGAGGGGA
56	5'-GGTTGTGAGCTCTTCTAGATGGT$_{17}$
80	5'-AGTATCGGCCTCAGGAAGATCG
59	5'-GGTTGTGAGCTCTTCTAGATGG
79	5'-ATTCAGGCTGCGCAACTGTTGG
-40 *LacZ* sequencing primer	5'-GTTTTCCCAGTCACGAC

2.1.10 Cellular protein preparation and analysis

2.1.10.1 Total protein extraction from mammalian cells

Total protein extracts were made from confluent 25 cm^2 tissue culture flasks. Cells were washed once in PBS, and lysed in 300µl PBS and 300µl of 2x SDS loading buffer (125 mM Tris [pH 6.5], 4% SDS [w/v], 10% 2-β-mercaptoethanol [β-ME] [v/v], 20% glycerol [v/v], 0.1% bromophenol blue [w/v]). Protein samples were then boiled for 10 min and sonicated on ice at 5A for 10 sec before being stored at -20°C until required.

2.1.10.2 Total nuclear protein extracts from mammalian cells

For each nuclear extract, two confluent 75 cm^2 tissue culture flasks were trypsinized and harvested by centrifugation at 1000 g for 3 min. Cells were then washed in PBS and resuspended in 5 ml of ice cold NBA (Nuclei Extraction Buffer A, 5.5% sucrose [w/v in dH_2O], 10 mM Tris-HCl [pH 8], 85 mM KCl, 0.5 mM spermidine, 250 µM PMSF [phenyl methyl sulfonyl fluoride], 0.2 mM EDTA). To this, 5 ml of ice cold NBB (Nuclei Extraction Buffer B, NBA and 0.1% NP-40 [v/v]) was added and the solution incubated on ice for 3 min. The resulting nuclei were then centrifuged at 500 *g* for 3 min at 4°C, washed in 5 ml of NBA and recentrifuged before finally resuspending in 200 µl NBA.

To measure the concentration of suspended nuclei, the nuclei were incubated with 0.1 U/μl of DNase I for 5 minutes at room temperature and the A_{260} reading taken. Since the concentration of DNA equals the concentration of the nuclei, the OD reading can be used to create a nuclear protein extract of known concentration. An equal volume of 2x SDS protein loading buffer was added to the sample and boiled and sonicated as 2.1.10.1

2.1.10.3 Extraction of cytoplasmic, insoluble nuclear and soluble nuclear protein fractions

Two confluent 75 cm^2 tissue culture flasks were trypsinized and harvested at 1000g for 3 minutes for each set of protein extracts to be made. After washing cells once in PBS and pelleting at 1000g for 3 minutes, the volume of cell pellet was estimated. This was then washed in 5 packed cell volumes (pcv) of hypotonic (10mM HEPES [pH7.9]; 1.5 mM $MgCl_2$,;10mM KCl;0.2 mM PMSF; 0.5mM DTT; 1x protease inhibitor cocktail, Invitrogen™) buffer, after which the pellet was resuspended, this time in 3 pcv of hypotonic buffer. After 10 strokes of a glass Dounce homogenizer, the mixture was transferred to a 1.5 ml eppendorf tube and the nuclei repelleted at 3300g for 15 minutes. The supernatant was removed and saved as the cytoplasmic protein fraction.

To create different nuclear protein fractions, nuclei were resupended in 1 packed nuclear volume (pnv) of low salt buffer (20mM HEPES [pH7.9]; 25% glycerol; 1.5 mM $MgCl_2$, 0.02 M KCl; 0.2mM EDTA; PMSF; 0.5mM DTT; 1 x protease inhibitor cocktail) buffer, to which 1 pnv of high salt buffer was added (low salt buffer with 0.4M KCl) drop by drop. Soluble nuclear proteins were then extracted by constant mixing at 4 °C for 30 minutes, after which the protein sample was centrifuged at 25,000g for 2 minutes. The supernatant was removed and stored as the soluble protein fraction, whilst the pellet was resuspended in PBS as the insoluble fraction. Equal volumes of 2x SDS loading buffer were added to all three samples and the samples boiled and subsequently sonciated as in 2.1.10.1.

2.1.10.4 Resolution of proteins on SDS PAGE denaturing gels

Cell protein extracts were resolved by sodium dodecylsuplphide polyacrylamide gel electrophoresis (SDS-PAGE). Denaturing polyacrylamide minigels (10-12% acrylamide [v/v], 0.39 M Tris-HCl [pH 8.8], 0.1% SDS [w/v], 0.1% ammonium persulfate [w/v], 0.04% TEMED [N, N, N', N-tetramethylethylene diamine] [v/v] in dH_2O) with stacking gels (5% acrylamide [v/v], 0.13 M Tris-HCl [pH 6.8], 0.1% SDS [w/v], 0.1% ammonium persulfate [w/v], 1% TEMED [v/v] in dH_2O) using 30% or 40% acrylamide (29:1 and 37:1 acrylamide:bis-acrylamide [v/v] respectively) (Severn Biotech) were run in presence of Tris-glycine running buffer (25 mM Tris base, 250 mM glycine, [pH 8.3], 0.1% SDS [w/v]) in electrophoresis tanks (Mighty Small, Hoefer) at 110 V for 2 hr. Pre-stained protein standards (Bio-Rad) were loaded alongside samples to aid with analysis.

2.1.10.5 Visualisation of resolved cellular proteins

Before visualisation of resolved proteins on SDS-PAGE gels, stacking gels were removed and the denaturating gel washed twice in ddH_2O. Gels were then submerged in Coomassie stain (0.25% Coomassie brilliant blue R-250 [w/v], 45% methanol [v/v], 10% glacial acetic acid [v/v] in dH_2O) for 1 hour at room temperature with gentle agitation. Stain was then discarded and gels incubated overnight in destain (30% methanol, 10% glacial acetic acid in dH_20), again with gentle agitation. Stained gels were used to quantify protein samples and ensure the equal loading of samples on gels to be western blotted.

2.1.10.6 Western blotting

After SDS-PAGE (section 2.1.10.4), the stacking gel was removed and protein samples transferred to polyvinylidene difluoride (PVDF) membrane (Hybond-P, Amersham Biosciences) for further analysis by semi-dry western blotting, PVDF membrane was soaked in methanol, followed by ddH_2O and equilibrisation in semi-dry transfer buffer (24mM Tris, 192mM Glycine, 20% methanol v/v). The gel and

membrane were then sandwiched between 3MM paper (Whatmann) equilibrated with semi-dry transfer buffer and transferred as per the manufactors instructions (WEB company, Washington).The apparatus was run at 200mA per gel, and at 25V for a minimum of 45 minutes. To determine the success of transfer, gels were stained with Coomassie stain as section 2.1.9.5 and/or the membrane stained with Ponceau S stain for 2 minutes. Proteins could then be seen on Ponceau S stained membranes after rinsing twice with ddH_2O.

Membranes were blocked to reduce background before the addition of the primary antibody using 1x TS (150 mM NaCl, 10mM Tris-HCl pH7.5) containing 5% milk proteins (Marvel) and gentle agitation for 1 hour at room temperature. Primary antibodies were then diluted to the appropriate concentration in 5% Milk protein, 1x TS and incubated with membranes at 4°C overnight with constant agitation.

Membranes were washed 3 times in TST (1x TS, 0.05% Tween-20 v/v) before incubation with secondary antibodies for at least 1 hour at room temperature, again with constant agitation. Finally washes in TST were repeated and membranes detected using enhanced chemiluminscent (SuperSignal® West Pico Chemiluminescent, Pierce). Signals were exposed on Hyperfilm Ecl (Amersham Biosciences)

All antibodies used are listed in table 2.3 and 2.4

Table 2.3 Primary antibody dilutions for Western blots

antibody	*Species*	*Source*	*Dilution factor*
Emerin	Rabbit polyclonal	Santa Cruz Sc-15378	1 in 400
Lamina associated polypeptide 2	Mouse monoclonal	Abcam Ab 11823	1 in 1000
Living colours GFP	Rabbit polyclonal	Clontech 632376	1 in 400
AcH4K5	Rabbit	Upstate 30417	1 in 5000
GAPDH	Rabbit polyclonal	Abcam Ab94585	1 in 1000

Table 2.4 Secondary antibodies for Western blots

antibody	*species*	*source*	*Dilution factor*
Anti-mouse IgG (Fab) Horseradish peroxidase conjugate (HRP)	Goat	Sigma, A9917	1:5000
Anti-rabbit IgG (whole molecule) HRP	Goat	Sigma, A0545	1: 5000

2.2 MAMMALIAN CELL CULTURE

2.2.1 Cell counting

A haematocytometer was used to count cells (Weber Scientific International Limited). This has a chamber 0.1 mm in height with an etched grid of $1mm^2$, subdivided into 400 squares. Therefore the total volume defined by the grid is $1x10^{-4}$ ml and cell concentrations per ml are obtained by multiplying the total number of cells in the grid by 10^4.

2.2.2 Thawing cells from storage in liquid nitrogen

Aliquots of cell suspensions in 10%DMSO with foetal calf serum (FCS) were stored in liquid nitrogen. After thawing at 37°C, cells were diluted in 10mls of fresh culture medium and pelleted by centrifugation at 400g for 4 minutes to remove DMSO. Cells were then resuspended in fresh medium and seeded into the appropriate $25cm^2$ culture flasks.

2.2.3 Culture of mammalian cell lines

All cells were cultured at 37 °C with 5% CO_2 and tissue culture medium containing penicillin (10000 units/ml) and streptomycin (650μg/ml). For immunofluorescence and 3D FISH, cells were counted and seeded directly onto Superfrost® plus microscope slides (BDH laboratory supplies). Prior to cell seeding, slides were soaked for at least 1 hour in ethanol with a few drops of HCl and flamed inside a laminar flow sterile fume hood (Heraeus). Quadriperm slide chambers (Greiner bio-one) were used to culture cells on slides overnight. For the growth of ES cells slides were coated in 0.1% gelatin (v/v PBS).

2.2.3.1 Culture of transformed human cell lines

HT1080 (male fibrosacroma-derived) (Chen et al., 1983) and 293T (human embryonic kidney transformed with SV40) (Pear et al., 1993) cells were cultured in high glucose Dulbecco's Modified Eagle Medium (DMEM)(Invitrogen™), supplemented with 10% FCS. Cells were grown to near confluency before passaging into new culture flasks. To split cells, spent tissue culture medium was removed, and cells washed once in PBS before the addition of a small volume of 10% trypsin-EDTA and incubation at 37°C for 5 minutes. Cells were dislodged by simple agitation, medium added, and cells pelleted at 400g for 4 minutes before replating or fixation.

2.2.3.2 Culture of mouse embryonic stem cells

ES cells were grown in Glasgow Modified Eagle Medium (GMEM, Invitrogen™) with supplements as follows: 10% FCS (v/v), 100 U/ml LIF (Leukaemia inhibitory factor, pers.com F.Kilanowskia), 50 μM β-mercaptoethanol, 100 mM sodium pyruvate, 1% NEAA (non-essential amino acids) (v/v), L-Glutamine 2mM, and as described (Smith et al., 1988). Cells were grown to near confluence before splitting into fresh tissue culture flasks coated in 0.1% gelatin. To split cells, medium was poured off, cells rinsed with PBS and covered with a thin layer of 10% trypsin-EDTA before incubation at 37°C for 5 min to allow cells to dislodge. Fresh medium was then added, and the cells pelleted at 1000 *g* for 5 min before being replated or harvested for experiments. ES cells used in this study are as described in table 2.5.

2.2.3.3 *In vitro* differentiation of ES cells

HT2 ES cells contain a fusion of hygromycin-thymidine kinase under the promoter of *Oct4*, an important marker for stem cells. To select for undifferentiated cells, ES cells were grown in the presence of hygromycin (100μl/ml) for seven days. To differentiate HT2 cells, the differentiation protocol described by Billon et al., 2002, and subsequently adapted by Chambeyron and Bickmore, 2004 was used. To begin

LIF was removed from the tissue culture medium for one day before the addition of retinoic acid. Cells were then grown in the presence of 5x 10^{-6} M retinoic acid (all-*trans*-retinoic acid, stock solution 3.3x 10^{-3} M in DMSO, stored in the dark at -20°C), for two days, after which retinoic acid was removed from the culture and ganciclovir (2.5 μM) added for a further 4 days to kill off any undifferentiated cells. After 7 days of growth in LIF free media, *Oct4* expression was no longer detectable by RT-PCR.

2.2.4 Determination of drug concentrations suitable for selection

To determine drug concentrations that would be suitable to select for drug resistance cells within a population, kill curves were carried out before the transfection of cells with the appropriate drug selection cassette. To do this cells were plated out in 6 well plates (Greiner bio-lab) at a concentration of approximately 1 x10^5 cells per well. A wide range of different drug concentrations, spanning across the recommended concentration were then applied to each well. Fresh media with the appropriate drug concentration was applied to each well every 48 hours. Cells were monitored over a suitable time period to determine the lowest concentration of drug required to kill all the cells in one well. This concentration was then used in subsequent transfections to select for cells expressing the transfected DNA construct.

Table 2.5: Mouse Embryonic stem cell lines used in this study

Name	*Description*	*Source*
E14	Wt mouse ES cell, (129/Ola). In house.	Gift, A. Smith (Hooper et al., 1987)
Suv39h wt (WT41)	E14 wt ES cells *Suv (3-9)* targeted knockout	Gift, T. Jenuwein (Peters et al., 2001)
MeCP2$^{-/y}$	*Mecp2* targeted knockout ES cells	Gift, A Bird (Guy et al., 2001)
Dnmt3ab wt	J1 wt ES cells (129S4/SvJae)	Gift, E. Li (Chen et al., 2003)
Dnmt3ab$^{-/-}$ (KOV-1)	Targeted disruption of *Dnmt3a* and *3b* in mouse J1 ES cells	"
Dnmt3b^{res}	*Dnmt3ab*$^{-/-}$ ES cells with a transgene of *Dnmt3b*	Gift, B.Ramashoye (Jackson et al.,2004)
HT2 wt	*Oct4-HygTK* into CGR8	Gift, A. Smith (CGR8-Mountford et al., 1994)

2.2.5 Transfection of mammalian cells

2.2.5.1 Transfection of mammalian cell lines using Lipofectamine 2000.

Cells for transfection were seeded at a concentration of 2.4 x 10^5 cells into each well of a 6 well plate the day before transfection (the surface area of each well =10cm^2). For cells seeded directly onto slides this concentration was doubled, as were subsequent concentrations of Opti-MEM (Invitrogen™), Lipofectamine 2000 (Invitrogen™), DNA and media. For each transfection, 3 μg of DNA and 5μl of Lipofectamine 2000 was used per well. For every well to be transfected 200 μl of

Opti-MEM was mixed with 5µl of lipofectamine and a further 200µl of Opti-MEM mixed with the appropriate volume of DNA. After 5 minutes incubation at room temperature both the Lipofectamine 2000 mixture and the DNA mixture were added to each other, mixed well and left to incubate for a further 20-60 minutes. During this incubation time, cells were washed once in PBS and 1.6 ml of fresh antibiotic free medium added to each well awaiting transfection. The lipofectamine /DNA mixture was then applied to cells and cells left to culture overnight before fixation for immunofluorescence, harvesting for protein extracts or seeding at various densities onto 9 cm and /or 14 cm plates to select for stable cell lines expressing recombinant proteins.

2.2.5.2 Transfection of mouse embryonic stem cells using electroporation

For each electroporation to be carried out, 6 confluent $75cm^2$ tissue culture flasks were harvested and the cells resuspended in PBS to a final concentration of 1.4×10^8 cells/ ml. 700µl of cells were then placed in a 0.4mm disposable electroporation cuvette (Geneflow) together with 100µl of DNA (concentration 1.5 µg/µl). Electroporation using a BioRad Genepulser was then performed at 800V, 3µF (low capacitance). The time constant for these conditions should be between 0.04-0.1 milliseconds. Cells were allowed to recover for 20 minutes at room temperature before plating out at various concentrations.

2.2.5.3 Selection for stable cell lines

Selection at the appropriate drug concentration was applied to the cells 24 hours after transfection, and the medium changed every two days until visible colonies could be seen, usually 8-14 days after the initial addition of selection to the culture. At this stage, plates were washed twice in PBS, and a thin layer of PBS left on the cells. Individual colonies were taken up using a filtered pipette tip, placed in a very small volume of trypsin-EDTA in one well of a 96 well plate (Greiner bio-one) and gently broken up by pipetting up and down before transfer to a single well of a 24 well plate

(Greiner bio-one). Colonies were grow in selection medium until splitting into larger plates.

2.2.6 Cultures for live cell analysis

For live cell analysis, cells were seeded at 1-2 x 10^5 in 2ml of the appropriate medium in Delta 0.17mm live cell chambers (Biotech's Inc, Pennysylvania), with heat conductive glass bases, the day before analysis. For ES cells, live cell chambers were coated with 0.1% gelatin before cells were seeded. 25mM of HEPES (pH7) was added to the medium in each chamber to help regulate pH during analysis. For observation of transient transfections, cells were seeded into chambers and left for 6-8 hours to ensure cells had plated down before carrying out transfection by Lipofectamine 2000 for analysis the next day. For each dish to be transfected, 3μl of Lipofectamine 2000, 2 μg DNA and 150 μl of Opti-MEM was used, and transfections performed as described previously (section 2.2.5.1).

2.3 IMMUNOHISTOCHEMISTRY

2.3.1 Immunofluorescence

Mammalian cells were grown on slides as described (section 2.2.3) and all subsequent steps performed at RT and with PBS containing 1.5 mM $MgCl_2$ and 1 mM $CaCl_2$. Slides were rinsed in PBS and fixed in 4% paraformaldehyde (pFa) w/v/PBS for 10 minutes. Following fixation slides were washed three time in PBS, quenched with 50mM NH_4Cl in PBS for 10 minutes and permeabilised in 0.5% Triton-X100 (v/v) in PBS for 12 minutes. Slides were washed for a further three times before blocking, in 5% serum/PBS (v/v) for a minimum of 20 minutes using serum from the same species that the secondary antibody was derived from. Primary antibodies were then diluted in the blocking solution to the appropriate concentration and incubated with slides overnight at room temperature in a humidified chamber. After primary antibody incubation, slides were washed a further three times in PBS,

blocked once more and secondary antibodies applied for 45 minutes. All coverslips used for antibody incubations and blocking were derived from parafil
m (Pechiney plastic packing). Finally slides were washed three more times in PBS and mounted in 4,6-diamidino-2-phenylindole (DAPI) in Vectashield (Vector). For human cells the DAPI concentration used was 1μg/ml and for mouse 0.5μg/ml.

Table 2.6 Primary antibodies used for Immunofluorescence

Antibody	*Species*	*Source*	*Dilution Factor*
β–galactosidase	Rabbit monoclonal	Europa Bioproducts CR7001RP2	1:3000
LacI	Mouse monoclonal	Upstate 05-503	1:200
Myc-tag	Rabbit polyclonal	Upstate 06-549	1:200
Lamin A	Goat polyclonal	Santa Cruz Biotechnology Sc-6214	1:200
Lamin B	Goat polyclonal	Santa Cruz Biotechnology Sc-6216	1:200
Lamin C	Goat polyclonal	Santa Cruz Biotechnology Sc-6218	1:200
Emerin	Goat polyclonal	Santa Cruz Biotechnology Sc-8084	1:200
AcH4K5	Rabbit	Sigma, A0545	1:200
Ki67	Mouse monoclonal	Sigma, p6834	1:100

Table 2.7 Secondary antibodies used for Immunofluorescence

Antibody	*Species*	*Source*	*Dilution Factor*
Anti-rabbit FITC conjugate (IgG, heavy & light chain specific [H&L])	Donkey	Jackson Labs, 711-095-152	1:200
Anti-rabbit TR conjugate (IgG, H&L)	Donkey	Vector Labs	1:200
Anti-mouse FITC conjugate (IgG, H&L)	Donkey	Vector Labs	1:200
Anti-mouse TR conjugate (IgG, H&L)	Donkey	Jackson Labs, 715-075-150	1:200
Anti-Goat TR conjugate (Fab2, H&L)	Donkey	Sigma TR7367	1:200

2.3.2 X-Gal staining

X-Gal (5-bromo-4-chloro-3-indolyl-b-D-galactoside) staining solution was prepared by fully dissolving 250 mg X-Gal in 5 ml dimethylformamide (DMF) before the addition 5 mM potassium ferricyanide [$K_3Fe(CN)_6$], 5 mM potassium ferrocyanide [$K_4Fe(CN)_6$], 0.25 mg/ml spermidine, and 2 mM $MgCl_2$. This was then made up to 500 ml in wash solution (0.05% BSA [w/v], 2 mM $MgCl_2$, 0.02% NP-40 (v/v), 0.1% sodium desoxycholate [w/v] in 0.1 M phosphate buffer [21:6 1M NaH_2PO_4 and 1 M Na_2HPO_4 (pH 7.3)]) and filtered before use. After fixation of cells using 0.5% glutaraldehyde made up in 0.1M phosphate buffer, 2mM MgCl2, and 5mM EGTA, cells were washed in 0.1M phosphate buffer, 2mM $MgCl_2$, 0.05% BSA and stained o/n in X-Gal staining solution (maximum 15 hr) at 37°C whilst protected from the light. Staining solution was removed the following morning and the samples stored in fix until required. Stained cells were visualised with microscopy (section 2.5.2).

2.4 FLUORESCENCE *IN SITU* HYBRIDISATION (FISH)

2.4.1 Preparation of mouse chromosomes for 2D Fluorescent *in situ* hybridsation (FISH)

To increase the number of mitotic cells within a cell population, and therefore the amount of chromosome spreads KaryoMAX® colcemid® (0.1μg/ml) was added to tissue culture medium and incubated for 30 minutes. Colcemid inhibits cell division by depolymerising microtubules. Cells were then harvested, washed once in PBS (phosphate-buffered saline), and fixed in 3:1 methanol:acetic acid (MAA) for 2D FISH as described in section 2.4.1.2.

2.4.2 Harvesting and fixing cells in 3:1 methanol: acetic acid (MAA)

Cells for two-dimensional (2D) FISH were harvested, washed once in PBS and resuspended in 10ml hypotonic solution (0.033 M KCl v/v dH_2O). This was added drop-wise with constant agitation (the concentration of cells in hypotonic should be $<2x\ 10^7$/ml). The cells were then left to swell for 10 min at RT before centrifugation at 400 *g* for 5 min. The hypotonic solution is then aspirated off the nuclei pellet and cells were fixed in fresh 3:1 methanol: glacial acetic acid. To do this, the first 2ml of fix are added drop wise with constant agitation, followed by the addition of a further 8ml of fix. Cell preparations are then stored at -20°C indefinitely. Before slides were prepared from new cell preparations, cells were fixed a minimum of three times.

2.4.3 Preparation of three dimensionally fixed nuclei

Cells were plated on slides the day before paraformaldehyde (pFa) fixation as described in section 2.2.3. To prepare slides for 3D FISH and ImmunoFISH, slides were first washed three times in PBS, before transfer to CSK buffer (100mM NaCl, 300mM sucrose, 3mM $MgCl_2$,10 mM PIPES pH6.8, 0.5% Triton x100) on ice for 5 minutes to permeabilise the cells. Slides were then washed a further 3 times in PBS

and fixed in 4% pFa v/v/PBS for 10 minutes at room temperature, followed by three addition washes in PBS and transfer to 20% glycerol in PBS (v/v) for at least 30 minutes at room temperature or overnight at 4°C.

To permeabilise cells further, slides were put through several cycles of freeze/thaw using liquid nitrogen. Slides were immersed in liquid nitrogen until all fizzing and cracking has stopped, allowed to thaw completely, and then incubated in 20% glycerol/PBS for one minute before repeating the cycle. The number of cycles of freeze/thaw is dependent on the cell line. For ES cells, 7 cycles were used and for HT1080 cell lines, 5. If more than 5 cycles are required a 30 minute incubation in 20%glycerol:PBS at room temperature, is included in the middle. At the end of the final freezing slides are not allowed to defrost and are placed in the -80 freezer until required for *in situ* hybridisation.

2.4.4 Preparation of fluorescence *in situ* hybridisation (FISH) probes.

2.4.4.1 Nick translation

The analogues biotin-16-dUTP and digoxigenin-11-dUTP were used to label all DNA probes used. These analogues were incorporated into DNA by nick translation. Following incorporation, unbound nucleotides were removed and the efficiency of labelling measured.

1-1.5µl of supercoiled DNA was added to 4µl of nick translation salts (0.5M Tris-HCl pH7.5, 0.1M $MgSO_4$, 1mM DTT, 500µg/ml Bovine serum albumin [BSA]), alongside 4µl each of 2mM dATP, dCTP and dGTP, 2µl of 0.5mM dTTP and 4µl of either biotin-16-dUTP or digoxigenin-11-dUTP. Freshly diluted DNase I was then added to the translation to create a final concentration of 1 unit/ml, alongside1 µl of T4 DNA polymerase (Invitrogen™ , 10 units per µl). The total reaction volume was made up to 40 µl by the addition of dH_2O, mixed thoroughly and left to proceed at 16°C for 90 minutes. To subsequently stop the reaction after the incubation period was over, the reaction was placed at -20 °C or immediately processed for removal of unincorporated label.

2.4.4.2 Removal of unincorporated label

Quick spin columns (Roche) containing G50 Sephadex beads were used, as per the manufactors instructions to remove unincorporated nucleotides by size exclusion. Labelled probes were then eluted in TE pH7.5.

2.4.4.3 Quantification of label incorporation

To begin, gridded nitrocellulose membranes were soaked briefly in dH_2O, followed by immersion in 20x SSC for 10 minutes and allowed to air dry. 1µl of labelled DNA diluted to 1 $x10^{-4}$ and 1x 10^{-3} in TE was spotted twice on to membranes, and allowed to dry. After drying a further 1µl spot was added to one of each dilution. Onto the same membrane 20,10,2, and 1 pg of labelled lambda DNA standards were also spotted (Roche). Once all DNA spots had air dried, the DNA was crosslinked onto the membrane by exposure to 30mJ of UV irradiation.

The membrane was immersed in buffer 1 (0.1M Tris-HCl pH7.5, 0.15M NaCl) for 5 minutes at room temperature with constant agitation, before blocking in 3% BSA in buffer 1 for 60 minutes at 60 °C. The membrane was then incubated at room temperature, with constant agitation and the appropriate antibody (10 µl of either streptavidin-alkaline phophatase, and/or anti-digoxigenin-alkaline phosphatase [Boehringer] depending on the probes being quantified) for 30 minutes. 2 washes of 15 minutes in buffer 1 were then carried out, before equilibration for 5 minutes in 0.1 M Tris-HCl pH 9.5. To develop the colour reaction the membrane was incubated in a sealed polythene bag, with 5ml of 0.1M Tris-HCl pH9.5 containing two drops from each of the bottles 1-3 from the alkaline phosphatase substrate kit IV (Vector labs). The substrates in this colour reaction are 5-bromo-4-chloro-3-idolyl phosphate and nitroblue tetrazolium, which produce a blue reaction product. A complete colour reaction could be observed within a few hours and an estimate of the concentration of labelled DNA obtained from comparison with the lambda standards.

2.4.5 Fluorescence *in situ* hybridisation (FISH) on MAA-fixed nuclei

2.4.5.1 Slide preparation of MAA-fixed nuclei

Glass slides were stored in a dilute solution of HCl in ethanol for at least one hour prior to use. Slides were then dried and polished with muslin before use. MAA fixed cells (section 2.4.2) were removed from storage at -20°C and centrifuged at 1000 *g* for 5 min. Fresh MAA fix was then added until the cell suspension reached a 'milky' appearance. One drop of this suspension was then dropped onto a horizontal microscope slide from a height of 30 cm using a fine tipped pastette (to obtain good chromosomal spreads slides were preferably dropped when air humidity was ~50% and slides coated with a thin layer of moisture, usually achieved by breathing on the slides immediately before and after dropping). The quality of the spread was monitored by phase contrast microscopy. Slides were preferably stored for 2-6 days prior to hybridisation, however if slides were to be used the following day, they were artificially aged by baking at 60°C for 1 hour prior to FISH.

2.4.5.2 Hybridisation on MAA-fixed nuclei

Slides were treated with 100 μg/ml RNaseA in 2x SSC for 1 hr at 37°C, washed briefly in 2x SSC and dehydrated through an ethanol series (2 min each in 70%, 90% and 100% ethanol). Slides were then allowed to air dry before heating in a 70°C oven for 5 min and denaturation in 70% formamide (v/v) in 2x SSC (pH 7.5) at 70°C for 90 seconds. Following denaturation slides were immediately plunged in 70% ethanol at 4°C for 2 min before further dehydration through 90% and 100% ethanol.

Labelled probes (section 2.4.4) were prepared by precipitating ~75 ng probe with 5 μg salmon sperm DNA and mouse Cot 1 DNA (Invitrogen™, 2.5-10 μg depending on repeat content of probe) per slide. After the addition of 2x volume ethanol, probes were spun down under a vacuum before resuspension in 10 μl hybridisation mix per slide (50% deionised formamide [v/v], 10% dextran sulphate [v/v], 1% Tween 20 [v/v], in 2x SSC). All chromosome paints used were commercial

and therefore supplied in their own hybridisation buffer in a ready to use format (13µl paint per slide) (Cambio). All probes were denatured at 70°C for 5 min and reannealed at 37°C for 15 min before being spotted onto coverslips and picked up by slides. Slides were sealed with rubber solution (TipTop) before incubation o/n in a covered tray in a 37°C water bath.

2.4.5.3 Washing and detection of 2D and 3D FISH signals

After o/n hybridisation of slides, rubber solution was removed from the coverslips and slides washed in 2x SSC at 45°C for 4x 3 min. The coverslips were allowed to fall off slides naturally in the first few FISH washes. Slides were washed a further 4x 3 min in 0.1x SSC at 60°C before transfer to 0.1% Tween 20 [v/v] in 4x SSC. Detection was carried out in a moist chamber pre-heated to 37°C. Biotin was detected with sequential layers of fluorochrome-conjugated avidin (FITC- or TR-avidin), biotinylated anti-avidin, and a further layer of fluorochrome-conjugated avidin. Digoxigenin was detected with sequential layers of Rhodamine (R)-conjugated anti-digoxigenin and TR-conjugated anti-sheep IgG. Detection reagents were diluted in SSCM (4x SSC, 5% Marvel milk powder [w/v]) to the appropriate concentration (Table 2.10), mixed thoroughly and centrifuged at 1200g for 15 minutes to precipitate any clumps of antibody. After blocking with 40 µl of SSCM for 5 min at RT, 40 µl of the appropriate detection layer was applied to each slide. Slides were incubated with each antibody layer for 60 min in a moist chamber at 37°C. In between antibody layers and following the last antibody incubation slides were washed for 3x 2 min with 0.1% Tween 20 [v/v] in 4x SSC at 37°C. All slides were mounted in the appropriate DAPI concentration in Vectashield. Coverslips were sealed with rubber solution (PANG) and slides were stored in the dark at 4°C until imaged.

Table 2.8 Antibodies and fluorochrome-conjugates used for FISH

Antibody or fluorochrome-conjugate (cell sorting grade)	*Species in which the antibody/ conjugate was raised*	*Source*	*Stock concentration (mg/ml)*	*Dilution*
FITC-avidin	Goat	Vector	2.0	1:500
TR-avidin	Goat	Vector	2.0	1:500
Biotinylated anti-avidin	Goat	Vector	0.5	1:100
R-anti-digoxigenin	Sheep	Roche	0.2	1:20
TR-anti-sheep (IgG, H&L)	Rabbit	Vector	0.5	1:100

2.4.6 FISH on three dimensionally preserved nuclei

This method was used to maintain the three dimensional architecture of nuclei throughout the process of FISH (Kurz et al., 1996; Croft et al., 1999).

Slides were prepared as described previously described in section 2.4.3. To begin, slides were thawed from -80° C to RT and placed in PBS for at least 2x30 minutes. Slides were then incubated in 100μg/ml RNaseA in 2 x SSC for 60 minutes at 37° C, returned briefly to PBS and incubated in 0.1M HCl in dH_2O for 7 minutes, before returning once more to PBS. Slides were denatured in 70% deionised formamide, 2 x SSC (pH 7.0) for three minutes followed by 50% formamide, 2 x SSC(pH 7.0) for 1 minute, both at 75-78 ° C. Probes were applied immediately after denaturation. These were prepared, detected and hybridised as described in 2.4.5.2.

2.4.6.2 ImmunoFISH on 3-D preserved nuclei

Slides for immunoFISH were made as described in section 2.4.3. and the hybridisation of FISH probes performed as described in section 2.4.6 minus the HCl incubation step as this can destroy the antigen to be studied. After overnight hybridisation of FISH probes slides were washed and probes detected as described for 2D FISH, however to decrease background slides were first washed for 4 x 3 minutes in 50% formamide, 2 x SSC (pH7.0), and washes continued as in section 2.4.3.3. After detection of the FISH probe, slides were washed in PBS for 3 x 1 min and incubated with primary antibody o/n at RT after a 20 min blocking step as described in 2.3.1. The next day, slides were rinsed in PBS, blocked and incubated with secondary antibody, before mounting and storing as previously described (section 2.3.1).

2.5 FLUORESCENCE AND BRIGHTFIELD IMAGING AND PROCESSING

2.5.1 Brightfield analysis of cells or tissue sections

Xgal stained cells were analysed with brightfield (using differential interface contrast [DIC] optics) and images taken with a Photometrics CoolSnap HQ monochrome CCD camera (Roper Scientific, Arizona). IPLAB Spectrum (Scanalytics Inc., VA) wrote the image capture scripts that were used to control camera capture.

2.5.2 Capture of 2D fluorescence images

After FISH or immunofluorescence experiments, images were captured using either a Zeiss Axioplan II or Zeiss Axioplan fluorescence microscope, both using 100 watt mercury bulbs and equipped with a triple band-pass filter (Chroma # 83000). Grey scale images for each fluorochrome were collected with a cooled CCD camera depending on the model of microscope (Pentamax with a Kodak KAF 1400 sensor or

Micromax with Kodak KAF 1400e sensor respectively, Princeton Instruments) using IPLAB software v. 3.6 (Scanlytics, USA).

Slides were scanned in a methodical manner beginning at the bottom left hand corner, scanning to the right, and then moving upwards and scanning the next row of nuclei from right to left etc. For chromosome and probe position analysis, fifty bin 2 images (using x63 oil immersion objective, Zeiss) were collected of consecutive nuclei that fulfilled the inclusion criteria, mainly intact nuclei containing visible signals. For chromosome position analysis images of nuclei containing two clear distinct territories only were captured and for the purpose of running scripts only single nuclei not touching any other were imaged.

2.5.3 Capture and analysis of 3D images

2.5.3.1 Fluorescence imaging and processing

3-D stacks of colour images were captured using an Axioplan microscope fitted with a 100 watt mercury bulb, Ludl filter wheel, Chroma filter set #81000 and motorised stage attached to a cooled CCD Kodak KAF 1401e sensor camera (Princeton Instruments). A script was devised (P.Perry) using IPLAB v3.6 software (Scanlytics) to capture bin1 or bin2 resolution level images. To capture a 3D stack, the Dapi excitation filter is selected and a "live" focus window displayed. The plane of best focus is interactively selected, as is a region of interest to capture. The number of optical slices to be collected, the z distance between each optical slice and the exposure times for each flurochrome signal are also determined. The optimal exposure time is determined by capturing a 2D test image. The microscope focus motor then moves the stage downward for half the total depth of the focus series to the starting point for capture. To compensate for backlash in the focus mechanism , the stage is moved a further 200 microns downwards, followed by a movement of upwards of the same distance. Image capture begins, collecting the specified images at each focal plane and placing each into a stacked file. The stage is then moved upwards by the specified z distance before repeating the same capture sequence. After capture of the final image, the stage returns to its original "best focus" plane.

Stack files are then merged to provide a colour stack file that can be animated or projected. For each nucleus 30-35 bin 1/bin 2 image planes were captured at 0.5μm intervals, so as to include the whole nucleus in the image stack.

2.6 LIVE CELL CONFOCAL IMAGING

Cells growing on DeltaT 0.17mm culture dishes (Biotech's Inc) were mounted on a heated stage (Biotech's Inc) on a Zeiss LSM510 confocal microscope. An objective warmer system (Biotech's Inc) was then used to help maintain a stable temperature in the tissue culture medium. To capture movies, the time series software option was used specifying the appropriate time delay between rounds of 3D stack capture. To ensure cells were healthy, the number of mitotic cells was constantly monitored throughout image capture. A large number of these cells should be visible. An additional indicator of cell health was the retention of polarized cell morphology, and images were only collected for as long as the cells retained this.

2.6.1. Fluorescence recovery after photobleaching

In fluorescence recovery after photobleaching experiments (FRAP), a region of GFP-recombinant protein was selected, bleached once and the cell imaged over a recovery period. To bleach a selected region of interest (ROI) 15 iterations using 100% of total laser output (~6.1mA) was used. Immediately following the bleach, 2D images were captured every 7 seconds until 60 images were taken, using 8% laser power. By this stage fluorescence had fully recovered in all of my experiments.

2.6.1.2 Calculating relative fluorescence intensity for data analysis

During the course of image capture in FRAP experiments, cells would rotate, change shape and move. To correct for this IPLAB (v3.6) scripts were devised and used to ensure the ROI in each z stack captured did not change its position during the course of analysis (described further in box 4.1 and figure 4.2). The sum of pixel counts within a selected ROI was calculated using the selected option in IPLAB v3.6

software. It is accepted that repeated fluorescence imaging of samples will result in a small but significant loss of fluorescence over time within a selected ROI. To correct for this, the data was normalised to the intensity of the whole cell over time using the normalisation equation summarised as follows:

$$I_{REL} = \frac{T_O I_T}{T_T I_O}$$

Where T_o is the total cellular intensity of whole cell at the time zero (pre-bleach), T_t is the total cellular intensity of this same cell at the time point T, I_o is the intensity of the ROI at time zero and I_t is the intensity of the ROI at time point T (Phair and Misteli 2000).

2.7 COMPUTATIONAL METHODS

The Bioinformatics programmes and resources referred to in this thesis are listed below, together with the relevant World Wide Web (www) link.

Ensembl	http://www.ensembl.org/
ExPASy-Tools	http://ca.expasy.org/tools/
InterProScan	http://www.ebi.ac.uk/InterProScan/
NCBI (BLASTN/P, TBLASTN)	http://www.ncbi.nih.gov/BLAST/
NCBI (Entrez)	http://www.ncbi.nlm.nih.gov/Entrez/index.html
PSORT II Prediction	http://psort.nibb.ac.jp/
SMART	http://smart.embl-heidelberg.de/

CHAPTER 3

CHROMATIN DYNAMICS DURING THE CELL CYCLE AND THE ESTABLISHMENT OF NUCLEAR ARCHITECTURE

For nuclear compartmentalisation to have a role in gene regulation, either in maintaining the stable expression of a gene, or in varying its expression dependant on nuclear position, chromatin mobility must be compatible with this. On the one hand chromatin mobility must be restricted, but on the other hand chromatin must be able to move in the nucleus to accommodate changes in gene expression. It is therefore important to know how stable or dynamic chromatin is and how and when chromatin organisation is established and maintained.

Previously the motion of several different GFP tagged LacO loci, in human fibrosacroma cells, over the time period of a few minutes has been analysed (Chubb et al., 2002). This reported an average chromatin movement in the range of 0.5μm for nucleoplasmic loci. Although this value is comparable with the motion observed in yeast and *Drosophila*, the actual diffusion constant of human chromatin is several times lower (table 3.1).

I have looked at chromatin motion in human cells in more detail, in particular to determine whether long or short-range components exist, and whether chromatin motion is cell cycle regulated. The motion and positioning of GFP-tagged loci through mitosis was also followed to determine whether cell architecture is established before or after cell division.

3.1 ANALYSIS OF CHROMATIN MOTION

I analysed the motion of LacO-tagged loci in human fibrosacroma HT1080 cells, using four different clonal cell lines each with a large LacO integration at a different

genomic site. These cell lines were previously made in the lab by J.Chubb and the sites of integrations havey been mapped to the G-band of 5p14, the R-band of 11q13, 13p near the rDNA, and the pericentromeric region of 19q12 (Chubb et al., 2002, unpublished data). To visualise the LacO arrays in these cells, GFP-LacI was expressed. This was taken from the p3'SS-GFP-Lac-NLS vector and so ensures that LacI is imported into the cell nucleus (Robinett et al., 1996) (see figure 1.10). To exclude error in measurement caused by z-axis resolution and nuclear rotation, cells in which the chromosome carrying the original array had duplicated were selected for analysis. This means that each cell analysed contains two visible foci of concentrated GFP-LacI. To calculate the three-dimensional distance between two loci in a cell, over time periods that are greater than one second, a series of images were taken through the z-axis for each time point in the study. This series of images is called a Z stack (figure 3.1). The position of each locus as defined by the brightest pixels was calculated by measuring the x, y and z co-ordinates. The three dimensional distance between two loci is then calculated using the formula $d= \sqrt{(x_2-x_1)+(y_2-y_1)+(z_2-z_1)}$ (Marshall et al., 1997). The change in distance between two foci (Δd) is plotted against time (t).

3.2 A SHORT-RANGE COMPONENT OF CHROMATIN MOVEMENT EXISTS

To determine whether short-range chromatin movements were detectable in HT1080 cells, cells were visualized using the 488nm laser line of the LSM510, with laser power at 75% with 6% transmission and a pinhole of 1AU. Cells containing two GFP tagged loci on the same plane of the z-axis were used for analysis. This was in order to track movement in as small a time frame as possible. If the loci had been on two different planes of the z-axis, a Z stack through the cell would have been required to calculate the 3D distance between loci, and this would have greatly increased the required scan time. 34 cells were imaged for each cell line with images captured over a time period of 30s with an image captured every second. Figure 3.2.a shows confocal sections taken at 1s intervals of an HT1080 cell line with GFP tagged 5p14 loci (arrowed in figure 3.2.a). To correct for any motion due to vibrations or

the heat from the heated stage used to capture images of live cells and vibrations from any other source, the analysis of short-range chromatin movement was also performed on fixed cells.

Chromatin displacements from movies taken of cells tagged at the loci 11q13, 13p and 5p14 were all calculated using the same methodology. Figure 3.2.b shows the $<\Delta d>$ plots of single second displacements on a dimensionless x-axis. Each graph contains 986 displacements. A comparison of the motion in fixed and live cells containing the GFP-tagged 5p14 loci shows a clear elevation of movement in live cells as opposed to fixed cells. Calculation of the t value using a Paired t test shows this difference to be statistically significant ($p< 0.0001$). Furthermore an analysis of variation between all three tagged cell lines suggests the movement in each cell line is significantly different to the movement observed in the other three cell lines measured ($p< 0.001$).

Significant levels of motion over the time period of one second were recorded in all three cell lines analysed, and the maximum motion recorded was 0.8 μm/s. The average overall motion recorded is approximately 0.2μm/s. From these observations it was concluded that human chromatin motion does contain a short-range component, like that seen in *Drosophila* and *S.cerevisiae*. Furthermore, the movement observed in this study does not show any of the restrictions observed in chromatin motion when followed over a long time period (figure3.3 and figure 3.5). Plots of the mean squared displacements ($<\Delta d^2>$) calculated over time can be used to determine if loci move randomly within the nucleus (Qian et al., 1991, Platani et al., 2002). Three classes of motion can be deduced from such plots: random diffusion, constrained motion, and diffusion with flow (figure 1.10). The Δd^2 plot calculated from the short-range movement of GFP tagged 5p14 loci in fixed cells shows very constrained movement. The Δd^2 values can be observed to initially increase and then level off, as expected for this type of motion. The Δd^2 plots for both the tagged 5p14 and 11q13 cell lines suggest that over short time periods the chromatin moves with random diffusion. The diffusion co-efficient (D) for these tagged loci are 1.25×10^{-3} μm^2/sec and 1.5×10^{-3} μm^2/sec respectively (table 3.1).

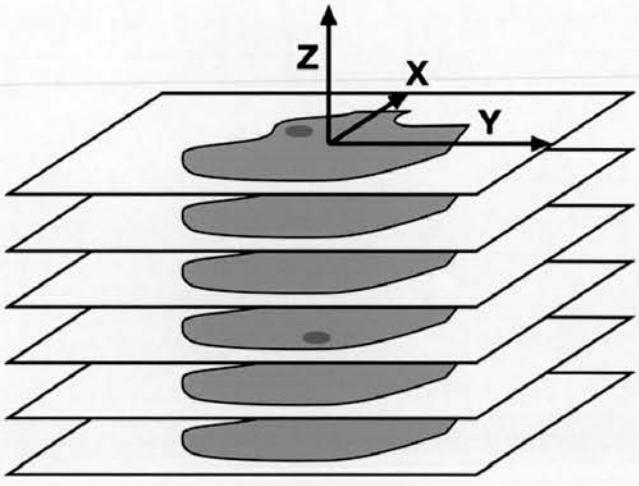

Figure 3.1: Schematic of a Z stack showing how images through a 3D cell are collected. In order to measure the three dimensional distance between a pair of GFP tagged LacO loci in a cell, images at regular intervals through the z axis of a cell were collected.

These were calculated from the gradients of the $<\Box d^2>$ plots, which are equal to 4D. This is ten-fold smaller than the diffusion co-efficient calculated for human chromatin over the time period of a few minutes (table 3.1). In contrast to 11q13 and 5p14, the Δd^2 plot of 13p suggests diffusion with flow is taking place. It has been previously shown that this cell line displays constrained motion of the tagged loci over the time period of a few minutes (Chubb et al., 2002). This was proposed to be due to anchoring of the locus to the nucleolus to which it is adjacent. Diffusion with flow implies that external forces have an impact on the movement of the locus, suggesting that this locus may not be tethered but simply confined to a region of the nucleus (Platani et al., 2002).

Organism	**Diffusion co-efficient**
Yeast	5×10^{-8} μm^2/sec (Marshall et al.,1997)
Drosophila	2.0×10^{-7} μm^2/sec (Marshall et al., 1997)
Human	1.5×10^{-3} μm^2/sec (tagged 11p14), 1.25×10^{-3} μm^2/sec (tagged 5p14), 1.25×10^{-4} μm^2/sec (Chubb et al.,2002)

Table 3.1. Diffusion co-efficients of chromatin in different organisms. Known diffusion co-efficients of yeast, *Drosophila,*and human chromatin, alongside the diffusion co-efficients obtained from the short-range chromatin motion of tagged loci.

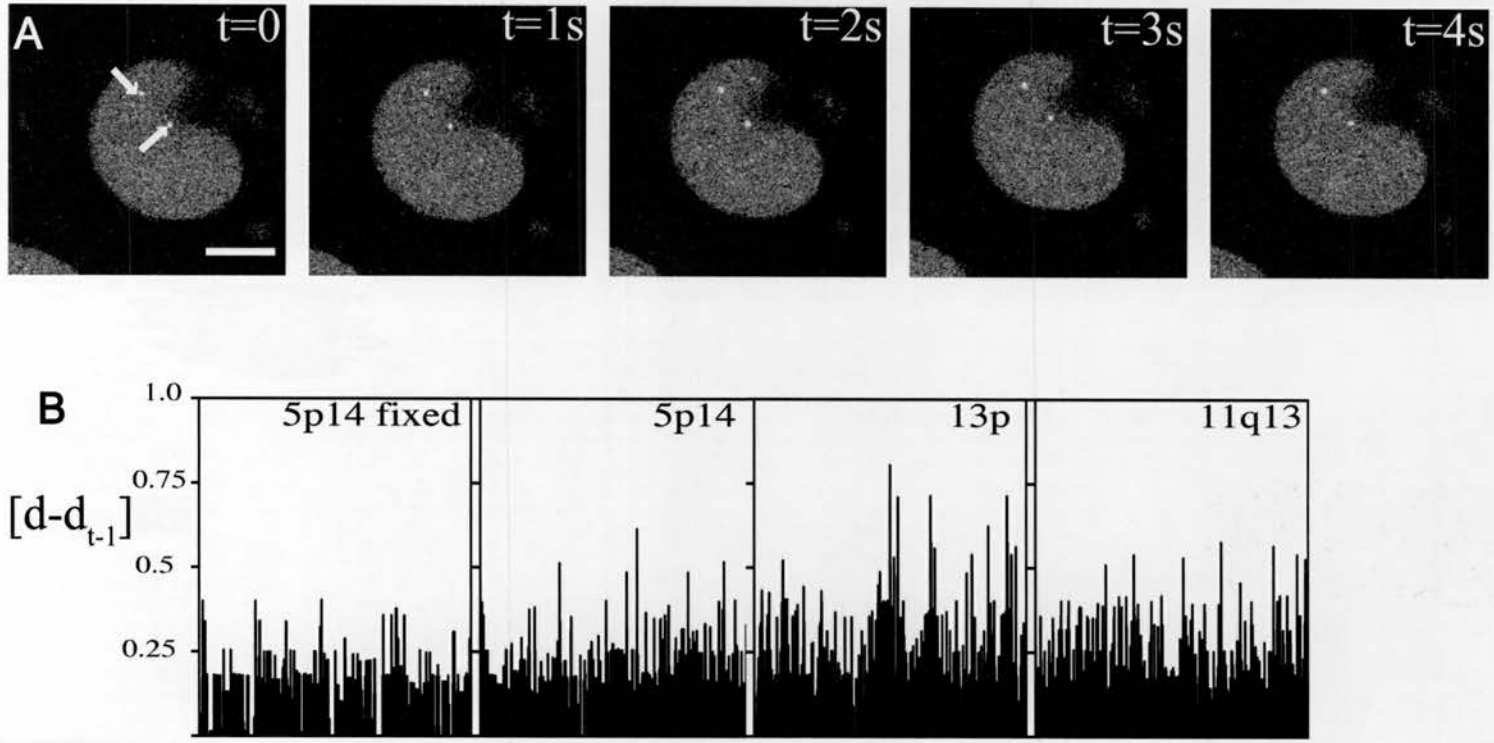

Figure 3.2: Rapid short range movement of human chromatin. A)Images captured at one second intervals of a HT1080 cell containing two copies of a GFP tagged 5p14 locus on the same plane of the z axis. The scale bar represents 10 μm. B)Changes in distance per second, d_{t1-t} , for live and fixed 5p14 cells and for cells with tagged loci at 13p and 11q13 in μm. The data from 34 movies is on each graph, giving 984 data points per graph. The x axis is dimensionless

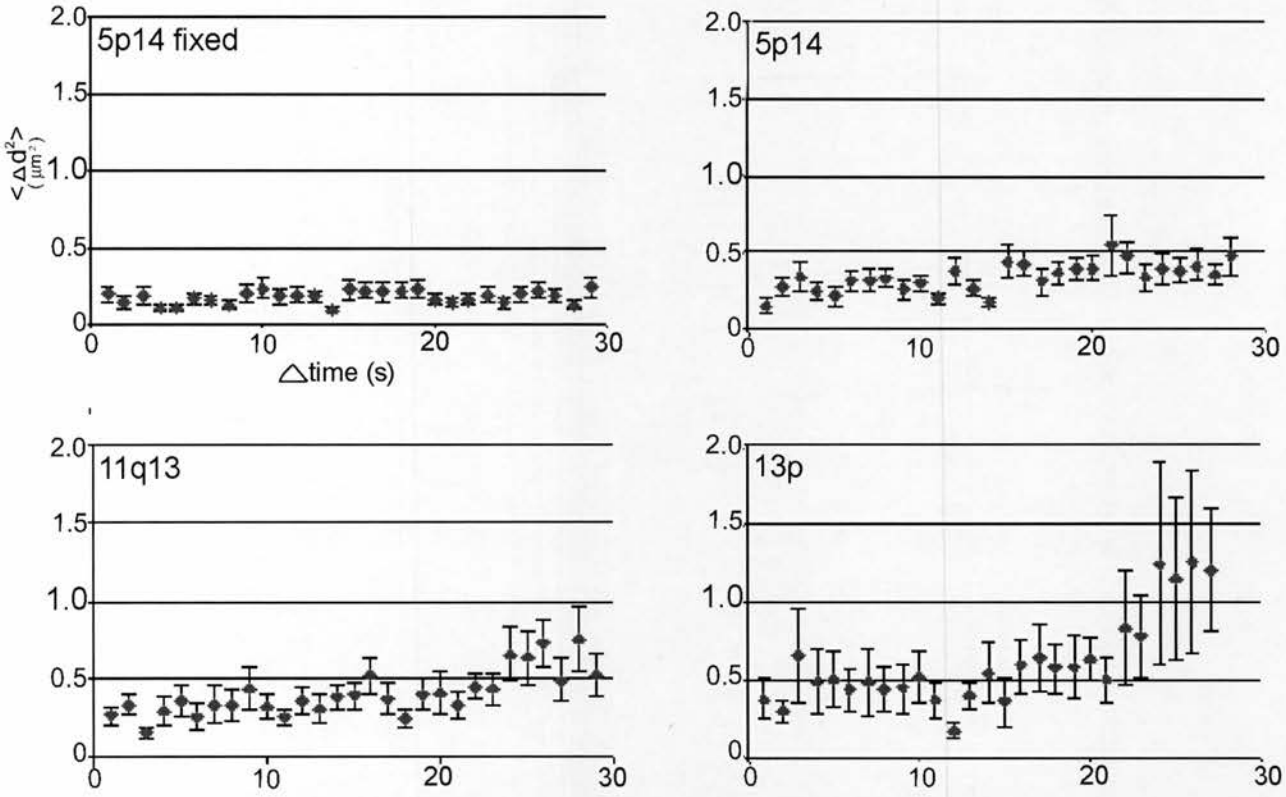

Figure 3.3: Mean squared displacements of rapid human chromatin motion show unconstrained movement. Graphs showing the mean squared displacements for each of the four cell lines captured, plotted against the time in(s).

3.3 A LONG-RANGE COMPONENT OF CHROMATIN MOTION

Previous studies looking at chromatin motion in mammalian cells using photobleaching, have suggested that chromatin is stable within a 1μm range for long time periods (Edelmann et al., 2001, Walter et al., 2003). However these studies follow large regions of chromatin over time and do not look at the motion of individual loci. The stability they propose is in contrast to the large dynamic movements of specific loci seen in *Drosophila* (Gunawardena and Rykowski, 2000). The labeling of such large chromatin areas may well obscure the movement of smaller individual chromatin fibers. Therefore to determine the level of long-range motion at individual loci in mammalian cells, 5 cells tagged at 5p14 and at 11q13 were imaged over a time period of 2 hours. Z stacks of cells containing two GFP-tagged loci were captured every 10 minutes over the observation period, using the 488nm laser line with 75% laser power at 6% transmission and a pinhole of 1AU. The three-dimensional distance (d) between each pair of loci was then calculated for each time point recorded and plotted against time (figure 3.4). Figure 3.4a shows images of cells tagged at 11q13 taken at 0,10,30 and 60 minutes after the start of observation. Two of the nuclei in these images contain two visible GFP-tagged loci. Despite changes in nuclear morphology and position the loci remain relatively stable over the course of analysis. However one of the loci in the bottom right hand cell can be observed moving from the nuclear periphery to a more internal position, during the first 30 minutes of observation.

Many of the cells captured show little movement of tagged loci over time, however other cells from both lines show more dramatic changes in position (figure 3.4.b). The mean change in distance over the two-hour observation period for both cell lines was 2.3μm and a Student t test shows the difference in the level of motion between different cell lines is not significant ($p=0.51$). My results suggests that individual loci are able to move in the order of 2-3 μm over the space of 2 hours, a level of motion up to four fold more than previously reported (Chubb et al., 2002). Plots of the mean squared displacement for both cell lines show that in

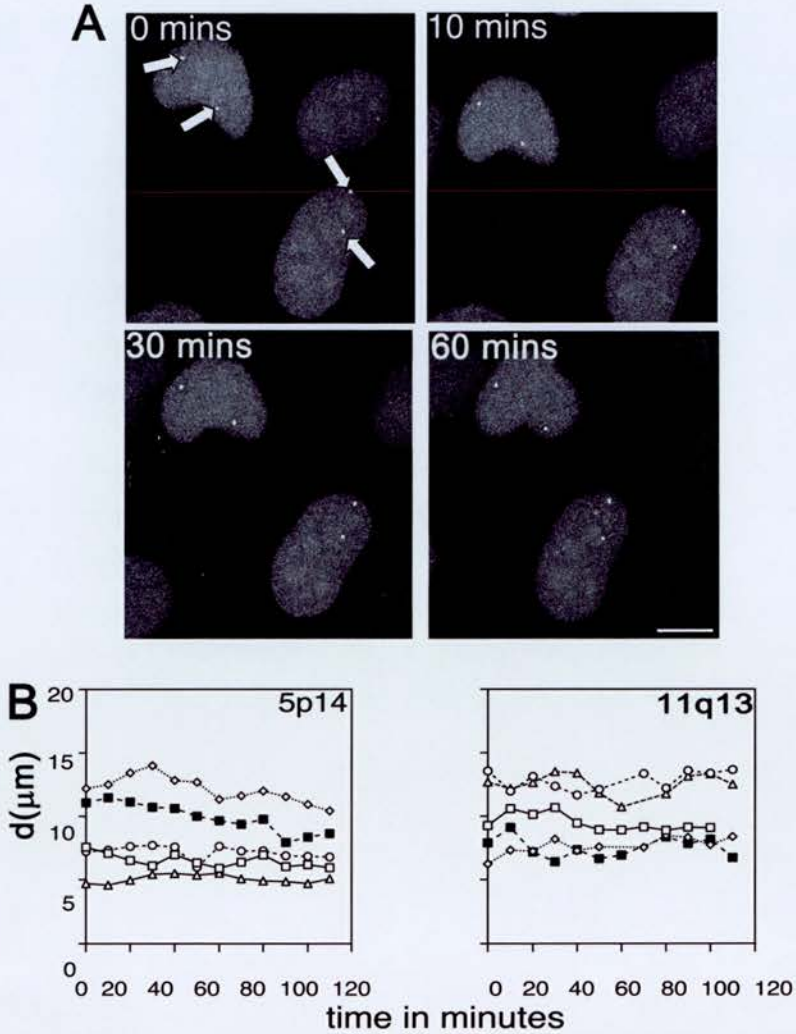

Figure 3.4: Long range motion of human chromatin during interphase. A) Frames taken at various time points from a movie of HT1080 cells with tagged 11q13 loci (arrowed in the first frame). The movie was captured as a series of z stacks which have been flattened to allow the stimultaneous visualisation of all loci. The scale bar represents 5 μm. B) The 3D distance(d) between two loci for the 5p14 and 11q13 loci measured at 10minute intervals over a 2 hour period.

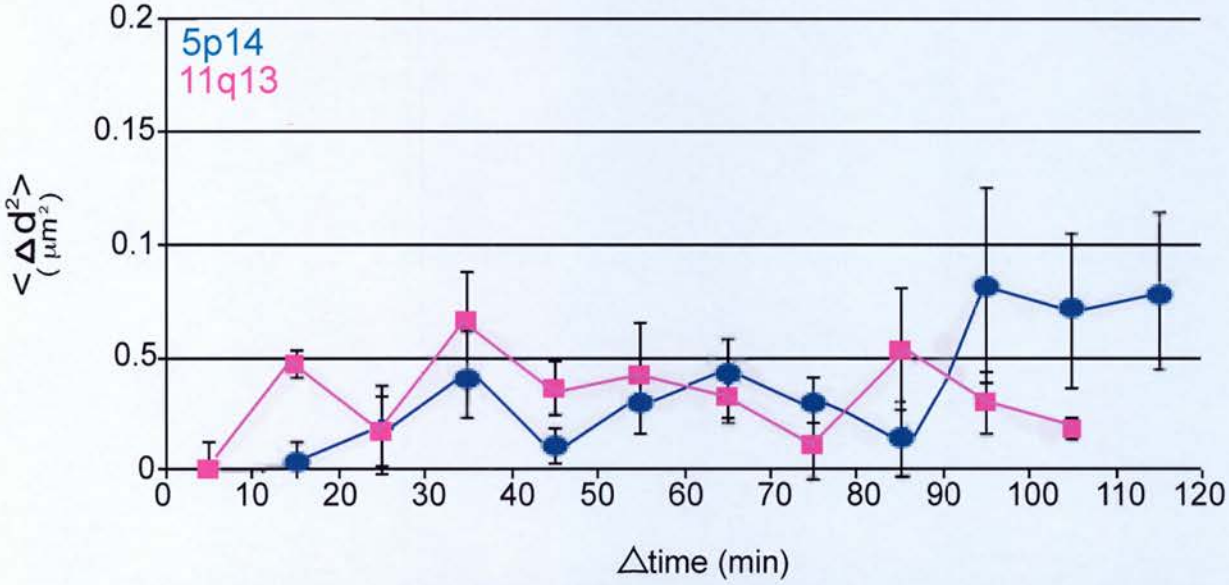

Figure 3.5: Mean squared displacements of long range human chromatin movement, shows that motion is constrained. Graphs showing the mean squared displacements of chromatin motion in both cell lines analysed, plotted against the change in time (min).

contrast to rapid short-range chromatin movement, movement over a longer time period is constrained (figure 3.5). In order to obtain an accurate diffusion co-efficient for the tagged chromatin in both cell lines the sample size would have to be significantly increased.

3.4 CHROMATIN MOVEMENT DURING EARLY G1

Several studies have suggested that there is enhanced chromatin movement in early G1 (Shelby et al., 1996; Tumbar and Belmont 2001; Walter et al., 2003; Dimitrova and Gilbert 1999; Bridger et al., 2000). To determine if chromatin is more mobile at this stage of the cell cycle, mitotic HT1080 cells with two bright GFP-tagged loci were imaged using the 488nm laser line with 75% laser power at 6% transmission and a pinhole of 1AU. To identify mitotic cells the breakdown of the nuclear envelope was used as a marker. This results in very rounded cell morphology and the redistribution of background GFP-LacI-NLS to the entire cell (t0 min in figure 3.6). In some cells, the condensed sister chromatids can be seen, and are marked by a pair of bright GFP foci very close together (t0 in figure 3.6). The start of G1 is marked by the re-concentration of GFP-LacI-NLS into the nucleus as the membrane is reformed in daughter cells (t10 min in figure 3.6). Z stacks were captured every 10 minutes for a time period of two-three hours throughout completion of mitosis and for the first part of G1. During the first hour of G1 dramatic changes in cell morphology occur as cells flatten and expand (figure 3.6). Mitotic cells containing GFP tagged loci were analysed and the distance between the two loci calculated throughout the course of the movie. Figure 3.7 shows plots of the change in distance between loci during the first two hours of G1 in the GFP-tagged 11q13 cell line. The broken vertical line on each graph represents the metaphase to anaphase transition, as defined by the separation of tagged loci on the sister chromatids.

The first conclusion that can be made from these graphs is that many large chromatin movements occur in early G1, when compared to motion present in interphase nuclei. A comparison of the mitotic and subsequent daughter cells to the interphase cell in the top left hand corner of figure 3.7 presents an example of this. In

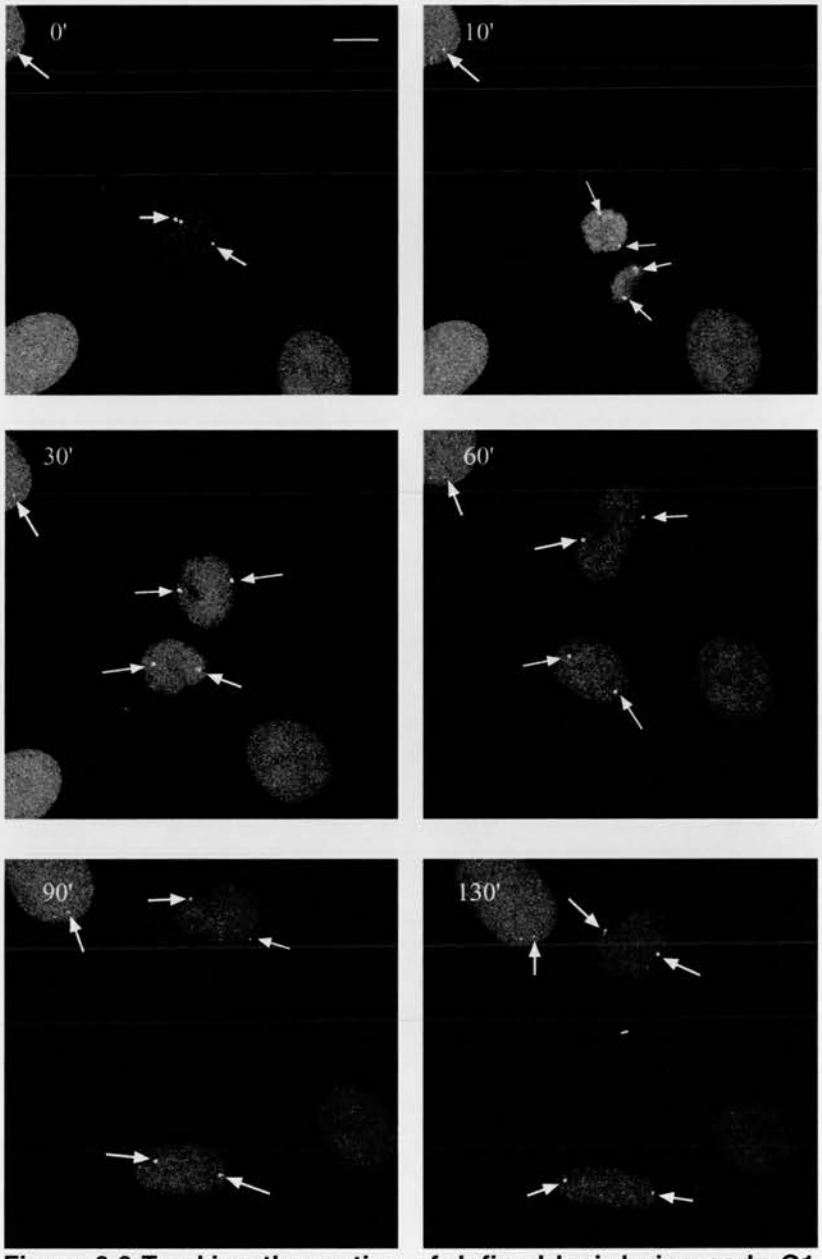

Figure 3.6:Tracking the motion of defined loci during early G1. Mitotic cells were identifed by the dispersal of GFP-lacI-NLS fusion throughout the entire cell volume in the absence of the nuclear envelope (0' frame). Confocal z stacks were captured at 10 minute intervals for a 2 hour period after the completion of mitosis, and are shown flattened to allow the stimultaneous visualisation of all spots. Considerable changes in the distance seperatingthe tagged loci in newly formed daughter nuclei occur over time.Note the relative lack of motion in an interphase cell that has not just exited mitosis (top left). Scale bar=10 m

the interphase cell the two GFP-LacI foci remain relatively immobile, however the foci present in the daughter cells display more motion. Overall many movements of > 5μm were observed to take place in time periods as little as 10 minutes during the early part of G1 (figure 3.7). One movie in particular shows extreme movement of tagged loci in early G1 (figure 3.6). As G1 progresses the bottom daughter cell expands and then elongates. The two tagged loci in this cell are positioned along the axis of elongation and thus as the nucleus elongates the two loci are pulled further apart. The second daughter cell also undergoes a similar expansion and elongation, however in contrast to the first daughter cell the tagged loci are not positioned along the axis of elongation resulting in only a small increase in the distance between them. This pair of daughter cells provides an example of how, in some cases, the changing cell morphology characteristic of early G1 can result in large movements of tagged loci.

During mitosis transcription ceases and begins anew with the formation of the nuclear envelope in early G1 (Prescott and Bender 1962). To determine if the reinitiation of transcription is driving the large chromatin movements observed, cells were followed through mitosis and early G1, in the presence of (50μg/ml) 5,6-dichloro-D-ribofuranosylbenzimidazole (DRB). This is a potent inhibitor of transcription, which exerts its effect by preventing the elongation of RNA transcripts by RNA polymerase II (Chodosh et al., 1989). DRB was added to the tissue culture medium just before live cell analysis was carried out. The graphs of chromatin motion in the presence of DRB show movements as large as those in untreated cells (figure 3.7). This suggests that transcription is not driving large chromatin movements in early G1. In yeast, large chromatin movements are repressed by the presence of carbonyl cyanide chlorophenyl hydrazone, an inhibitor of ATP synthesis and are unaffected by the presence microtubule destabilizing drugs (Heun et al., 2001). This would suggest chromatin movement is energy dependent but does not require microtubule dependent motors. It would be interesting to carry out similar experiments in my GFP-LacO tagged cell lines, although such experiments may prove to be very difficult technically as these processes are required for mitosis.

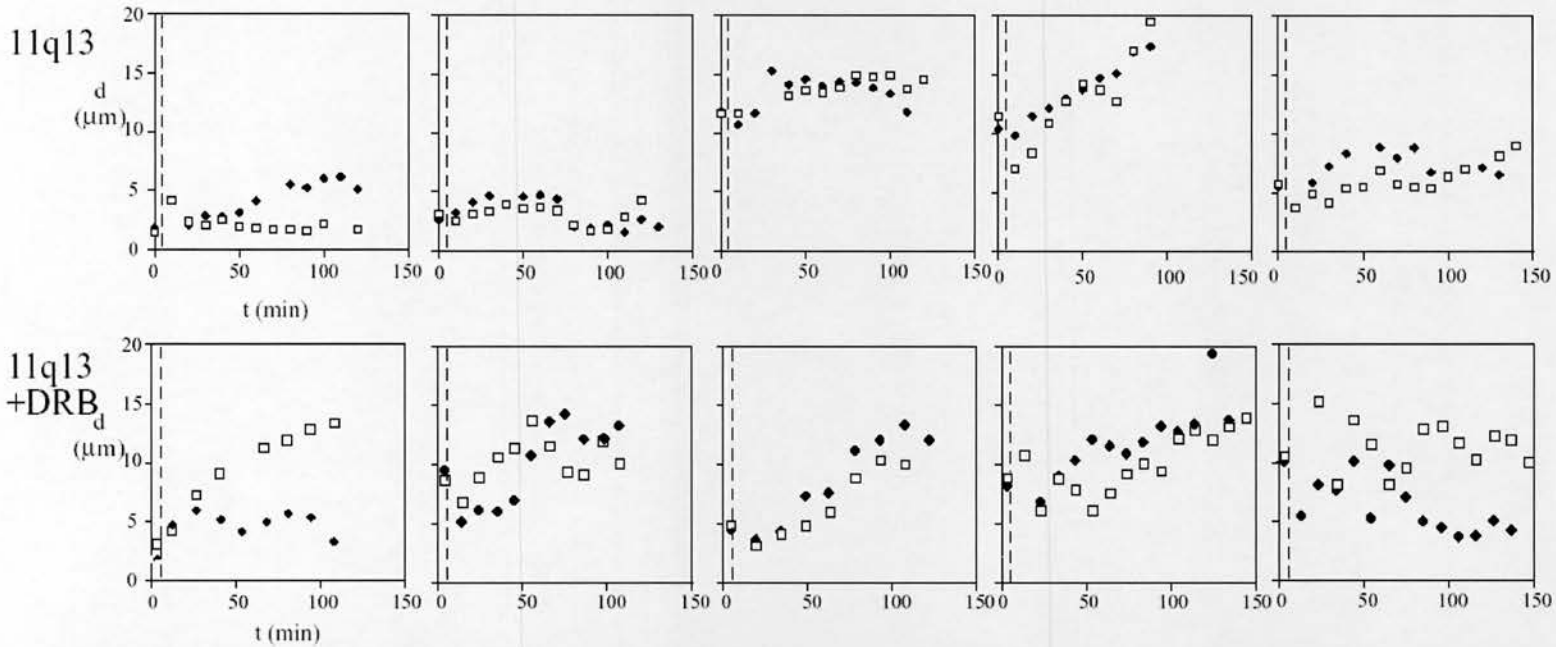

Figure 3.7: Enhanced but restricted human chromatin motion in early G1. Each graph corresponds to the daughters (squares or diamonds) of a single mitotic cell and plots the distance (μm) between homologous loci in the same cell, against time (min). Data for the 11q13 tagged loci with and without the presence of DRB(50μg/ml) is shown. Dashed line=metaphase to anaphase transition.

3.5 INTERACTIONS WITH NUCLEAR COMPARTMENTS ARE ESTABLISHED DE NOVA IN EARLY G1

The range of movement observed in early G1 suggests that chromatin is able to move between different nuclear compartments as substantial nuclear reorganization takes place. However, by comparing the positioning of GFP tagged loci in pairs of daughter cells, the questions of when in the cell cycle chromatin position is established, and to what extend the enhanced chromatin mobility of early G1 contributes to the establishment of nuclear architecture can be answered (figure 3.8). At present there are two contrasting views on when chromatin position is established. The first proposes that chromatin position is established *de novo* every cell cycle, and the second that chromatin position is inherited from the mother cell to the daughter cell via the organisation of chromosomes on the metaphase plate. Evidence in support of both models has been published (Gerlich et al., 2003; Walter et al., 2003). However these studies address the question of when chromatin position is established by following the positioning of large chromatin domains, rather than individual loci through mitosis and G1. Both Gerlich et al., 2003, and Walter et al., 2003, used mammalian cell lines expressing GFP tagged to the histone H2B. Areas of chromatin were then photobleached and the pattern of bleaching followed through mitosis. This approach is dependent on the slow turnover of histone H2B into chromatin. Despite the similar approach, both papers reach contrasting conclusions. Walter et al., concluded that reorganisation of chromatin positioning occurs in G1, as 60% of the cells bleached showed substantial reorganising of bleached domains in daughter cells. However, Gerlich et al., concluded that position is inherited through mitosis, although some mixing of bleached and unbleached domains is present in their data. To resolve the differences in opinion of when chromatin position is established, I have looked at the positioning of individual LacO tagged loci in daughter cells. If two daughter cells have similar positioning of tagged loci this would suggest position is already determined before or during metaphase. However, if two daughter cells show different positioning this would suggest that positioning is established in early G1 (figure 3.8).

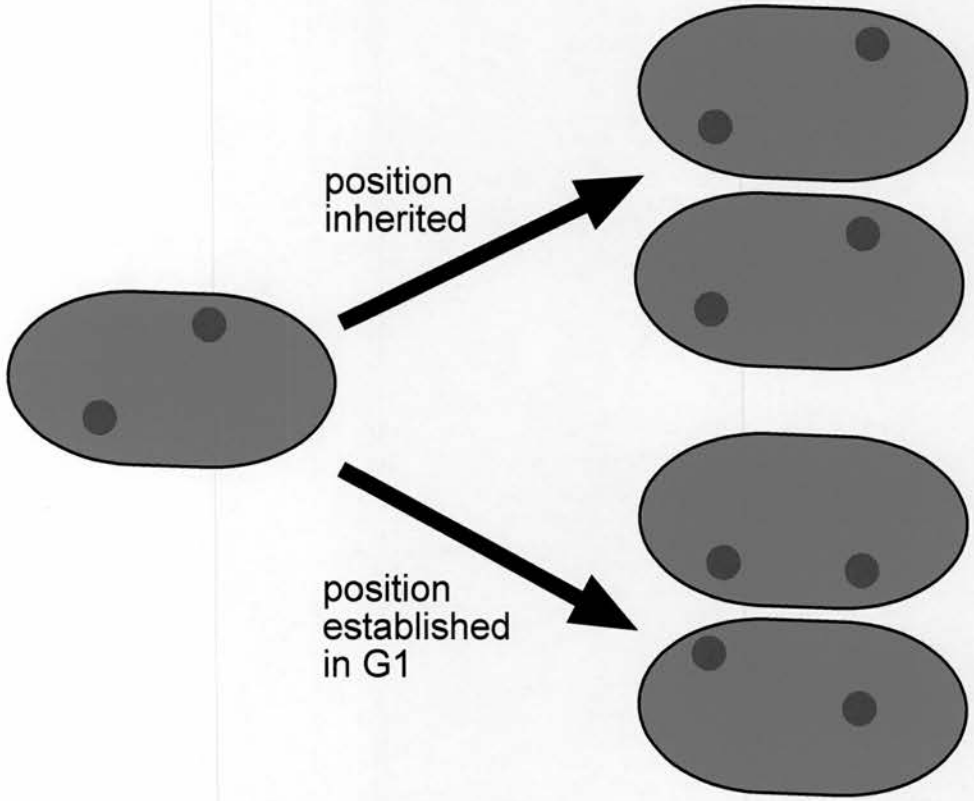

Figure 3.8:How to determine when in the cell cycle chromatin position is established. Comparing loci position in pairs of daughter cells , provides insights into when chromatin position is established.

I have analysed the position of LacO tagged loci in daughter cells relative to the nuclear periphery. Many of the cells I followed through mitosis showed asymmetrical positions of tagged loci in the resulting daughter cells. One such Z stack of a pair of daughter cells taken 110 minutes after metaphase is shown in figure 3.9. This pair of daughter cell has tagged loci at the chromosomal position 5p14. In the daughter cell on the left, the GFP tagged loci have relatively internal positions (>1 μm from the nuclear periphery, and present in slices 1μm and 2μm of the Z stack). However, the daughter cell on the right appears to have more peripheral locations of both its GFP tagged loci. This is especially apparent in the locus present in the 4μm slice of the Z stack, in that this locus is inseparable from the nuclear periphery, as defined by the edge of the GFP-LacI-NLS signal. Similarly the other locus in this daughter cell is very close to, but not quite touching, the periphery in the 6μm slice of the Z stack. Therefore it can be concluded that this particular pair of daughter cells has asymmetrical nuclear organisation and radial positioning of its chromatin. Five cells in total for the 5p14 cell line were followed through mitosis, of which 2 had asymmetrical positioning of GFP tagged loci in their daughter cells. The graphs of chromatin mobility in these cells was previously discussed in my M(Res), and hence not show here.

To investigate the positioning of tagged loci in pairs of daughter cells further, the positioning of tagged loci with respect to different nuclear compartments was analysed in two cell clones from the 19q12 and the 5p14 tagged cell lines (figure 3.10). Both of these cell lines have tagged loci distributed between more than one nuclear domain (Chubb et al., 2002, Chubb personal communication). To investigate the positioning of tagged loci in daughter cells, cells were seeded at a very low density onto coverslips, and fixed with 4% pFa, 24 hours later. At this stage most cells were in well-isolated pairs. Cell pairs with a similar nuclear size, expression of GFP, and over 500μm for any other cell pair, were assumed to be pairs of daughter cells. The position of GFP tagged loci was then scored using a protocol similar to that of Walter et al., and with respect to three nuclear compartments which were the nuclear periphery, the nucleolus (marked using immunofluorescence with an antibody against pKi67)(figure 3.10.a) and the nucleoplasm. Many daughter cells

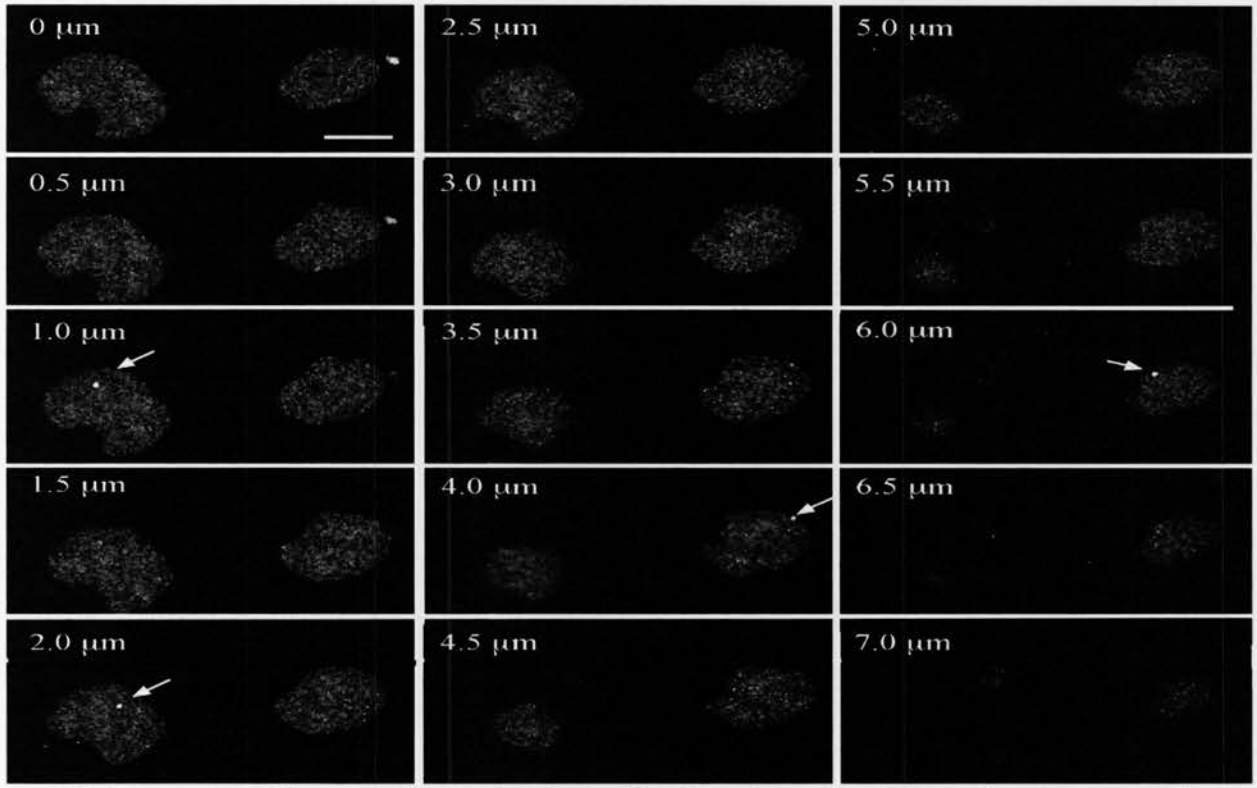

Figure 3.9: Asymmetry of locus position in daughter cells. 0.5µm interval confocal sections from a z stack captured 110 minutes after the completion of mitosis,through a pair of daughter nuclei tagged at 5p14. In the left nucleus both loci are internal (sections 1µm and 2µm. In the right nucleus one locus abuts the nuclear edge (4 µm) and the other is close to, but not at the upper surface of the nucleus (6µm). Scale bar=10µm.

were observed to have asymmetrical positioning of their loci (figure 3.10.b). For the 5p14 cell line 17/30 pairs of cells analysed had different positioning of their loci. This high frequency of asymmetrical daughter cells was also conserved in the 19q12 cell line.

Using a null hypothesis of no inheritance of nuclear position, the probability of a locus associating with a particular compartment was directly related to the population frequency the association, and was independent of the behavior of the sister locus in the other cell of a clone pair. The population frequencies of tagged loci in the 19q12 cell line were 0.19 for nucleoplasmic association, 0.35 for the nuclear periphery and 0.46 for association with the nucleolus (figure 3.10.c). To calculate the expected (E) numbers of tagged loci associated with each nuclear compartment in two cell pairs, each cell was classed as having one of three possible locations for the tagged loci (nucleoplasm (i), nuclealor (n), or peripheral (p)). For the null hypothesis of no inheritance the observed distribution in 2 cell clones should simply reflect their population frequencies. There are nine different possible outcomes of clone pair associations. These are 1) p/p p/n p/i 2) n/p,n/n.n/i and 3) i/p i/n, i/i. To calculate the expected frequency of each combination the observed population frequencies are multiplied together. Multiplying the expected frequencies by the population size then generates E values. After pooling like combinations (e.g. p/n and n/p), the E values were tabulated and compared to the observed values(O) using a X^2 test giving X^2 a value of 7.2 for 5 degrees of freedom. $X^2 = \Sigma(O-E)^2/E$. For the 19q12 locus this results in a p value between 0.2 and 0.3 meaning the null hypothesis of no inheritance of locus position cannot be ruled out.

Both the enhanced mobility, and the asymmetry, of daughter cells suggests that chromatin can form and lose associations with nuclear compartments during the early part of G1. Examples of this can be seen in figure 3.11, which shows confocal sections from Z stacks of cells taken directly after mitosis. Figure 3.11.a. shows a cell in which one tagged locus is located relatively internally immediately after the completion of mitosis, however as G1 progresses and the nucleus expands and elongates, the tagged locus is observed to move towards the nuclear periphery and is

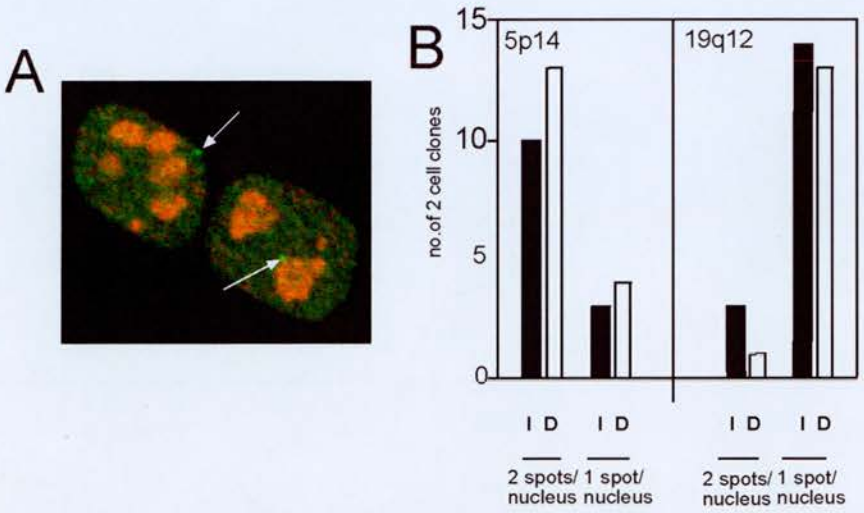

C

Position of 19q12 in daughter nuclei		Observed (O) n=27	Expected (E)
symmetric	periphery/periphery	4	3.3
	nucleolus/nucleolus	7	5.8
	nucleoplasm/nucleoplasm	3	0.92
asymmetric	periphery/nucleoplasm	2	3.5
	periphery/nucleolus	9	8.8
	nucleolus/nucleoplasm	2	4.6

Figure 3.10. Associations of loci with nuclear compartments are not inherited through cell division. A) Confocal image of a two cell clone of the GFP-LacI expressing 19q12 cell line. The tagged GFP loci are visble in both cells as a green dot.Nucleoli are detected (red) using immunofluorescene with an antibody recognising Ki67. B) Proportions of two cell clones where the daughter cells have indentical (I) and different (D) positions of loci relative to nuclear compartments. C) Statistical analysis of the data from B). There are 3 symmetric and 3 asymmetric expected combinations of locus-nuclear compartment association. The observed patterns of association (O) are compared to the expected frequencies (E), calculated from the incidence of association throughout the population of cells.

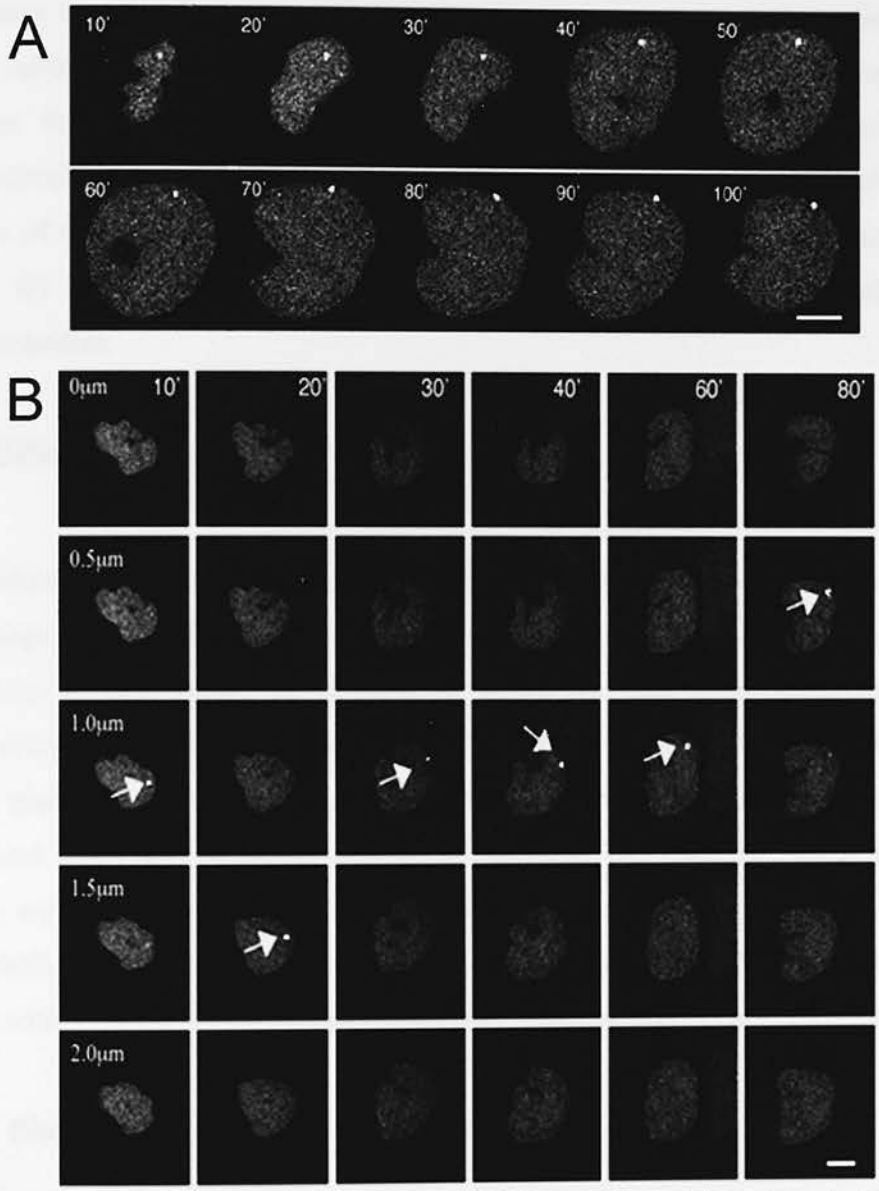

Figure 3.11. Changing associations with the nuclear periphery in early G1. A) Progressive establishment of peripheral localisation for a 5p14 tagged locus during G1. Each frame is a z slice captured at 10 min intervals after the metaphase -anaphase transition. Scale bar = 10μm. B) Z stacks from an 11q13 tagged nucleus taken at 10 and then 20 min intervals after mitosis, showing changing associations with the periphery. Scale bar= 5μm

located here 70 minutes after the nuclear envelope has been established. The locus then remains here for the rest of the movie. Likewise figure 3.11.b. also shows the tagged locus in a cell from the 11q13 cell line, moving from an internal location to the nuclear periphery. However in contrast to figure 3.11.a, this locus moves to the periphery over the time period of 40 minutes, and does not remain here. Instead this locus moves back into the nucleoplasm by 80 minutes of G1. Both of these movies suggest that chromatin associations with the nuclear envelope are not set up immediately after nuclear envelope formation, but are instead established over the course of G1. The position of chromatin relative to the periphery is plastic during early G1 allowing loci to be repositioned with respect to several nuclear compartments.

3.6 DISCUSSION

To understand how chromatin position is established and maintained in dividing cells it is important to first understand the behaviour of chromatin in living cells. How dynamic is chromatin? Is it able to move to and from different nuclear compartments? Is chromatin more dynamic at different cell cycle stages? To answer these questions the dynamics of chromatin over time in living human cells was followed using the GFP-LacI protein to visualize Lac operator repeat sequences which are stably integrated at different genomic sites (Robinett et al., 1996, Chubb et al., 2002). These cell lines were also used to determine whether the association of a locus with a nuclear compartment is inherited from one cell cycle to the next.

3.6.1 Short and long range chromatin motion

Previous studies in mammalian cells have shown that chromatin is able to move in the order of approx. 0.5μm in the space of a few minutes (Chubb et al., 2002). I have shown for the first time that human chromatin also has a short-range component to its motion. By tracking the movement of loci over the period of a few seconds I have observed chromatin movement averaging 0.2μm/sec. In addition, the movement observed does not display any of the constraints observed over larger time periods,

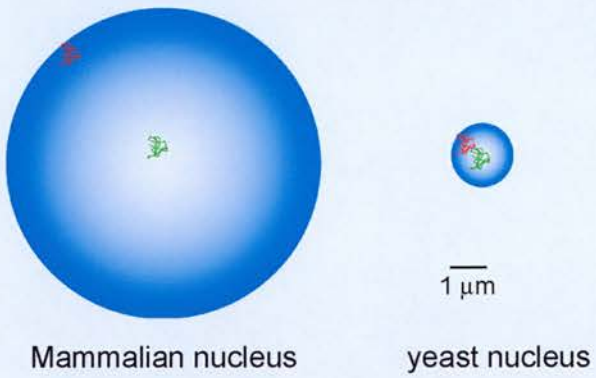

Figure 13.12. Schematic diagram showing the range of chromatin movement in mammals and yeast. Although both yeast and mammalian chromatin can display movements in the region of 0.5µm within a relatively short time period, the volume of the total cell nucleus chromatin can access in both differs dramatically. The green and red lines indicate the volume able to be accessed by loci in both nuclei.

and in the case of the tagged 13p locus displays movement described as diffusion with flow. This suggests external factors may have a role in its movement. This locus is known to associate near the nucleolus, a very active site of RNA pol I transcription, which may explain the motion seen. Overall my results are similar to the motion previously reported in simpler eukaryotes (Heun et al., 2001, Vazquez et al., 2001). Individual loci in *Drosophila* spermocytes nuclei are able to move up to 0.3μm over the space of a few seconds, and over the time period of a few minutes can access chromosome territory-sized regions of the nucleus (Vazquez et al., 2001). Yeast chromatin also displays rapid short- range movements of up to 0.5μm in the space of 10 seconds (Heun et al., 2001).

In addition to the short-range motion of chromatin in humans cells, I have also observed chromatin movement over longer time periods which is greater than previously reported. Over the time period of a couple of hours, loci move 2-3μm, four fold greater than chromatin movement previously reported in mammalian cells (Chubb et al., 2002). However, my analysis does not take into account changes in cellular morphology over the period of observation, and it is possible that changes in nuclear shape could account for some of the motion observed. To overcome this, measuring the position of loci with respect to the nuclear periphery may allow the scale of motion due to nuclear enlongation to be determined. Movements of 2-3μm could allow individual genes to move in and out and of their chromosome territory during the course of activation (Chamberyon and Bickmore, 2004). The level of the movement I observed also allows chromatin to be able to move from one nuclear compartment to another, and is comparable in scale to motion observed in yeast. Despite this, chromatin in human cells has access only to a very small area of the total cell nucleus. In contrast, yeast chromatin is able to access up to half of the nuclear volume (figure 3.12) and *Drosophila* embryonic chromatin can move up to 75% of the nuclear volume over a period of a few hours (Gunawardena and Rykowski 2000).

3.6.2 Chromatin dynamics and the establishment of chromatin position in G1.

My results show that chromatin is considerably more dynamic in early G1 than in other stages of the cell cycle. Both the maximum, and average, movement observed is greater than that recorded for the rest of interphase. These results are in agreement with previous studies, which have recorded increased movement of labelled DNA, photobleached domains and GFP labelled centromeres in early G1 (Walter et al., 2003, Shelby et al., 1996). Why should chromatin movement be increased at this stage of the cell cycle? Analysis of the movies captured suggests that, in some cases, enhanced motion is due to changes in nuclear organisation and morphology as the nucleus reassembles after mitosis, as suggested by Williams and Fisher 2003. However, it is not all simply due to isomorphic expansion of the nucleus. I saw loci that moved towards the nuclear periphery and it is known that HSA18 can also move towards the nuclear periphery during early G1 (Bridger et al., 2000). In early G1, nucleolar organizer regions form from pre-nucleolar bodies, which fuse together to form the nucleoli, dependent on the reinitiation of RNA polymerase I transcription. (Scheer et al., 1993, Fompoix et al., 1998). RNA pol I is repressed from prophase through to late anaphase, leading to the hypothesis that enhanced mobility of chromatin in early G1 could be due to the re-intiation of general transcription. To test this cells were followed through mitosis in the presence of DRB, to inhibit the reinitiation of transcription. However, the results of these experiments suggest that large movements occur independent of transcription. Both Tumbar and Belmont 2001, and my results show in some cases that loci are able to move between nuclear compartments in early G1 suggesting that active reorganisation of the nucleus is taking place at this stage of the cell cycle.

3.6.3 Is chromatin position inherited or established anew each cell cycle?

My results also allow us to determine when in the cell cycle chromatin position is established. Before my study two recent papers, which followed the positioning of photobleached domains through mitosis and early G1, published two different conclusions to the question of when chromatin positioning is established. The first concluded that the position of chromatin in the mother cell was retained on the metaphase plate and propagated through mitosis to daughter cells (Gerlich et al., 2003). However some mixing of photobleached domains is present in their data. The second, used the same approach as Gerlich et al., 2003, but in contrast, concluded that some aspects of chromatin position were preserved during mitosis but that other aspects were established *de novo* every cell cycle (Walter et al., 2003). They showed substantial loss of chromatin organization as chromosomes in the mother cell were captured on the mitotic spindle. In particular they also analysed the specific relative localisations of human chromosomes in clones of HeLa cells. Whilst daughter cells contained similar positioning of chromosomes, the position of chromosomes in grand daughter cells did not. From their studies, they concluded that locally constrained chromatin movements were sufficient during the transition of a cell from interphase to mitosis and vice versa (Both papers are reviewed in Williams and Fisher, 2003; Bickmore and Chubb, 2003; Parada et al., 2003).

My study rather than following large domains with unknown chromatin content looks at the positioning of individual GFP-tagged loci. By tracking the movement and spatial distribution of these loci through mitosis my results suggest that the positioning of chromatin in daughter cells is similar although not identical, agreeing with the results of Walter et al,. Figures 3.9 and 3.10 show that there is non-symmetrical behaviour of loci in daughter cells and a large portion of cells from two cell clones display non-symmetrical locations of tagged loci. Moreover, there is no evidence statistically that chromatin position is inherited with respect to nuclear compartments.

Although chromatin is able to move further distances in early G1 than at any other stage in the cell cycle, movement is still restricted to a very small volume

of the total cell nucleus. This suggests that some aspects of chromatin position are already restricted immediately after mitosis takes place. Images taken from my movies also suggest that loci can form and lose associations with different nuclear compartments. Overall I conclude that chromatin position is not globally inherited through its positioning on the metaphase plate. The chromatin movements observed in early G1 suggest that chromatin is already restricted to a small volume of the total cell nucleus immediately after mitosis, however the level of motion recorded is large enough to allow chromatin to undergo substantial remodeling. Locus position appears to be plastic allowing movement between compartments before progressive restrictions results in a more stable organisation for the rest of interphase.

CHAPTER 4

EPIGENETIC MODIFICATIONS AND THEIR EFFECT ON LINKER HISTONE MOBILITY

In contrast to chromatin, which is relatively immobile in human cells, many chromatin-associated proteins have been shown to be dynamic (Misteli et al., 2000; Lever et al., 2000; Phair et al., 2004). This indicates that they are not stably bound to the chromatin fibre, but rather in equilibrium between bound and unbound states. Measuring the mobility of these proteins in different experimental situations can give insights into the factors that govern binding. Previously FRAP with wild-type and mutant reporter proteins has been used to determine the contribution of different protein domains to chromatin binding (Lippincott-Schwartz, Altan-Bonnet, and Patterson 2003). However for the first time here I have used FRAP in cells with different genetic backgrounds to analyse the contribution of different epigenetic mutations to the binding of linker histones.

DNA methylation is thought to primarily influence gene silencing by altering the structure of the chromatin fibre, however what levels of chromatin compaction are regulated by DNA methylation are not known (see section 1.1.3). Moreover, mutations in the Suvar39h enzymes responsible for H3K9me3 at constitutive heterochromatin can cause chromosome instabilities and the loss of DNA methylation at major satellite sequences (Peters et al., 2001, see also section 1.1.8). Both DNA methylation and H3K9me3 are found at their highest concentrations at constitutive heterochromatin (Lewis et al., 1992; Aagaard et al., 2000), which has been shown to have a very compact chromatin structure (Gilbert et al., 2004). In addition, experimentally and genetically inducing hypomethylation of satellite DNA can cause its visible decondensation (Schmid et al., 1984; Brown et al., 1995). Likewise inducing hypermethylation of DNA with 3-aminobenzamide (3-ABA), a drug that introduces new methyl groups into the 5' position of cytosine residues in

CpG dinucleotides, can cause chromatin to condense dependent on the presence of linker histone H1 (Karymov et al., 2001). Furthermore, over expression of the methyl-CpG binding protein MeCP2 can cause chromatin to aggregate into compact structures (Brero et al., 2005).

Since linker histones, such as H1, are involved in chromatin folding and the formation of higher chromatin structures, DNA and histone methylation may have roles in H1 binding. Evidence suggesting that linker histones may preferably bind to methylated DNA comes from miccrococcal nuclease (MNase) digests in which 80% of all methylated cytosine residues are found in mononucleosomes that contain H1 (Ball et al., 1983) and unmethylated CpG islands appear to be depleted in H1 (Tazi and Bird 1990). In addition, *in vitro* competition assays, and other binding experiments, have shown that there is an increased affinity of methylated DNA for H1 (Levine et al., 1993; McArthur and Thomas 1996). The link between H1 and DNA methylation is also highlighted in recent RNAi experiments in *Arabidopisis,* in which 90% of H1 expression was inhibited. This caused both hypo- and hyper- DNA methylation at specific sequences in a stochastic manner (Wierzbicki and Jerzmanowski, 2005). However, the influence of DNA methylation in linker histone binding is not clear cut, as studies, from both *Xenopus* and the mouse, have revealed no difference between the ability of methylated and unmethylated DNA to bind H1 (Nightingale and Wolffe, 1995; Hashimshony et al., 2003).

Therefore to analyse the *in vivo* effects of DNA methylation, and H3K9me3 on linker histone binding, I have performed fluorescence recovery after photobleaching (FRAP) experiments for H1 and H5 in a range of mouse ES cell lines, that carry different mutations in genes that affect these epigenetic modifications.

4.1 EGFP TAGGED LINKER HISTONES

In order to use FRAP as a means to measure the binding of linker histones in different epigenetic backgrounds, the linker histones, H1.4 and H5 were both tagged at the N-terminus with EGFP (figure 4.1.a). EGFP was placed at the N terminus of H1 and H5 as this part of the linker histone is not strictly required for the formation

of the higher order chromatin fibre (Allan et al., 1986; Hendzel et al., 2004) and fusions of GFP to the C terminus of H1 have been shown to result in a lower affinity for chromatin than GFP fusions to the unstructured N-terminal (Hendzel et al., 2004). DNA fragments encoding each linker histone were cloned in frame into the vector backbone pEGFP-C1 (Clontech). Both vectors were created and characterised by N. Gilbert.

Several variants of linker histone exist, with roles in ageing, DNA repair, and apoptosis (Barra et al., 2000; Downs et al., 2003; Konishi et al., 2003). However two of the best characterised are H1.4 and H5. Linker histone H1.4 is from the human family of H1 linker histones, whilst H5 is expressed in the chicken (SWISSPROT accession numbers: P10412 and P02259 respectively). The linker histone variant H1.4 accounts for 60% of all expressed H1 protein (Swiss-Prot), whilst H5 maintains a more specialised function and is expressed in a developmentally regulated manner in the erythrocytes of birds (Cole,1984). The different expression patterns and functions of these linker histone variants are reflected by differences in their amino acid composition. H1 has a higher proportion of lysine residues at the carboxyl domain whilst H5 has a higher proportion of arginine residues (see figure 1.3). Both these variants were used in subsequent FRAP experiments.

Fusion proteins expressing EGFP-H1 and EGFP-H5 (gift N.Gilbert) were transiently transfected in mouse HT2 ES cells to confirm that the presence of the EGFP tag did not alter the binding of linker histone to chromatin (figure 4.1.b). EGFP was detected in a diffuse pattern throughout the nucleoplasm of the cell nuclei, with some dense patches of EGFP corresponding to sites of heterochromatin. Both fusion proteins have previously been shown to associate with chromatin through sucrose gradient sedimentation and by the analysis of nucleosomes prepared from transfected cells and run on native gels (personnel communication N.Gilbert).

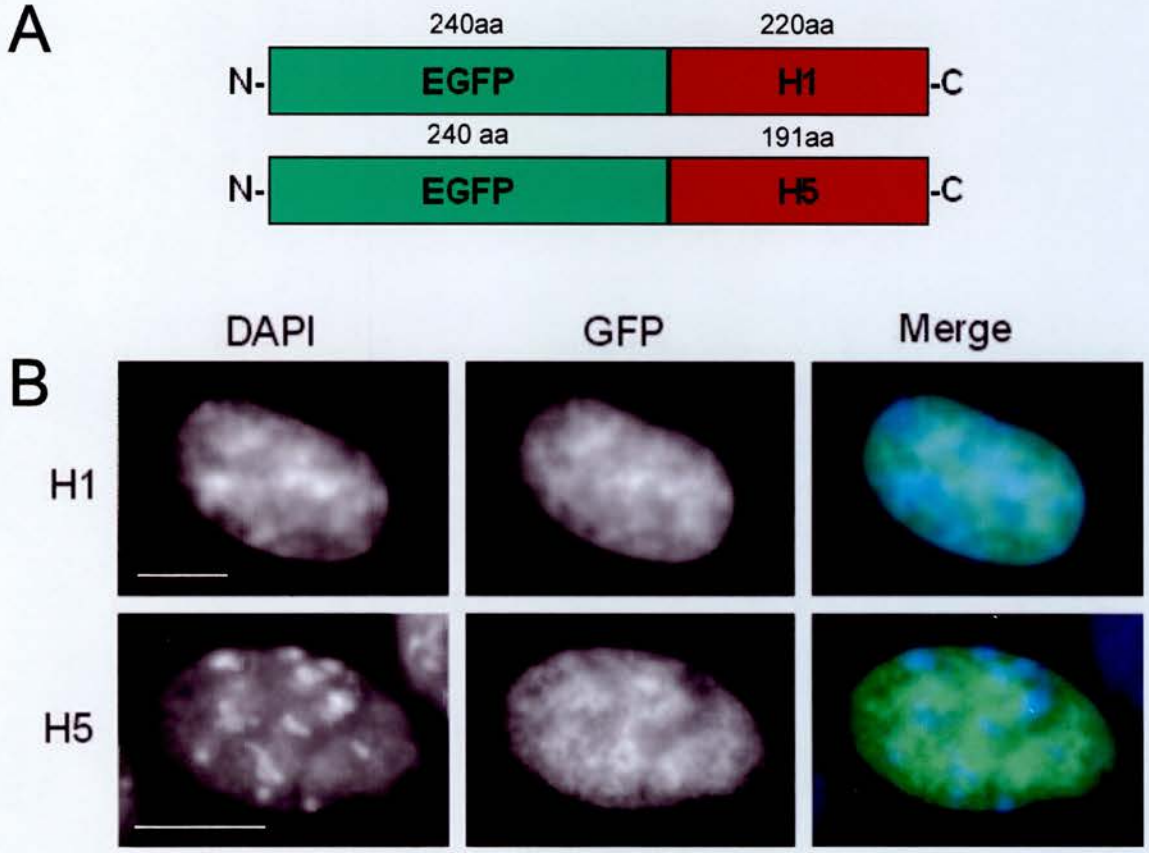

Figure 4.1: EGFP tagged linker histones and their expression. A) Fusion constructs encoding H1 and H5 with EGFP tags at the N terminus were used to measure the mobility of linker histones in different cell types. B) To ensure the EGFP tag did not disrupt the binding of the linker histone to chromatin, both constructs were transiently transfected into HT2 ES cells. Cells were then fixed and stained with DAPI.Scale bars= 10μm.

4.2 FLUORESCENCE RECOVERY AFTER PHOTOBLEACHING

4.2.1 Wild-type ES cells:

Previous recovery halftimes for H1 in somatic cells ($t_{1/2}$ = ~20-50 s Misteli et al., 2000; Hendzel et al., 2004; Phair et al., 2004) have shown that H1 is relatively immobile compared to many other chromatin associated proteins, but more mobile than the core histones (Kimura and Cook 2001, table 1.1). I transiently expressed EGFP tagged H1 and H5 in wild-type mouse ES cells and measured the subsequent mobility of the EGFP tagged linker histone approxiamately 24 hours after transfection. The mobility of EGFP-H1 and EGFP-H5 was measured in 10 wild-type ES cells transiently expressing each fusion protein. Cells expressing very high levels of tagged linker histones as judged by the cellular level of EGFP were excluded from the analysis as over expression of the fusion protein may saturate the cell, resulting in free unbound EGFP tagged linker histones able to freely diffuse around the nucleoplasm. This would then affect the results of the FRAP experiment by increasing the rate of fluorescence recovery. A selected region of interest (ROI) was irreversibly photobleached in each cell and images of the whole cell captured every 7 seconds for a total of 340 seconds, at which time fluorescence had fully recovered.
Analysing the region of interest (ROI) presented a problem as experiments were performed on live rather than static cells. FRAP is concerned with the fluorescent intensity of a ROI before and after photobleaching, however even over the course of 340 secs, ES cell nuclei rotate and move across a culture dish, and can in some cases drift out of focus. Hence at the end of each experiment the ROI is in a different position, and direct comparisons of before and after cannot be performed.

To address this, each image from a time series was processed with IPLAB v3.6 scripts that enabled images to be aligned and the rotation corrected. These are described in box 4.1 and shown in figure 4.2 (P.Perry, v3.6 IPLAB scanlytics).
To investigate H1 and H5 dynamics correctly aligned FRAP data sets were analysed. To calculate the loss of fluorescence attributed to the imaging process alone, the sum of the pixel intensity for the whole cell in each image of a time series was measured using a third IPLAB script that interactively segmented the nuclear edge, with a

defined threshold value. Using a normalisation equation (section 2.6.12), the relative fluorescence intensity over time was calculated for each defined ROI. This was averaged over 10 cells and plotted against time.

Figure 4.3.a shows the relative recovery of fluorescence of the bleached area for wild-type ES cells. This data represents the average recovery of each time point for 10 different cells. The recovery kinetics of EGFP-H5 are slower than EGFP-H1 and recovery half times of H1 and H5 were approx. 50s and 70s respectively. As well as having a slower recovery time, H5 also had a larger immobile fraction (~20%) when compared to H1 (~15%).

4.2.2 ES cells carrying mutations affecting DNA and histone methylation

As both DNA methylation and methylation of H3K9 have interrelated roles in heterochromatin formation, the mobility of linker histones in ES cells lacking both DNMT3a and 3b (herein called Dnmt 3$^-$) (Okano et al., 1999), lacking MeCP2 (Guy et al., 2001), and lacking both Suv39h1 and Suv39h2 (Peters et al., 2001) were examined. Dnmt 3$^-$ cells in which the Dnmt3b mutation (Dnmt $^{3res)}$ has been rescued by a transgene were also analysed (Jackson et al., 2004).

Dnmt 3$^-$ cells, at the time of their establishment showed small reductions in the level of CpG methylation (Okano et al., 1999). Since then, prolonged culture has resulted in the further massive losses of methylation and only 0.6% of CpGs remain methylated when compared to wild-type ES cells (~70%) by nearest neighbour analysis (Ramsahoye, 2002; Jackson et al., 2004). Both the MeCP2 $^-$ and Dnmt 3 ^{res} cells have near normal levels of methylation. Although DNMT3b is concentrated at areas of heterochromatin in mouse cells (Bachmann et al., 2001), exogenous expression in the Dnmt 3 ^{res} cells has resulted in the remethylation of both major and minor satellites and B2 repeats. B2 repeats are short interspersed repetitive DNA sequences found in more than 10^5 copies scattered throughout the genome. Levels of H3K9me3 in Dnmt 3$^-$ cells are normal, although AcH3K9 levels have increased

BOX 4.1 Alignment and analysis of fluorescence after photobleaching images

Individual frames from each time series were grouped together to create a movie of the cell over the analysis period. Using IPLAB scripts each movie was processed to correct for nuclear rotation and cell movements as follows:

1.To correct for cell movement the script, Segmented centriod is used. This isolates the first image of a time series (cell pre-bleach) and the signal in this image is then subjected to interactive segmentation. The user can increase or decrease the threshold of segmentation to determine the appropriate threshold for clearly defining the nuclear edge (figure 4.2.b).

2.The area and centroid co-ordinate of each image in the stack is then calculated, using the defined segementation value. Each image is then re-aligned, so that the calculated centroid of each image overlays the previous.

3. A second script called Interactive rotate is then used to correct for nuclear rotation. The first image in a stack is shown as red, and the second as green, superimposed on the calculated centroid. Here, the second image can be rotated around the centroid to the left or right to ensure the exact overlaying of the second image with the first (figure 4.2.c)

4. Each remaining image in the stack is then manually rotated, with the first image of the stack presented as the reference each time.

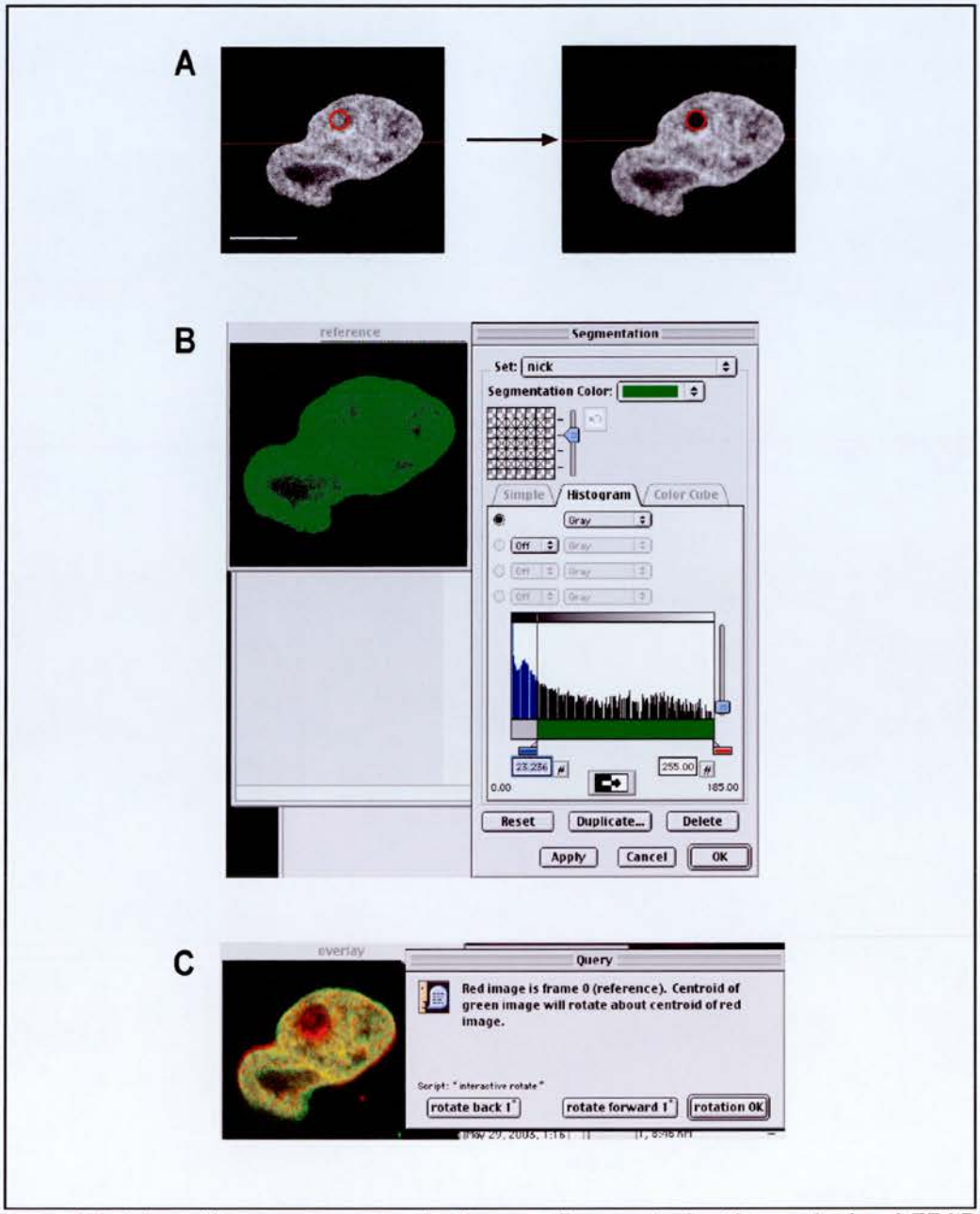

Figure 4.2: Interactive programmes for image alignments for the analysis of FRAP data. A) Image analysis was required to quantify the loss of fluorescence within a cell in FRAP experiments. ES cells transiently expressing GFP-tagged H1 or H5 were bleached at a region of interest (ROI,red circle). Scale bar = 10μm (A). Each series of images taken at regular time periods before and after photobleaching are then segmented at the nuclear edge using a defined threshold value. The calculated centriod of each cell nucleus is then used to stack images on top of one another (B). This corrects for cell movement. C) Each image (green) in turn is then superimposed upon the pre-bleach image of each stack (red), and interactively rotated around the calculated centriod of the nucleus to correct for nuclear rotation.

100% (personnel communication N.Gilbert, Jackson et al., 2004). Upon "rescue" of DNMT3b, levels of DNA methylation are restored, whilst AcH3K9 remains elevated.

Suv39h double null (dn) ES cells, lack H3K9me3, have more diffuse H3S10 phosphorylation and enriched levels of H4K12 acetylation at heterochromatin (Peters et al., 2001). These cells also lack DNA methylation at major satellite sequences (Peters et al., 2001; Lehnertz et al., 2003).

FRAP experiments were carried out and analysed as described for wild-type ES cells and figure 4.3 shows the relative recovery of fluorescence of the bleached ROI for each mutant ES cell line compared to wild-type ES cells. Again, this data represents the average recovery of each time point for 10 different cells.

The recovery kinetics of both EGFP-H1 and EGFP-H5 were slower in Dnmt 3^- cells when compared to wild-type ES cells (figure 4.3.a and 4.4). Recovery half-times (t ½) for EGFP-H1 increased from ~50 seconds in wild-type cells to 70 secs in Dnmt 3^- cells, and the values for EGFP-H5 increased from 70 secs to 100 secs (figure 4.3.a). Alongside altered kinetics of recovery, the fraction of EGFP-H1 and EGFP-H5 that was immobile was greater for both H1 and H5 in the Dnmt 3- cells when compared to wild-type ES cells (table 4.1).

These altered kinetics of linker histone binding are due to the lack of DNA methylation *per se*, rather than the loss of subsequent methyl-CpG-binding of MeCP2, as the mobility of EGFP-H1 and EGFP-H5 in cells carrying mutations in this gene was indistinguishable from wild-type (figure 4.3.b).

Dnmt 3^- cells as well as lacking DNA methylation have elevated levels of histone acetylation. Altering histone acetylation levels using the HDAC inhibitor TSA has been shown to increase the mobility of H1 (Misteli et al., 2000). In agreement with this, Dnmt 3^{res} with normal DNA methylation levels but increased histone acetylation levels display very rapid turnovers of both EGFP-H1 and EGFP-H5 (figure 4.3.c). This was reflected in the shorter recovery half times of both EGFP-H1 and EGFP- H5, which were only ~25-28s and in the decreased level of immobile EGFP-H1 and EGFP-H5 (table 4.1). These were both considerably different to wild-type ES cells. Figure 4.4 shows examples of FRAP experiments upon transiently

expressed GFP tagged EGFP-H5 in wild-type, Dnmt 3^{-} and Dnmt 3^{res} ES cells. In these images, the altered kinetics of EGFP-H5 binding can be seen.

Despite links between DNA and histone methylation, the absence of SuVar39h has no effect on the general binding of H1 or H5 to chromatin (figure 4.3.d). Recovery half times of both the wild-type *Suvar* and the mutated ES cells are similar. The wild-type *Suvar* and the *Suvar 39h* dn cell lines both display increased recovery half times for EGFP-H1 and EGFP-H5, when compared to the wild-type Dnmt3^{-} cells. However EGFP-H1 mobility is still faster than EGFP-H5. Although the recovery half times are similar, the amount of immobile protein is reduced in the mutant cells. All recovery half times and immobile fractions are summarised in table 4.1.

4.3 DISCUSSION

Previous studies have implicated DNA methylation in chromatin compaction, especially at sites of constitutive heterochromatin (Brown et al., 1995; Schmid et al., 1984; Karymov et al., 2001; Ma et al., 2005). However it has not been shown whether alterations in chromatin compaction due to DNA methylation, are at the level of the nucleosome, the chromatin fibre or the tertiary chromatin structure. By using FRAP in ES cells with different epigenetic backgrounds I have shown that the mobility kinetics of EGFP-H1 in mouse ES cells is similar to that seen in other cell types and that DNA methylation can directly affect the chromatin structure.

The FRAP experiments I performed show EGFP-H5 has a slower turnover than EGFP-H1 suggesting it is bound more tightly to the chromatin fibre. Given the role of H5 in inducing the repression of large proportions of the genome when injected into mammalian cells (Bergman et al., 1988), and its proposed function to compact chromatin in the absence of HP1 proteins in chicken erythrocytes (Gilbert et al., 2003), this finding is not unexpected. Moreover, H5 (pI=12.18) has a higher basic charge than H1 (pI= 11.03), which suggests it is able to bind more tightly to DNA.

In addition, tighter binding of linker histones to chromatin in the absence of DNA methylation was seen. Recovery times are normal in MeCp2^{-} cells suggesting this is

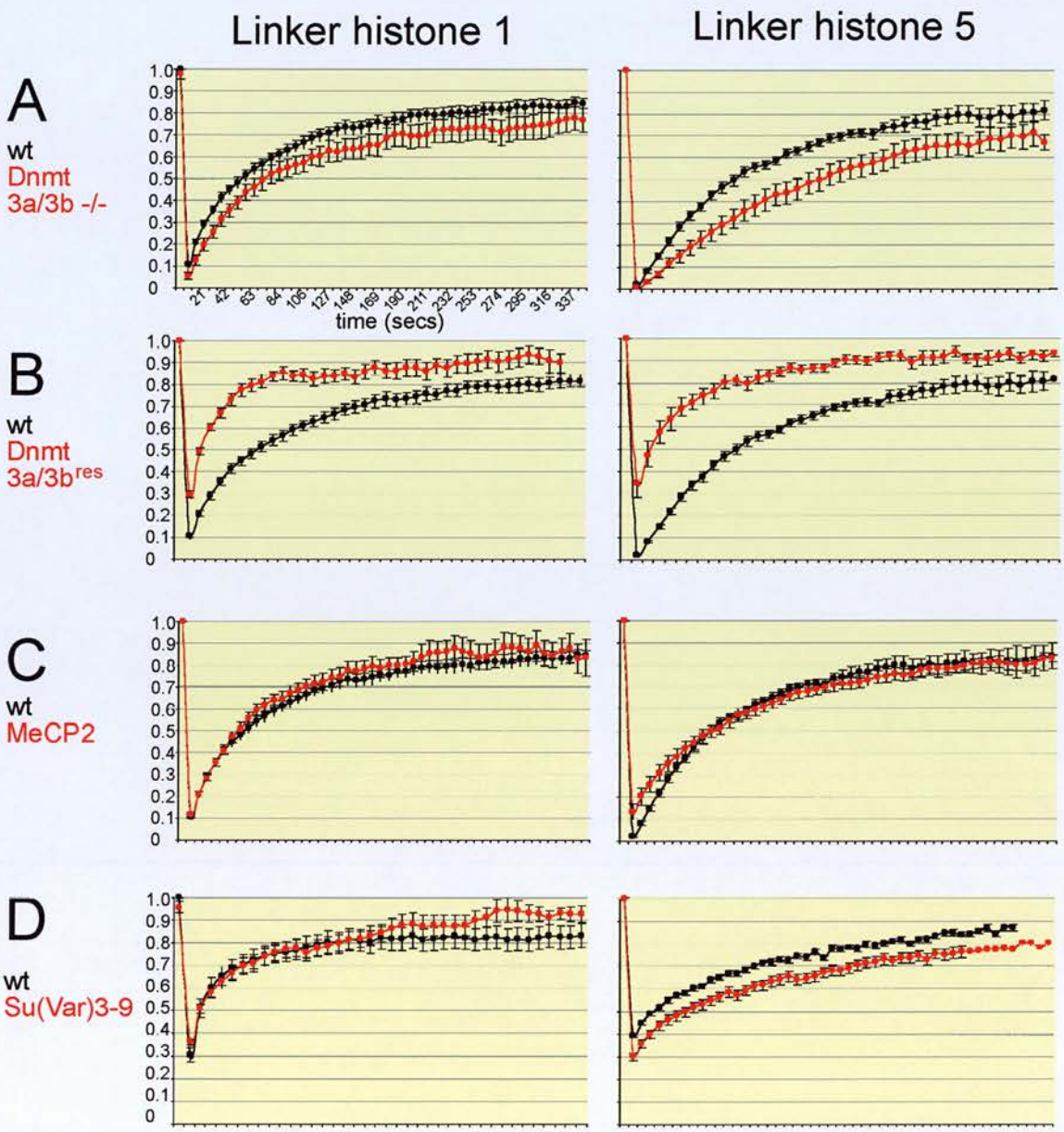

Figure 4.3. Fluorescence recovery after photobleaching recovery curves. EGFP tagged H1 and H5 were followed in FRAP experiments. The recovery of the relative intensities of defined ROIs in each cell was calculated and the average data from 10 different cells from each cell line plotted. Error bars= s.e.m. Cell lines are as described in the main text.

Figure 4.4: The mobility of H5 is altered by loss of DNA methylation and increased histone acetylation. Images taken from FRAP experiments performed in three different cell types at set time points, show the altered dynamics of H5 binding, upon the photobleaching of a ROI (red circle) in each cell. When compared to FRAF in wild-type ES cells, ES cells in which there is no DNA methylation (*Dnmt 3a/3b -/-*) take longer to recover their fluorescence within the ROI. In cells in which the Dnmt 3b mutation has been rescued by a transgene (Dnmt 3^{res}), the opposite is seen. Recovery of the photobleached area when compared to the wild-type ES cells is significantly quicker.

H1

Cell line	Immobile fraction (%)	T half (in secs)
wt	15	50
Dmnt 3a/3b -/-	22	70
Dnmt 3^{-res}	10	25-28
MeCP2 -/-	15	53
SuVar(3-9) parent line	18	30
SuVar(3-9) -/-	7	32

H5

Cell line	Immobile fraction (%)	T half (in secs)
wt	20	70
Dmnt 3a/3b -/-	30	100
Dnmt 3^{-res}	8	25-28
MeCP2 -/-	20	64
SuVar(3-9) parent line	20	45
SuVar(3-9) -/-	13	47.5

Table 4.1: Summary of FRAP kinetics and immobile linker histone populations in different epigenetic backgrounds.
For a description of each cell line see text.

the direct effect of the absence of DNA methylation and not an indirect effect due to the loss of methyl-CpG binding proteins. DNA methylation could primarily control gene transcription by altering the structure of the chromatin at the level of the nucleosome.

Cell lines in which there was more rapid recovery of fluorescence, i.e. , Dnmt 3^{res} and Suvar39h wt and Suvar3-9 dn, were not be photobleached at the start of experiments to the same extend as cell lines which recovered more slowly, despite indentical photobleaching conditions. This is due to some recovery of fluorescence between the time the cell was photobleached and the first image was captured (~ 3 secs). Increased photobleached did increased the amount of photobleaching at the start of experiments in these cell lines, but in order to make direct comparions with other cell lines, the level of photobleaching was not increased.

Recently it has been shown that linker histones can inhibit chromatin remodelling enzymes in the absence of phosphorylation (Horn et al., 2002). Phosphorylation of H1 has also been shown to result in a quicker recovery time in FRAP experiments (Dou et al., 2002). Therefore by altering the binding kinetics of linker histones, DNA methylation could also influence the activity of Swi/snf, Mi-2 or ISWI complexes. This in turn could have a direct impact on mechanisms of transcriptional regulation that are mediated by DNA methylation. Other factors that may alter the binding of H1 to chromatin include the methylation of the histone residue K26 by PRC2. This modification can induce HP1 binding and phosphorylation of the adjacent S27 (Daujat et al., 2005).

Dramatically decreased residence times of EGFP-H1 and EGFP-H5 are observed in Dnmt 3^{res} cells. These cells have normal DNA methylation levels but increased levels of acetylation. Increased histone acetylation has previously been implicated to increase the turnover of H1 (Misteli et al., 2000).

Mutations in *Suv39h1* and *Suvar39h2*, affect only a subset of the chromatin (i.e. constitutive heterochromatin) in ES cells, hence no alteration in the binding kinetics of either H1 or H5 in the Suv39 dn cells may be due to these mutations affecting only a small proportion of the cellular chromatin. However DNA methylation is also concentrated at sites of pericentric heterochromatin within mouse cells, and the effects of its absence on linker histone binding were still seen. To

address whether the binding of linker histones specifically at heterochromatin is affected in Suvar39h dn ES cells, FRAP experiments, in which either euchromatin or heterochromatin is bleached could be performed. However, such experiments have two main obstacles. Firstly, to distinguish between euchromatin and heterochromatin may prove problematic. In mouse ES cells stained with DAPI, bright patches of stain are associated with centromeric heterochromatin, on this basis brighter patches of EGFP expression within a cell nucleus transiently expressing either EGFP tagged H1 or H5 may also correspond to heterochromatin. However as figure 4.1.b shows, while brighter patches of EGFP tagged H1 generally do overlap heterochromatin, EGFP tagged H5 does not. Expression levels of EGFP may therefore be an inaccurate measure of hetero- or euchromatin. Secondly, the foci of heterochromatin in ES cell nuclei are relatively small and ES cells themselves are quite dynamic. In the time between selecting a small area and bleaching it, the cell has in many cases moved slightly. This can result in a different area being bleached from that selected. This slightly altered ROI could contain a mixture of euchromatin and heterochromatin.

Although there is no difference in the recovery kinetics between the *SuVar39* parent cell line and the *SuVar39* dn ES cells, the fraction of immobile linker histones is reduced in cells lacking the Suvar39 HMTases, suggesting their may be a small effect of these mutations upon chromatin structure. It would be interesting to study the recovery kinetics of EGFPH1 and EGFPH5 in *SuVar39h* dn ES cells before and after differentiation. During differentiation large proportions of the genome are transcriptional silenced and levels of H3K9me3 increase. Therefore the lack of SuVar39 HMTases may have a more pronounced affect on the binding of linker histones in differentiated cells.

In summary, DNA methylation can induce changes in chromatin structure. In its absence, linker histones are more tightly bound to the chromatin fibre. Given the role of DNA methylation in gene repression, it might have been expected that the opposite would be true i.e. in the absence of DNA methylation, the chromatin fibre becomes less compact and the linker histones are not bound as tightly. My results therefore suggest that DNA methylation effects linker histone binding at the level of the nucleosome and not at the level of either the 10 or 30nm chromatin fibre.

CHAPTER 5

THE RADIAL DISTRIBUTION OF CHROMOSOMES IN THE MOUSE

It is now generally accepted that the three dimensional organisation of the human genome correlates to gene density (Croft et al., 1999; Boyle et al., 2001) with gene poor chromosomes found towards the nuclear periphery and gene-rich chromosomes towards the interior of the nucleus in several different cell types, including human ES cells (Wiblin et al., 2005). However, in addition to a gene density related radial positioning of chromosomes, it has recently been proposed that a size related distribution can exist in some cells which have flat-ellipsoidal nuclei such as fibroblasts (Cremer et al., 2003; Bolzer et al., 2005). The spatial organisation of chromosome territories (CTs) is conserved in other vertebrates including new and old world primates and the chicken, spanning over 300 million years of evolution and irrespective of highly divergent karyotypes (Habermann et al., 2001, Tanabe et al., 2002a, Tanabe et al., 2005b). In all of these organisms the chromosomes have widely different gene densities from each other and most of the chromosomes are either metacentric or sub-metacentric. In contrast, the mouse genome is very different. Although the size of the mouse genome is comparable to the human genome (approx. 3000 MB of DNA), it is arranged on 20 pairs of similarly sized acrocentric chromosomes (figure 5.1). In addition, the mouse genome does not contain any such thing as a gene -rich or gene poor chromosome; genes are more evenly spread across the whole genome (the mouse genome consortium, www.ensembl.org). To determine the parameters that contribute to spatial organisation of the murine chromosome, I have chosen to analyse the radial distribution of mouse chromosomes in undifferentiated and differentiated mouse embryonic stem (ES) cells.

Chromosome:	1	2	3	4	5	6	7	8	9	10	11	12	13	14	15	16	17	18	19
Chr.size(Mb):	195	182	161	154	149	150	133	129	124	131	122	115	116	117	104	99	94	91	61
Genes per Mb (x10-6):	8.4	10.7	8.6	10	10.3	9.7	14.8	10.2	11.7	9.4	16	5.5	8.8	8.8	9.5	8.7	13.2	7.5	14.2

Figure 5.1: The mouse karyotype. Schematic of the mouse genome showing the differences in size and gene content of mouse chromosomes.Chromosomes containing rDNA in mouse cells analysed are indicated by a (*).

5.1 EMBRYONIC STEM CELLS

Studying the spatial organisation of the mouse genome in mES cells will allow the genome organisation in undifferentiated pluripotent cells to be compared with that of terminally differentiated cells, and will address the question of when during development chromosome positioning is established. In humans, ES cells already have a gene-density related radial organisation but there is evidence of some specific differences with differentiated cells (Wiblin et al., 2005). Two recent studies have suggested that CTs are found at different positions in different mouse cell types, and both propose that the mouse genome is organised in a tissue specific manner (Parada et al., 2004; Kim et al., 2004). Similarly, the architecture and positioning of chromosome 1 has been shown to be different in chicken cell lines at different stages of haematopoietic differentiation (Stadler et al., 2004).

Mouse embryonic stem cells (mES) are pluripotent cells derived from the inner cell mass of a 3.5dpc embryo, and have the ability to remain pluripotent for innumerable cell divisions (Evans and Kaufman 1981). The pluripotency of mES cells gives them the unique property of being able to differentiate into cell types from all three germ layers, and the ability to produce an animal (Bradley et al., 1984; Nagy et al., 1993). *In vitro* differentiation can be induced by the withdrawal of Leukaemia inhibitory factor (LIF), and the addition of retinoic acid (RA) (Smith et al., 1988). ES cells can be maintained indefinitely in an undifferentiated state in culture through a mechanism of self-renewal in the presence of the cytokine, LIF (Smith et al., 1988). However even under these culture conditions, ES cells can spontaneously differentiate. Thus in order to obtain a homogenous population of undifferentiated cells, HT2 ES cells were used for my analysis. These cells are a derivative of the CGR8 cell line and express a hyg-TK gene (Lupton et al., 1991) under the control of the *Oct4* promoter (Hitoshi, unpublished). The use of the hyg-TK gene allows positive and negative selection to be used in these cells. The hygromycin phosphotransferase portion of the fusion gene allows positive selection of *Oct4* expression in undifferentiated cells, whilst the HSV-1 TK portion of the gene allows negative selection. Cells expressing HSV-1 TK convert ganciclovir into a cytotoxic

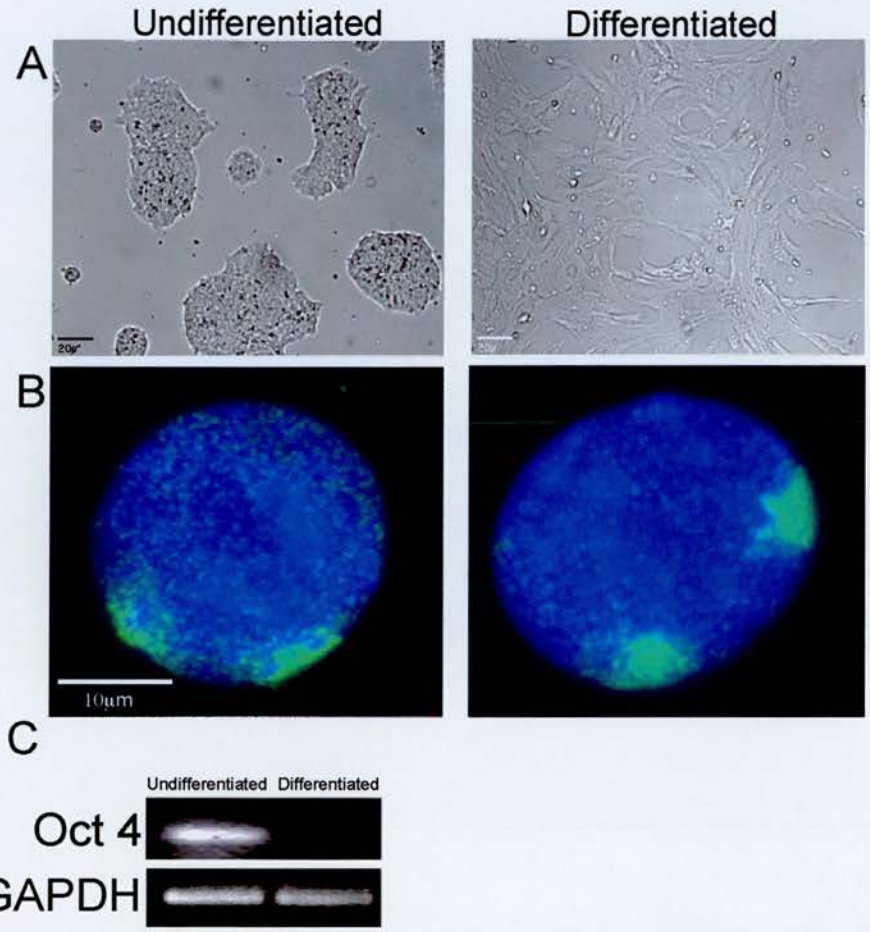

Figure 5.2: Differentiation dramatically changes the appearance of ES cells and results in the silencing of *Oct4*, however chromosome territory morphology stays the same.
A:Brightfield images of undifferentiated and differentiated cells. B:2D FISH analysis of chromosome territory positioning using whole chromosome paint for chromosome 5 in undifferentiated and differentiated mouse ES cells. C:RT-PCR showing the silencing of *Oct4* in differentiated cells, with GAPDH used as a positive control.

nucleotide. Therefore, ganciclovir can select for cells in which *Oct4* is no longer expressed. *Oct4* is an important POU domain transcription factor that regulates multiple genes (Nichols et al., 1998) and is expressed in blastomeres, pluripotent early embryo cells and the germ lineage (Rosner et al., 1990; Scholer et al., 1990). It is also essential to maintain ES cells in an undifferentiated state (Matin et al., 2004). *Oct4* is down regulated as stem cells differentiate making HT2 cells ideal for studies of differentiation. Undifferentiated cells can be selected for using hygromycin and selected against by using ganciclovir, as this will kill any cells still expressing TK. Undifferentiated HT2 cells were grown for 7 days in 100μg/ml of hygromycin before harvesting and analysis of chromosome territory positioning was carried out. Figure 5.2.b shows the dramatic change in the morphology of ES cells as they become differentiated. Undifferentiated ES cells grow in small tight colonies, with a spherical nucleus and very little cytoplasm. In contrast, differentiated ES cells have a flatten appearance with more cytoplasm and resemble fibroblasts (figure 5.2). Despite the obvious changes in cellular morphology, the appearance of CTs detected by FISH is generally the same in both cell populations.

5.1.2 The radial distribution of chromosomes

The 2D radial position of each chromosome (except chromosomes X and Y) was analysed using 2D FISH with whole mouse chromosome paints (Cambio), as described in box 5.1. Figure 5.3 gives examples of the three main types of radial distribution observed within my analysis.

The analysis I performed in undifferentiated mES cells reveals an enrichment of most chromosomes towards the edge of the nucleus (figure 5.4). A comparison of the percentage of total chromosome signal present in segments 5 and 4 of the nucleus was shown to be significantly different to the percentage of signal in segments 1 and 2 by Students paired t tests ($p<0.05$ for every chromosome except MMU14). The only exception to this is chromosome 14 ($p=0.93$). This could be due to exclusion of territories from the nucleolus, which is frequently found in the centre of the nucleus and central location of centromeric heterochromatin, which is not detected by the chromosome paints. In addition the 2D analysis performed splits the nucleus into

BOX 5.1: 2D analysis of the radial distribution of mouse chromosomes:

The radial distribution of each mouse chromosome was analysed using 2D FISH with commercial mouse whole chromosome paints (Cambio). The distribution of chromosome paint signal in an interphase nucleus was then analysed using a previously designed analysis script (Figure 5.3, Croft et al., 1999). For each chromosome, fifty fluorescent images from a single plane of focus were captured and processed in turn. To capture images, slides were scanned in a methodical manner, from one side to the other and only intact cell nuclei with two clear territories captured. To calculate the distribution of signal across a nucleus, the Dapi signal was outlined and the total area of the nucleus (i.e. the Dapi signal) calculated. This area was then divided into five concentric shells of equal area (Figure 5.3), with segment 1 at the edge of the nucleus and segment 5 in the middle. The intensity of the Dapi and the fluorochrome signal (i.e chromosome paint signal) were then calculated per segment. The relative intensity (%dapi/% fluorochrome) of signal per nuclear segment was calculated over fifty images to allow the generation of a distribution curve of the mean value of paint signal over the cell nucleus. This data is graphed as a histogram and examples of the typical data obtained for different distributions of chromosome territories are shown in Figure 5.3.B. A straight line through 1 represents an equal distribution of DNA/chromosome paint in each nuclear shell, suggesting random distribution. Enrichment of signal in the outer segments suggests a localisation towards the periphery and enrichment in the inner segments, an internal chromosome location.

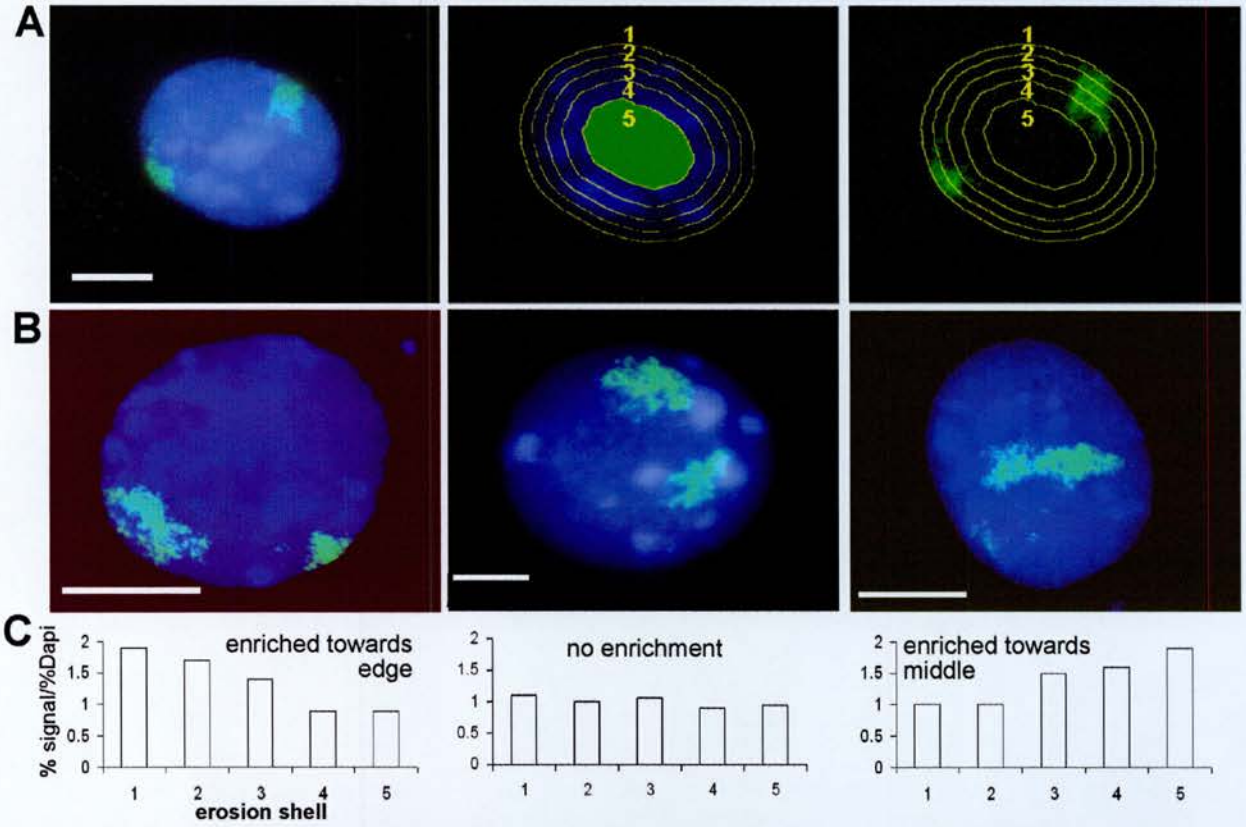

Figure 5.3:2D analysis of the radial distribution of chromosome signal across an interphase nucleus. A) 2D FISH images of interphase nuclei with whole chromosome paints were analysed using a script to divide the cell nuclei into 5 segments of equal area. The amount of flurochrome signal in each segment was then calculated, indicating the radial distribution of a chromosome territory across the nucleus. The amount of signal present in each segment can then be graphed (C). B) shows examples of chromosome territories in different positions and C) shows examples of the graphs obtained for each of these images. Scale bars represent 10 μm.

five segments of equal area but does not take into account nuclear volume, most of which is found in the outer nuclear segments. Despite the similar distributions for each chromosome territory, a Fisher least significant difference (LSD) test using the percentage of signal present in each segment, for each of the 50 images captured per CT, reveals significant differences in the positioning of some chromosomes (Table 5.1). For example chromosomes 1 and 13 appear to be very peripheral, and chromosomes 9, 14 and 19 are the most internal.

Chromosome 1 is the largest chromosome and chromosome 19 the smallest. Several studies have suggested that size is an important factor governing radial positioning with smaller chromosomes in more internal nuclear locations (Bridger et al., 2000; Sun et al., 2000; Cremer et al., 2001; Bolzer et al., 2005). To investigate this in more detail, chromosome size was plotted against the % of CT signal in the outer two segments (1 and 2) (figure 5.5). Spearman rank-order correlation, was then used to determine if a correlation existed between chromosome size and position and whether this was significant. This test returned a r_s value of 0.526, suggesting both a positive and significant ($p=0.021$) correlation between chromosome size and territory signal across the nucleus. Regression analysis also identified chromosomes 13 and 14 as outliners in this analysis.

Why chromosome 13 should have a very peripheral location is not clear, and the more internal positioning of chromosome 14 was initially thought to be due to the presence of less centromeric chromatin on this chromosome (figure 5.6). HT2 ES cells, like several other mouse cell lines have less centromeric DNA on chromosomes 8 and 14 (figure 5.6). However, analysis of the radial position of chromosome 8 would suggest centromeric DNA does not have a significant effect on chromosome position. Centromeric DNA is highly repetitive and the centromere is composed of a large block of heterochromatin, traditionally associated with gene silencing and enriched at the nuclear periphery.

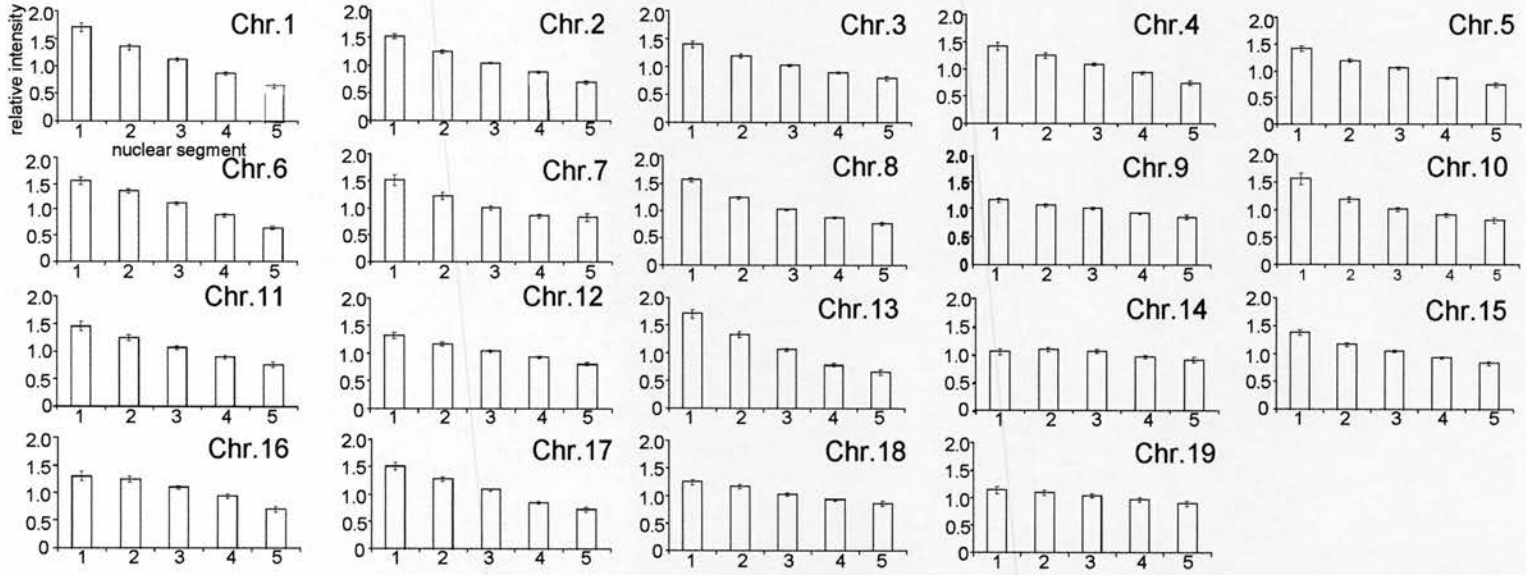

Figure 5.4 : Mouse chromosome territories are enriched towards the nuclear periphery. The location of each chromosome territory within the cell nucleus was mapped as described in figure 5.3. 50 images of interphase nuclei were analysed for each territory and the average signal in each nuclear segment graphed.errors bars=st.dev

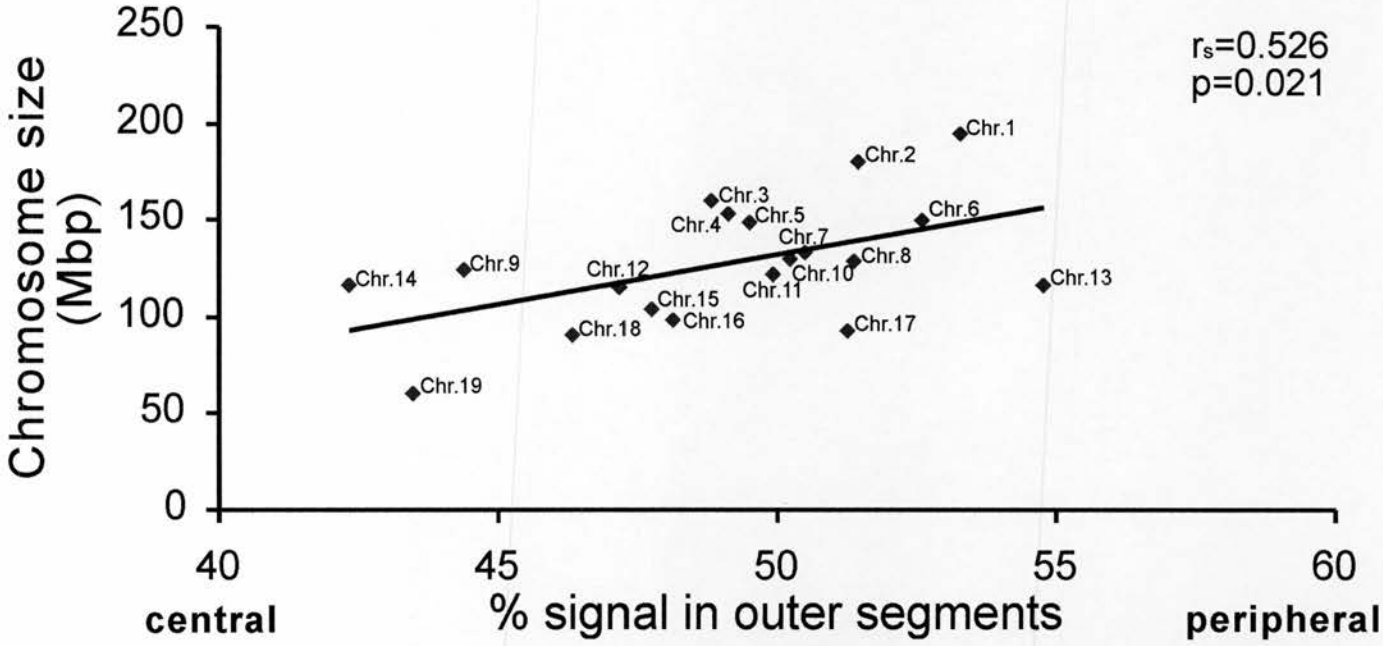

Figure 5.5. A correlation between chromosome size and position exists.
A dotplot of chromosome size plotted against the % of chromosome signal found in the outer two segments of the nucleus suggests a correlation between size and position.

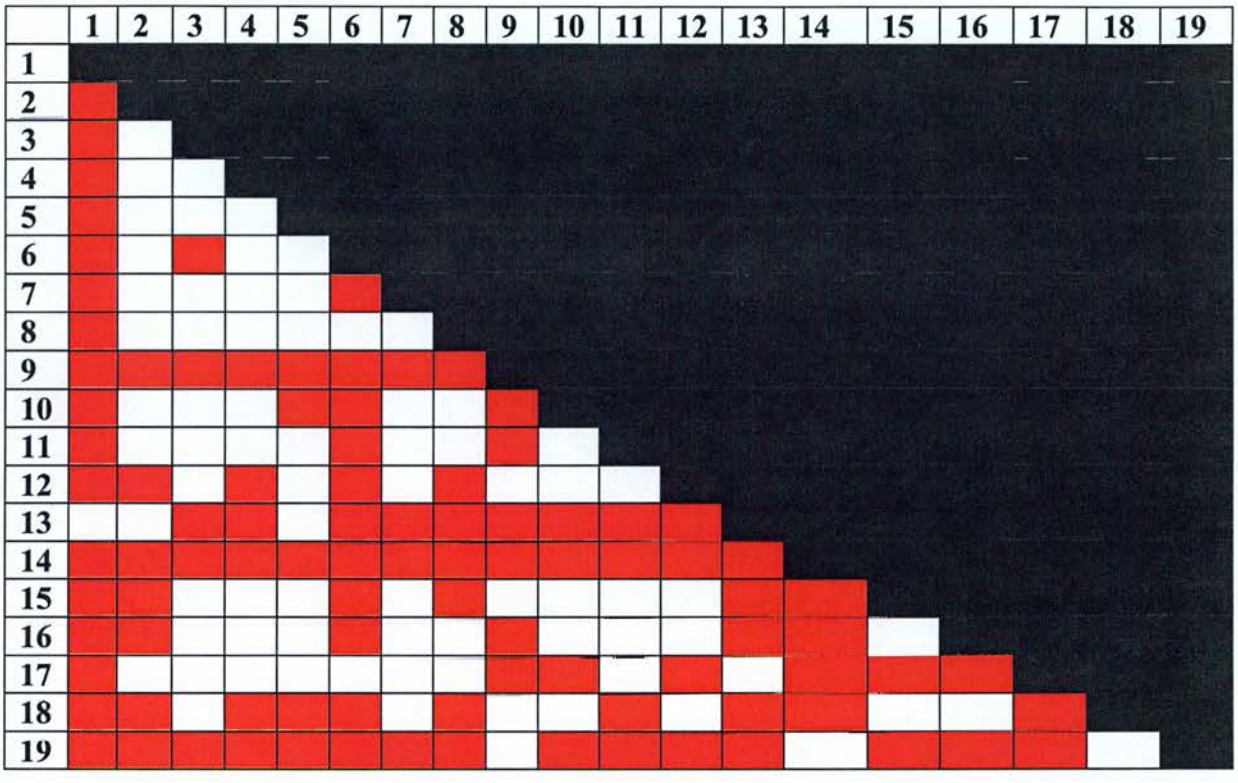

Table 5.1: Summary of the differences in radial positioning between chromosomes. Results of a Fishers LSD test to show which pairs of chromosome territories have significantly different radial positioning. Chromosomes that are different to one another are represented by a red box. Where no significant difference exists, the chromosome numbers are met with a white box.

However, 2D analysis of centromere positioning using a probe against minor satellite sequences (Kipling *et al.,* 1994) in undifferentiated mES cells shows only a slight enrichment of centromeres towards the periphery ($p<0.05$). Minor satellite sequence is composed of tandem arrays of a 120bp repeat (Wong et al., 1990, Rattner et al., 1988, Kipling et al., 1991) and is found adjacent to a large block of major satellite DNA on the short arm of the mouse chromosome (Pietras et al., 1983, Wong and Rattner 1988, Joseph et al., 19890. In differentiated ES cells, centromeres appear enriched both at the periphery and at the centre of the nuclei. A Student paired t test shows that the distribution of centromeres in undifferentiated and differentiated are statistically different ($p<0.05$). Centromeres have been shown to cluster together at the nuclear periphery in mouse lymphocytes (Weierich et al., 2003), however centromere clustering has not yet been examined in mouse ES cells. The internal localisation of some centromeres could reflect the association of NOR containing chromosomes with the nucleolus (figure 5.7).

NORs are regions of ribosomal gene repeats, which together form the basis of the nucleolus as they recruit all the processing and assembly components required for ribosomal biosynthesis to it (e.g. Spector 1990, Lawrence et al., 1988, Carmo-Fonseca et al., 1991). As NOR regions preferentially associate with the nucleolus any chromosome containing one of these regions may be expected to be found in a more internal location. In Humans, the acrocentric chromosomes 13,14,15,21 and 22 containing rDNA preferentially localise with the nucleolus (Bobrow and Heritage 1980, Sullivan et al., 2001). In mice, NOR regions have been mapped to the chromosomes 12,15,16,17,18 and 19 (Dev et al., 1977), but these regions vary in size and location amongst inbred mouse strains. In HT2 ES cells, I mapped rDNA to chromosomes 12,16,18 and 19 using FISH with a probe against the coding regions of human 18S and 28S rDNA (figure 5.7) (Sullivan et al., 2001). As chromosomes 16,18, and 19 are also amongst the smallest mouse chromosomes, it is extremely difficult to tell whether the subtle differences observed in their radial positioning when compared to larger chromosomes, are due to size or the presence of a NOR. However, chromosome 12 when compared to the two chromosomes closest to it in size e.g. 11 and 13, does have a less pronounced enrichment to the periphery, which may be due to the presence of a NOR. Likewise chromosome 17, which does not

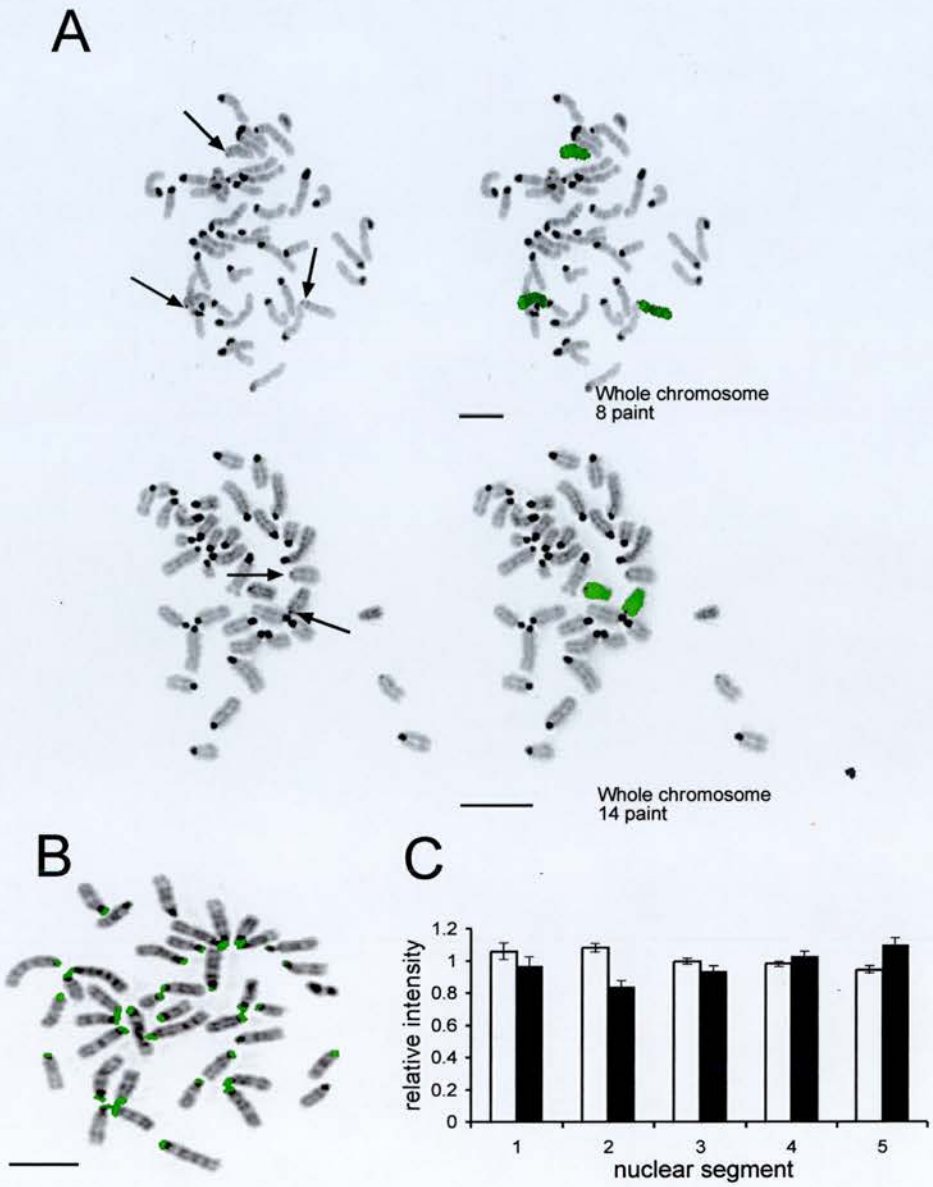

Figure 5.6: HT2 mouse chromosomes 8 and 14 are depleted in centromeric DNA and centromeres show no obvious radial distribution when mapped in 2D. A:2D FISH using whole chromosome 8 and 14 paints reveals that chromosomes 8 and 14 are depleted in centromeric DNA. B: A probe against minor satellite was used to analysis the radial distribution of centromeres. C:In both differentiated and undifferentiated ES cells, centromeres have an even radial distribution across the whole nucleus, when analysed in 2D.Unfilled bars represent undifferentiated cells and filled bars, differentiated cells. error bars=st.dev The scale bars in each image represent 10μm.

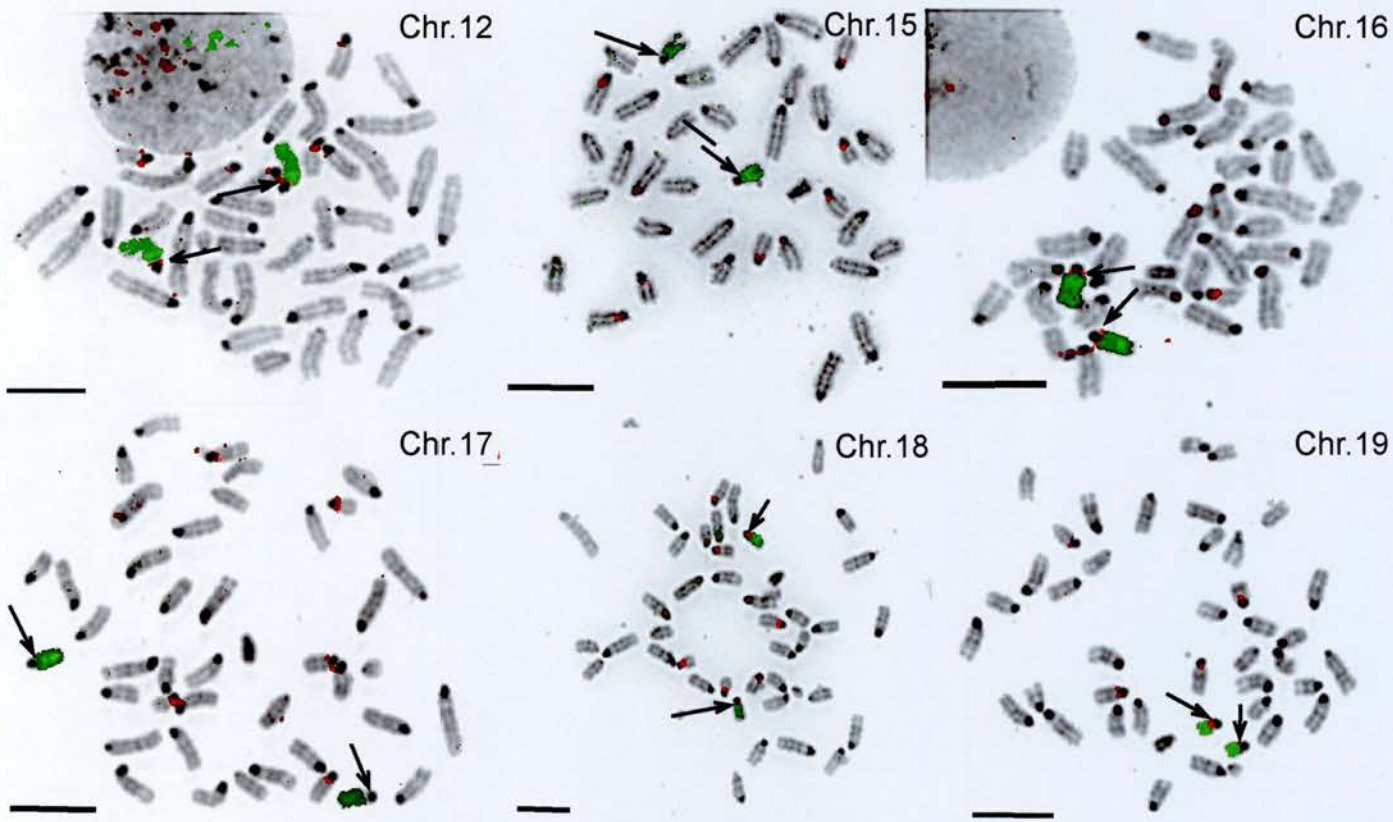

Figure 5.7: HT2 chromosomes 12,16,18 and 19 contain rDNA. 2D FISH using whole chromosome paints and a probe against human 47s rDNA was used to map chromosomes containing rDNA.The scale bar in each image represents 10μm.

contain rDNA, is found in a more peripheral location when compared to its nearest neighbours chromosomes 16 and 18, which do.

Only one other chromosome stands out as having a different radial distribution when compared to the rest of the genome, MMU9. No obvious reason for this can be found.

5.2 THE EFFECT OF DIFFERENTIATION UPON RADIAL CHROMOSOME POSITIONING

It has been suggested that chromosome position is altered in different murine cell types (Kim et al., 2004, Parada et al., 2004). Therefore I examined the radial distribution of chromosomes in mES cells after differentiation. Differentiation may have effects on the global organisation of the nucleus as many genes become permanently silenced or induced as cells differentiate down specific lineages. For example there is a dynamic reorganisation and clustering of centromeres in differentiating mES cells (reviewed by Arney and Fisher, 2004), C2C12 myoblasts differentiating into myotubes (Arney and Fisher, 2004), and differentiating promyelocytic leukaemia cells (Beil et al., 2002). Furthermore the positioning of several genes can undergo dynamic changes depending on transcriptional status (Brown et al., 1997; Francastel et al., 2001; Skok et al., 2001; Williams et al., 2002; Chamberyon and Bickmore, 2004).

The protocol used to differentiate HT2 ES cells was an adaptation of that used by Chamberyon and Bickmore, 2004. Cells were differentiated using RA, a potent inducer of differentiation, which is able to induce cells to differentiate primarily into endoderm-like or fibroblast-like cells (figure 5.2) (Smith et al., 1988). Undifferentiated cells were selected against using ganciclovir and to ensure that no undifferentiated cells remained and only differentiated cells had been obtained, RT-PCR was performed using primers for *Oct4* (figure 5.2). *Oct4* expression was only detected in the undifferentiated cell population.

To determine if changes in gene expression brought about by differentiation affect the global positioning of chromosomes, 2D analysis of the radial positioning of

chromosomes 1,5,6,7,10,13, and 15 was carried out as described previously in differentiated HT2 cells (figure 5.8). Chromosomes 1 and 13 were selected for this analysis as they are very peripheral in undifferentiated cells (figure 5.5). Chromosomes 5, and 15 were chosen as previous studies have suggested these chromosomes have several locations in different murine tissues (Parada et al., 2004). Chromosome 6 was analysed, as this is the location of the gene *Nanog* that has essential roles in self-renewal, and is highly expressed in ES cells (Chambers et al., 2003). Moreover, it is also surrounded by other several stem cell genes and in humans *Nanog* is found on chromosome 12, which has recently been reported to have different positions in differentiated and undifferentiated human cells (Wiblin et al., 2005). MMU6 shares around 30Mb of synteny with the p-arm of HSA12. Finally chromosomes 7 and 10 were analysed as the positioning of these chromosomes has not previously been investigated in differentiated murine cells. Paired Student t-tests comparing the radial positioning of each chromosome before and after differentiation showed there to be no significant changes in position for chromosomes 1,5,7,10, and 15($p < 0.05$ for each test). However, for chromosomes 6 and 13 there is. Chromosome 13 shows a small but significant movement towards the nuclear interior in differentiated ES cells, whilst chromosome 6 shows a more substantial change in nuclear location, also towards the nuclear interior.

5.3 3D ANALYSIS OF CHROMOSOME POSITIONING

All the data discussed so far has been of chromosome signals in a 2D image. This is generally representative of the 3D situation (Bridger et al., 2000, Mahy et al., 2002a). However to confirm this, 3D FISH was used to determine the nuclear localisation of a small subset of chromosomes. This type of analysis is a lot more technically demanding and the statistics of 3D modelling a lot more complex.

3D FISH was performed on chromosomes 5,7 and 15 in undifferentiated ES cells and 20 Z stacks at 0.3μm steps for each chromosome were captured (figure 5.9a). These were deconvolved using "Microtome" software (Scanalytics Corp, Fairfax, VA), which uses a constrained iterative frame algorithm (Agard & Sedat

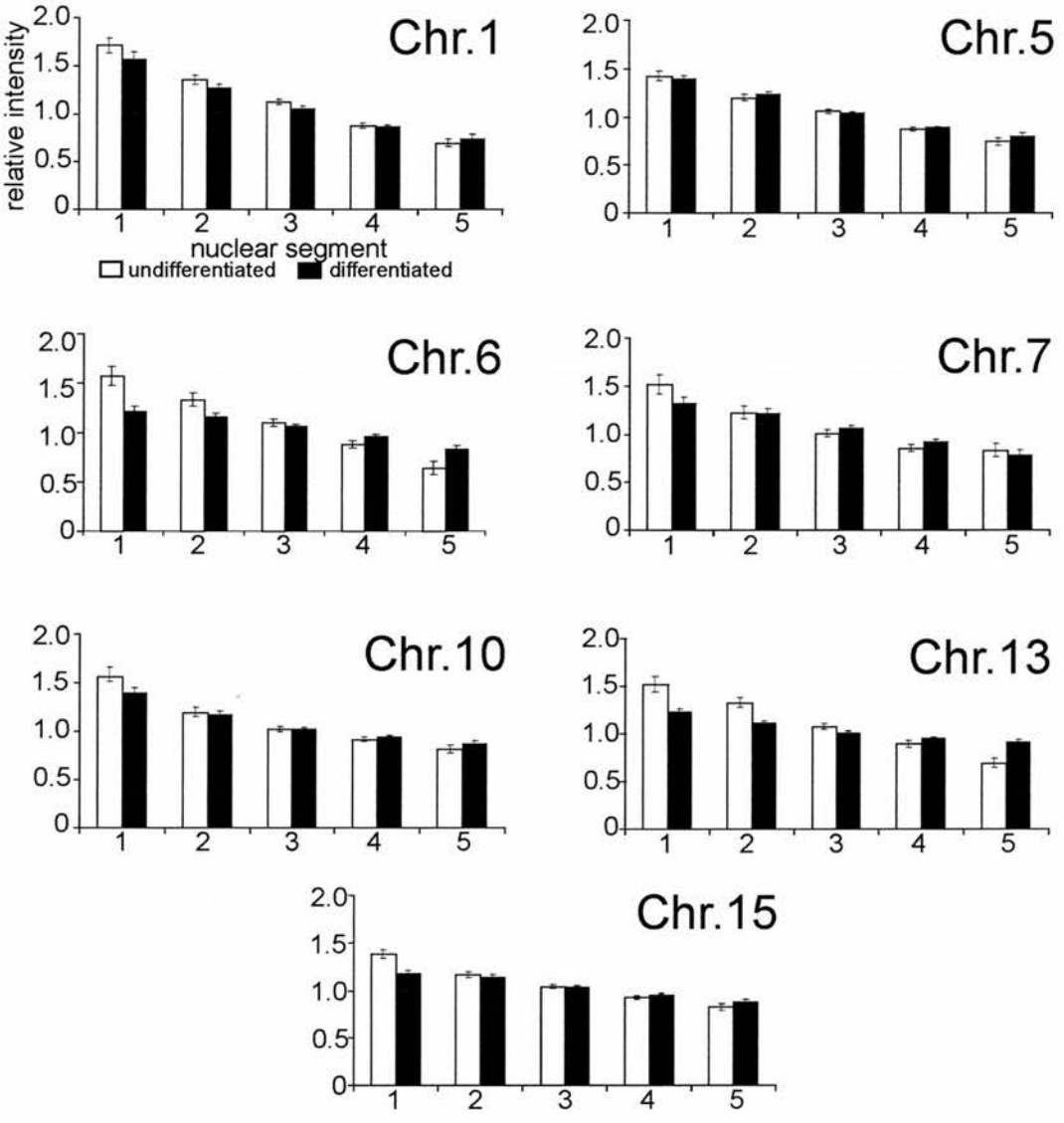

Figure 5.8: Differentiation of ES cells can affect the radial distribution of a subset of chromosomes. Graphs showing the radial positioning of chromosomes before and after differentiation.error bars=st.dev

(UCSF)) to remove out of focus haze from an image. The Z slice containing the greatest amount of chromosome signal was then calculated using IPLAB software. From this the weighted centroid of the chromosome territory could be located. This co-ordinate was taken to be the middle of the CT and from this the distance of the territory from the edge of the nucleus was calculated both along the x and y-axis. This was converted to a fraction of the total length of the radius along each axis with the edge as 0 and the centre as 1. The percentage of territories located at each of the fractional distances was plotted (figure 5.9).

The results obtained agree with the 2D analysis of these chromosomes, which suggests chromosome 5 is the most peripheral, followed by chromosome 7 and then chromosome 15. Chromosome 5 is peripheral even along the z axis and chromosomes 7 shows enrichment of chromosome signal towards the edge of the both the x and y axes as in agreement with the 2D FISH result, although the result is not as pronounced.

The discrepancies observed between the 2D and 3D data may be able to be explained by the analysis performed. Firstly, the 3D data was from a relatively small sample number of cells (n=20), whereas for each chromosome in 2D the sample size is larger (n=50). Secondly, the analysis performed here, is less accurate than that performed on the 2D data. Deconvolution does not remove all of the out of focus haze from an image, making it particularly difficult to determine the exact top and bottom of a cell, differences of one or two extra stacks at the top or bottom of a cell will have significant effects on the positioning of a territory along the z axis. The amount of nuclear volume captured in each z slice will also differ significantly from the top to the bottom of the cell, with the middle z slices containing the most nuclear volume, it therefore follows that more chromosome signal is found in these slices. The position of territories along the x and y-axis is determined manually from a single co-ordinate calculated to be the centre of the CT, to the nuclear edge. Both the distance from the centre of a territory to the edge and the radius of the nucleus are determined manually and may be subject to error. If these measurements could be automated this error would be significantly reduced. A much more accurate analysis of chromosome positioning in 3D would be to split the nucleus into segments of

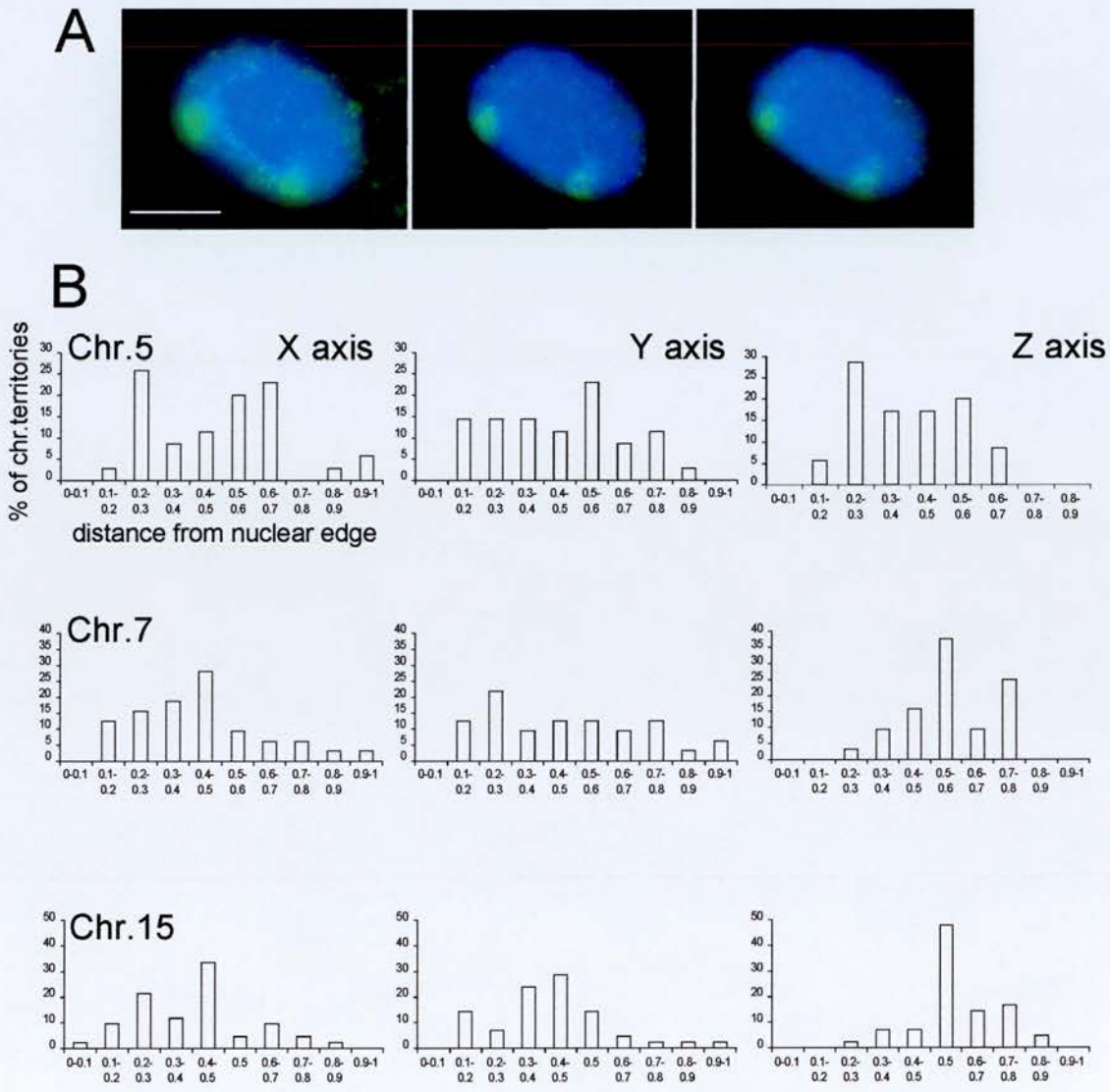

Figure 5.9: 3D analysis of chromosome territory positioning. A) Images taken at 0.3 μm intervals through the Z axis of a HT2 ES cell probed with whole chromosome 5 paint. Scale bar=10 μm. B) Graphs showing the positioning of chromosome territories along the z,y and x axis of the cell nuclei.

equal voxels and calculate the amount of signal in each segment, as used in the 2D analysis and the 3D analysis by other groups (Cremer et al., 2001; Parada et al., 2004; Kim et al., 2004). Such software is presently unavailable to our group.

5.4 THE EFFECT OF GENE EXPRESSION ON RADIAL POSITIONING

Although the mouse genome does not contain any chromosomes greatly enriched in gene content, do chromosomes containing a higher proportion of expressed genes have more internal locations? Figure 5.10 plots the gene content of a chromosome against the % of CT signal present in the two outer nuclear segments. This shows a positive correlation between gene content and position (Spearman rank order correlation r_s=0.533, p=0.019). This is similar to the correlation between size and position. Chromosomes with low gene density are more peripheral. To address whether chromosomes containing a higher proportion of expressed genes are located more towards the interior of the nucleus, the results of a microarray experiment investigating gene expression in undifferentiated and differentiated ES cells was used (Tanaka et al., 2002). The portion of expressed genes located on a particular chromosome was compared to the portion of the whole genome located on that chromosome. Therefore chromosomes containing a higher than expected number of expressed genes can be identified and their radial position compared with chromosomes containing a lower than expected number of expressed genes (table 5.2). This analysis was performed using the NCBI build 30 mouse assembly and Ensembl version 18.30.1. Since it was performed in November 2003 updated versions of the mouse genome have been released which suggest the total number of genes per chromosome is slightly different to those used in the analysis.

When looking at genes showing a 100 fold or more enrichment in expression levels in mouse ES cells, several chromosomes appear to have enriched or depleted levels of expressed genes. MMU6 has almost 2 fold more genes expressed than expected in undifferentiated ES cells, based upon the % of the genome located on MMU6 and the % of genes from the microarray assay found there. Chromosome 13 is also enriched in genes highly expressed in undifferentiated ES cells. MMU6 and

MMU13 both move to more internal nuclear positions in differentiated cells (figure 5.8), when genes indentified in the microarray analysis will become silent. This could suggest that large changes in gene expression levels could have an effect on chromosome positioning. However the number of genes in this category is relatively small (78) and when looking at the locations of genes showing a 10 fold or more enrichment of expression, for which there is greater sample size (251), only chromosome 16 appears to have very large difference in the number of expected genes versa the number of observed genes. The radial positioning of chromosome 16 does not indicate any obvious enrichment towards the nuclear interior when compared to chromosomes 15 and 17, the two chromosomes in the genome most similar to it in size and gene content. Although there may well be a subtle influence of the increased number of expressed genes upon the position of chromosome 16, it is hard to differentiate this from other factors such as the presence of a NOR, or its size.

A: Genes upregulated 100 fold in ES cells

Chromosome	Number of genes identified on chromosome	% of genes identified chromosome	Difference between % of the genes identified and the % of genome found on chromosome.	Deviation
1	4	5.1	-0.9	-14.9
2	4	5.1	-3.1	-37.8
3	1	1.3	-3.7	-74.1
4	6	7.7	1.7	28
5	6	7.7	1.8	29.8
6	8	10.3	5.1	99.6
7	7	9.0	0.9	11.8
8	5	6.4	1.6	34.5
9	5	6.4	0.8	14.7
10	2	2.6	2.3	-46.9
11	5	6.4	1.1	-14.8
12	3	3.8	0.4	12.6
13	5	6.4	2.4	58
14	1	1.3	2.3	-64.4
15	4	5.1	1.3	34.2
16	3	3.8	0.6	18.3
17	1	1.3	3.4	-72.4
18	2	2.6	0.0	1.9
19	3	3.8	0.7	20.7
X	3	3.8	0.6	-14

B: Genes upregulated 10 fold in ES cells

Chromosome	Number of genes indentified on chromosome	% of genes indentified on chromosome	Difference between % of the genes indentified and the % of genome found on chromosome.	Deviation
1	18	7.2	1.1	19
2	24	9.6	1.3	15.9
3	9	3.6	-1.4	-27.7
4	19	7.6	1.6	26
5	17	6.8	0.8	14.3
6	10	4	-1.2	-22.5
7	15	6	-2.1	-25.6
8	12	4.8	0	0.3
9	16	6.4	0.8	14.1
10	11	4.4	-0.4	-9.3
11	18	7.2	-0.4	-4.7
12	6	2.4	-1	-30
13	12	4.8	0.7	17.9
14	6	2.4	-1.2	-33.6
15	7	2.8	-1	-27
16	14	5.6	2.3	71.6
17	12	4.8	0.1	3.1
18	7	2.8	0.3	10.8
19	7	2.8	-0.4	-12.5
X	11	4.4	-0.1	-2.0

C: Summary of the distribution of genes across the mouse karyotype

Chromosome	Gene number	% of genome
1	1504	6
2	2058	8.2
3	1237	5
4	1499	6
5	1478	5.9
6	1282	5.1
7	2003	8
8	1189	4.8
9	1394	5.6
10	1205	4.8
11	1877	7.5
12	852	3.4
13	1012	4.1
14	898	3.6
15	953	3.8
16	811	3.3
17	1157	4.6
18	628	2.5
19	795	3.2
X	1116	4.5

Table 5.2. Summary of the location of genes highly expressed in mouse ES cells. Table A: Analysis of location of genes found to be upregulated 100 fold or more in ES cells when compared to trophoblast stem (TS) cells. Table B: Analysis of the location of genes upregulated 10 or more fold. The % of upregulated genes on one chromosome was compared to the % of the total genome found there. Table C: Gene number per chromosome, as used in the analysis, taken from ENSEMBL version 18.30.1.

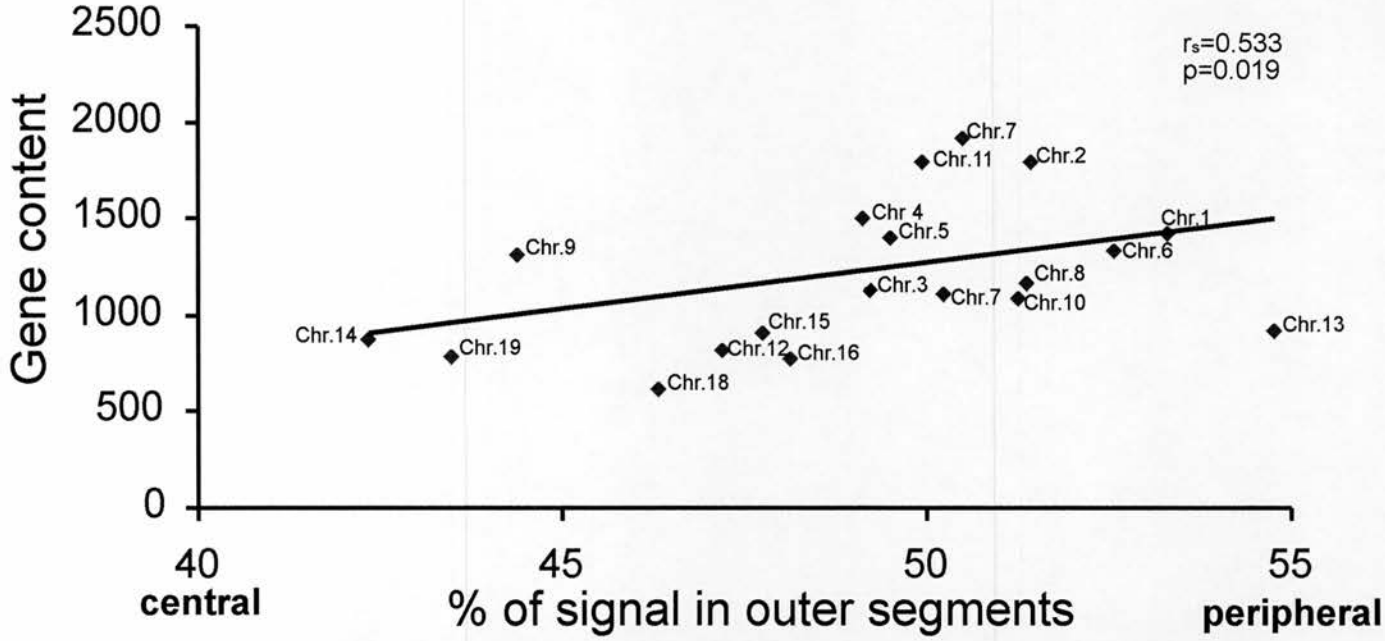

Figure 5.10: A correlation between gene content and position exists. A dotplot of gene content plotted against the average percentage of chromosome signal found in the outer nuclear segments shows a correlation between gene content and position. Chromosomes with higher gene contents are more peripheral.

5.5 DISCUSSION

The most striking characteristic about the radial positioning of mouse CTs in undifferentiated ES cells, is that chromosomes do not show a large range of different positions. Each chromosome tends to be enriched towards the edge of the nucleus, and no chromosome has a clear interior position. This may be due to exclusion of chromosome territories from the nucleolus, the location of undetected centromeres, or due to most of the nuclear volume residing in the outer nuclear segments. However, a positive correlation between chromosome size and position was found, with smaller chromosomes in more internal positions.

This agrees with other studies which also suggest a relationship between size and position in cells with flat/ellipsoid nuclei (Sun et al., 2000; Cremer et al., 2001; Cremer et al., 2003; Bolzer et al., 2005). However, in contrast to fibroblasts and aminocytes, in which a size related radial distribution of chromosomes exists, mouse ES cells have round spherical nuclei, similar to the shape of human lymphocyte nuclei in which a gene density related radial positioning of chromosomes has been reported.

It has been recently suggested by other groups that the mouse genome is organised in a tissue specific fashion. I have found some evidence of this in my studies. Parada and colleagues have analysed the positioning of chromosomes 1,5,6,12,14 and 15 in several primary cell populations, and have proposed differential positioning for each chromosome in at least three different tissues (Parada et al., 2004). In addition, each chromosome was stated to have a significantly different radial position to the other chromosomes studied. This contrasts my results, as I observed several chromosomes with very similar radial locations. Parada and colleagues also noted that the most similar chromosome distributions are in cell types sharing common differentiation pathways, such as large and small lung cells and myeloblasts and lymphoblasts, suggesting that positioning is established during the process of differentiation itself. A second study from the same group has analysed the positioning of chromosome 6 during T cell differentiation alongside the positioning of two key differentially expressed T-cell markers: CD4 and CD8. As the cells began to differentiate down more and more specific lineages differences in the

location of chromosome 6 were noted (Kim et al., 2004). Changes in position were correlated with permanent gene silencing. If this is the case I would expect to see significant differences in the positioning of several chromosomes in undifferentiated and differentiated cells. However, chromosomes 6 and 13 which are enriched in the number of genes expressed in undifferentiated ES cells do show significant differences in position when compared to differentiated cells (table 5.2), suggesting gene expression levels may have some affect chromosome position. To investigate this possibility further, a more comprehensive microarray analysis which takes into account genes up regulated by only two fold in undifferentiated ES cells could be used.

Finally one last study analysing the radial positioning of chromosomes in chicken cell lines as they differentiated down specific haematopoietic cell lineages showed chromosome 1 but not chromosome 8 to alter in positioning and suggested the morphology of CTs changed with differentiation. Stadler and colleagues noted as the cells differentiated territories became more diffuse and in some cases disintegrated in several small domains (Stadler et al., 2004). However, I have noted no obvious changes in the morphology of mouse CTs (figure 5.2.b).

The differences between my results and those of published studies may be due to the cell types being analysed. Both the Parada and Kim studies look at cells from very specific lineages and pure cell populations. The Parada study isolated several primary tissues and tried to minimise the time in culture to as little as possible in order to try and analyse the positioning of chromosome territories *in vivo*. Kim and co-workers have analysed territories in very specific cell populations that they have shown to be over 95% pure. In contrast to this, I have analysed positioning in a more heterogenous population and ES cells and their differentiation in monolayers in culture may be considerably different to differentiation in 3D tissues *in vivo*, nevertheless if chromosome positioning was tissue specific, I would expect to see more differences in positioning between a very pure undifferentiated ES population and a heterogenous population.

The reported differences in positioning between cell types may in part be due to changes in nuclear size and shape, but again undifferentiated and differentiated ES cells have a very different morphology (figure 5.2), and no

difference in the positioning of several chromosomes is apparent. Furthermore chromosome positioning has been shown to be generally conserved in three very different human cell lines: primary fibroblasts, lymphoblasts, and ES cells (Boyle et al., 2000, Wiblin et al., 2005), although a small change in the positioning of chromosome 12 is observed between undifferentiated human ES cells and lymphocytes. The position of chromosome 12 may be altered as this is the location of the IgH locus which has been shown to have different locations in both lymphocyte and mouse ES cells (Skok et al.,2001, Kosak et al., 2002).

I therefore propose that chromosome position is established early in development, and generally maintained during the differentiation of stem cells into different cell types, although large changes in gene expression may induce some changes in position.

Whether chromosome positioning is established by a passive or an active mechanism is still not clear. Positioning may arise as the consequence of other cellular processes, and may simply be the exclusion or association of territories with nuclear bodies, such as the nucleolus. However an active mechanism would imply some functional role of territory positioning. As chromosome 6 and 13 are able to move during differentiation, this would suggest that there may be an active mechanism of chromosome positioning.

Chapter 6 will explore the role of nuclear position in gene expression in more detail.

CHAPTER 6

THE ROLE OF NUCLEAR POSITION IN GENE REGULATION

It is well established in primates and chicken cells that CTs are arranged non-randomly in nuclei (Boyle et al., 2001; Bolzer et al., 2005; Croft et al., 1999). I have also shown in chapter 5, that mouse chromosome territories are non-randomly arranged, in agreement with other published studies (Kim et al., 2004; Parada et al., 2004). These studies suggest that there is a functional constraint to maintain certain portions of the genome at the nuclear periphery. Histone modifications are known to be key determinants in the regulation of gene expression, but little is known about the higher order structures of chromatin and how the spatial organisation of chromatin can effect gene expression. This remains a key question in addressing the role of spatial organisation in genomic function. Changes in nuclear position have been observed to accompany changes in the transcriptional status of a gene in several organisms, which include; *Saccharomyces cerevisiae*, *Drosophila*, *Mus musculus* and *Homo sapiens* (Casolari et al., 2004; Dreesen et al., 1991; Csink and Heinkoff 1996; Chamberyon and Bickmore, 2004; Kim et al., 2005; Brown et al., 1997; Bartova et al., 2000), but only in yeast is there direct evidence that localisation at the nuclear periphery has an impact on gene expression. In yeast, artificially tethering a defective mating type locus to the nuclear periphery was shown to restore its repression, in a SIR dependent manner (Andrulis et al., 1998).

To address directly whether position alone can change the expression of a gene in the mouse genome, I aimed to artificially tether a gene to the nuclear periphery of mouse ES cells (figure 6.1). To achieve this aim I took advantage of the tight binding of the *E.Coli* LacI protein to Lac operator (LacO) array sequences. LacI has been shown to have a very high affinity for LacO sequences (Miller and

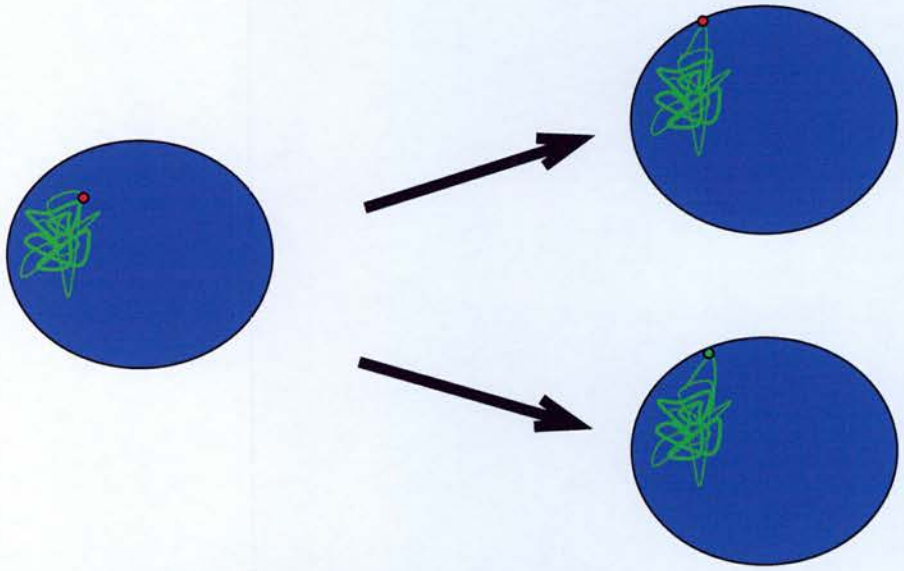

Figure 6.1: Schematic representing how the the role of nuclear compartments in gene regulation will be investigated. By artifically tethering an endogenous gene to the mouse nuclear periphery, the effects of this nuclear compartment upon gene regulation can be investigated (red circle= active gene, green circle= inactive gene).

Rezinkoff 1980), and this system was previously used to study chromatin motion in chapter 3. By inserting Lac operator sequences into or next to genes and expressing a fusion protein of LacI with an integral nuclear membrane protein, I hypothesised that the LacI fusion protein would bind to the Lac operator sequences and drag the gene to the nuclear periphery.

To create an anchoring protein that would localise to the nuclear edge and be able to bind to Lac operator sequences, two fusion proteins encoding myc-tag-LacI and emerin or LAP2β were made (Figure 6.2). Emerin and LAP2β are integral nuclear membrane proteins (section 1.2.8) and have conserved LEM domains. LEM domains are thought to bind chromatin via an interaction with the DNA binding protein BAF (Foisner and Gerace 1993, Shumaker et al., 2001). Both of these proteins are likely to have a role in binding endogenous chromatin to the nuclear periphery, implicating them as endogenous DNA anchors in the mammalian nucleus, therefore it was decided to use both proteins as potential anchors of Lac operator sequences.

6.1 INSERTING LAC OPERATOR ARRAYS INTO ACTIVE GENES

I first inserted LacO sequences into a variety of endogenous mouse genes. To do this, the plasmid pGT1 was modified to contain 16 copies of the Lac operator sequence (appendix1 figure A.1). This vector has previously been used in a gene trap screen in mammalian cells looking for novel chromosomal and nuclear proteins within the lab (Tate et al., 1998, Sutherland et al., 2001). pGT1 contains a β-galactosidase neomycin phosphotransferase (βgeo) reporter gene, which lacks a promoter and ATG but is preceded by a 5' slice acceptor from the mouse *en2* gene. This results in the vector inserting into the intron of an expressed gene such that the reporter is spliced in frame to the gene transcript to create a fusion protein possessing both neomycin (G418) resistance and β-galactosidase (lacZ/β-gal) activities (Freidrich and Soriano 1991) (figure 6.3). Xgal staining to detect β-gal activity is then used to follow the expression of trapped genes. Using a gene trap approach to insert Lac operator

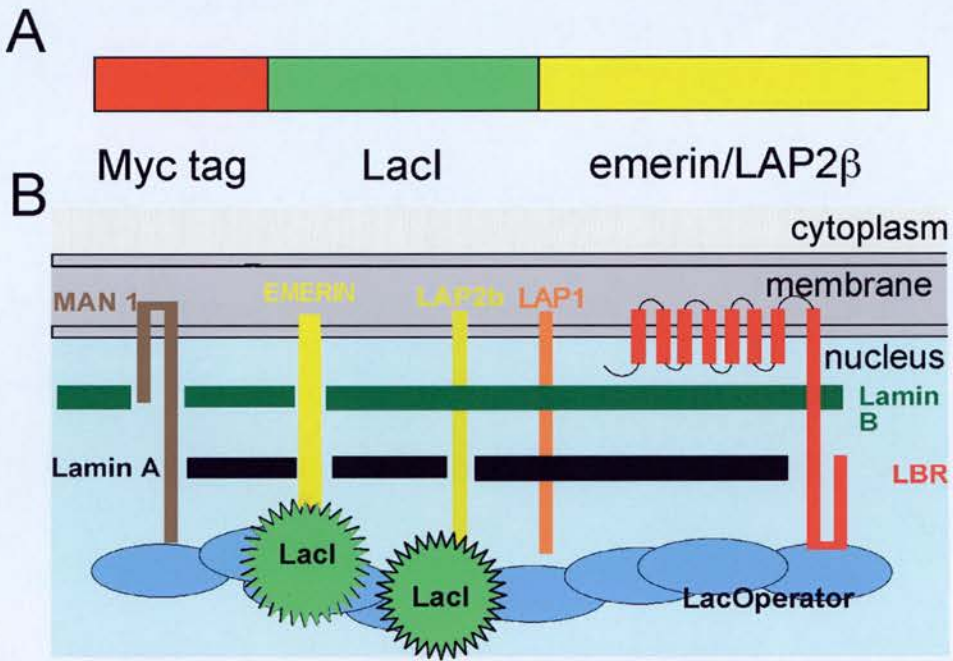

Figure 6.2: Schematic showing how active genes will be tethered to the nuclear edge. A) Schematic of the two fusion proteins created to tether genes to the nuclear periphery.These encode myc-tag for visualisation, and LacI fused to the N terminus of LAP2β or emerin. The N terminal domains of both membrane proteins, protrude into the nucleoplasm. B) How the anchoring proteins will work. Emerin and LAP2β are integral membrane proteins resulting in the localisation of each anchoring protein at the nuclear edge. LacI is known to bind to Lac operator sequence with high infinity, thus this portion of the anchor will bind to Lac operator sequences that have been inserted into active genes and drag them to the nuclear periphery.

sequences into mammalian genes ensures that prokaryotic sequences are kept away from the genes promoter, reducing the likelihood of silencing of the disrupted gene. Previous studies using Lac operator arrays to visualise genes in live cells have generally used arrays covering up to 10kb and containing up to 256 copies of the operator sequence, although a direct repeat less than 1kb has been visualised in *Drosophila* (Marshall et al., 1997). Previously in the lab multiple insertions of a 128-copy array were used to create cell lines with bright GFP tagged LacO loci, which were easily visible *in vivo* (Chubb et al., 2002, Chapter 3). The size of the LacO array inserted into pGT1 will probably not be large enough for trapped genes to be detected *in vivo* using GFP-LacI. However, despite the small size of the array it was hoped that 16 copies would be sufficient for tethering a gene, given the very high affinity of LacI for operator DNA.

Restriction digests with ScaI only, BamHI only, XhoI and NotI, and NotI and ScaI were used to determine in which orientation the LacO array had inserted into the gene trap vector. These indicated that the array had inserted with the NotI site closest to the splice acceptor and the XhoI site downstream of the LacO array (figure A.1). Therefore, linearising pGTXN6 with NotI places the Lac array downstream of the gene trap components and linearising with XhoI places the array upstream of the gene trap components (figure 6.3.c).

pGTXN6 was linearised with XhoI and NotI and electroporated in HT2 mouse ES cells as described Sutherland et al., 2001 and section 2.2.5.2 (figure 6.3). HT2 ES cells are as described in chapter 5, section 5.1.

Colonies were selected for with the antibiotic G418 (conc.200μg/ml) for 10 days and then screened for Xgal activity to determine those containing an expressed trapped gene. Several different expression patterns were observed (figure 6.4). From the 5.6×10^7 cells plated for each transfection, 288 colonies were obtained when the Lac array was placed downstream of the gene trap machinery, by linearising pGTXN6 with NotI, and 196 colonies obtained when the array was upstream, via linearisation with XhoI. In both transfections approx. 55% of the clones showed no Xgal staining and thus were discarded. Colonies that contained no staining could be due to the greater sensitivity of G418 selection when compared to the Xgal stain. In

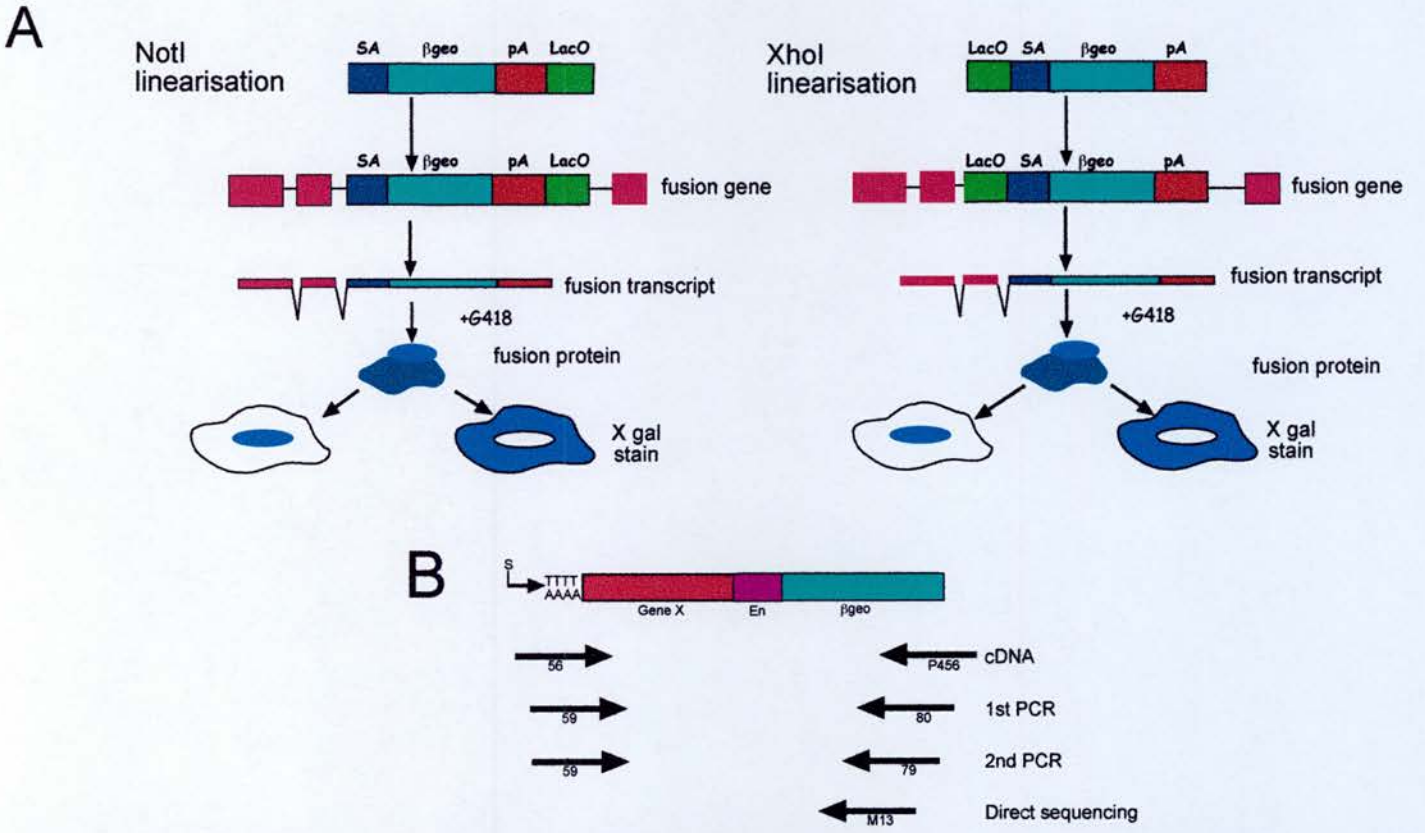

Figure 6.3: Schematic of gene trap and screening strategy. A)pGTXN6 containing the ßgeo reporter gene,is integrated into the intron of an expressed gene downstream of coding exons (stippled boxes). The fusion gene is spliced in frame into the gene transcript via its slice acceptor (SA), taken from the mouse *engrailed* 2 gene (En2). The polyA signal ensures that the gene transcript ends after ßgeo. Linearisation of pGTXN6 with NotI places the LacO array downstream of the SA, and linearisation of pGTXN6 with XhoI places it upstream. pGTXN6 also encodes neomycin resistance, therefore drug selection can identify cells that have integrated pGTXN6 in the correct orientation into an active gene. X-Gal staining was then used to assess the sub-cellular distribution of the resulting fusion proteins. B) The sequence of trapped genes is established by 5'RACE. Products of the second PCR are sequenced directly. Primers used are as described in section 2.1.9.2 and Sutherland et al .,2001.

addition there may have been inactivation of βgal activity in some of the colonies (Tate et al., 1998; Freidrich and Soriano, 1991; Skarnes et al., 1995) Of the remaining colonies a further, 16% and 18%, respectively, stained positive for what is most likely to be misfolded and mislocalised proteins. These are visible as intense spots of stain close to but outside the periphery of the nucleus (figure 6.4). Only colonies, which had staining in the cytoplasm and/or nucleus were kept and grown up for further analysis. In total 69 cell lines were kept that contained the LacO array downstream of the gene trap machinery and 44 with the array upstream. The results of both transfections are summarised in figure 6.4.b.

6.2 CHARACTERISATION OF GENE TRAP CELL LINES

6.2.1. Sub cellular localisation of trapped gene products

A subset of 10 cell lines was selected for further analysis (figure 6.5). These were named depending on the location of the LacO array relevant to the splice acceptor. 6x cell lines contain the LacO array upstream of the splicing acceptor and 6n cell lines have the LacO array downstream of the splice acceptor.

Expression of lacZ in each cell line must be quite strong in order for changes in the expression of a trapped gene to observed upon tethering. In addition understanding the expression pattern of each trapped gene is important in order to understand what changes in expression may take place when genes are tethered. Therefore immunofluorescence using an antibody against βgal (Europa Bioproducts) was used to further characterise the expression of trapped genes at higher resolution (figure 6.5). The subset of cell lines analysed showed a variety of expression patterns: from the cytoplasm (6n 3d4, 6x 4b1) through to nuclear speckles (in cell lines 6n 3b3, 6n 4d1,6x 1c1, 6x 2c6) the nucleolus (cell lines 6x 6d5, 6x 8d3, 6n 11b5) and splicing speckles (6x 7c5) (figure 6.5 and table 6.1).

A

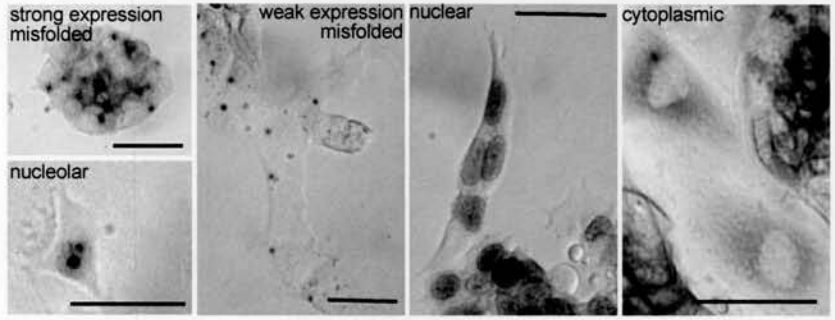

B

	Colonies picked	No stain/no growth	Misfolded protein	Unidentified /mixed Staining pattern	Cytoplasmic	Nuclear	Nucleolar
Lac array downstream (6N)	**288**	**158**	**45**	**21**	**29**	**24**	**2**
Lac array upstream (6X)	**196**	**110**	**35**	**14**	**19**	**15**	**3**

Figure 6.4: Summary of genetrap transfection with pGTXN6.
A)Brightfield images showing examples of Xgal staining patterns of trapped genes in HT2 ES cells. The scalebar represents 20 μm in each image. B)Table summarising the results of each transfection carried out with both forms of the linearised pGTXN6. Cell lines in which the LacO array was downstream of the splice acceptor were named 6N, and cell lines with the LacO array upstream were named 6X.

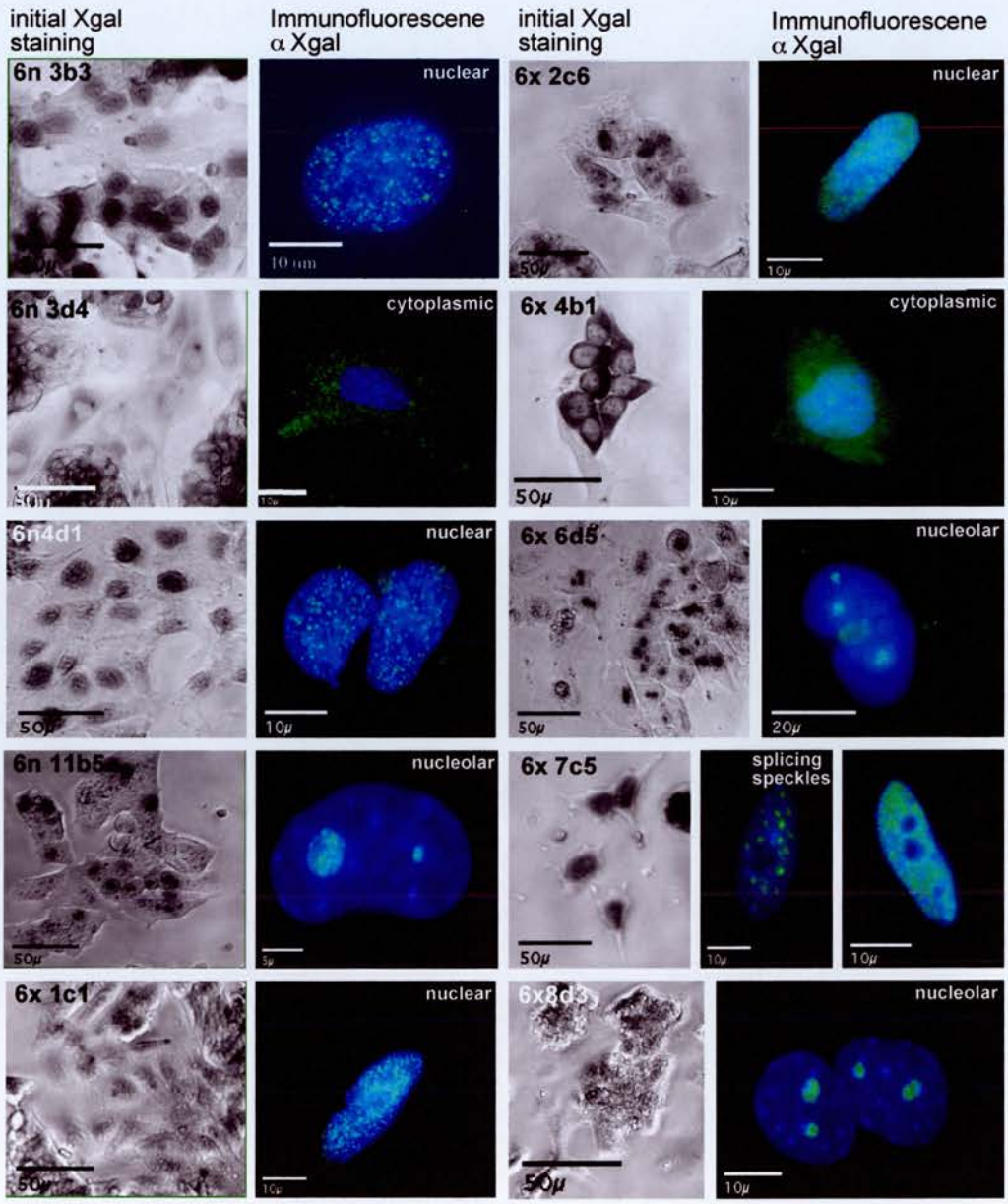

6.5 Characterisation of the expression patterns of the trapped genes in a subset of cell lines. Expression patterns of trapped genes were initially analysed using Xgal staining. Immunofluorescence with antibody that recognises the βgal protein was then used to look at expression patterns in cell lines at higher resolution (blue=Dapi staining, green=βgal protein).Each image has its own scale bar.

6.2.2 Determining the presence of the Lac operator array within trapped cell lines.

The most important factor to determine, was whether gene-trapped cell lines still contained the LacO array as sometimes the ends of a vector are lost, through cell nucleases, when it is transfected into a cell line (Lechardeur et al., 1999; Pollard et al., 2001). Genomic DNA from each cell line was digested with EcoRI and a Southern blot performed with LacO array DNA used as a probe. Digestion with EcoRI should release the LacO array from the trapped gene, as a 400bp fragment. To create the LacO array probe, the plasmid, pJRC35 was also digested with EcoRI, and the corresponding 400bp fragment containing the LacO sequences isolated. For a negative control genomic DNA from a mouse containing an integration of pGT1 was used (gift from H.Sutherland). As a positive control, this same DNA was spiked with 0.1pg of LacO array DNA. 0.1pg of the Lac array DNA should contain as many copies of the array as 10μg of genomic DNA, the amount of DNA loaded onto the blot for each cell line. This is based on the following; each cell has approximately 12pg of DNA and one copy of the LacO array, therefore 10μg of genomic DNA contains 4×10^5 copies of LacO. As the average molecular weight of a single stranded nucleotide is 330kDa, 1 copy of a 400 bp probe will have a molecular weight of 132,000 kDa and as 1 mole of probe will contain 6×10^{23} molecules of the array, then 4×10^5 molecules will weigh $(6 \times 10^{23} / 4 \times 10^5) \times 132000$, which equals 0.1 pg. Figure 6.6 suggests that the Lac array is present clearly as a single integration in at least 4 of the 10 cell lines. These results are summarised in table 6.1. In other cell lines, LacO may have been present at less than one copy per cell and below the level of detection.

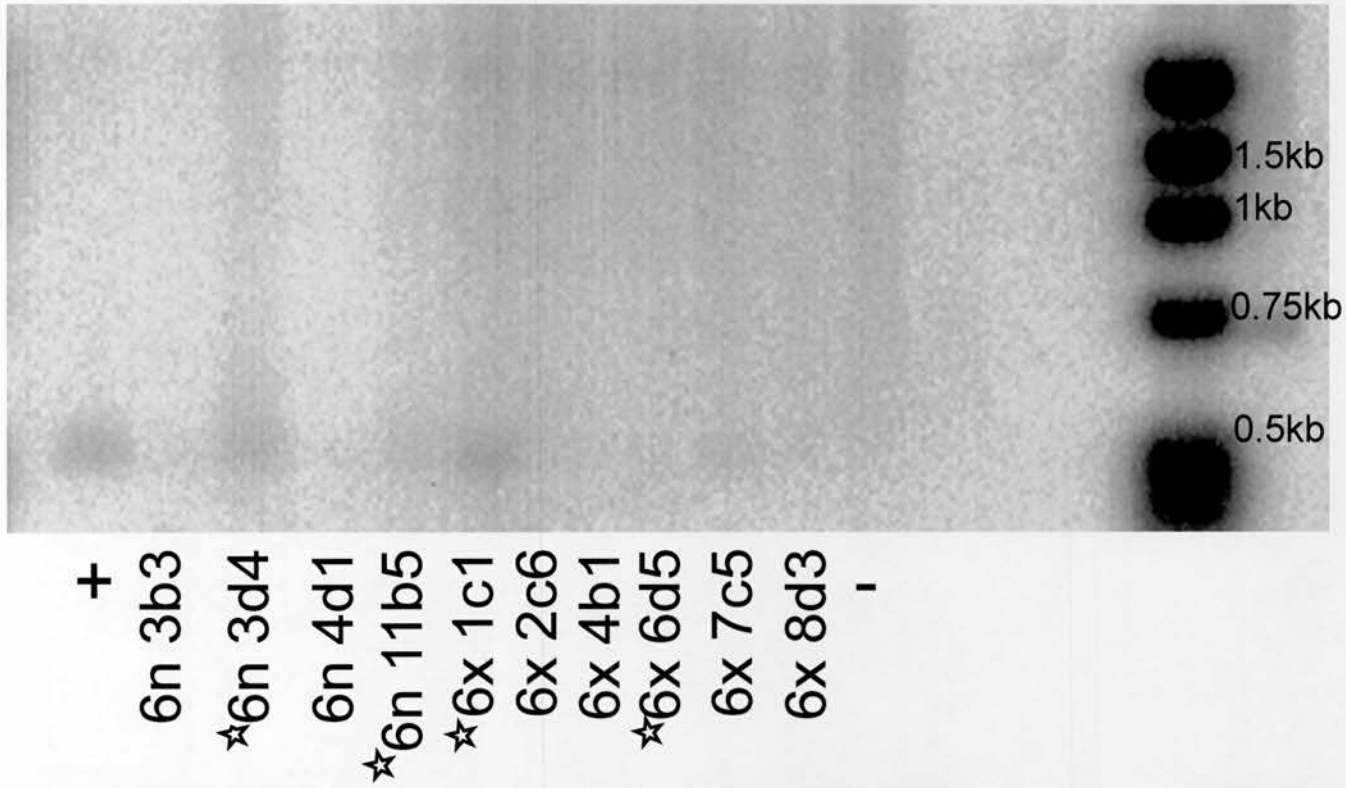

Figure 6.6: Dectection of LacO arrays in pGTXN6-trapped cell lines. Southern blot with genomic DNA from each gene trap cell line digested with EcoRI and probed with Lac Operator sequence shows the Lac array to be present in at least 4 cell lines. Cell lines thought to be positive are indicated by a star. (+= genomic DNA from pGT1 containing mouse spiked with 1pg of pGTXN6 plasmid DNA, - = genomic DNA from pGT1 containing mouse).

6.2.3 Determining the sequences and genomic locations of trapped genes

The sequence of trapped genes was obtained with 5' rapid amplification of cDNA (5'RACE) as previously described (Tate et al., 1998) (figure 6.3), with primers as described in section 2.1.9.2. These sequences were then compared to those in databases using the BLAST algorithm (http://www.ncbi.nlm.nih.gov/BLAST/). The identity of the trapped gene and its genomic location were successfully obtained for seven cell lines (table 6.1). 2D FISH with a probe made from the plasmid pGTXN6 and commercial whole mouse chromosome paints confirmed which chromosome the gene trap had inserted into (table 6.1, figures 6.7). Chromosome paints will hybridise to both copies of a homologous chromosome pair, however the pGTXN6 probe should only hybridise to one copy of the chromosome, as it should only have integrated the genome once (figure 6.7).

Two of the cell lines 6x 1c1 and 6x 2c6 have insertions within the same gene, *erythroid differentiation regulator 1*, found on the pseudoautosomal region of chromosomes X and Y (figure 6.7, figure 6.8). This gene has not yet been assigned a genomic location by ENSEMBL (www.ENSEMBL.org) and has an unknown function, a NLS protein domain, an uncharacterised transcript and no CpG islands, TATA or CAAT boxes in or near its promoter. ENSEMBL can predict the locations of CpG islands and can be used to view the upstream sequence of a gene. Determining the type of promoter for each trapped gene may prove important, as different promoter types may be affected differently by tethering to the nuclear periphery. CpG islands, TATA and CAAT consensus sequences are common components of promoter sequences and can be found in varying combinations in a range of promoters. CpG islands have been reported to be predominantly associated with house keeping genes and genes expressed in the early embryo (Bird, 1984; Ponger et al., 2001; FitzGerald et al., 2004; Schug et al., 2005). In contrast, TATA boxes are associated with tissue specific genes (FitzGerald et al., 2004). *Erythroid differentiation regulator 1*, must lie in a region of the genome particularly prone to insertions as previous gene traps in the lab have trapped this gene in approx. 10% of their clones, and always at the same site within the gene (Sutherland et al., 2001).

The RACE sequences for the cell lines 6N 3b3 and 6x 6d5 have been obtained and used to determine the upstream sequence of both trapped genes through blast searches. Both map to uncharacterised genes. The gene trap vector in 6N 3b3 has inserted relatively near the start of a gene with unknown function called 3110082I17Rik. The RACE sequence also maps the trapped gene to chromosome 5, band G1 (figure 6.7, 6.8). This gene has a bipartite nuclear localisation signal and so is predicted to localise to the nucleus by PSORT (http://psort.nibb.ac.jp/), consistent with the Xgal and immunofluorescence staining results for this cell line (figure 6.5). Furthermore, 6N 3b3 contains the LacO array downstream of the NLS. The transcript is 729bp long with 6 exons, of which the gene has been trapped in intron 2, and the protein is 222 residues in length. The gene also has no CpG island TATA or CAAT boxes in/near its promoter, as determined by ENSEMBL.

The cell line 6x 6d5 also contains an insertion of pGTXN6 in a gene with unknown function, this time the gene is named 2810430MO8Rik and maps to chromosome 1 band H5 (figure 6.7, 6.8). The transcript is 1298bp in length with 5 exons and encoding 281 residues. Again the gene has been trapped in intron 2. The protein encoded by this gene contains a coiled coil domain at residues 108-138. As with 3110082I17Rik, this gene also has no CpG islands, TATA or CATA box in/near its promoter.

The cell line 6N 4d1 contains what is essentially a knock out of *diaphanous-related formin 3* (figure 6.8). This is a member of the Rho family of GTPases that regulate diverse cellular processes ranging from cytoskeletal organization to gene expression and cell transformation (Alberts et al., 1998). The gene trap vector has inserted into the first intron of the *diaphanous-related formin 3* gene knocking out all of the protein domains. The genomic location of this gene is chromosome 14, band D3 and FISH results agree with this location (figure 6.7). Again this trapped gene also has no CpG islands, TATA or CATA box in/near its promoter.

In the cell line 6x 7c5 the vector has inserted into a gene called *SF3b1* or *SAP155*, which is involved in the assembly of the spliceosome. The spliceosome removes introns from the transcripts of pre-mRNA. Sf3b1 is part of the U2 snRNP. The vector has inserted relatively near the start of this gene at base 1345 of 6231, and protein prediction programs fail to pick up any known motifs in the translated protein

sequence. The gene has been isolated and mapped to the central part of chromosome 1, band C1. Karyotyping results agree with this location on chromosome 1 (figure 6.7) and immunofluorescence of the trapped gene shows the localisation of the fusion protein to splicing speckles (figure 6.5). SF3b1 contains a CpG island in its promoter.

Cell line 6x 8d3 has been identified as a DEAD box RNA helicase, called *Ddx10*. DEAD box proteins are required for a variety of RNA metabolic processes. They all contain a highly conserved motif composed of the amino acids D-E-A-D (Asp-Glu-Ala-Asp) (Linder et al., 1989). The DEAD box family of proteins has been grouped into the super family II of RNA helicases. The vector has inserted near the end of the trapped gene and both the DEAD box and Helicase motifs remain intact. The BLAST results obtained for this cell line also suggest the trapped gene is upon chromosome 9 band C, in agreement with the karyotyping results shown in figure 6.7. Furthermore, immunofluorescence using an antibody against βgal, localises the expression of this trapped gene to the nucleolus (figure 6.5). This localisation would agree with the proposed role in RNA metabolism of the gene product as suggested by the RACE sequence obtained. Furthermore DDX10 in humans, is known to be nucleolar (Scherl et al., 2002; Anderson et al., 2002). Again no CpG islands, TATA or CATA box in/near the promoter of the trapped gene could be found.

In the seven cell lines in which the identify of the trapped gene is known, only one contains a CpG island, and none contain TATA or CAAT boxes in or near their promoters. This result is not entirely unexpected as a recent study, which has analysed the sequence of over 13,000 human gene promoters found only 7.6% to contain a CAAT box and only 2.6 %, a TAAT box. CpG islands were found to vary in frequency dependent on the function of the gene and only 9% of tissue specific genes contained a CpG island in contrast to 80% of non-tissue specific genes (FitzGerald et al., 2004).

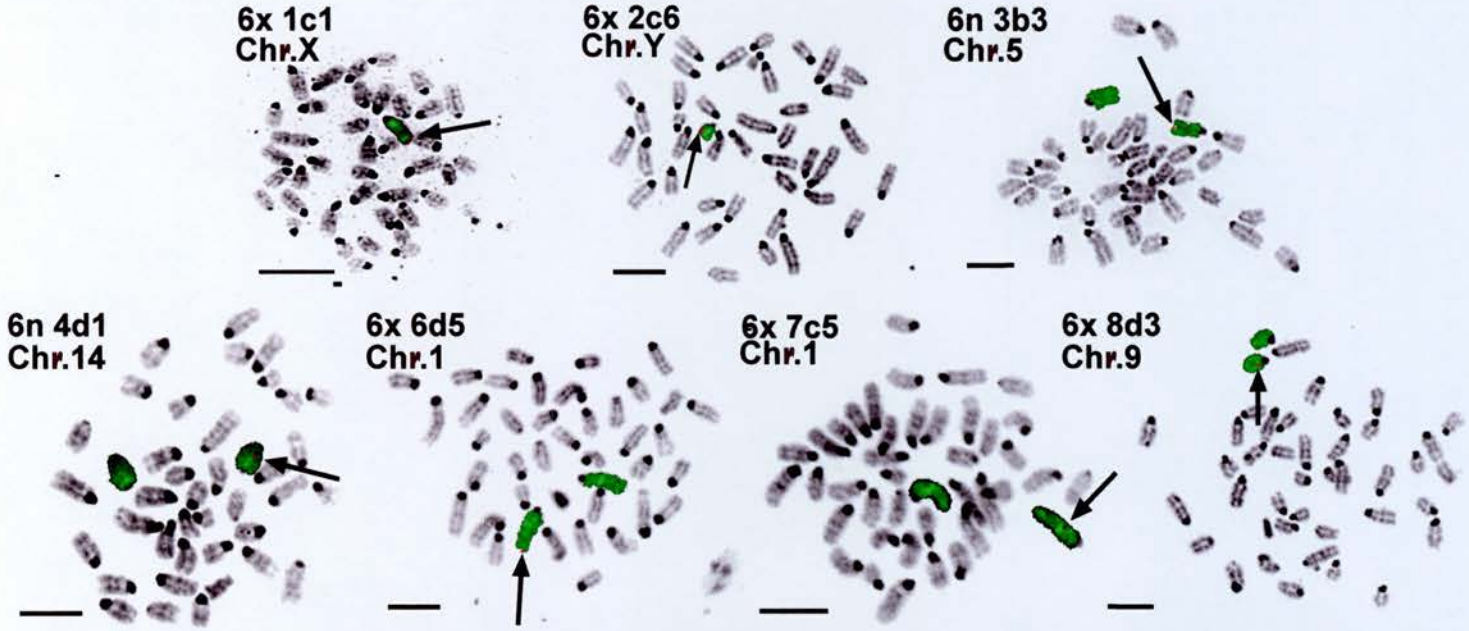

6.7 .2D FISH confirmed the genomic location of 7 trapped genes as predicted by 5'RACE sequences. 2D FISH using whole chromosome paints and a probe against the gene trap vector was used to map the location of trapped genes in seven out of ten gene trap cell lines chosen to be characterised. The scale bar in each image represents 10 μm.

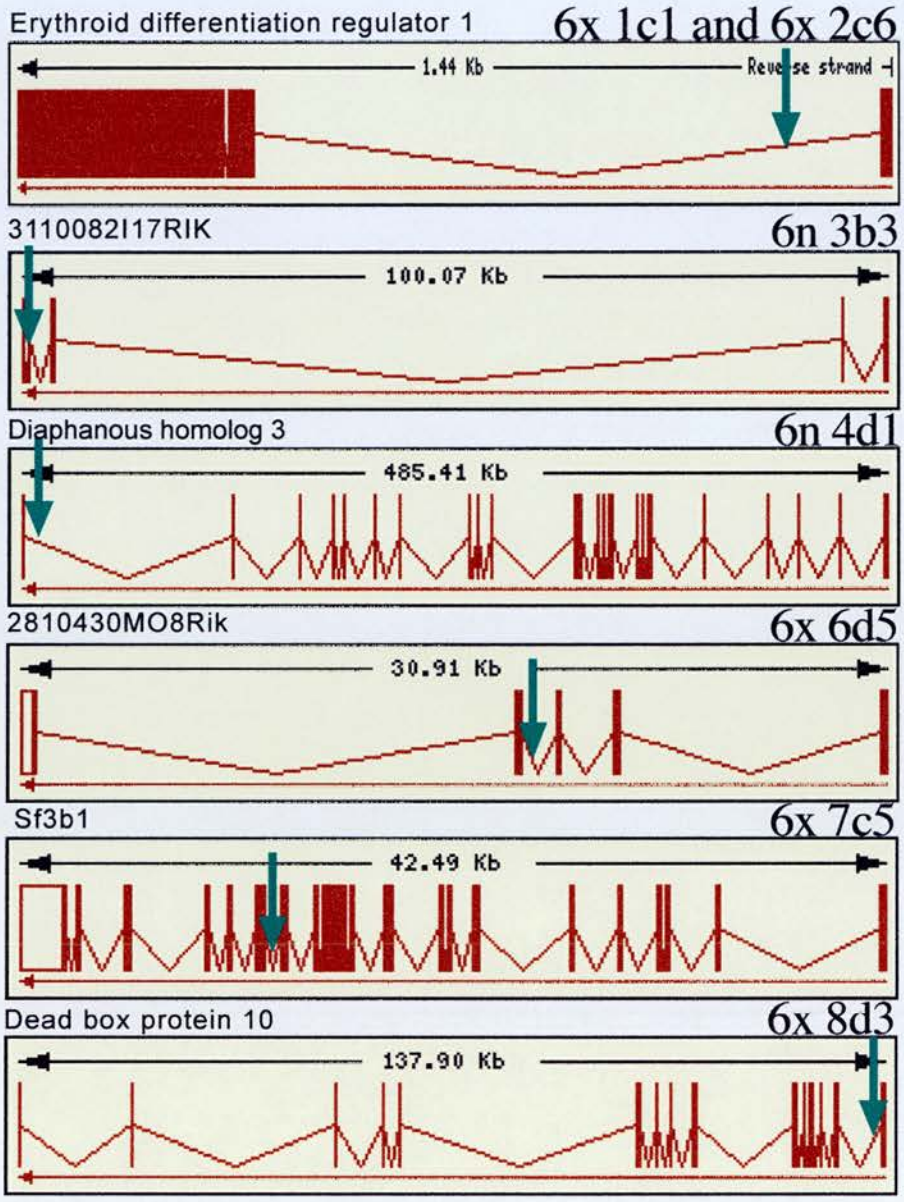

Figure 6.8:The gene trap vector can insert into a range of sites within a gene. Schematic showing the site of insertion of the gene trap vector in the 5 trapped genes as determined from the 5' RACE sequence obtained for each cell line. Each gene is presented as a series of filled boxes and interconnecting lines. The filled boxes represent gene exons, whilst introns are the thin lines connecting each box. Green arrows show the site of pGTXN6 insertion into each gene.Images adapted from ENSEMBL.

The trapped genes are found in a range of different chromosomal positions; from near the telomere in cell lines 6n 3b3, 6x 1c1 and 6x 6d5, to the middle of the chromosome in cell lines 6n 4d1 and 6x 7c5, to relatively near the centromere in cell line 6x 8d3. In addition the gene trap has inserted into chromosome Y, in the cell line 6x 2c6, this chromosome is gene -poor and highly heterochromatic making this cell line an unlikely candidate for tethering experiments. The location of each trapped gene on its chromosome was hoped to provide insights into which cell lines would contain suitable trapped genes to try and tether. It may be that genes already located near heterochromatin will not experience an effect on their expression if anchored to the heterochromatic environment of the nuclear periphery.

In addition to mapping to several different genomic locations, the site of insertion of pGTXN6 within a gene also varied (figure 6.8).

I failed to obtain, 5' RACE sequences for the three cell lines, 6N 3d4, 6N 11b5 and 6x 4b1. This may be due to a number of reasons. Firstly, the trapped genes may not be expressed at a level high enough to be detected in the nested PCR step. However Xgal staining and immunofluorescence performed on these cell lines showed them to have a moderate level of trapped gene expressed (figure 6.5), and a higher level of protein expression than some of the trapped genes which were successfully determined by 5'RACE. The quality of the RNA preparation from these cell lines may be too poor or degraded for 5' RACE or the RNA may have co-precipitated with polysaccharides or small RNAs such as tRNA or 5S RNA during preparation, resulting in poor synthesis of the 1st strand of cDNA. However as all RNA preparations were made using the same protocol and several were prepared together, this is unlikely. A more likely reason for failure of the 5'RACE in these three cell lines could be due to secondary structures in the mRNA transcript, as this can be a problem in transcripts with a high GC content.

With no RACE sequences obtained for the cell lines 6n 3d4, 6n 11b5 and 6x 4b1 attempts to karyotype the genomic location of pGTXN6 in these cell lines were also unsuccessful. With no candidate chromosomes to look upon, karyotyping is very difficult. The mouse genome is very difficult to decipher as unlike the human genome, all the chromosomes are acrocentric, and distinctions in size between chromosomes are not as clear.

6.2.4 Determining the radial position of trapped genes within the interphase cell nucleus

In order to monitor any changes in the nuclear positioning of trapped genes when anchoring protein is expressed, 2D FISH on the interphase nuclei of each cell line with a probe that detects pGTXN6 was used to determine the radial positioning of each trapped gene (figure 6.9). Furthermore, if trapped genes were already at the nuclear edge, there would be no point in trying to tether the gene to the nuclear membrane. The radial distribution of each trapped gene was analysed as described in box 5.1, however instead of using IPLAB3.6 software to calculate the nuclear segment containing the majority of probe signal, the nuclear segment containing the gene trap probe in each cell line was scored manually from fifty images. Two main types of distribution were seen between all the cell lines. Cell lines in which the trapped gene was found to be mostly in the middle nuclear segments 4 and 5 included : 6n 3d4, 6n 11b5, 6x 1c1, 6x 2c6, 6x 4b1, 6x 6d5, 6x 8d3 and cell lines in which the gene trap was found mostly in segments 2,3 and 4 i.e. with no strong preference for either the nuclear edge or interior included: 6n 3b3, 6n 4d1 and 6x 7c5. The very internal location of the trapped gene in the cell line 6x 2c6 is surprising as this gene is upon the heterochromatic chromosome Y. Heterochromatin is traditionally believed to be located mostly at the nuclear periphery although portions of it can be found near the nucleolus and in the nucleoplasm. Despite mapping to the same chromosome the radial distribution of the gene trap in the cell lines 6x 6d5 and 6x 7c5 is different. This may reflect differences in the precise chromosomal location of each trapped gene. Furthermore, the only trapped-gene to have a similar radial distribution to its host chromosome is 6n 4d1, located on chromosome 14. Table 6.1. summarises the radial positions of each gene.

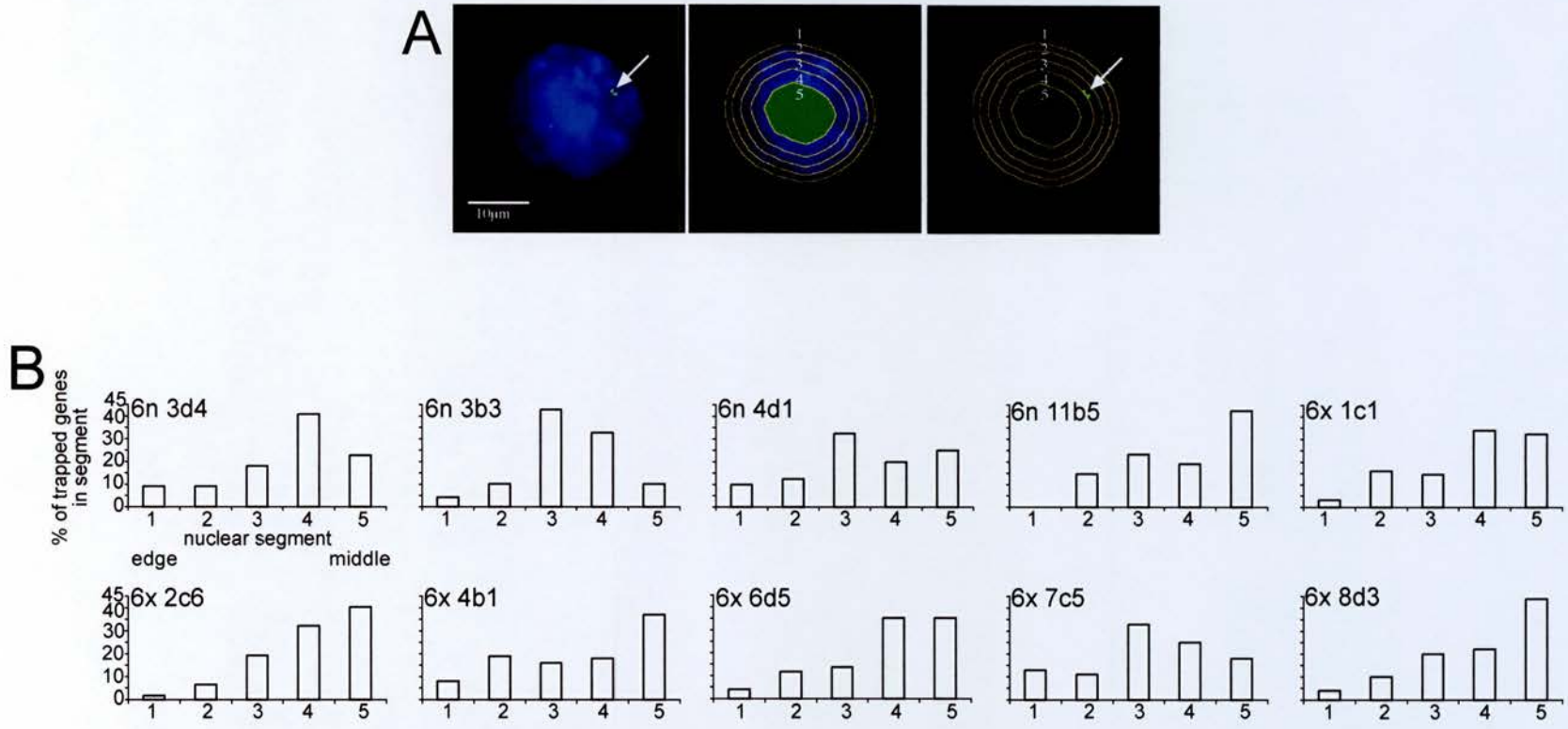

Figure 6.9: Radial position of trapped genes within the nucleus. A) 2D FISH with a probe against pGTXN6 was used to detect the position of the trapped gene in each cell line. The nucleus in each image was then divided into five erosion shells of equal area and the location of the trapped gene scored. B) Histograms showing the distribution of pGTXN6 signals within the nuclei of gene-trapped cell lines, relative to 5 erosion shells from edge (1) to centre of the nucleus (5), n=50.

Although table 6.1 does not contain a complete data set for each of the 10 cell lines chosen for further analysis, enough information had been obtained from all five different characterisations to decide which cell lines were suitable candidates to undergo tethering experiments. Cell lines in which the identity of the trapped gene and its genomic location were unknown were, in general, discarded from further experiments. Likewise the cell lines 6x 1c1 and 6x 2c6 were also discarded, as the trapped gene in both lines was upon the psuedoautosomal region of the X and Y chromosomes. This region of the genome appears to be unstable as it is particularly prone to gene insertions and recombination. As complete data sets had been obtained for the cell lines 6x 6d5, 6x 7c5, and 6x 8d3, and 6n 3b3, initial attempts to anchor trapped genes were performed in these cells. Although Southern blots failed to show the presence of the LacO array in the cell lines 6x 6d5, 6x 8d3 and 6n3b3, it could not be concluded that it was absent either due to the resolution of the blot. As 4 out of the 10 cell lines were believed to still contain the array, it was decided to use the 6x 6d5 cell line anyway. Unfortunately only one of the four cell lines chosen for anchoring experiments contained the Lac array downstream of the fusion transcript generated by the trapped gene.

6.3 TETHERING GENES TO THE NUCLEAR PERIPHERY

6.3.1 Anchoring proteins

In order to relocalise the Lac operator tagged genes, a fusion protein of the Lac repressor (LacI) with a protein found at the nuclear periphery must be introduced into the cells. Fusion proteins have previously been created in the lab encoding fusions of myc-tag-LacI-emerin (JRC73) and myc-tag-LacI-LAP2β (JRC74). The expression of these is driven by a CMV promoter and both contain a DsRed-N1 backbone (appendix 1 figure A.2). The CMV promoter is derived from the human cytomegalovirus and is able to drive high expression of transgenes in a variety of cell types and in both transient and stable cell lines (Thomsen et al., 1984; Boshart et al., 1985; Foecking and Hofstetter 1986). From the knowledge I have about the location of wild-type emerin and LAP2β in the nucleus (figure 6.10), I expected these two

Cell Line	Trapped gene	Expression pattern	Genomic location	Radial position	Lac array?
6n 3b3	3110082I17Rik (NM_028469)	nuclear	Chr.5 band G1	No strong preference (mostly nuclear segments 3-4)	?
6n 3d4	unknown	cytoplasmic	unknown	Middle (mostly nuclear segments 4-5)	+
6n 4d1	Diaphanous Homolog 3 (NM_019670)	weak nuclear	Chr.14 band D3	Middle (mostly nuclear segments 3-5)	?
6n 11b5	unknown	nucleolar	unknown	Middle (mostly nuclear segments 4-5)	+
6x 1c1	Erythroid differentiation regulator 1 (NM_133362)	nuclear	Chr.X pseudoautosomal region	Middle (mostly nuclear segments 4-5)	+
6x 2c6	Erythroid differentiation regulator1 (NM_133362)	nuclear	Chr.Y pseudoautosomal region	Middle (mostly nuclear segments 4-5)	-
6x 4b1	unknown	cytoplasmic	unknown	Middle (mostly nuclear segment 5)	-
6x 6d5	2810430M08Rik (NM_026041)	nucleolar	Chr.1 band H5	Middle (mostly nuclear segments 4-5)	-
6x 7c5	SF3b1 (NM_031179)	Splicing speckles	Chr.1 band C1	No strong preference (mostly nuclear segments 3-4)	+
6x 8d3	Ddx 10 (gene id: 77591)	nucleolar	Chr.9 band C	Middle (mostly nuclear segment 5)	-

Table 6.1: Summary of the characterisation of a subset of pGTXN6 gene trapped cell lines

anchoring proteins to be found in the inner nuclear membrane (INM) in transfected cells, with the N terminal of both proteins protruding into the nucleoplasm. However, by fusing LacI to the N terminus of emerin and LAP2β, I may have blocked the BAF binding LEM domain and thus have blocked accessibility to normal nuclear rentention signals. To test this, both vectors were transiently transfected in 293T cells. These cells are derived from human embryonic kidney cells, which have been immortalized by the adenovirus E1A gene product, and express the large T antigen of SV40. These cells were used to determine the expression pattern of both anchor proteins as they have a very high transfection frequency.

Immunofluorescence with antibodies against the myc-tag (Upstate, catalog number 06-549) and LacI (Upstate, catalog number 05-503) were used to confirm the presence of the fusion protein at the nuclear periphery in transfected cells (figure 6.10.a). As these transfections are only transient, it is likely that both anchoring proteins are very highly expressed resulting in some of the protein remaining in the endoplasmic retiliculum (ER). This can be seen in some of the images captured. Brightfield images were overlapped with fluorescent images to confirm the presence of the anchor protein was not simply in the entire cytoplasm surrounding the nucleus (figure 6.10.b). Most importantly, no fusion protein could be detected in the nucleoplasm. To further confirm both anchoring proteins were being correctly expressed, Western blots using antibodies against amino acids 3-254 of emerin Santa Cruz, catalog number sc-15378) and amino acids 29-50 of LAP2 (Abcam, catalog number ab11823), which is common to all LAP2 isoforms, were performed (figure 6.10). Bands of the expected protein sizes were detected for both anchoring proteins. Endogenous emerin is 37kDa in size, whilst endogenous LAP2α and LAP2β are 76 kDa and 50kDa respectively. This makes the fusion protein of myc-tag-LacI-emerin 70kDa and myc-tag-LacI-LAP2β, 90kDa. To confirm that the anchoring proteins were inserted in the nuclear membrane, Western blots were performed on different fractions of cellular proteins including a whole cell, cytoplasmic, nuclear, insoluble nuclear and soluble nuclear extracts. Proteins localised at the nuclear membrane should be found in the insoluble nuclear fraction. This was indeed where the anchoring proteins were (figure 6.10.c). In the emerin Western blot some anchor protein is also seen in the cytoplasmic fraction, this is due

to the presence of emerin expression in the ER (Vaughan et al.,2001, Fairley et al., 1999). In addition, the LAP2 Western blot confirms that the LAP2β isoform is expressed in the anchor protein, this is important as the LAP2α isoform is expressed in the nucleoplasm. This is visible in the soluble extract of nuclear proteins, probed with the LAP2 antibody (figure 6.10.c).

Once it had been confirmed that the anchoring proteins were both expressed as expected at the nuclear periphery, it was important to ensure stable cell lines expressing both anchor proteins could be made. High levels of some proteins can be toxic to cells over a long time making it impossible to create stable cell lines expressing them. Both pJRC73 and pJRC74 were transfected into HT2 mouse ES cells as this is the parent cell line used in the gene trap. Both vectors were linearised for transfection via the BsaI site located near the kanamycin gene away from the fusion transcript. G418 selection was then used to select for ES cell colonies expressing each anchoring protein. After 10 days of G418 selection ES cell colonies were picked, gently trpysinsed and plated out into 24 well plates. Once colonies had been expanded to the 6 well stage, they were assayed by immunofluorescence using an antibody against LacI. 25 cell lines were screened for each anchor protein, and a wide range of expression levels of anchor protein was seen for both vectors. Although each cell line is clonally derived there is a wide range of expression levels both within and between lines. Position effect variegation (PEV) is problem when creating stable cell lines expressing transgenes. The longer cells are expressing a transgene in culture the greater the number of cells within the population in which the gene is silenced. The five best cell lines for each anchor were expanded further, and 73GB15 (emerin anchor) and 74GB1(LAP2β anchor) used in Western blots to determine the level of anchor protein expression relative to endogenous emerin or LAP2β (figure 6.11). Both the anchors were calculated to be expressed at approximately 10-15% of the level of the endogenous protein in stable cell lines. However in the cell line 74GB1 approx 90% of cells expressed pJRC74, compared to approx. 60% of cells in 73GB15 expressing pJRC73 (figure 6.11).

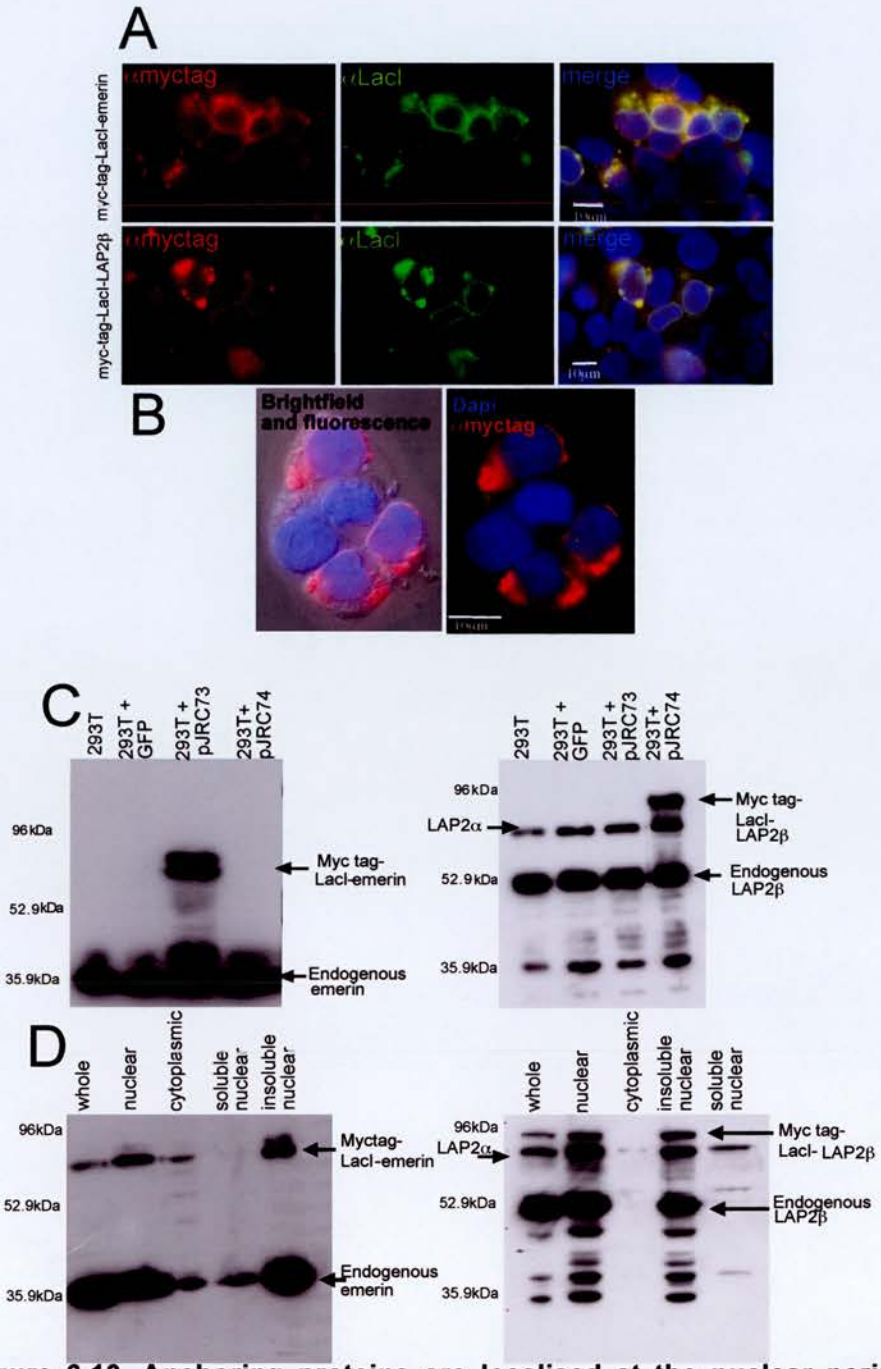

Figure 6.10. Anchoring proteins are localised at the nuclear periphery. A)Immunofluorescence with antibodies against myc tag and LaclI proteins show that in 293T cells transiently transfected with pJRC73and pJRC74, both anchoring proteins appear to be localised at the nuclear edge, although high expression levels have resulted in some protein localising to the ER. B) Overlapping immunofluorescent images with brightfield images reveals the anchoring proteins are at the edge of the nucleus and not in the surrounding cytoplasm. C) Western blots of whole cell extracts from 293T cells transiently transfected with pEGFP-N1, pJRC73 and pJRC74 and antibodies against emerin and LAP2 reveal high expression levels of both anchoring proteins. D) Western blots using different cellular protein extracts from ES cell lines stably expressing both anchoring proteins. These fractions included a whole cell extract, a nuclear protein extract, cytoplasmic extract and insoluble and soluble membrane proteins. Antibodies against emerin(left blot) and LAP2(right) were used. This confirms expression of both pJRC73 and pJRC74 is localised to the insoluble nuclear protein fraction. This cellular fraction will contain the membrane proteins.

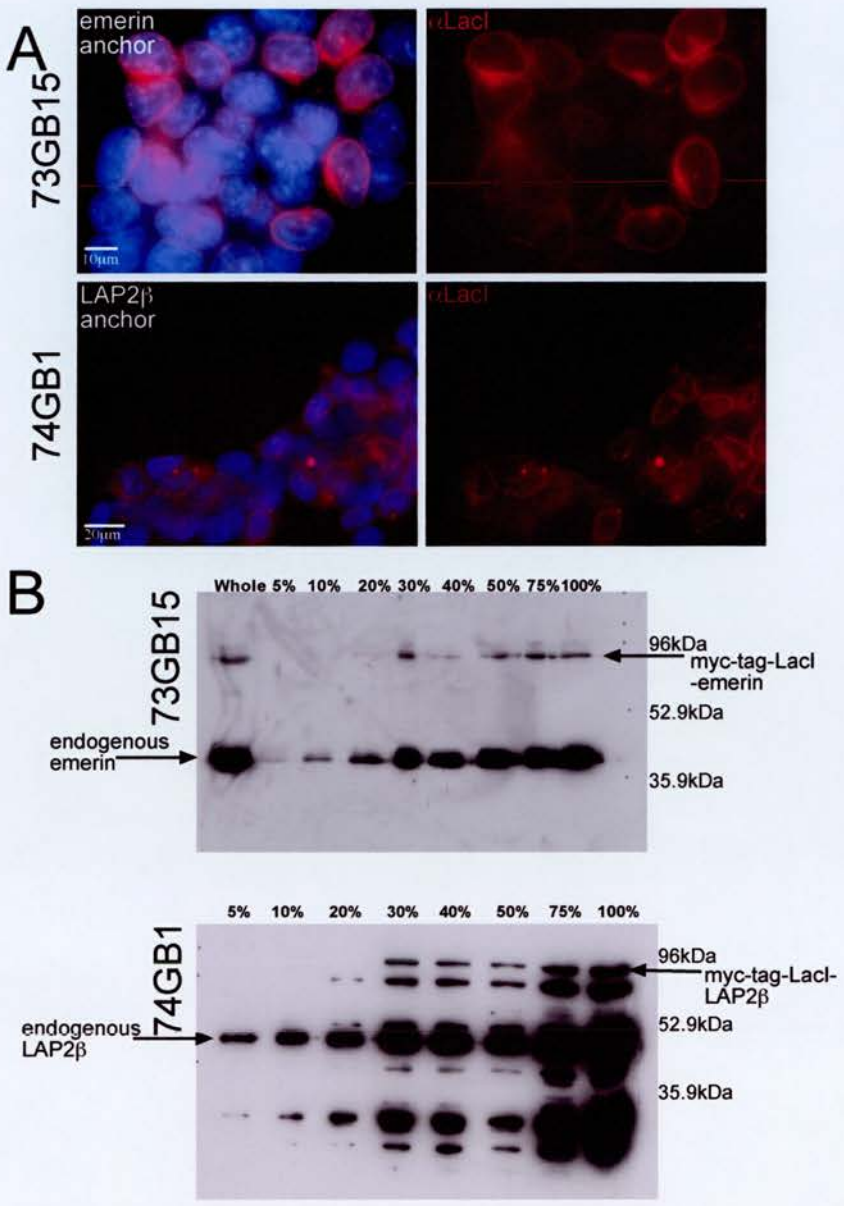

Figure 6.11. Stable cell lines expressing both anchoring proteins A) Immunofluorescence using an antibody against LacI proteins in stable HT2 ES cell lines expressing both anchoring proteins.B) Western blots using serial dilutions of whole cell protein extracts were used to determine the level of expression of the anchoring protein relevant to the endogenous protein. In both cell lines, the anchoring protein was expressed at around 10-20% of the level of the endogenous protein.

6.3.2 Using anchoring proteins to tether genes

pJRC73 and pJRC74 are both driven by the CMV promoter and are in the plasmid backbone DsRed-N1. To select for stable expression of each anchor protein, in these vector backbones requires the use of G418 selection, however the gene trap vector used to tag active genes with Lac operator sequences also uses G418 resistance to select for stable cell lines, therefore this drug selection can not be used to select for cell lines containing both trapped genes and expressing an anchoring protein. As the initial stable cell lines created in HT2 cells also revealed problems with silencing of the anchor protein expression, it was decided to change to the vector backbone of both anchoring proteins to pCAGASIZ (a gift from B.Ramashoye, appendix 1 figure A.2). This vector will not only overcome the problem of PEV but will also solve the problem of selecting for cell lines expressing both a trapped gene and the antibiotic zeocin. However for a cell to be resistant to zeocin, it must encode a discistroninc mRNA for alkaline phosphatase and the zeocin resistance gene *Sh ble*. The initiation of translation of *Sh ble* then occurs via the IRES structure present on anchor protein. pCAGASIZ encodes resistance to the copper-chelated glycopeptide the dicistronic mRNA, which recruits and activates translation machinery in the absence of a 5' cap. The 5' cap of mRNA is usually critical for recognition and proper attachment of mRNAs to ribosomes. Furthermore, pCAGASIZ also contains a small exon and a chimaeric intron present just after the promoter. These help to increase the stability of the final transcript.

Both the pCAGASIZ73 and pCAGASIZ74 anchoring vectors were transfected into the cell lines 6x 6d5, 6x 8d3, 6x 7c5, 6x 4b1 and 6n 3b3 using Lipofectamine2000. Before transfection of each vector into ES cells, both plasmids were linearised via the PvuI restriction site (figure A.2). 24 hours after transfection, cells were passaged and zeocin selection applied (10μg/ml). Transfections were initially performed only in the cell lines 6x 6d5 and 6x 8d3, however these yielded no viable colonies. As zeocin is encoded via an IRES structure, it was expected that fewer colonies than normally would be achieved, as clones in which the transgene has become silent are no longer be able to encode zeocin resistance. As initial transfections in the cell lines 6x 6d5, and 6x 8d3 yielded no colonies, it was decided

to carry out transfections into three new cell lines: 6x 7c5, 6n 3b3 and 6x 4b1. These transfections were more successful and colonies were obtained. However initial clonal expansion proved difficult due to the sensitivity of ES cells to zeocin. Once colonies had been picked they would often grow slowly and spontaneously differentiate. Differentiation may affect gene expression therefore, to combat this, selection with zeocin often had to be reduced or removed temporarily.

Furthermore, FISH analysis of metaphase spreads prepared from three of the cell lines derived from the parent cell line 6n 3b3 and probed with pGTXN6, revealed that the trapped gene appeared to have moved in its genomic location. As this is extremely unlikely, the most obvious explanation would be that the parent cell line had been mixed up with another trapped gene line, thus these colonies were discarded from further analysis. As the trapped gene sequence is still unknown for the cell line 6x 4b1, it was decided to mainly concentrate on colonies derived from the cell line 6x 7c5. Expression of the anchor protein in the newly derived cell lines 6x 4b1.t1, 6x 7c5.t3 and 6x 7c5.t6 was detected by immunofluorescence using a LacI antibody, and it was immediately obvious that there was more uniform expression of the anchor protein within the vast majority of the cell population (figure 16.12.a).

To test whether the presence of anchoring protein affected the radial distribution of a trapped gene, 2D FISH on the newly derived cell lines 7c5.t3 and 7c5.t6, both expressing the emerin anchor, and the cell line 6x 4b1.t1, expressing the LAP2β, anchor was performed as before with a biotin labelled probe against the gene trap sequence (figure 6.14.b). Although pGTXN6 and pCAGASIZ73/74 both contain prokaryote sequences, they do not encode any of the same transcripts, therefore any cross-hybridisation between pGTXN6 and pCAGASIZ73/74 in the cells should be minimum. In the 2D FISH images captured only one bright signal of pGTXN6 could be seen. Radial position was analysed as before (section 6.2.4). The trapped gene moved towards the periphery in the cell lines 6x 7c5.t3 and 7c5.t6, but in the cell line 6x 4b1.t1, movement towards the interior was observed. In all cases the movement of the trapped gene was not significant, as p values obtained using a Kolmogorov-Smirnov test were approximately 0. 42-0.44 for each cell line. Therefore, it was concluded that trapped genes were not being tethered to the periphery as hoped.

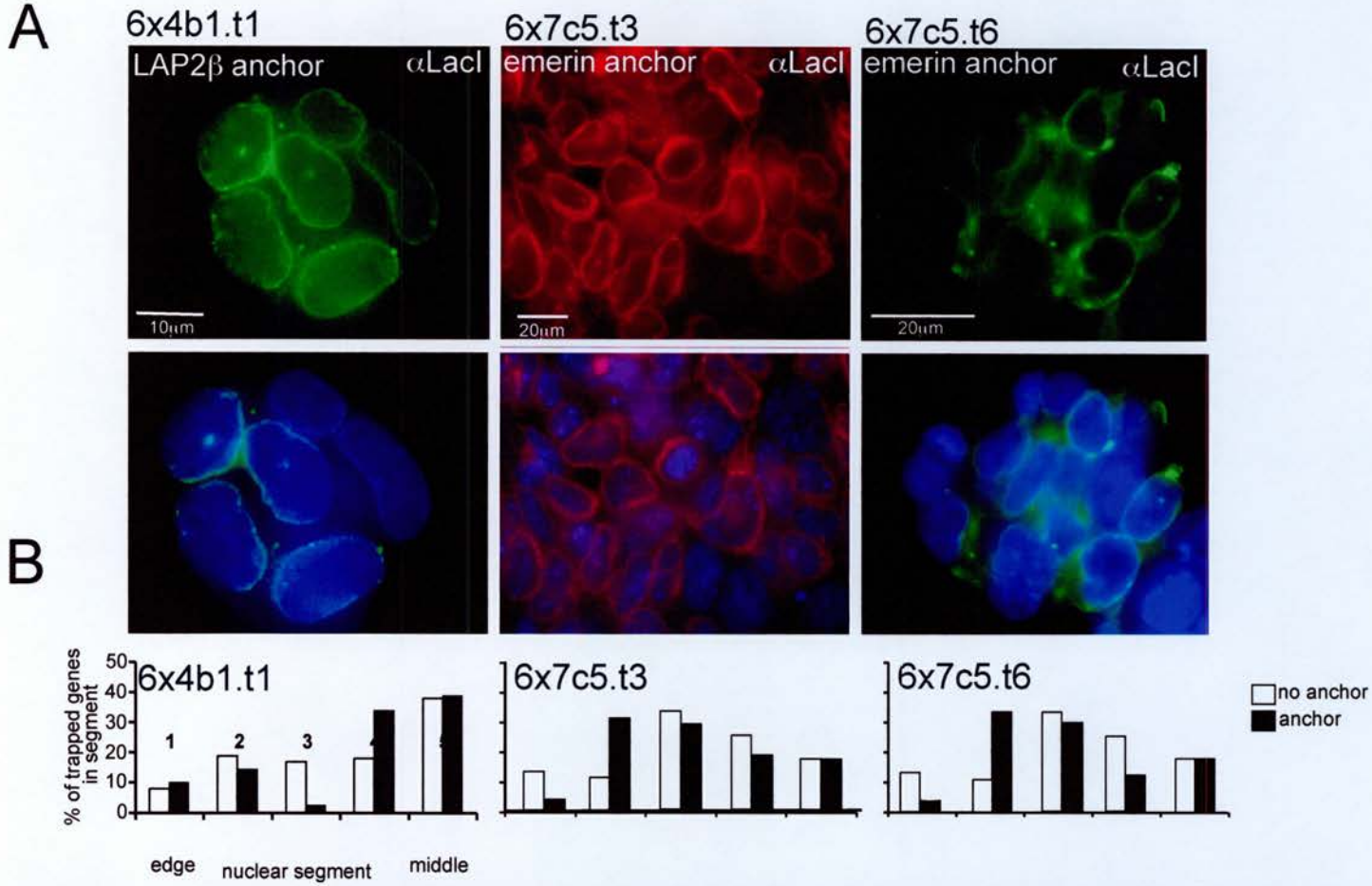

Figure 6.12: Expression of anchoring proteins in gene trap cell lines fails to reposition trapped genes to the nuclear periphery. A) Immunofluorescence against LacI shows the expression of anchoring protein in the gene trapped cell lines 6x 4b1.t1, 6x 7c5.t3 and 6x 7c5.t6. B) 2D FISH with a probe against pGTXN6 was used to determine the position of the trapped gene in each cell line before and after expression of anchoring protein. 50 images of interphase nuclei were collected for each cell line and the nucleus in each image split into five segments of equal area. The % of trapped genes in each segment for each cell line was then calculated and graphed. Open bars= % of trapped genes in nuclear segment in parent cell line.Closed bars= % of trapped genes in nuclear segment after expression of an anchor protein.

6.4 TETHERING LARGE LAC OPERATOR ARRAYS TO THE NUCLEAR PERIPHERY

One possible reason for the failure of tagged genes to tether to the nuclear periphery may be that the trapped genes simply do not contain a large enough LacO array for binding tightly to LacI. To address this question, it was decided to try and determine if larger arrays could indeed be anchored. Present already within the lab were HT1080 cell lines containing large stable integrations of LacO. The cell line B49.5 contains an integration of approximately 12 copies of the 128mer LacO into human chromosome 5 p14. This integration has been shown to be in the nucleoplasm of the nucleus and not near the nuclear periphery (Chubb et al., 2002). pCAGASIZ73 and pCAGASIZ74 were transfected into this cell line and zeocin selection (100μg/ml) used to obtain stably expressing cell lines. The emerin anchor transfection was the most successful and the radial position of LacO arrays in two of the cell lines obtained was analysed, using 2D FISH with a probe against the Lac operator array (figure 6.13).

This time a larger shift of position of the LacO arrays towards the nuclear periphery was observed in both cell lines and a Kolmogorov-Smirnov test deemed this to be significant for the cell line B49.5.t2 ($p< 0.007$), whilst for the cell line B49.5.t4, $p=0.076$. Although the change in the distribution of arrays was not significant for both of the cell lines, the movement observed was much larger than the movement observed in the trapped gene cell lines.

6.5 CO-LOCALISATION OF LACO SEQUENCES WITH THE NUCLEAR MEMBRANE

During the screening cell lines for the expression of anchoring protein it was observed that many large invaginations of the nuclear membrane were present, alongside foci of anchoring protein located internally within the nucleoplasm. These foci are most likely to also be invaginations of the membrane.

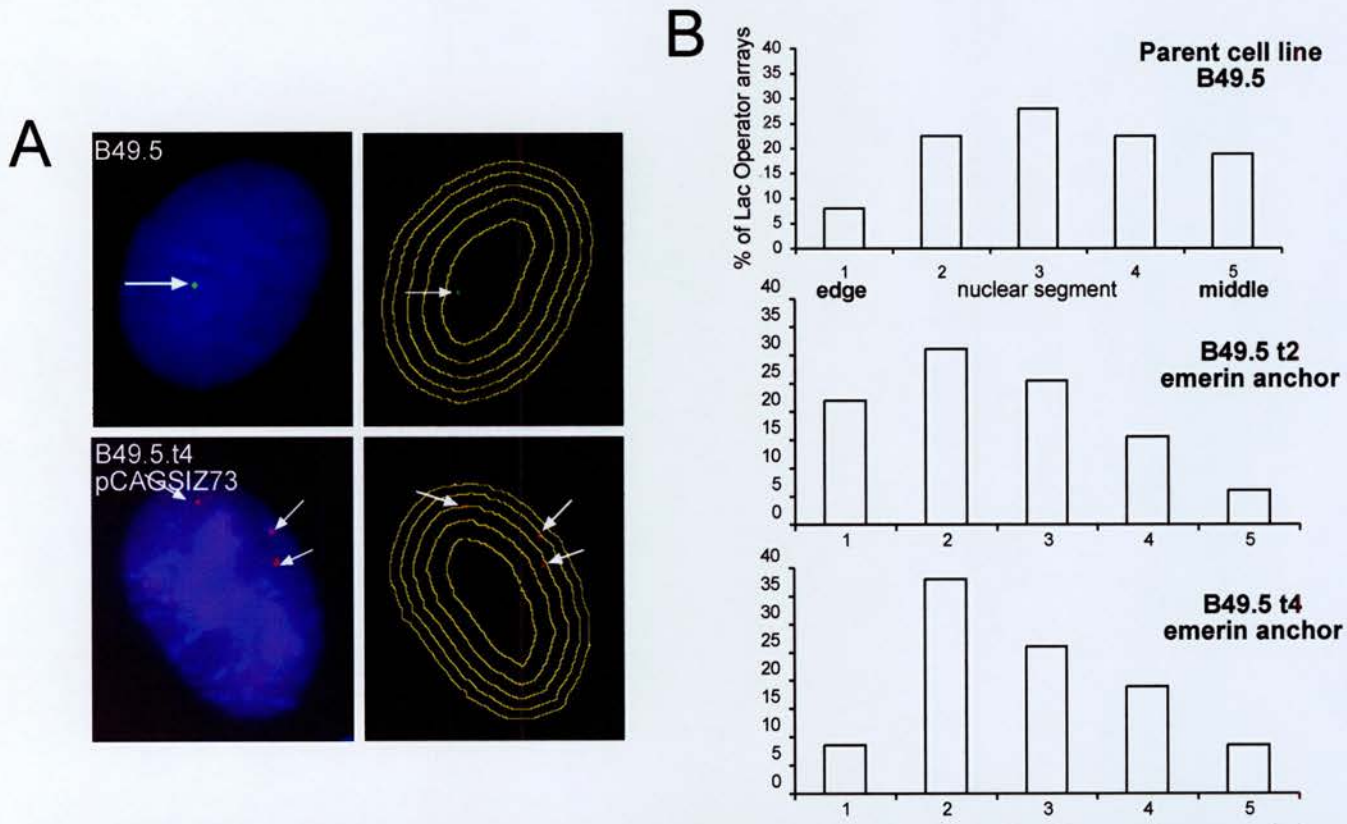

Figure 6.13. Large lac operator arrays can be tethered towards the nuclear periphery. **A)** 2D FISH using a probe against the Lac operator array was used to analysis the radial position of the arrays in the parent cell line B49.5 and 2 cell lines stably expressing the emerin pCAGSIZ73 anchor. 50 images of interphase nuclei were collected for each cell line and the nucleus in each image split into 5 segments of equal area and the segment/s containing LacO array/s scored. B) Graphsof the radial distribution of LacO arrays in each cell line were then plotted.

Immunofluorescence using an antibody against lamin A showed that invaginations and foci of membrane proteins in the nucleoplasm were also present in the parent cell line, B49.5 (figure 6.14). Closer analysis of the gene trap cell lines also revealed that many of these cells contained membrane invaginations, although these were not as pronounced as those seen in the HT1080 cell lines. These can be seen in figure 6.17. Membrane invaginations have been reported for a number of different cell types (Fricker et al., 1997).

Immunofluorescence was used to determine the frequency of invaginations in a range of cells including: HT2 ES cells, HT2 ES cells transiently transfected with a GFP reporter construct containing 128 copies of LacO, HT2 cells stably expressing anchor protein, the parent line 6x 7c5 and its derivative, 6x 7c5.t3. This revealed that over 60% of the cells in both the parent cell line 6x 7c5 and the subsequent daughter cell line 6x 7c5.t3 contained invaginations of the membrane suggesting that the high level of invaginations present in the tethered gene cell line is a characteristic of the cell line it was derived from (figure 6.15).

However it was still possible that the nuclear membrane was being dragged towards the LacO arrays, or that LacO arrays were preferentially localising at the intra-nuclear foci. To address this question, the LacO arrays and the nuclear periphery were required to be visualised together, by ImmunoFISH.

ImmunoFISH was performed on the cell line B49.5 t2, and 3D stacks through the z-axis of a cell captured (figure 3.1 shows a z stack). The co-localisation of the Lac operator probe with lamin A was then scored (figure 6.16). This revealed that the majority of the Lac operator arrays in this cell line were indeed co-localised with lamin A.

To determine if trapped genes also co-localised with lamin proteins, ImmunoFISH was performed on the cell line 6x 7c5.t3. Previous FISH on this cell line to look at the position of the trapped gene has used the plasmid pGTXN6 as a probe, however 3D FISH is a more difficult technique than 2D FISH and often contains more background. Attempts at using the pGTXN6 probe in 3D FISH were unsuccessful due most likely to its relatively small size (6kb). Therefore to obtain a probe that would cover a larger region of the genome and be detected more easily, a probe was derived from the BAC RP23-409J18, which covers the region of the

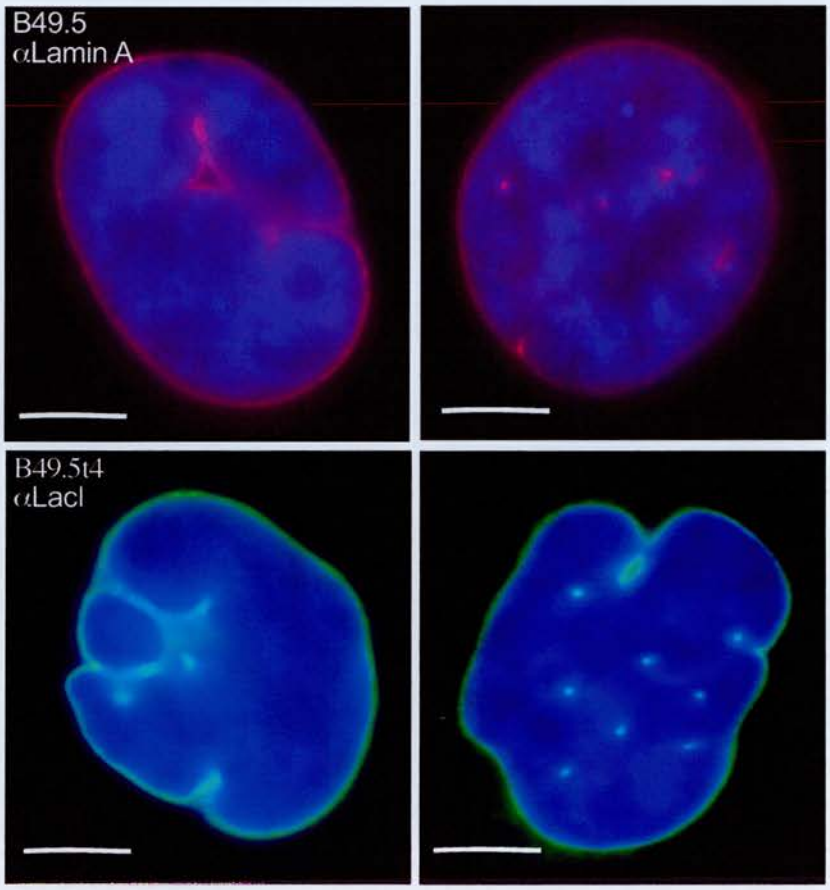

Figure 6.14. B49.5 HT1080 cells contain large nuclear membrane invaginations. Immunofluorescene using antibodies to detect Lamin A at the nuclear membrane in the parent cell line B49.5, and LacI to detect the nuclear membrane in the cell line B49.5t4 reveals that both the parent cell line B49.5 and the daughter cell line B49.5t4, expressing the emerin anchor, contain large invaginations in their nuclear membranes and foci of Lamin A and LacI proteins in their nucleoplasm.Scale bar =10μm

mouse genome that contains the gene *Sfb1*, the gene trapped in this cell line. This means that in the nucleus of each cell, two signals can be detected, one for the endogenous gene and one for the trapped gene. If the gene has been tethered one signal in each cell will co-localise with membrane proteins, and one will not. As lamin A is not expressed in ES cells, ImmunoFISH was performed with an antibody against lamin B (Santa Cruz). 25,3D stacks were captured for this analysis and the co-localisation of BAC signal with lamin B scored (figure 6.17). Over 60% of the cells did contain only one BAC signal co-localised with lamin B, however the same analysis carried out on the parent cell line 6x 7c5, showed this to be the case in just under 40% of the cells. An increase in the number of cells containing two BAC signals co-localised with lamin B was also seen in the presence of anchor expression. These results would suggest that LacO tagged genes are able to co-localise with lamin B.

6.6 ANALYSING THE EXPRESSION OF TRAPPED GENES IN THE PRESENCE OF ANCHOR PROTEIN

Based on the results of the ImmunoFISH in the cell line 6x 7c5.t3, the expression of the LacO tagged gene in this cell line was investigated. The large size of the gene trapped β-galactosidase protein (540kDa) makes it extremely difficult to determine the level of expression by Western blotting. Therefore expression of the trapped gene in the cell line 6x 7c5.t3 was initially analysed using immunofluorescence with an antibody against βgal (figure 6.18). The nature of immunofluorescence and subsequent image capture means that no direct quantitative comparison between the strength of expression of βgal in the parent and the anchored cell line is possible. However initial impressions of the immunofluorescence performed suggested that there was no obvious difference in expression between the parent cell line 6x 7c5 and the cell line 6x 7c5.t3 expressing the emerin anchor protein. If the trapped gene had been silenced to a large extent this would have been apparent.

Despite this, closer analysis of the expression of βgal in the cell line 6x 7c5.t3 revealed that in some neighbouring cells, one cell would contain high levels of

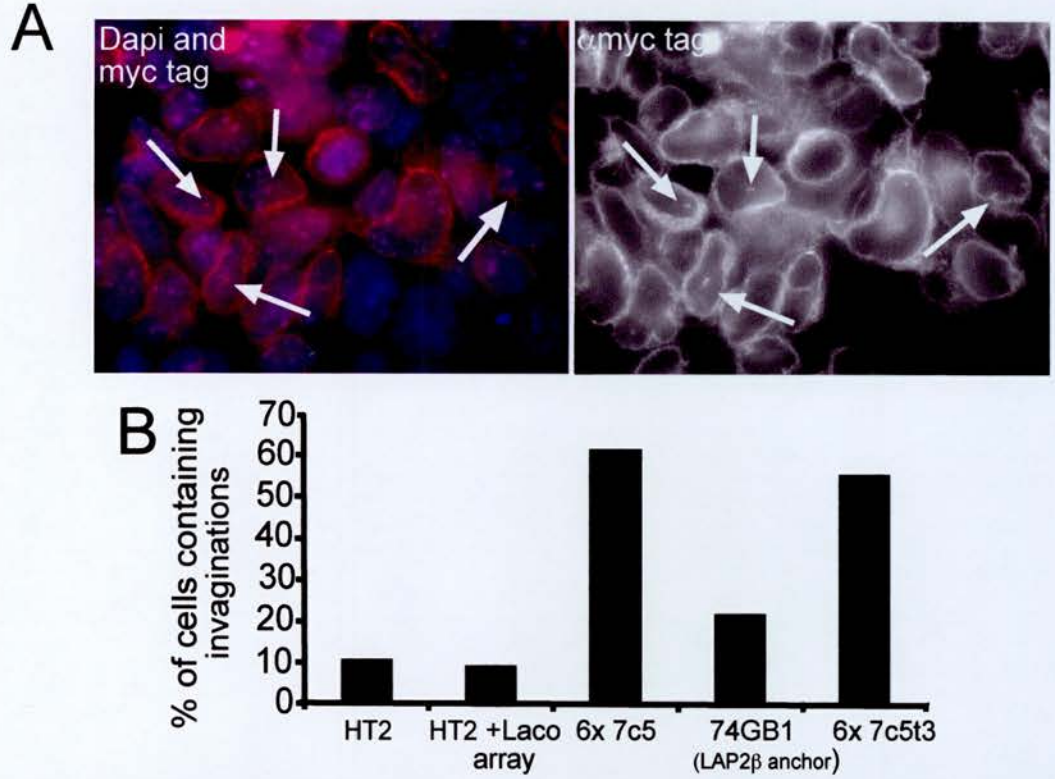

Figure 6.15: Membrane invaginations are not due to the expression of anchor protein in the gene trap cell line 6x 7c5.t3. A) Immunoflurescence in the cell line 6x 7c5.t3 with an anitbody against myc-tag, reveals a high proportion of cells with either invaginations of the membrane or foci of anchoring protein in the nucleoplasm.B) Quantification of the % of cells from different cell populations, with either membrane invaginations of foci of membrane proteins in the nucleoplasm, suggest the high proportion of invaginations seen in the cell line 6x 7c5.t3 is a characteristic of the parent cell line 6x 7c5, and not due to the binding of Lac operator sequences with membrane proteins (n=50).

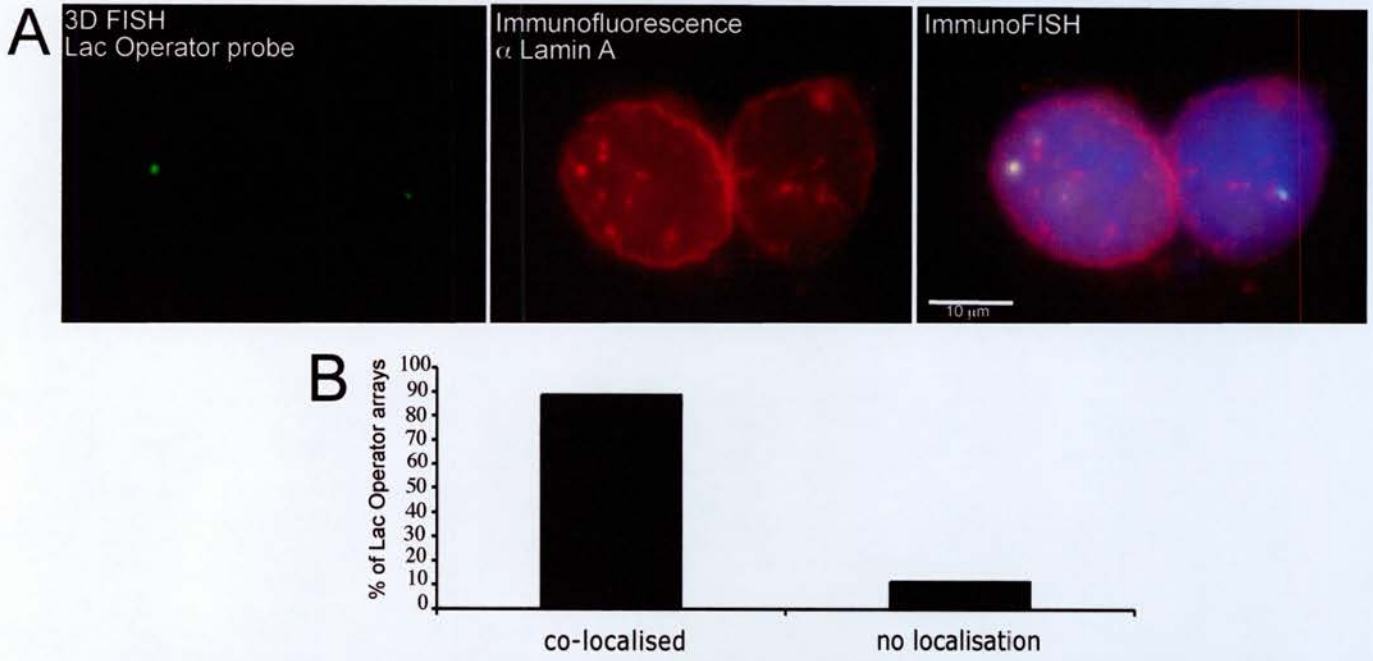

Figure 6.16:Lac operator arrays co-localise with components of to the nuclear periphery. A) A single z stack plane taken from ImmunoFISH used to visualise Lac operator arrays and the nuclear membrane together showing that Lac operator arrays co-localise with membrane proteins upon the stable expression of the LAP2 anchor. B) Quantification of the % of Lac operator arrays co-localised with the membrane shows the majority of arrays are tethered (n=62).

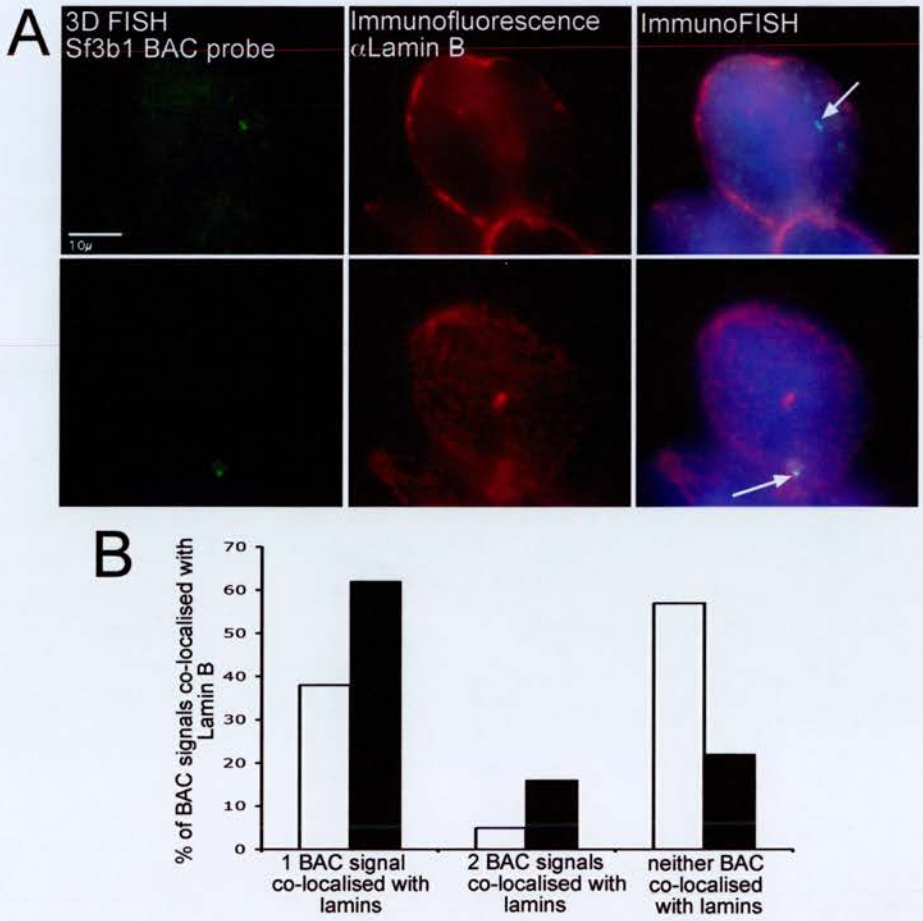

Figure 6.17: Trapped genes co-localise with membrane proteins in some cells. A) Different z stack planes of a cell nuclei from the cell line 6x 7c5.t3 upon which ImmunoFISH using a BAC probe covering the genomic region containing the trapped gene Sfb1 (green) was performed. These planes show the localisation of one BAC signal with the nuclear edge and one BAC signal with the nucleoplasm (arrows), suggesting the trapped gene may be tethered. B) Quantification of the number of cells in which the BAC signal is localised with lamin B proteins in cells expressing and not expressing anchor protein, open bars = 6x 7c5, filled bars=6x 7c5t3 (n=30).

the anchoring protein and low levels of βgal expression and vice versa (figure 6.18.b). This was quantified in 50 images of cell pairs, with different levels of expression of anchor protein. A line was drawn through the centre of both cells, which was 6 pixels wide, and the signal along the line calculated, this was then plotted as a line graph using IPLAB 3.6 software. In approximately 50% of cell pairs captured there was no or little difference in the expression level of βgal between the cell expressing the higher level of anchor protein and the cell expressing the lower level. About 35% of the cells pairs had increased expression of the trapped gene in the cell expressing the higher anchor level, and only 15% of cells showed silencing of βgal in the presence of increased anchor protein. From this analysis I concluded that the presence of anchoring protein had little effect on the expression of the trapped gene.

Immunofluorescence looks at gene expression at the level of the final protein product, therefore to determine if there was any difference at the level of RNA transcription, RT-PCR was used. Primers were designed to cover the junction of the gene trap with the endogenous gene (table 2.1). cDNA was prepared from DNaseI treated RNA preparations from both the parent cell line, 6x 7c5 and anchor expressing cell line, 6x 7c5.t3. To ensure all genomic DNA was destroyed, RNA was treated with DNaseI, ethanol precipitated, resuspended in fresh distilled water, before being DNaseI treated a second time. Primers against GAPDH were used as a control. RT-PCR was initially performed using 30 cycles of PCR (table 2.1). This showed no obvious difference in expression levels of the trapped gene between the two cell lines. RT-PCR was then performed using 25,26,27 and 28 cycles of PCR. 25 and 26 cycles of PCR yielded no detectable PCR product and quantification of the amount of signal present after 27 and 28 cycles of PCR using Aida 3.52 (Raytest) software showed no obvious difference in expression (figure 6.19).

Figure 6.18

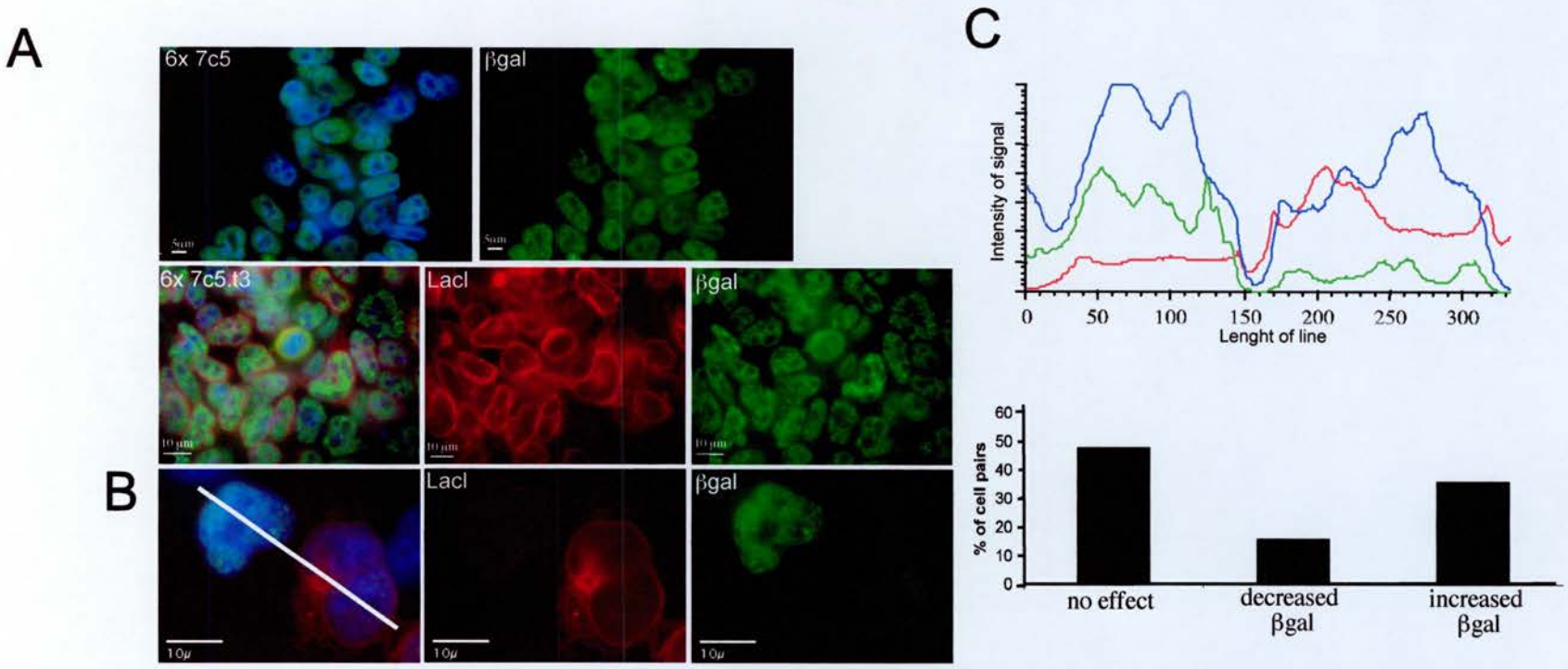

Figure 6.18: Expression of anchoring protein does not effect the expression of the trapped gene. A) Immunofluorescence in both the parent cell line 6x 7c5, and the daughter cell line, 6x 7c5.t3 expressing the LAP2β anchor revealed little difference in the overall level of expression of the trapped gene, Sfb1.C) Pixel intensity along the line drawn through cell pairs as shown in B for Dapi (blue) LacI (red) and βgal (green). This line was 6 pixels in width.This was plotted for 50 pairs of cells and the level of βgal in the cell expressing the higher level of anchor level compared to the level of βgal in the cell with lower anchor expression. This was plotted as either decreased or increased trapped gene expression (D).

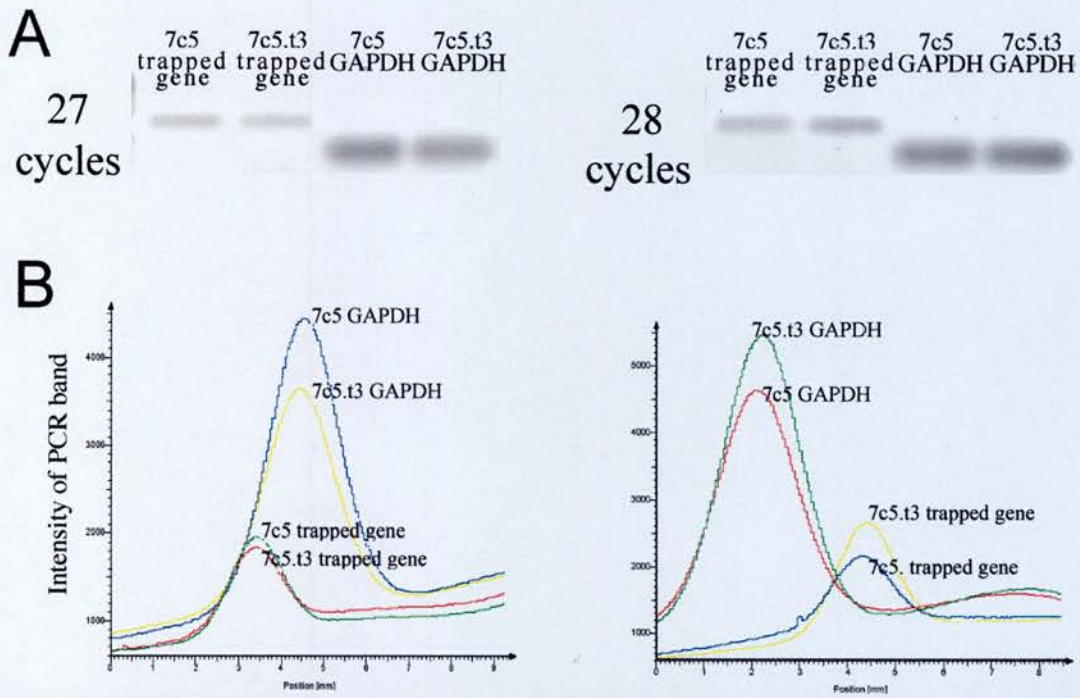

Figure 6.19: RT-PCR reveals no difference in the expression of a trapped gene in the presence of emerin anchor expression. RT-PCR using primers to cover the junction between the gene trap vector and the endogenous trapped gene, was performed at various cycle numbers. At the lowest number of cycles required to see a visible product, the difference in the expression of the trapped gene with and without anchor protein was not significant. Aida 3.52 software was used to quantify and plot the amount of PCR product present in each PCR.

6.7 ANALYSIING THE ABILITY OF ANCHORING PROTEINS TO TETHER PLASMIDS TO THE NUCLEAR PERIPHERY

The results of the anchoring experiments in which there is little movement of LacO arrays which are integrated into the mammalian genome, agrees with the knowledge that genomic DNA packaged into chromatin is locally constrained within the cell nucleus (Chubb et al., 2002, Chapter 3). Therefore I wanted to ask if it would be easier to tether DNA that is not integrated into the genome, to the nuclear periphery. To test this hypothesis, the original emerin and LAP2β anchor expressing HT2 cell lines, 73GB15 and 74GB1 (figure 6.11), initially created to test the toxicity of the anchor protein were utilised. A cell line expressing only myc-tag-NLS-LacI, was also created as a control to determine the effect of free LacI on the ability of LacO arrays to be tethered to the nuclear periphery. This cell line was called, 74LacI.9 (figure 6.20).

A linker sequence encoding a stop codon in each of the three different possible reading frames was then ligated into the plasmid backbone to create the new plasmid, myc-tag-LacI, encoding a fusion protein of the myc-tag, NLS and LacI only. This was sequenced to ensure that LAP2β had been excised and immunofluorescence carried out using an antibody against LacI to confirm that this protein is localised throughout the nucleus and is not at the nuclear periphery (figure 6.20).

Transfections using Lipofectamine 2000, of a plasmid containing 128 copies of the Lac operator sequence, pJRC49, (figure A.3) were carried out in HT2 cells and HT2 cells expressing the LAP2β anchor, the emerin anchor, and myc-tag-LacI. Cells were then harvested and fixed at the set time points of 6hrs, 18hrs and 24 hrs after transfection and the radial position of the transfected plasmids determined. For cells expressing the LAP2β anchor an additional time point, 48 hours, was also collected. 2D FISH using a probe against the plasmid pJRC49 was used to map plasmid locations. 50 images of each transfection were captured and analysed as before (box 5.1). The interphase nucleus of each image was divided into 5 segments of equal area, and the number of plasmid signals in each segment manually counted (figure 6.21). The results of this showed that HT2 cells expressing anchoring proteins

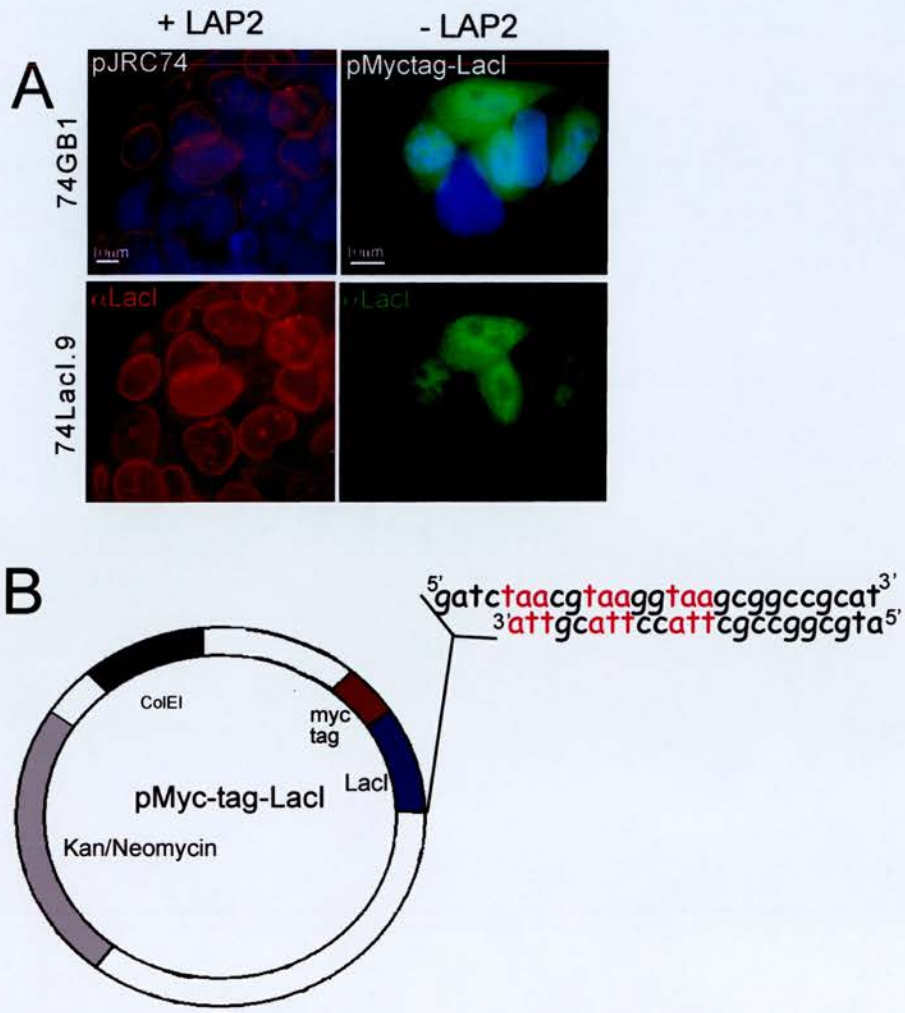

Figure 6.20: Removal of LAP2β from the plasmid pJRC74 results in the loss of LacI expression at the nuclear periphery. A) Immunofluorescence in ES cells stably expressing the plasmids pJRC74 and pMyc-tag-LacI using a LacI antibody. B) To create the myc-tag-LacI encoding plasmid, the LAP2β protein was removed from pJRC74 by digestion with SmaI and BamHI and a linker sequence containing stop codons in each reading frame (red) inserted into the plasmid backbone.

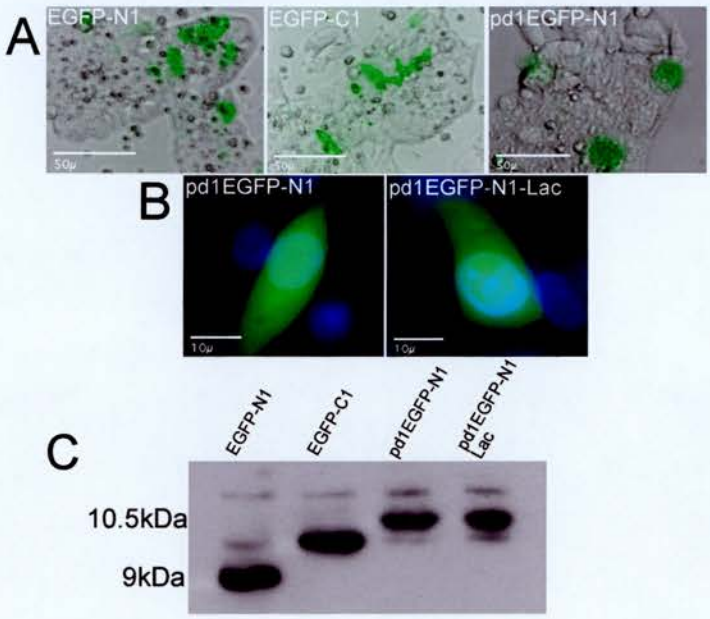

Figure 6.21: Expression of pd1EGFP-N1 and pd1EGFP-N1 in in wildtype ES and 293T cells. A) Brightfield images of HT2 ES cells overlapped with fluorescence show that although pd1EGFP-N1 protein is degraded quickly, this does not effect its transfection efficiency. B)ES cells transfected with both pd1EGFP-N1 and pd1EGFP-N1-Lac,do not display any signifcant difference in the level of EGFP protein expressed. C) Western blots probed with antibodyagainst EGFP with whole cell extracts derived from transiently transfected 293T cells also show no significant difference in the level of protein expression between pd1EGFP-N1 and EGFP-N1 and EGFP-C1 and
between pd1EGFP-N1 and pd1EGFP-N1-LacI.

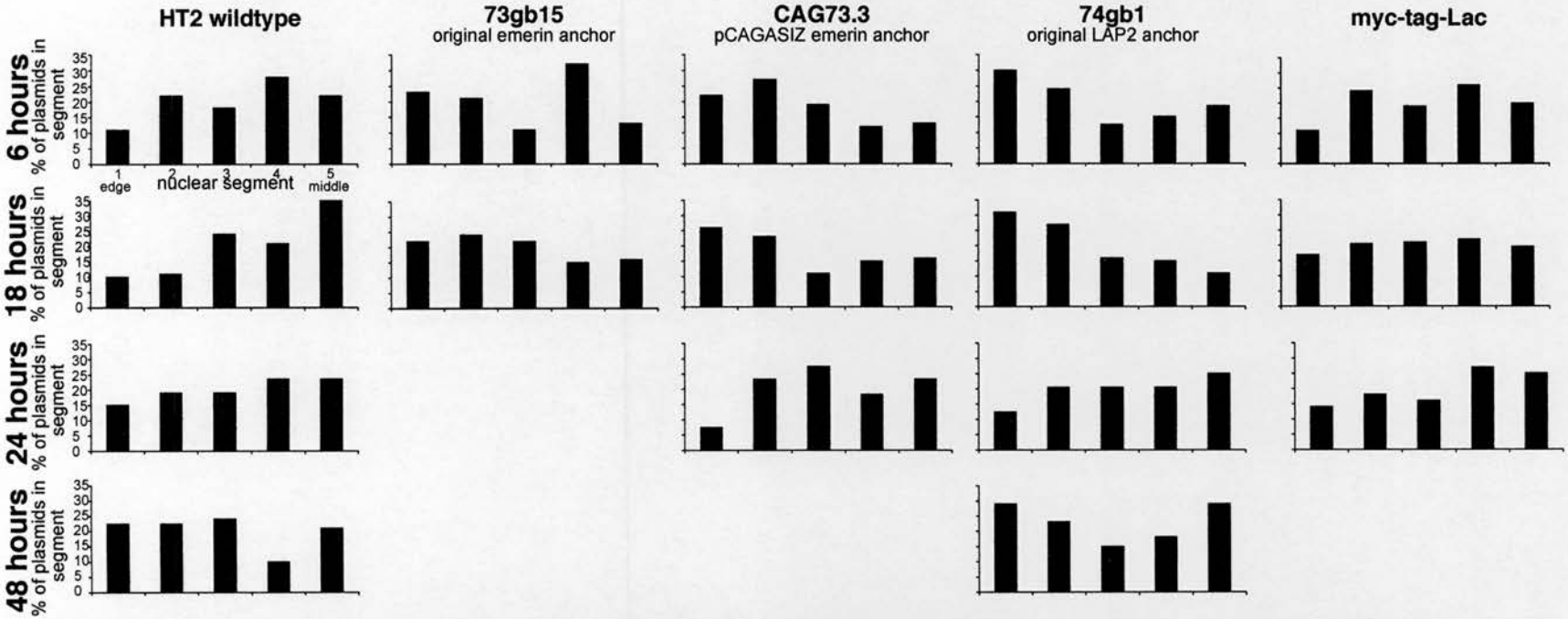

Figure 6.22: Stable cell lines expressing anchoring proteins are able to transiently tether pJRC49 to the nuclear periphery. Cell lines expressing various anchoring proteins were transfected with the Lac operator containing plasmid pJRC49,and fixed at set timepoints after transfection. 2D FISH using a Lac Operator probe was then used to map plasmid locations. 50 Interphase images of each cell line were captured and split into 5 segments of equal area. The % of plasmids mapping to each segment was then manually counted for each of the time points and cell lines analysed.

are able to tether plasmids to the periphery between 6 and 18 hours after transfection. Furthermore at 48 hours after transfection, LAP2β expressing anchor cells contain an enrichment of plasmids both in the outer and inner segments, suggesting two possible populations of plasmid, tethered and non-tethered. On closer examination of the images for this time point, both plasmid populations can be found within one cell (figure 6.22).

Overall, tethering of plasmids to the nuclear periphery is especially apparent in the LAP2β anchor expressing cell line. Immunofluorescence revealed that this cell line contained a higher proportion of cells expressing the anchoring protein compared to the emerin anchor cell line (figure 6.11). To address this, a cell line, HT2.CAGASIZ73.3, expressing pCAGASIZ73 (figure A.2) was made, in which over 95% of cells express the anchor. Transfections and subsequent mapping of plasmid positioning in this cell line revealed anchoring to the periphery takes place, although the LAP2β anchor is more effective.

6.8 ANALYSIS OF THE EFFECT OF NUCLEAR POSITIONING UPON GENE EXPRESSION

Cell lines expressing anchoring proteins are able to transiently tether LacO containing plasmids to the nuclear periphery for a short time period, between 6 and 18hrs after transfection. Therefore the effect of nuclear positioning upon the expression of a reporter gene can be investigated during these times after transfection. As this time period is relatively short the product of any reporter gene used will have to have a short half life, to allow an accurate analysis of the kinetics of transient gene expression to be performed. The plasmid pd1EGFP-N1 (BD Biosciences) was used for this purpose. The EGFP encoding portion of this plasmid was ligated into pJRC49 to create the plasmid, pd1EGFP-N1-Lac (appendix 1, figure a1.3). This plasmid encodes the d1EGFP destabilised, red-shifted variant of the wild-type GFP from *Aequorea victoria* (Prasher et al., 1992). pd1EGFP-N1 has residues 422-461 of the mouse ornithine decarboxylase (MODC) gene fused to the C terminus of EGFP (Li et al., 1998). These residues contain a PEST sequence that targets

proteins for rapid destruction and is composed of proline (P), glutamic acid (E), serine (S) and threonine (T) residues (Rogers et al., 1986). To reduce the half-life even further, additional amino acid substitutions in the MODC residues have created a half life of 1 hour, making it ideal for my study.

To ensure that the presence of a large region of repetitive sequence did not compromise the expression of EGFP, pd1EGFP-N1 and pd1EGF-N1-LacO constructs were transfected into 293T cells, and the expression of each analysed. This revealed no obvious effect of the Lac operator array upon either the transfection efficiency or the expression level of the reporter gene (figure 6.23).

pd1EGFP-N1 and pd1EGFP-N1-Lac were then transfected into HT2, 74GB1, Ht2.CAGASIZ73.3 and 74LacI.9 cell lines, to determine the effect of nuclear position upon expression. In the cell lines 74GB1 and HT2.CAGASIZ73.3, transfections of the plasmid pd1EGFP-N1-Lac result in the plasmid being anchored to the nuclear periphery at 6 and 18 hours after transfection (figure 6.21). After set time points of 6,18 and 24 hours after transfection, cells were counter-stained with Hoechst 33342 (5μM) and imaged. The % of cells expressing EGFP in each transfection was then manually counted. For each time point in each transfection, 5 or 6 images were collected, which in total contained between 400-600 cells. The values plotted are the average of three independent transfections in both the cell lines 74GB1 and 74LacI.9 and five independent transfections of HT2 cells. Silencing of pd1EGFP-N1 in the cell lines 74GB1 and HT2.CAGASIZ73.3 was apparent even before transfection frequencies had been calculated (figure 6.24.a). Quantification of the % of EGFP expressing cells allowed the true extent of this silencing to be investigated further (figure 6.24.b). Graphs plotting the % of cells in each transfection expressing pd1EGFP-N1-Lac divided by the % of cells expressing pd1EGFP-N1 show that nuclear position has a strong effect on gene expression (figure 6.24.b). At 6 hours, after transfection there is approx. 3 fold fewer cells expressing pd1EGFP-N1-Lac compared to pd1EGFP-N1 in wild-type HT2 cells, however in cells expressing free myc-tag-LacI, there is a further 2 fold reduction in expression from the LacO plasmid suggesting that free LacI has some effect on the expression of pd1EGFP-N1-Lac. A more striking change in expression levels

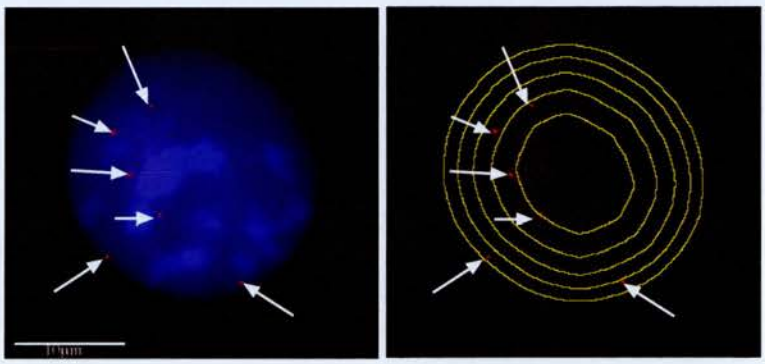

Figure 6.23: 48 hours after transfection, LacO plasmids can be found both at the nuclear edge and in the nucleoplasm of cells expressing pJRC74. 2D FISH on cells expressing the LAP2β anchor 48 hours after transfection shows that LacO plasmids ar located both at the nuclear periphery and in the nucleoplasm. 50 Images were divided into 5 segments of equal area and the % of LacO plasmids in each segment calculated.

between pd1EGFP-N1 and pd1EGFP-N1-LacO vectors is apparent in the LacI-LAP2β and LacI-emerin anchor expressing cell lines. In 74GB1, there is a massive 40 fold repression of expression from the LacO containing plasmid at 6-18 hours post-transfection when this plasmid is anchored at the nuclear periphery. Similar repression is seen in the HT2.CAGASIZ73.3 cell line, and no cells expressing pd1EGFP-N1-Lac at 6 hours were ever observed in the emerin anchor expressing cell line. However, at 24 hours after transfection there is an increase in the expression of pd1EGFP-N1-Lac in both cell lines, corresponding to the change in position of the plasmid from the nuclear edge to the nucleoplasm. In the cell line expressing myc-tag-LacI the ratio of expression of both plasmids remains fairly constant with no significant changes in expression seen from 6 hours through to 24 hours. At 24 hours expression from pd1EGFP-N1-LacO comparable in cells expressing LacI in nucleoplasm and cells expressing LacI at the nuclear periphery.

6.9 ELUCIDATING THE MECHANISM BEHIND SILENCING AT THE NUCLEAR PERIPHERY

Using the pd1EGFP-N1 reporter gene I have shown that the nucleus does indeed contain sub-compartments that can repress or promote gene expression and has provided direct evidence of the role of the nuclear periphery in gene silencing. However, what is the mechanism behind this gene silencing? Could it simply be an exclusion effect of transcription factors and other proteins from the nuclear periphery, or due to a more fundamental difference in the structure of chromatin forming on the plasmids dependent on their location?

6.9.1 Determining the role of histone acetylation in peripheral gene silencing

Histone hypoacetylation has been associated with transcriptional repression in some systems such as chromosome X inactivation (Jeppesen and Turner, 1993), and there is a zone of histone hypoacetylation for H3K9, H4K5 and H4K8 around the nuclear periphery (Sadoni et al., 1999; Taddei et al., 2001; Gilchrist et al., 2004,).

TSA is a potent inhibitor of HDACs and adding it to cells at low concentrations results in the accumulation of H3 and H4 acetylation throughout the cell nucleus, and in particular at the nuclear periphery (figure 6.25.b) (Gilchrist et al., 2004, Taddei et al., 1999). Low levels of TSA have previously been shown to cause large increases in the expression of transiently transfected genes (Ishiguro and Sartorelli, 2004) and have been shown to lift LAP2β mediated repression of transcription factors (Somech et al., 2005). I treated HT2 cells with 50ng/ml of TSA for set time points, and performed Western blots with an antibody against AcH4K5 (Upstate 07-327) to show that global levels of H4K5 acetylation increased with increased times of TSA treatment (figure 6.25.a). An antibody against GAPDH (Abcam ab9485) was used as a loading control to determine the level of protein on the blot for each sample. GAPDH is a housekeeping gene expressed in the cytoplasm of almost all tissues.

The % of cells expressing pd1EGFP-N1 and pd1EGFP-N1-Lac at each time point after transfection with Lipofectamine 2000, in the presence of TSA was calculated (figure 6.25.c). This was done for the three cell lines HT2, 74GB1, and 74LacI.9 with three independent transfections performed for each time point. Despite increased acetylation after 6 hours of transfection, there appears to be little effect on the ratio of expression of pd1EGFP-N1-Lac and pd1EGFP-N1 in the cell line 74GB1 when compared to HT2 cells and 74LacI.9. At 18 hours after transfection there is an increase of pd1EGFP-N1-Lac expression in the 74GB1 cell line, resulting in a reduction of the 46.5 fold difference in expression between both vectors to a 10 fold difference. Expression of myc-tag-LacI has been shown to induce some silencing of the pd1EGFP-N1-Lac vector in section 6.8, presumably due to free LacI binding to the Lac operator array and blocking transcription. In the presence of TSA at 18 hours after transfection, the ratio of pd1EGFP-N1 expression to pd1EGFP-N1-Lac in this cell line, is greater than that seen in HT2 cells with no TSA. This suggests that TSA can overcome silencing due to free LacI in the cell. This may also account for the increased expression of pd1EGFP-N1-Lac observed in the presence of the LAP2β anchor at 18 hours and suggesting that silencing of expression from the plasmid anchored at the nuclear periphery is not due to hypoacetylated histones.

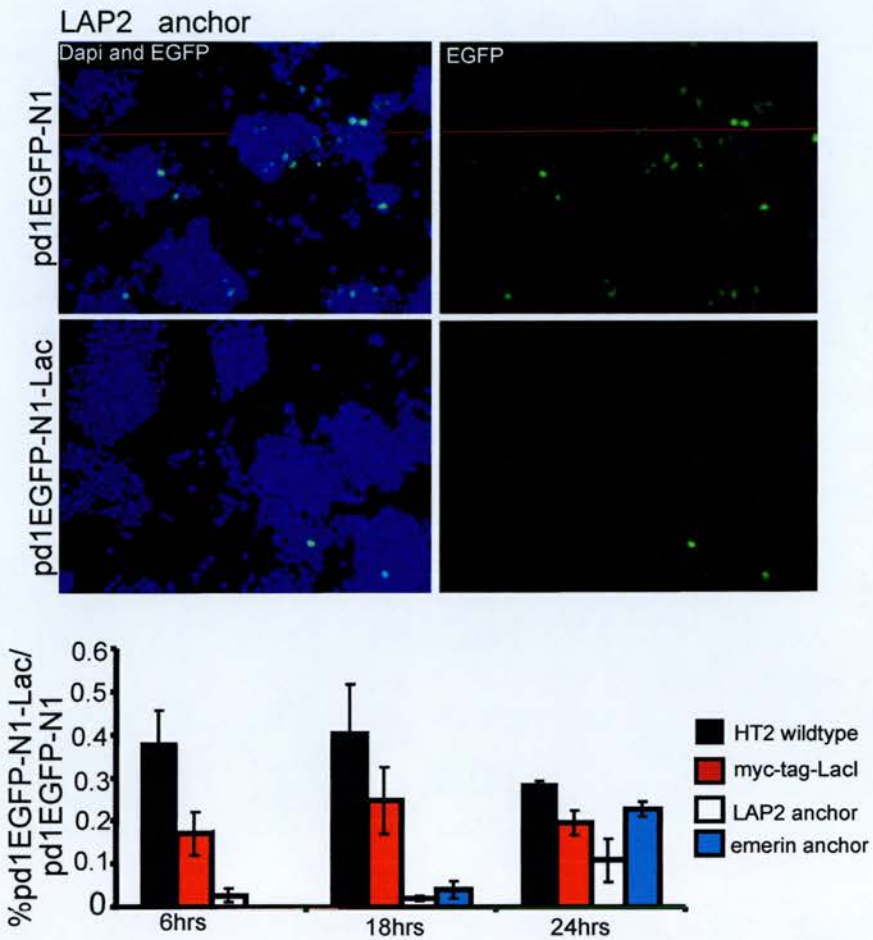

Figure 6.24: Localisation at the nuclear periphery induces gene silencing. A) Images from transient transfections of pd1EGFP-N1 and pd1EGFP-N1-Lac into 74GB1 cells.B) Ratio of pd1EGFP-N-Lac/pd1EGFP-N1 expresion in HT2, 74lacI, 74GB1, and HT2 CAGASIZ73.3 cells at 6,18 and 24 hours after transfection. No HT2 CAGSIZ73.3 cells expressing pd1EGFP-N1-Lac at 6 hrs were ever observed.Graphs are the mean of three different transfections,error bars= s.e.m.

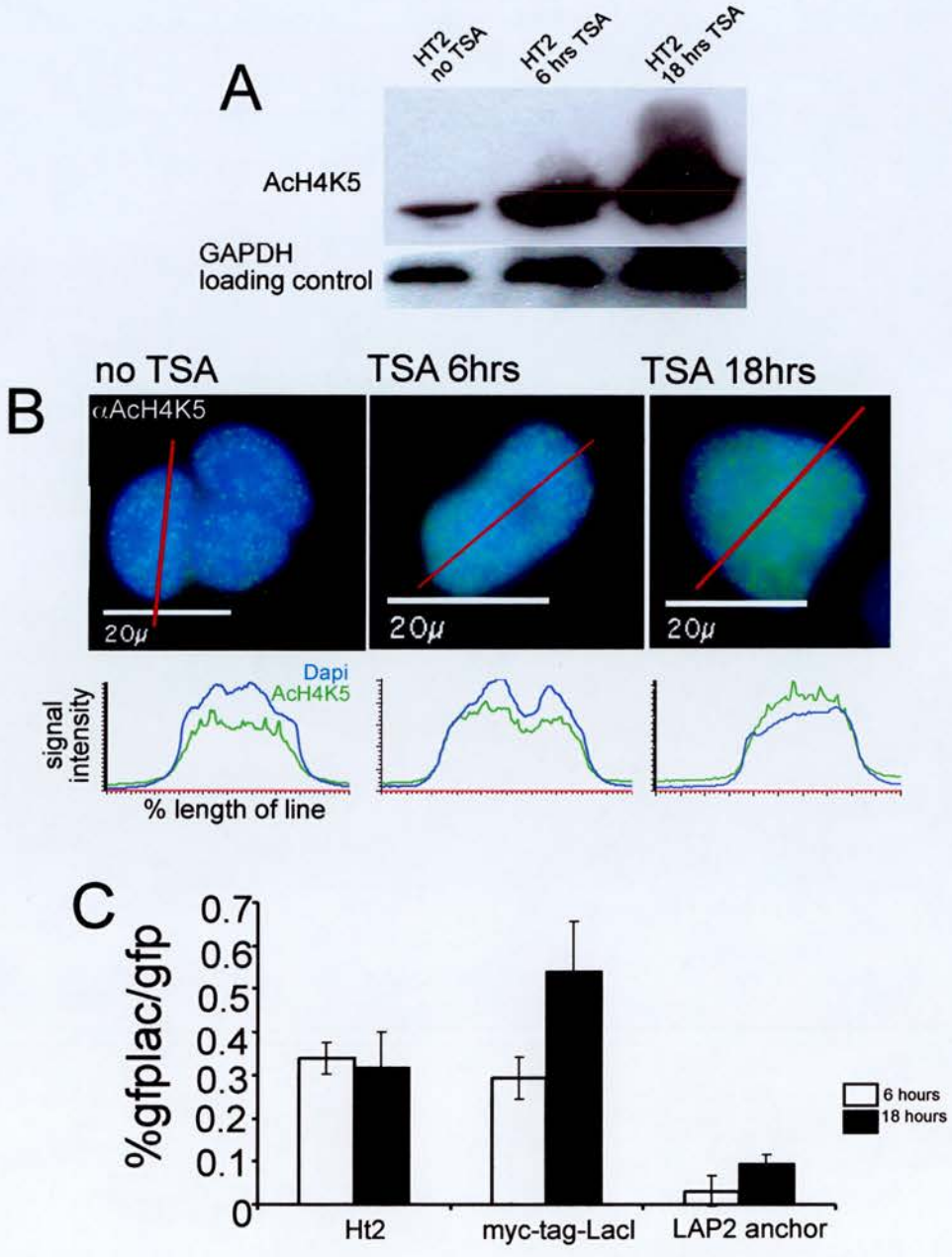

Figure 6.25: TSA reduces silencing at the periphery 18 hrs after transfection and removes the silencing induced by free LacI. A) Western blots using an antibody for AcH4K5 show that acetylated H4K5 increases with TSA treatment time.An antibody against GAPDH was used as a loading control. B) Immunofluorescence using the same antibody on cells treated with TSA for set time periods shows that acetylation increases with time of treatment especially at the nuclear edge.Pixel intensity along a 6 pixel wide line (red) through a cell for each time period was plotted (blue=Dapi, green =AcH4K5). C) Transfectionsof HT2 cells and cells expressing myc-tag-LacI and the LAP2β anchor proteins with plasmids expressing pd1EGFP-N1 and pd1EGFP-N1-Lac in the presence of 50ng/ml TSA were performed. The % of cells expressing EGFP at 6 and 18 hours after transfection was calculated and graphed as the % of EGFP-Lac expressing cells/ %EGFP expressing cells. All transfections were performed 3 times. Error bars=s.e.m.

6.10 DISCUSSION

Previously it has been shown in budding yeast that tethering a gene to the nuclear periphery can facilitate gene silencing (Andrulis et al., 1998). Here, I have tried to perform a similar experiment in the mouse nucleus. The mouse genome is 241 times bigger than the yeast genome and there is a large difference between the size of the nucleus in both species (figure 3.12). This has made tethering a gene to the periphery of mammalian cells a much more difficult process.

Although initial attempts to tether endogenous mouse genes to the nuclear periphery via 16 copies of LacO were unsuccessful, further experiments to tether large arrays with 1500 copies of LacO to the nuclear edge in human cells were and may have provided important insights into the structure of the nucleus. However, these arrays carried no reporter gene whose expression could be monitored. To tether endogenous mouse genes to the nuclear periphery would require the insertion of a larger LacO array into active genes. However, this could introduce problems with silencing of the endogenous gene, caused by changes in histone modifications and the higher order structure of chromatin due to the presence of a large block of heterochromatin *in cis*. In addition the presence of a larger array may itself induce changes in the position of the endogenous gene. The insertion of a large block of heterochromatin into the *Drosophila* locus *Brown* resulted in both the disrupted gene and its undisrupted homolog localising to a heterochromatin environment (Dreesen et al., 1991; Csink and Heinkoff, 1996). Despite this, FISH studies in HT1080 cell lines containing arrays approximately 100 times larger than the arrays used in my gene trap cell lines, appear to induce no changes in their nuclear positioning relative to their untagged homologs (Chubb et al., 2002). Determining the minimal size of array required for tethering could prove problematic as a plasmid containing 128 copies of the Lac operator sequence and 6kb of repetitive sequence is tethered to the nuclear periphery for only a short time after transfection, and may suggest that even an array of this size is not sufficient for long term tethering of an endogenous locus. Highly repetitive sequences such as a large LacO array are difficult to clone as they are unstable in *E.Coli* and can form deletions or rearrangements upon propagation. Cloning must be performed in an *E. coli* strain, which is recombination deficient.

The technical problems of cloning an even larger array into the gene trap vector make this experiment very difficult.

The B49.5.t2 and B49.5.t4 cell lines show that it is possible to tether DNA to nuclear membrane proteins and introduce it to a new nuclear environment. In both cell lines analysed there is a change in the location of arrays towards the nuclear edge suggesting that the binding of LacI to LacO containing DNA, is strong enough to move both chromatin and the membrane. However, analysis of the radial position of the Lac operator arrays would suggest that they are limited in the distance they are able to move. This agrees with the limited range of 2-3μm, of chromatin movement observed in live cells within the time period of a couple of hours (Chapter 3) and with previous studies which suggest specific parts of the genome can be tethered to different nuclear compartments such as the nuclear periphery or the nucleolus (Chubb et al., 2002; Zink and Cremer 1998; Marshall et al., 1996). Such tethering may create an anchor that is stronger than the interaction between LacI protein and Lac operator DNA and would thus limit the range of movement possible for specific loci.

To answer the question of what happens when DNA is not part of the genome and is able to move around the nucleoplasm, plasmids containing a Lac operator array were transfected into cells expressing LacI-anchoring proteins. FISH was used to show that these plasmids were indeed tethered to the nuclear edge between 6-18 hours after transfection (figure 6.22). Furthermore the insertion of a reporter gene into these plasmids showed that nuclear position does effect gene expression. Location of the reporter gene to the nuclear edge induced silencing. These experiments prove directly that nuclear positioning can have a role in gene regulation in mammalian cells. In yeast, it is known that silent chromatin is anchored at the nuclear edge through pathways dependent on the proteins yKu and SIR4 (Andrulis et al., 1998, Gartenberg et al., 2004, Taddei et al., 2004, Taddei et al., 2005). However in mammalian cells yKu is a nucleolar protein involved in double strand break repair, and there is no SIR4 homolog. Therefore the mechanisms for silencing chromatin at the nuclear periphery must be different.

To try and elucidate the mechanisms behind the peripheral silencing of genes in the mouse genome, the histone acetyltransferase inhibitor TSA was added to

cells at the point of transfection. The nuclear periphery is depleted in histone acetylation, associated with gene activation. However, increasing the level of histone acetylation at the nuclear periphery did not have a large effect on the level of pd1EGFP-N1-LacO repression observed in the LAP2β anchor expressing cell line, although repression due to free-LacI was lifted after 18 hours of treatment. Repression of transcription factors by LAP2β has recently been shown to be lifted in the presence of TSA, my results therefore suggest that pd1EGFP-N1-LacO is not silenced by LAP2 β mediated mechanisms (Somech et al., 2005).

There are two other possible causes for the peripheral silencing observed; differences in the chromatin structure of transfected plasmids dependent on location or the exclusion of transcription factors or enrichment of transcriptional repressors at the nuclear edge. Peripheral silencing could also be due to a combination of both factors.

CHAPTER 7

NUCLEAR ORGANISATION AND ITS ROLE IN REGULATING GENE EXPRESSION

In this thesis several new observations and findings regarding the spatial organisation of the genome within the mammalian nucleus are presented. I have looked at when chromatin position is established in both the cell cycle (chapter 3) and during differentiation (chapter 5) and have investigated some of the factors that may control nuclear positioning (chapters 5 and 6) and chromatin structure (chapter 4). In Chapter 3, the mobility of chromatin is analysed and I have looked at whether the positioning of a locus is conserved from one cell cycle to the next. In Chapter 4, the mobility of linker histones in different cell lines, each with a different mutation in an epigenetic modification of chromatin is investigated. This has allowed me to determine the affect of each mutation upon chromatin structure. In Chapter 5, the radial positioning of the mouse karyotype is analysed and the effect of differentiation and gene expression on chromosome positioning investigated and finally in Chapter 6, rather than analysing chromatin mobility or positioning, the nuclear position of reporter genes in mouse ES cells is experimentally manipulated and used to investigate the direct effect of nuclear position upon gene regulation.

7.1 MULTIPLE REGIMES OF CHROMATIN MOTION EXIST

Human chromatin, like yeast and *Drosophila* has both short and long range components to its mobility, and over long time periods can move distances further than previously thought. My studies also highlight increased mobility of chromatin during early G1 with loci moving up to 5μm in the space of 10 minutes. This agrees with previous work by Walter et al., 2003, which followed the pattern of photobleached domains thorugh mitosis and early G1, the behaviour of GFP labelled

centromeres (Shelby et al., 1996), and the long range chromatin reorganisation that has been inferred by cell cycle analysis of gene and chromosome position by FISH (Dimitrova and Gilbert 1999; Bridger et al., 1999). The question of whether chromosome position in the nucleus can be transmitted to daughter nuclei through mitosis is important for understanding whether nuclear organization can contribute to some form of epigenetic cellular memory. After analysing the motion of specific loci in human cells in the period immediately after exit from mitosis, I was able to conclude that the position of chromatin relative to nuclear compartments such as the nuclear periphery is not directly inherited through mitosis into daughter nuclei. Although the gross nuclear position of a locus becomes restricted by its position on the metaphase plate, and the angular relationship between two chromosomes can be transmitted, subsequent chromatin movements in early G1 are large enough to allow for substantial repositioning of loci within the nucleus relative to nuclear compartments.

Interestingly, the 13p locus located near the nucleolus displays what is described as motion with flow at short time intervals. This differs to the 5p14 and 11q13 loci, which are not located near either the nucleolus or the nuclear periphery. Investigating the short-range motion of the 13p locus in the presence of the transcriptional repressor DRB would be interesting as the nucleolus is primarily concerned with rDNA transcription and is a hub of transcriptional activity. Previous work has provided evidence that the 13p locus is anchored to the nucleolus and displays increased motion in the presence of DRB (Chubb et al., 2002). Could the forces driving the mobility of 13p locus over short periods be due to its location near the nucleolus? To test this, the mobility of other loci associated with the nucleolus could be analysed. It would be informative to undertake these experiments and to look at other loci associated with different nuclear compartments (i.e. the nuclear periphery) over short periods.

Over the course of 2 hours chromatin can move up to 2-3μm. This is similar in absolute terms to the mobility in *Drosophila* spermocytes and yeast, but as human nuclei are larger, loci are still restricted to small volumes of the total nucleus (Vasquez et al., 2001; Heun et al., 2001, figure 3.12). Despite this, the amount of movement observed would allow highly expressed genes to loop out with their

territories (Volpi et al., 2000; Williams et al., 2002; Mahy et al., 2002b; Chamberyon and Bickmore 2004) and could also allow genes to co-localise with centromeric heterochromatin upon repression (Brown et al., 1997; Brown et al., 1999; Skok et al., 2001;Merkenschlager et al., 2004; Rolden et al., 2005). To maintain the stable expression of a gene, chromatin is also required to remain relatively immobile. Examples of this were also seen in my analysis. Interestingly, studies in yeast have implicated chromatin motion to be controlled by ATP and replication. Could these same factors affect chromatin mobility in humans? In human cells, DNA replication during S phase has been shown to increase the mobility of only some loci (Chubb personal communication), which is the opposite situation to yeast, in which S phase reduces mobility (Heun et al., 2001). The high mobility of chromatin observed in early G1 was not driven by transcription, and although some of the motion may be due to changes in nuclear morphology, ATP could be essential for the larges changes seen. ATP is required for mitosis, making it impossible to determine if ATP is essential for the increased mobility of chromatin in early G1. However, it would be interesting to look at chromatin motion in interphase nuclei, both over long and short time periods, after the depletion of ATP. The requirement of ATP in yeast suggests mobility may be affected by chromatin remodelling. If ATP also plays a role in chromatin motion in humans, it may be informative to analyse chromatin motion in cell lines with defects in remodelling.

7.2 THE ABSENCE OF DNA METHYLATION CAN ENHANCE LINKER HISTONE BINDING TO CHROMATIN

Using fluorescence recovery after photobleaching, DNA methylation and histone acetylation, but not H3K9 methylation or the presence of MeCP2 has been shown to affect the binding of linker histones to chromatin. FRAP experiments in both mouse ES cells and in cell lines carrying different germline mutations were performed, both of which have never been done before. Using cell lines carrying mutations, rather than mutating the protein to be used, means that these experiments are very accurate as the GFP tag has not been altered. This sort of analysis is important as it provides insights into how epigenetic modifications may be able to regulate gene expression

through altering chromatin structure. DNA methylation is thought to regulate transcription by physically blocking transcription factors binding to chromatin. My results agree with this, and indicate that DNA methylation can also control the degree to which linker histones bind to chromatin. As linker histones stabilise higher chromatin structures and have roles in chromatin compaction, my results suggest that DNA methylation blocks transcription by altering the structure of chromatin. Linker histones can inhibit chromatin remodelling enzymes in the absence of phosphorylation (Horn et al.,2002) suggesting DNA methylation may influence the activity of Swi/snf, Mi-2 or ISWI complexes. It would be interesting to look at the binding abilities of chromatin remodelling complexes and other chromatin associated proteins in the *DNMT3a*$^{-/-}$ */3b* $^{-/-}$ cell line to test this idea. PRC2 is able to methylate H1K26 and this modification mark induces HP1 binding. Likewise,Ezh2, part of thc PRC2 complex, can methylate histoneH3K27, another mark of epigenetic silencing. Therefore the kinetics of HP1 and PRC2 binding to chromatin in *DNMT3a*$^{-/-}$ */3b* $^{-/-}$ cells may be interesting. Performing these experiments in the SuVar39h dn ES cell line could also be informative and these experiments could provide further insights in the effects of DNA and histone methylation upon chromatin structure and the interplay between different epigenetic modifications.

7.3 NON-RANDOM POSITIONING OF CHROMOSOMES IN MOUSE ES CELLS AND THE INFLUENCE OF GENE EXPRESION

The distribution of the mouse genome across its chromosomes is very different to that of humans, where gene rich chromatin is localised to the nuclear interior (Boyle et al., 2001). After I had started my PhD, two studies were published that suggested that chromosome position in the mouse nucleus is tissue specific (Parada et al., 2004; Kim et al., 2004). To determine if the radial positioning of the mouse genome is related to tissue type, I analysed the radial position of the mouse karyotype in undifferentiated ES cells and of several chromosomes in terminally differentiated ES cells. In undifferentiated ES cells, plotting both chromosome size and gene content against chromosome position shows little difference and both return very similar

Spearman rank order correlation values, making it impossible to decipher which factor maybe influencing chromosome position. Larger chromosomes with higher gene contents are found in more peripheral locations. However, from what we know about the radial positioning of human chromosomes, chromosomes with a higher gene content might be expected to be more internal rather than peripheral, suggesting that size is the influencing factor (Boyle et al., 2001; Cremer et al., 2001; Bolzer et al., 2005). Mouse chromosomes are relatively similar in size and gene distribution and in striking contrast to the radial distribution of the chromosomes seen in human cell lines, only subtle differences between the radial position of chromosomes is found in the mouse making it difficult to make any firm conclusions. This may be a reflection of the more even distribution of the mouse genome across its chromosomes. However, my results indicate that differentiation, and the global changes to chromatin structure that it induces, may have a role in the nuclear positioning of chromosomes. This would agree with the results of both Parada et al.,2004, and Kim et al., 2004. Chromosomes 6 and 13 are enriched with genes highly expressed in undifferentiated but not differentiated ES cells and my results show that these two chromosomes can occupy different regions of the nucleus in undifferentiated and differentiated ES cells. Furthermore, MMU6 that is further enriched in highly expressed genes in undifferentiated ES cells than MMU13 shows a more substantial change in its position. Five other chromosome territories analysed in both undifferentiated and differentiated cells do not show any change in their position, suggesting that chromosomes 6 and 13 may be the exception rather than the rule and that very large differences in gene expression may be required to alter chromosome position. The differences between my observations and those of Parada and colleagues may be due to the differences in the cell types analysed. However, in human cells CT position is conserved in primary and transformed cells as well as primary tissues suggesting that the spatial organisation of the nucleus is not grossly perturbed during cell transformation (Cremer et al., 2003). My results would suggest this is generally the case in mouse, as only small changes in CT position are seen in a subset of the CTs analysed. To answer questions regarding chromosome positioning and gene expression in different tissues would require a comprehensive analysis of

chromosome position in different mouse cell types before and after differentiation and the level of gene expression on each chromosome to be quantified.

To determine what other factors may play a role in CT positioning, genes with HDAC/HAT/HMTase or DNMT activities could be down regulated using RNAi, or CT position analysed in cell lines with mutations in genes involved in these processes. Perturbation of these processes using drugs has varying degrees of specificity and experimental results may not be representative of the role histone modifications or DNA methylation play in nuclear organisation. Furthermore, TSA is the obvious candidate for perturbing a process that may have a role in chromosome position, has previously been reported to have little effect on nuclear organisation (Gilchrist et al., 2004).

There is some evidence that chromatin may be anchored to nuclear compartments (Chubb et al., 2002; Croft et al., 1999), therefore mutating the protein structure or down regulating the expression of genes that may have a role in anchoring chromatin could provide further insights into CT positioning, as could experimentally manipulating the sequence content of a chromosome. Chromosomes could be altered to become either enriched or depleted in DNA sequences with potential roles as binding sites for proteins. Obvious candidates to investigate would include the lamin family of proteins and integral membrane proteins with LEM domains.

7.4 NUCLEAR POSITION CAN HAVE A DIRECT EFFECT ON GENE TRANSCRIPTION

By artificially anchoring a gene to the nuclear periphery in mouse ES cells it has bene shown that nuclear position can directly influence the expression of a gene. Although many studies have implicated nuclear compartments to have a role in gene regulation, only in yeast is there been direct proof that the location of a gene can control its expression (Andrulis et al., 1998). My results may provide important insights into why the genome is organised, the way it is. In human cell lines there is strong evidence to suggest gene-rich chromatin is located in the interior of the

nucleus and gene -poor chromatin at the nuclear edge (Boyle et al., 2001; Bolzer et al., 2005). My results suggest the nuclear periphery is a repressive environment therefore arranging the genome so that gene-rich chromosomes with, presumably, higher levels of transcription are located in the interior of the nucleus may prevent them from being silenced. The next step in this project is to determine the mechanism behind silencing at the nuclear periphery. Exclusion of transcription factors, or chromatin modifications or a combination of both factors may be responsible. In yeast high concentrations of silencing factors are concentrated at the nuclear edge. This is believed to function as a preventative measure, restraining these proteins from silencing large fractions of the genome. Although the proteins that mediate this, Ku and SIR4, have either a different function or no equivalent homolog in mammals (Gartenberg et al., 2004), nuclear compartmentalisation may serve a similar function in mammalian cells. Silencing factors may be enriched at the periphery of the nucleus. In support of this hypothesis is the recent finding that the integral membrane protein LAP2β is able to recruit HDAC3 to the nuclear periphery (Somach et al., 2005). In yeast, the SIR2 protein has HDAC activity. In addition HP1 proteins can interact with the Lamin B receptor, and emerin and LAP2β can both interact with the transcriptional regulator, GCL (Holmer et al., 2001; Nili et al., 2001;de la Luna et al., 1999; Haraguchi et al., 2004). Furthermore, levels of histone acetylation, a histone modification required for transcription are depleted at the nuclear periphery (Taddei et al., 2001; Gilchrist et al., 2004). To determine if whether chromatin has formed on the transfected plasmids will be the first step in elucidating the mechanisms behind silencing at the nuclear periphery. Chromatin immunoprecipitation could then be used to further characterise the nature of the chromatin in the control and anchor cell lines. For example different histone modifications may be present on plasmids dependent on location. ChIP could also be used to follow the recruitment of other non-chromatin proteins to plasmids, which also have a role in transcription activation or repression, such as HP1, RNA pol II, or chromatin remodelling factors.

To improve the tethering system it would be useful to increase the length of time a plasmid is tethered to the nuclear edge. In my experimental system plasmids are only tethered for a short time after transfection with maximum gene

repression seen at 18hrs. There are several reasons why this may be. These could include the inability of plasmids to replicate independently allowing them to remain as discrete chromatin circles within the cell nucleus. Failure to replicate could mean that plasmids are integrated into genomic DNA and the anchor lost. Other reasons could be the anchoring of plasmids to a nuclear scaffold restricting movement and thus preventing contact with the nuclear edge (Mearini et al., 2004, Jeong and Stein 1994), loss of the tether upon cell division, the assembly of chromatin and chromatin associated proteins upon the plasmid blocking the LacI-LacO interaction, or the targeting of plasmid DNA for destruction as the cells machinery recognises it as foreign. The replication of transfected plasmids has been reported to occur around 24-48 hrs after transfection and plasmids are not yet integrated into the genome in this time frame. Furthermore, plasmids unable to replicate become degraded around 40-50 hours after transfection (Cereghini and Yaniv 1984). These observations are from COS-1 monkey cells, and it may well be that mouse ES cells are different. Nevertheless, these observations suggest that the key events taking place in the plasmid tethering system at 24 hours are the inability of plasmids to replicate and/or the anchoring of plasmids to the nuclear scaffold and/or cell division. The only factor that can be easily altered is the ability of plasmids to replicate. In future plasmids could be used which are able to support episomal replication. This would be a key experiment to try and improve my tethering system.

7.5 PREDICTED ROLES OF NUCLEAR ORGANISATION

Some aspects of nuclear organisation may be conserved from yeast to mouse, spanning millions of years of evolution, but what drives the nucleus to be organised this way?

It has been proposed that the radial arrangement of the genome helps to maintain its integrity and that chromosomes rich in genes are protected from damage by having a more interior location (Tanabe et al., 2002). However, a recent study by Gazave and colleagues presents evidence to suggest this, "bodyguard hypothesis", is highly unlikely (Gazave et al., 2005). Nevertheless, the radial positioning of

chromosomes may still have some roles in maintaining genome integrity. The incidence of translocations between chromosomes is influenced by their nuclear locations (Bickmore and Teague 2002; Cornfleth et al., 2002). Therefore chromosome territories may be distributed to lower the frequency of such detrimental events.

Another hypothesis to explain nuclear organisation suggests that the nucleus is a self-organising entity and positioning is driven by gene transcription (Misteli et al., 2000; Kimura and Cook, 2002). Central to this hypothesis is the dynamic content and relative promiscuity of interactions amongst nuclear components. Nuclear proteins dynamically interchange and even major structural proteins have a high turnover suggesting nuclear proteins have unrestricted movement and are able to find specific binding sites within the nucleus (Chapter 4, Cheutin et al., 2003; Fesenstein et al., 2003; Lever et al., 2001; Misteli et al., 2001). This hypothesis, could explain the non-random position of chromosome territories and chromatin, as positioning may be the result of the interplay between the functional state of a gene or genes and the nuclear domains with which they interact. The results of Chapter 6 indicate that nuclear position alone can control gene expression and Chapter 5 presents evidence to suggest that chromosome position can be altered by differentiation. Moreover, chromosomes containing rDNA genes may be located more internally due to associations with the nucleolus, as has been shown to be the case in human cell lines (Bobrow and Heritage; 1980; Sullivan et al., 2001).

Gene loci upon either expression or repression are modified by local events such as histone modifications, DNA replication or transcriptional regulators, which in turn alter the chromatin state of the locus to either a more "open" structure or a more "closed" structure. In some cases these modifications can de-condense the chromatin fibre to a level that results in its expulsion from its territory (Volpi et al., 2000; Williams et al., 2002; Mahy et al., 2002; Chamberyon and Bickmore, 2004). Chromatin looping both *in cis* and *in trans* has been shown to mediate the expression of some genes in *Drosophila*, and chromatin looping of genes to specific nuclear compartments upon changes in transcription in both yeast and mammals has been reported. Combinations of chromatin loops from a central core body of a chromosome, may be able to associate with functionally distinct regions of the

nucleus and become preferentially associated with domains of functional equivalence, driving nuclear organisation. If very large genomic regions on one chromosome are either active or inactive, many of the genes on it may associate with the same or similar compartments, thus influencing the position of the whole chromosome. However, if chromatin looping and gene transcription are the driving forces behind nuclear organisation, then alterations in the radial positioning of a whole chromosome may not necessary take place during differentiation and might only be seen when very large changes in the level of transcription upon a chromosome is observed.

In Chapter 5, I have shown that CTs are generally static. This stability of interphase chromosome positioning may be due to tethering of chromosomes to nuclear compartments (Chubb et al., 2002), or nuclear matrices. The nuclear envelope has been proposed to play may a key part in this, as it has been suggested that some chromosomes interact with the reforming envelope after mitosis (Gerlich and Ellenberg, 2003). Quiescent cells with random chromosome positions, show global nuclear re-organisation upon re-entering mitosis as gene poor chromosomes re-localise to the nuclear edge (Bridger et al., 2000). Chromatin dynamics are increased during early G1, allowing chromosomes plenty of opportunity to associate with nuclear membrane proteins and with other factors that may also influence the position of whole chromosomes (Chapter 3). The idea of chromatin looping mediating gene expression is not new and it has long been suggested that chromatin in the nucleus is organised into loops anchored at their base by the nuclear matrix.

7.6 FUTURE DIRECTIONS

It is becoming increasingly clear from many studies that nuclear position influences gene regulation and I have shown for the first time that nuclear position can directly affect the expression of an exogenous gene in mouse ES cells, however we currently do not understand enough about nuclear architecture to understand why this may be. Our knowledge of the nuclear membrane and the function of the many proteins that are found there is particularly lacking. While the re-location of genes to pericentric heterochromatin may result in the spread of heterochromatin into the silenced gene,

or the the looping of genes through insulators may buffer them from silencing proteins, it is harder to imagine what components of the mammalian nuclear periphery may be controlling the repression of a reporter gene located there or how factors involved in repressing gene expression become enriched at the nuclear edge. The key to understanding this will be to analyse the structure of chromatin on plasmids tethered to the nuclear periphery and compare this to the structure of chromatin on plasmids located in the nuclear interior. Investigating the histone modifications on this chromatin will also be informative. Only by understanding what is different between the two populations of plasmid chromatin can we begin to dissect the mechanisms of peripheral gene silencing. This in turn will lead to our increased understanding of how nuclear compartmentalisation controls gene regulation.

Only by understanding these mechanisms, and the functional implications of chromatin composition and the spatial location of a gene or chromosome can we begin to develop efficient therapies for a wide range of genetic diseases. Many genetic diseases are caused by gene mis-regulation, and the molecular details for many individual diseases are not clear. Current research into potential therapies has a strong emphasise on the correction of the mutated gene sequence, however this will only be successful if the implications of chromatin structure, composition and position are fully understood and taken into account. From the results of my studies and the work of others, it is becoming increasingly clear that these factors may be just as significant to gene regulation as the primary DNA sequence alone.

REFERENCES

Aagaard,L., Schmid,M., Warburton,P., and Jenuwein,T. (2000). Mitotic phosphorylation of SUV39H1, a novel component of active centromeres, coincides with transient accumulation at mammalian centromeres. J. Cell Sci. *113 (Pt 5)*, 817-829.

Abney,J.R., Cutler,B., Fillbach,M.L., Axelrod,D., and Scalettar,B.A. (1997). Chromatin dynamics in interphase nuclei and its implications for nuclear structure. J. Cell Biol. *137*, 1459-1468.

Abranches,R., Beven,A.F., Aragon-Alcaide,L., and Shaw,P.J. (1998). Transcription sites are not correlated with chromosome territories in wheat nuclei. J. Cell Biol. *143*, 5-12.

Ahmad,K. and Henikoff,S. (2002). Epigenetic consequences of nucleosome dynamics. Cell *111*, 281-284.

Alami,R., Fan,Y., Pack,S., Sonbuchner,T.M., Besse,A., Lin,Q., Greally,J.M., Skoultchi,A.I., and Bouhassira,E.E. (2003). Mammalian linker-histone subtypes differentially affect gene expression in vivo. Proc. Natl. Acad. Sci. U. S A *100*, 5920-5925.

Alberts AS, Bouquin N, Johnston LH, Treisman R.Analysis of RhoA-binding proteins reveals an interaction domain conserved in heterotrimeric G protein beta subunits and the yeast response regulator protein Skn7. J Biol Chem. 1998 Apr 10;273(15):8616-22.

Allan,J., Mitchell,T., Harborne,N., Bohm,L., and Crane-Robinson,C. (1986). Roles of H1 domains in determining higher order chromatin structure and H1 location. J. Mol. Biol. *187*, 591-601.

Allis,C.D., Richman,R., Gorovsky,M.A., Ziegler,Y.S., Touchstone,B., Bradley,W.A., and Cook,R.G. (1986). hv1 is an evolutionarily conserved H2A variant that is preferentially associated with active genes. J. Biol. Chem. *261*, 1941-1948.

Alvarez,J.D., Yasui,D.H., Niida,H., Joh,T., Loh,D.Y., and Kohwi-Shigematsu,T. (2000). The MAR-binding protein SATB1 orchestrates temporal and spatial expression of multiple genes during T-cell development. Genes Dev. *14*, 521-535.

Anderson,J.D. and Widom,J. (2000). Sequence and position-dependence of the equilibrium accessibility of nucleosomal DNA target sites. J. Mol. Biol. *296*, 979-987.

Andrulis,E.D., Neiman,A.M., Zappulla,D.C., and Sternglanz,R. (1998). Perinuclear localization of chromatin facilitates transcriptional silencing [published erratum appears in Nature 1998 Oct 1;395(6701):525]. Nature *394*, 592-595.

Andrulis,E.D., Zappulla,D.C., Ansari,A., Perrod,S., Laiosa,C.V., Gartenberg,M.R., and Sternglanz,R. (2002). Esc1, a nuclear periphery protein required for Sir4-based plasmid anchoring and partitioning. Mol. Cell Biol. *22*, 8292-8301.

Angelov,D., Molla,A., Perche,P.Y., Hans,F., Cote,J., Khochbin,S., Bouvet,P., and Dimitrov,S. (2003). The histone variant macroH2A interferes with transcription factor binding and SWI/SNF nucleosome remodeling. Molecular Cell *11*, 1033-1041.

Arney,K.L. and Fisher,A.G. (2004). Epigenetic aspects of differentiation. J. Cell Sci. *117*, 4355-4363.

Ayer,D.E. (1999). Histone deacetylases: transcriptional repression with SINers and NuRDs. Trends Cell Biol. *9*, 193-198.

Ayyanathan,K., Lechner,M.S., Bell,P., Maul,G.G., Schultz,D.C., Yamada,Y., Tanaka,K., Torigoe,K., and Rauscher,F.J., III (2003). Regulated recruitment of HP1 to a euchromatic gene induces mitotically heritable, epigenetic gene silencing: a mammalian cell culture model of gene variegation. Genes Dev. *17*, 1855-1869.

Bachman,K.E., Rountree,M.R., and Baylin,S.B. (2001). Dnmt3a and Dnmt3b are transcriptional repressors that exhibit unique localization properties to heterochromatin. J. Biol. Chem. *276*, 32282-32287.

Bain,G. and Gottlieb,D.I. (1998). Neural cells derived by in vitro differentiation of P19 and embryonic stem cells. Perspect. Dev. Neurobiol. *5*, 175-178.

Ball,D.J., Gross,D.S., and Garrard,W.T. (1983). 5-methylcytosine is localized in nucleosomes that contain histone H1. Proc. Natl. Acad. Sci. U. S A *80*, 5490-5494.

Bannister,A.J., Zegerman,P., Partridge,J.F., Miska,E.A., Thomas,J.O., Allshire,R.C., and Kouzarides,T. (2001). Selective recognition of methylated lysine 9 on histone H3 by the HP1 chromo domain. Nature *410*, 120-124.

Bantignies,F., Grimaud,C., Lavrov,S., Gabut,M., and Cavalli,G. (2003). Inheritance of Polycomb-dependent chromosomal interactions in Drosophila. Genes Dev. *17*, 2406-2420.

Barak,O., Lazzaro,M.A., Lane,W.S., Speicher,D.W., Picketts,D.J., and Shiekhattar,R. (2003). Isolation of human NURF: a regulator of Engrailed gene expression. EMBO J. *22*, 6089-6100.

Barra,J.L., Rhounim,L., Rossignol,J.L., and Faugeron,G. (2000). Histone H1 is dispensable for methylation-associated gene silencing in Ascobolus immersus and essential for long life span. Mol. Cell Biol. *20*, 61-69.

Barreto,V. and Cumano,A. (2000). Frequency and characterization of phenotypic Ig heavy chain allelically included IgM-expressing B cells in mice. J. Immunol. *164*, 893-899.

Bartova,E., Kozubek,S., Kozubek,M., Jirsova,P., Lukasova,E., Skalnikova,M., and Buchnickova,K. (2000). The influence of the cell cycle, differentiation and irradiation on the nuclear location of the abl, bcr and c-myc genes in human leukemic cells. Leuk. Res. *24*, 233-241.

Bassing,C.H., Swat,W., and Alt,F.W. (2002). The mechanism and regulation of chromosomal V(D)J recombination. Cell *109 Suppl*, S45-S55.

Bassing,C.H., Suh,H., Ferguson,D.O., Chua,K.F., Manis,J., Eckersdorff,M., Gleason,M., Bronson,R., Lee,C., and Alt,F.W. (2003). Histone H2AX: A dosage-dependent suppressor of oncogenic translocations and tumors. Cell *114*, 359-370.

Baxter,C.S. and Byvoet,P. (1975). Intercalating agents as probes of the spatial relationship between chromatin components. Biochem. Biophys. Res. Commun. *63*, 286-291.

Beil,M., Durschmied,D., Paschke,S., Schreiner,B., Nolte,U., Bruel,A., and Irinopoulou,T. (2002). Spatial distribution patterns of interphase centromeres during retinoic acid-induced differentiation of promyelocytic leukemia cells. Cytometry *47*, 217-225.

Bell,A.C. and Felsenfeld,G. (1999). Stopped at the border: boundaries and insulators. Curr. Opin. Genet. Dev. *9*, 191-198.

Bell,A.C., West,A.G., and Felsenfeld,G. (1999). The protein CTCF is required for the enhancer blocking activity of vertebrate insulators. Cell *98*, 387-396.

Belmont,A.S., Bignone,F., and Tso,P.O.P. (1986). The Relative Intranuclear Positions of Barr Bodies in Xxx Nontransformed Human-Fibroblasts. Experimental Cell Research *165*, 165-179.

Belmont,A.S. and Straight,A.F. (1998). In vivo visualization of chromosomes using lac operator-repressor binding. Trends Cell Biol. *8*, 121-124.

Belmont,A.S., Li,G., Sudlow,G., and Robinett,C. (1999). Visualization of large-scale chromatin structure and dynamics using the lac operator/lac repressor reporter system. Methods Cell Biol. *58*, 203-222.

Belmont,A.S., Dietzel,S., Nye,A.C., Strukov,Y.G., and Tumbar,T. (1999). Large-scale chromatin structure and function. Curr. Opin. Cell Biol. *11*, 307-311.

Belmont,A.S. (2001). Visualizing chromosome dynamics with GFP. Trends Cell Biol. *11*, 250-257.

Belt,P.B., Jongmans,W., de Wit,J., Hoeijmakers,J.H., van de,P.P., and Backendorf,C. (1991). Efficient cDNA cloning by direct phenotypic correction of a mutant human cell line (HPRT-) using an Epstein-Barr virus-derived cDNA expression vector. Nucleic Acids Res. *19*, 4861-4866.

Benavente,R., Rose,K.M., Reimer,G., Hugle-Dorr,B., and Scheer,U. (1987). Inhibition of nucleolar reformation after microinjection of antibodies to RNA polymerase I into mitotic cells. JCB *105*, 1483-1491.

Bengtsson,L. and Wilson,K.L. (2004). Multiple and surprising new functions for emerin, a nuclear membrane protein. Curr. Opin. Cell Biol. *16*, 73-79.

Berger,R., Theodor,L., Shoham,J., Gokkel,E., Brok-Simoni,F., Avraham,K.B., Copeland,N.G., Jenkins,N.A., Rechavi,G., and Simon,A.J. (1996). The characterization and localization of the mouse thymopoietin/lamina-associated polypeptide 2 gene and its alternatively spliced products. Genome Res. *6*, 361-370.

Berger,S.L. (2002). Histone modifications in transcriptional regulation. Curr. Opin. Genet. Dev. *12*, 142-148.

Bergman,M.G., Wawra,E., and Winge,M. (1988). Chicken histone H5 inhibits transcription and replication when introduced into proliferating cells by microinjection. J. Cell Sci. *91 (Pt 2)*, 201-209.

Bernstein,B.E., Humphrey,E.L., Erlich,R.L., Schneider,R., Bouman,P., Liu,J.S., Kouzarides,T., and Schreiber,S.L. (2002). Methylation of histone H3 Lys 4 in coding regions of active genes. Proc. Natl. Acad. Sci. U. S A *99*, 8695-8700.

Bestor,T.H. (2000). The DNA methyltransferases of mammals. Hum. Mol. Genet. *9*, 2395-2402.

Bettinger,B.T., Gilbert,D.M., and Amberg,D.C. (2004). Actin up in the nucleus. Nat. Rev. Mol. Cell Biol. *5*, 410-415.

Bickmore,W.A. and Sutherland,H.G. (2002). Addressing protein localization within the nucleus. EMBO J. *21*, 1248-1254.

Bickmore, W.A and P Teague.2002. Influences of chromosome size,gene density and nuclear position on the frequency of constitutional translocations in the human population. Trends Genet 5:144-148

Bickmore,W.A. and Chubb,J.R. (2003). Chromosome position: now, where was I? Curr. Biol. *13*, R357-R359.

Billon,N., Jolicoeur,C., Ying,Q.L., Smith,A., and Raff,M. (2002). Normal timing of oligodendrocyte development from genetically engineered, lineage-selectable mouse ES cells. J. Cell Sci. *115*, 3657-3665.

Bione, S.; Maestrini, E.; Rivella, S.; Mancini, M.; Regis, S.; Romeo, G.; Toniolo, D. (1994).Identification of a novel X-linked gene responsible for Emery-Dreifuss muscular dystrophy. Nature Genet.*8*: 323-327, 1994.

Bird,A.P. (1984). DNA methylation versus gene expression. J. Embryol. Exp. Morphol. *83 Suppl*, 31-40.

Bird,A.P. and Wolffe,A.P. (1999). Methylation-induced repression--belts, braces, and chromatin. Cell *99*, 451-454.

Bobrow,M. and Heritage,J. (1980). Nonrandom segregation of nucleolar organizing chromosomes at mitosis? Nature *288*, 79-81.

Bode,J., Goetze,S., Heng,H., Krawetz,S.A., and Benham,C. (2003). From DNA structure to gene expression: mediators of nuclear compartmentalization and dynamics. Chromosome. Res. *11*, 435-445.

Boeke,J., Ammerpohl,O., Kegel,S., Moehren,U., and Renkawitz,R. (2000). The minimal repression domain of MBD2b overlaps with the methyl-CpG-binding domain and binds directly to Sin3A. J. Biol. Chem. *275*, 34963-34967.

Boggs,B.A., Allis,C.D., and Chinault,A.C. (2000). Immunofluorescent studies of human chromosomes with antibodies against phosphorylated H1 histone. Chromosoma *108*, 485-490.

Boggs,B.A., Cheung,P., Heard,E., Spector,D.L., Chinault,A.C., and Allis,C.D. (2002). Differentially methylated forms of histone H3 show unique association patterns with inactive human X chromosomes. Nat. Genet. *30*, 73-76.

Bolzer,A., Kreth,G., Solovei,I., Koehler,D., Saracoglu,K., Fauth,C., Muller,S., Eils,R., Cremer,C., Speicher,M.R., and Cremer,T. (2005). Three-Dimensional Maps of All Chromosomes in Human Male Fibroblast Nuclei and Prometaphase Rosettes. PLoS. Biol. *3*, e157.

Bone,J.R., Lavender,J., Richman,R., Palmer,M.J., Turner,B.M., and Kuroda,M.I. (1994). Acetylated histone H4 on the male X chromosome is associated with dosage compensation in Drosophila. Genes Dev. *8*, 96-104.

Borden,K.L. (2002). Pondering the promyelocytic leukemia protein (PML) puzzle: possible functions for PML nuclear bodies. Mol. Cell Biol. *22*, 5259-5269.

Bornfleth,H., Edelmann,P., Zink,D., Cremer,T., and Cremer,C. (1999). Quantitative motion analysis of subchromosomal foci in living cells using four-dimensional microscopy. Biophys. J. *77*, 2871-2886.

Borrow,J., Stanton,V.P., Jr., Andresen,J.M., Becher,R., Behm,F.G., Chaganti,R.S., Civin,C.I., Disteche,C., Dube,I., Frischauf,A.M., Horsman,D., Mitelman,F., Volinia,S., Watmore,A.E., and Housman,D.E. (1996). The translocation t(8;16)(p11;p13) of acute myeloid leukaemia fuses a putative acetyltransferase to the CREB-binding protein. Nat. Genet. *14*, 33-41.

Boshart,M., Weber,F., Jahn,G., Dorsch-Hasler,K., Fleckenstein,B., and Schaffner,W. (1985). A very strong enhancer is located upstream of an immediate early gene of human cytomegalovirus. Cell *41*, 521-530.

Boulikas,T. (1995). Chromatin domains and prediction of MAR sequences. Int. Rev. Cytol. *162A*, 279-388.

Boyle,S., Gilchrist,S., Bridger,J.M., Mahy,N.L., Ellis,J.A., and Bickmore,W.A. (2001). The spatial organization of human chromosomes within the nuclei of normal and emerin-mutant cells. Hum. Mol. Genet. *10*, 211-219.

Bozhenok,L., Wade,P.A., and Varga-Weisz,P. (2002). WSTF-ISWI chromatin remodeling complex targets heterochromatic replication foci. EMBO J. *21*, 2231-2241.

Bradbury,E.M., Cary,P.D., Crane-Robinson,C., and Rattle,H.W. (1973). Conformations and interactions of histones and their role in chromosome structure. Ann. N. Y. Acad. Sci. *222*, 266-289.

Bradley,A., Evans,M., Kaufman,M.H., and Robertson,E. (1984). Formation of germ-line chimaeras from embryo-derived teratocarcinoma cell lines. Nature *309*, 255-256.

Braunstein,M., Rose,A.B., Holmes,S.G., Allis,C.D., and Broach,J.R. (1993). Transcriptional silencing in yeast is associated with reduced nucleosome acetylation. Genes Dev. *7*, 592-604.

Braunstein,M., Sobel,R.E., Allis,C.D., Turner,B.M., and Broach,J.R. (1996). Efficient transcriptional silencing in Saccharomyces cerevisiae requires a heterochromatin histone acetylation pattern. Mol. Cell Biol. *16*, 4349-4356.

Brehm,A., Langst,G., Kehle,J., Clapier,C.R., Imhof,A., Eberharter,A., Muller,J., and Becker,P.B. (2000). dMi-2 and ISWI chromatin remodelling factors have distinct nucleosome binding and mobilization properties. EMBO J. *19*, 4332-4341.

Brero,A., Easwaran,H.P., Nowak,D., Grunewald,I., Cremer,T., Leonhardt,H., and Cardoso,M.C. (2005). Methyl CpG-binding proteins induce large-scale chromatin reorganization during terminal differentiation. J. Cell Biol. *169*, 733-743.

Brickner,J.H. and Walter,P. (2004). Gene recruitment of the activated INO1 locus to the nuclear membrane. Plos Biology *2*, 1843-1853.

Bridger,J.M. and Bickmore,W.A. (1998). Putting the genome on the map. Trends Genet. *14*, 403-409.

Bridger,J.M., Boyle,S., Kill,I.R., and Bickmore,W.A. (2000). Re-modelling of nuclear architecture in quiescent and senescent human fibroblasts. Curr. Biol. *10*, 149-152.

Broers,J.L., Kuijpers,H.J., Ostlund,C., Worman,H.J., Endert,J., and Ramaekers,F.C. (2005). Both lamin A and lamin C mutations cause lamina instability as well as loss of internal nuclear lamin organization. Exp. Cell Res. *304*, 582-592.

Broers JL, Machiels BM, van Eys GJ, Kuijpers HJ, Manders EM, van Driel R, Ramaekers FC.Dynamics of the nuclear lamina as monitored by GFP-tagged A-type lamins.J Cell Sci, *112* (Pt 20):3463-75.

Brosi,R., Groning,K., Behrens,S.E., Luhrmann,R., and Kramer,A. (1993). Interaction of mammalian splicing factor SF3a with U2 snRNP and relation of its 60-kD subunit to yeast PRP9. Science *262*, 102-105.

Brosi,R., Hauri,H.P., and Kramer,A. (1993). Separation of splicing factor SF3 into two components and purification of SF3a activity. J. Biol. Chem. *268*, 17640-17646.

Brown,D.C., Grace,E., Sumner,A.T., Edmunds,A.T., and Ellis,P.M. (1995). ICF syndrome (immunodeficiency, centromeric instability and facial anomalies): investigation of heterochromatin abnormalities and review of clinical outcome. Hum. Genet. *96*, 411-416.

Brown,K.E., Guest,S.S., Smale,S.T., Hahm,K., Merkenschlager,M., and Fisher,A.G. (1997). Association of transcriptionally silent genes with Ikaros complexes at centromeric heterochromatin. Cell *91*, 845-854.

Brown,K.E., Baxter,J., Graf,D., Merkenschlager,M., and Fisher,A.G. (1999). Dynamic repositioning of genes in the nucleus of lymphocytes preparing for cell division. Mol. Cell *3*, 207-217.

Brownell,J.E., Zhou,J., Ranalli,T., Kobayashi,R., Edmondson,D.G., Roth,S.Y., and Allis,C.D. (1996). Tetrahymena histone acetyltransferase A: a homolog to yeast Gcn5p linking histone acetylation to gene activation. Cell *84*, 843-851.

Brustle,O., Jones,K.N., Learish,R.D., Karram,K., Choudhary,K., Wiestler,O.D., Duncan,I.D., and McKay,R.D. (1999). Embryonic stem cell-derived glial precursors: A source of myelinating transplants. Science *285*, 754-756.

Bryk,M., Briggs,S.D., Strahl,B.D., Curcio,M.J., Allis,C.D., and Winston,F. (2002). Evidence that Set1, a factor required for methylation of histone H3, regulates rDNA silencing in S. cerevisiae by a Sir2-independent mechanism. Curr. Biol. *12*, 165-170.

Bulger,M., Schubeler,D., BENDER,M.A., Hamilton,J., Farrell,C.M., Hardison,R.C., and Groudine,M. (2003). A complex chromatin landscape revealed by patterns of nuclease sensitivity and histone modification within the mouse beta-globin locus. Molecular and Cellular Biology *23*, 5234-5244.

Byrd,K. and Corces,V.G. (2003). Visualization of chromatin domains created by the gypsy insulator of Drosophila. J. Cell Biol. *162*, 565-574.

Cai,S., Han,H.J., and Kohwi-Shigematsu,T. (2003). Tissue-specific nuclear architecture and gene expression regulated by SATB1. Nat. Genet. *34*, 42-51.

Cao,R., Wang,L., Wang,H., Xia,L., Erdjument-Bromage,H., Tempst,P., Jones,R.S., and Zhang,Y. (2002). Role of histone H3 lysine 27 methylation in Polycomb-group silencing. Science *298*, 1039-1043.

Cao,R. and Zhang,Y. (2004). SUZ12 is required for both the histone methyltransferase activity and the silencing function of the EED-EZH2 complex. Mol. Cell *15*, 57-67.

Capecchi,M.R. (1994). Targeted Gene Replacement. Sci. Amer. *March*, 34-41.

Carmi,I., Kopczynski,J.B., and Meyer,B.J. (1998). The nuclear hormone receptor SEX-1 is an X-chromosome signal that determines nematode sex. Nature *396*, 168-173.

Carmo-Fonseca,M., Pepperkok,R., Sproat,B.S., Ansorge,W., Swanson,M.S., and Lamond,A.I. (1991). In vivo detection of snRNP-rich organelles in the nuclei of mammalian cells. EMBO J. *10*, 1863-1873.

Carruthers,L.M. and Hansen,J.C. (2000). The core histone N termini function independently of linker histones during chromatin condensation. J. Biol. Chem. *275*, 37285-37290.

Carter,D., Chakalova,L., Osborne,C.S., Dai,Y.F., and Fraser,P. (2002). Long-range chromatin regulatory interactions in vivo. Nat. Genet. *32*, 623-626.

Casolari,J.M., Brown,C.R., Komili,S., West,J., Hieronymus,H., and Silver,P.A. (2004). Genome-wide localization of the nuclear transport machinery couples transcriptional status and nuclear organization. Cell *117*, 427-439.

Casolari,J.M., Brown,C.R., Drubin,D.A., Rando,O.J., and Silver,P.A. (2005). Developmentally induced changes in transcriptional program alter spatial organization across chromosomes. Genes & Development *19* , 1188-1198.

Cavalli,G. and Paro,R. (1998). The Drosophila Fab-7 chromosomal element conveys epigenetic inheritance during mitosis and meiosis. Cell *93*, 505-518.

Celeste,A., Fernandez-Capetillo,O., Kruhlak,M.J., Pilch,D.R., Staudt,D.W., Lee,A., Bonner,R.F., Bonner,W.M., and Nussenzweig,A. (2003). Histone H2AX phosphorylation is dispensable for the initial recognition of DNA breaks. Nature Cell Biology *5*, 675-U51.

Cereghini,S. and Yaniv,M. (1984). Assembly of transfected DNA into chromatin: structural changes in the origin-promoter-enhancer region upon replication. EMBO J. *3*, 1243-1253.

Chadwick,B.P. and Willard,H.F. (2001). A novel chromatin protein, distantly related to histone H2A, is largely excluded from the inactive X chromosome. J. Cell Biol. *152*, 375-384.

Chadwick,B.P., Valley,C.M., and Willard,H.F. (2001). Histone variant macroH2A contains two distinct macrochromatin domains capable of directing macroH2A to the inactive X chromosome. Nucleic Acids Res. *29* , 2699-2705.

Chalfie,M., Tu,Y., Euskirchen,G., Ward,W.W., and Prasher,D.C. (1994). Green fluorescent protein as a marker for gene expression. Science *263*, 802-805.

Chambers,I., Colby,D., Robertson,M., Nichols,J., Lee,S., Tweedie,S., and Smith,A. (2003). Functional expression cloning of Nanog, a pluripotency sustaining factor in embryonic stem cells. Cell *113*, 643-655.

Chambeyron,S. and Bickmore,W.A. (2004). Chromatin decondensation and nuclear reorganization of the HoxB locus upon induction of transcription. Genes Dev. *18*, 1119-1130.

Chang,Y., Bosma,M.J., and Bosma,G.C. (1999). Extended duration of DH-JH rearrangement in immunoglobulin heavy chain transgenic mice: implications for regulation of allelic exclusion. J. Exp. Med. *189*, 1295-1305.

Chao,M.V., Gralla,J.D., and Martinson,H.G. (1980). lac Operator nucleosomes. 1. Repressor binds specifically to operator within the nucleosome core. Biochemistry *19*, 3254-3260.

Chen,D., Ma,H., Hong,H., Koh,S.S., Huang,S.M., Schurter,B.T., Aswad,D.W., and Stallcup,M.R. (1999). Regulation of transcription by a protein methyltransferase. Science *284*, 2174-2177.

Chen,T., Tsujimoto,N., and Li,E. (2004). The PWWP domain of Dnmt3a and Dnmt3b is required for directing DNA methylation to the major satellite repeats at pericentric heterochromatin. Mol. Cell Biol. *24*, 9048-9058.

Chen T, Ueda Y, Dodge JE, Wang Z, Li E. (2003). Establishment and maintenance of genomic methylation patterns in mouse embryonic stem cells by Dnmt3a and Dnmt3b.Mol Cell Biol.23(16):5594-605.

Cheung,P., Allis,C.D., and Sassone-Corsi,P. (2000). Signaling to chromatin through histone modifications. Cell *103*, 263-271.

Cheutin,T., McNairn,A.J., Jenuwein,T., Gilbert,D.M., Singh,P.B., and Misteli,T. (2003). Maintenance of stable heterochromatin domains by dynamic HP1 binding. Science *299*, 721-725.

Chodosh,L.A., Fire,A., Samuels,M., and Sharp,P.A. (1989). 5,6-Dichloro-1-beta-D-ribofuranosylbenzimidazole inhibits transcription elongation by RNA polymerase II in vitro. J. Biol. Chem. *264*, 2250-2257.

Chow,C.M., Georgiou,A., Szutorisz,H., Silva,A.M.E., Pombo,A., Barahona,I., Dargelos,E., Canzonetta,C., and Dillon,N. (2005). Variant histone H3.3 marks promoters of transcriptionally active genes during mammalian cell division. Embo Reports *6*, 354-360.

Chubb,J.R., Boyle,S., Perry,P., and Bickmore,W.A. (2002). Chromatin motion is constrained by association with nuclear compartments in human cells. Curr. Biol. *12*, 439-445.

Chubb,J.R. and Bickmore,W.A. (2003). Considering nuclear compartmentalization in the light of nuclear dynamics. Cell *112*, 403-406.

Chung,H.M., Lee,M.G., Dietrich,P., Huang,J., and Van der Ploeg,L.H. (1993). Disruption of largest subunit RNA polymerase II genes in Trypanosoma brucei. Mol. Cell Biol. *13*, 3734-3743.

Chung,J.H., Whiteley,M., and Felsenfeld,G. (1993). A 5' element of the chicken beta-globin domain serves as an insulator in human erythroid cells and protects against position effect in Drosophila. Cell *74*, 505-514.

Chung,J.H., Bell,A.C., and Felsenfeld,G. (1997). Characterization of the chicken beta-globin insulator. Proc. Natl. Acad. Sci. U. S. A *94*, 575-580.

Clark,D., Reitman,M., Studitsky,V., Chung,J., Westphal,H., Lee,E., and Felsenfeld,G. (1993). Chromatin structure of transcriptionally active genes. Cold Spring Harb. Symp. Quant. Biol. *58*, 1-6.

Clark,K.L., Halay,E.D., Lai,E.S., and Burley,S.K. (1993). Co-Crystal Structure of the Hnf-3/Fork Head Dna-Recognition Motif Resembles Histone-H5. Nature *364*, 412-420.

Clemson,C.M., McNeil,J.A., Willard,H.F., and Lawrence,J.B. (1996). XIST RNA paints the inactive X chromosome at interphase: evidence for a novel RNA involved in nuclear/chromosome structure. J. Cell Biol. *132*, 259-275.

Cmarko,D., Verschure,P.J., Martin,T.E., Dahmus,M.E., Krause,S., Fu,X.D., van Driel,R., and Fakan,S. (1999). Ultrastructural analysis of transcription and splicing in the cell nucleus after bromo-UTP microinjection. Mol. Biol. Cell *10*, 211-223.

Cockerill,P.N. and Garrard,W.T. (1986). Chromosomal loop anchorage of the kappa immunoglobulin gene occurs next to the enhancer in a region containing topoisomerase II sites. Cell *44*, 273-282.

Cockerill,P.N. and Garrard,W.T. (1986). Chromosomal loop anchorage sites appear to be evolutionarily conserved. FEBS Lett. *204*, 5-7.

Cohen-Armon,M., Visochek,L., Katzoff,A., Levitan,D., Susswein,A.J., Klein,R., Valbrun,M., and Schwartz,J.H. (2004). Long-term memory requires polyADP-ribosylation. Science *304*, 1820-1822.

Cole,R.D. (1984). A Minireview of Microheterogeneity in H1-Histone and Its Possible Significance. Analytical Biochemistry *136*, 24-30.

Collins,N., Poot,R.A., Kukimoto,I., Garcia-Jimenez,C., Dellaire,G., and Varga-Weisz,P.D. (2002). An ACF1-ISWI chromatin-remodeling complex is required for DNA replication through heterochromatin. Nat. Genet. *32*, 627-632.

Colot,V. and Rossignol,J.L. (1999). Eukaryotic DNA methylation as an evolutionary device. Bioessays *21*, 402-411.

Comings,D.E. (1980). Arrangement of chromatin in the nucleus. Hum. Genet. *53*, 131-143.

Cook,P.R. and Brazell,I.A. (1975). Supercoils in human DNA. J. Cell Sci. *19*, 261-279.

Cook,P.R. and Brazell,I.A. (1976). Conformational constraints in nuclear DNA. J. Cell Sci. *22*, 287-302.

Cook,P.R., Brazell,I.A., and Jost,E. (1976). Characterization of nuclear structures containing superhelical DNA. J. Cell Sci. *22*, 303-324.

Cornforth, M.N., K.M. Greulich-Bode, B.D.Loucas, J.Arsuga, M.Vazquez, R.K. Scahs, M.Bruckner, M.Molls, P.Hahnfeldt, L.Hlatky and D.J.Brenner.(2002). Chromsomes are predominately located randomly with respect to one another in interphase human cells. J.Cell.Biol. *159*:237-244

Costa,T.E., Suh,H., and Nussenzweig,M.C. (1992). Chromosomal position of rearranging gene segments influences allelic exclusion in transgenic mice. Proc. Natl. Acad. Sci. U. S A *89*, 2205-2208.

Costanzi,C. and Pehrson,J.R. (1998). Histone macroH2A1 is concentrated in the inactive X chromosome of female mammals. Nature *393*, 599-601.

Craig,J.M. and Bickmore,W.A. (1993). Chromosome bands--flavours to savour. Bioessays *15*, 349-354.

Craig,J.M., Boyle,S., Perry,P., and Bickmore,W.A. (1997). Scaffold attachments within the human genome. J. Cell Sci. *110 (Pt 21)*, 2673-2682.

Cremer,C., Munkel,C., Granzow,M., Jauch,A., Dietzel,S., Eils,R., Guan,X.Y., Meltzer,P.S., Trent,J.M., Langowski,J., and Cremer,T. (1996). Nuclear architecture and the induction of chromosomal aberrations. Mutat. Res. *366*, 97-116.

Cremer,M., von Hase,J., Volm,T., Brero,A., Kreth,G., Walter,J., Fischer,C., Solovei,I., Cremer,C., and Cremer,T. (2001). Non-random radial higher-order chromatin arrangements in nuclei of diploid human cells. Chromosome. Res. *9*, 541-567.

Cremer,T., Cremer,C., Schneider,T., Baumann,H., Hens,L., and Kirsch-Volders,M. (1982). Analysis of chromosome positions in the interphase nucleus of Chinese hamster cells by laser-UV-microirradiation experiments. Hum. Genet. *62*, 201-209.

Cremer,T., Lichter,P., Borden,J., Ward,D.C., and Manuelidis,L. (1988). Detection of chromosome aberrations in metaphase and interphase tumor cells by in situ hybridization using chromosome-specific library probes. Hum. Genet. *80*, 235-246.

Cremer,T., Kurz,A., Zirbel,R., Dietzel,S., Rinke,B., Schrock,E., Speicher,M.R., Mathieu,U., Jauch,A., Emmerich,P., and . (1993). Role of chromosome territories in the functional compartmentalization of the cell nucleus. Cold Spring Harb. Symp. Quant. Biol. *58*, 777-792.

Cremer,T. and Cremer,C. (2001). Chromosome territories, nuclear architecture and gene regulation in mammalian cells. Nat. Rev. Genet. *2*, 292-301.

Croft,J.A., Bridger,J.M., Boyle,S., Perry,P., Teague,P., and Bickmore,W.A. (1999). Differences in the localization and morphology of chromosomes in the human nucleus. J. Cell Biol. *145*, 1119-1131.

Cross,S.H., Lee,M., Clark,V.H., Craig,J.M., Bird,A.P., and Bickmore,W.A. (1997). The chromosomal distribution of CpG islands in the mouse: evidence for genome scrambling in the rodent lineage. Genomics *40* , 454-461.

Cryderman,D.E., Cuaycong,M.H., Elgin,S.C., and Wallrath,L.L. (1998). Characterization of sequences associated with position-effect variegation at pericentric sites in Drosophila heterochromatin. Chromosoma *107*, 277-285.

Csankovszki,G., Nagy,A., and Jaenisch,R. (2001). Synergism of Xist RNA, DNA methylation, and histone hypoacetylation in maintaining X chromosome inactivation. JCB *153*, 773-783.

Csink,A.K. and Henikoff,S. (1998). Large-scale chromosomal movements during interphase progression in Drosophila. J. Cell Biol. *143*, 13-22.

Cubitt,A.B., Heim,R., Adams,S.R., Boyd,A.E., Gross,L.A., and Tsien,R.Y. (1995). Understanding, improving and using green fluorescent proteins. Trends Biochem. Sci. *20*, 448-455.

Cuthbert,G.L., Daujat,S., Snowden,A.W., Erdjument-Bromage,H., Hagiwara,T., Yamada,M., Schneider,R., Gregory,P.D., Tempst,P., Bannister,A.J., and Kouzarides,T. (2004). Histone deimination antagonizes arginine methylation. Cell *118*, 545-553.

Czermin,B., Schotta,G., Hulsmann,B.B., Brehm,A., Becker,P.B., Reuter,G., and Imhof,A. (2001). Physical and functional association of SU(VAR)3-9 and HDAC1 in Drosophila. EMBO Rep. *2*, 915-919.

Czermin,B., Melfi,R., McCabe,D., Seitz,V., Imhof,A., and Pirrotta,V. (2002). Drosophila enhancer of Zeste/ESC complexes have a histone H3 methyltransferase activity that marks chromosomal polycomb sites. Cell *111*, 185-196.

Dani,C., Smith,A.G., Dessolin,S., Leroy,P., Staccini,L., Villageois,P., Darimont,C., and Ailhaud,G. (1997). Differentiation of embryonic stem cells into adipocytes in vitro. J. Cell Sci. *110*, 1279-1285.

Daujat,S., Bauer,U.M., Shah,V., Turner,B., Berger,S., and Kouzarides,T. (2002). Crosstalk between CARM1 methylation and CBP acetylation on histone H3. Curr. Biol. *12*, 2090-2097.

Daujat,S., Zeissler,U., Waldmann,T., Happel,N., and Schneider,R. (2005). HP1 binds specifically to K26 methylated histone H1.4, whereas simultaneous S27 phosphorylation blocks HP1 binding. J. Biol. Chem.

Davey,C., Pennings,S., Meersseman,G., Wess,T.J., and Allan,J. (1995). Periodicity of Strong Nucleosome Positioning Sites Around the Chicken Adult Beta-Globin Gene May Encode Regularly Spaced Chromatin. Proceedings of the National Academy of Sciences of the United States of America *92* , 11210-11214.

Davie,J.R. (1995). The nuclear matrix and the regulation of chromatin organization and function. Int. Rev. Cytol. *162A*, 191-250.

Davie,J.R. and Chadee,D.N. (1998). Regulation and regulatory parameters of histone modifications. J. Cell Biochem. Suppl. *30-31:203-13*, 203-213.

de la,L.S., Allen,K.E., Mason,S.L., and La Thangue,N.B. (1999). Integration of a growth-suppressing BTB/POZ domain protein with the DP component of the E2F transcription factor. EMBO J. *18*, 212-228.

de Laat,W. and Grosveld,F. (2003). Spatial organization of gene expression: the active chromatin hub. Chromosome Res. *11*, 447-459.

de Napoles,M., Mermoud,J.E., Wakao,R., Tang,Y.A., Endoh,M., Appanah,R., Nesterova,T.B., Silva,J., Otte,A.P., Vidal,M., Koseki,H., and Brockdorff,N. (2004). Polycomb group proteins Ring1A/B link ubiquitylation of histone H2A to heritable gene silencing and X inactivation. Developmental Cell *7*, 663-676.

Dechat,T., Vlcek,S., and Foisner,R. (2000). Review: lamina-associated polypeptide 2 isoforms and related proteins in cell cycle-dependent nuclear structure dynamics. J. Struct. Biol. *129*, 335-345.

Dekker,J., Rippe,K., Dekker,M., and Kleckner,N. (2002). Capturing chromosome conformation. Science *295*, 1306-1311.

Dellaire,G. and Bazett-Jones,D.P. (2004). PML nuclear bodies: dynamic sensors of DNA damage and cellular stress. Bioessays *26*, 963-977.

Delmas,V., Stokes,D.G., and Perry,R.P. (1993). A Mammalian Dna-Binding Protein That Contains A Chromodomain and An Snf2 Swi2-Like Helicase Domain. Proceedings of the National Academy of Sciences of the United States of America *90*, 2414-2418.

Dennis,K., Fan,T., Geiman,T., Yan,Q., and Muegge,K. (2001). Lsh, a member of the SNF2 family, is required for genome-wide methylation. Genes Dev. *15*, 2940-2944.

Dernburg,A.F., Broman,K.W., Fung,J.C., Marshall,W.F., Philips,J., Agard,D.A., and Sedat,J.W. (1996). Perturbation of nuclear architecture by long-distance chromosome interactions. Cell *85*, 745-759.

Deuring,R., Fanti,L., Armstrong,J.A., Sarte,M., Papoulas,O., Prestel,M., Daubresse,G., Verardo,M., Moseley,S.L., Berloco,M., Tsukiyama,T., Wu,C., Pimpinelli,S., and Tamkun,J.W. (2000). The ISWI chromatin-remodeling protein is required for gene expression and the maintenance of higher order chromatin structure in vivo. Molecular Cell *5*, 355-365.

Dev,V.G., Tantravahi,R., Miller,D.A., and Miller,O.J. (1977). Nucleolus organizers in Mus musculus subspecies and in the RAG mouse cell line. Genetics *86*, 389-398.

Dietzel,S., Jauch,A., Kienle,D., Qu,G., Holtgreve-Grez,H., Eils,R., Munkel,C., Bittner,M., Meltzer,P.S., Trent,J.M., and Cremer,T. (1998). Separate and variably shaped chromosome arm domains are disclosed by chromosome arm painting in human cell nuclei. Chromosome. Res. *6*, 25-33.

Dietzel,S., Schiebel,K., Little,G., Edelmann,P., Rappold,G.A., Eils,R., Cremer,C., and Cremer,T. (1999). The 3D positioning of ANT2 and ANT3 genes within female X chromosome territories correlates with gene activity. Exp. Cell Res. *252*, 363-375.

Dillon,N., Trimborn,T., Strouboulis,J., Fraser,P., and Grosveld,F. (1997). The effect of distance on long-range chromatin interactions. Mol. Cell *1*, 131-139.

Dillon,N. and Festenstein,R. (2002). Unravelling heterochromatin: competition between positive and negative factors regulates accessibility. Trends Genet. *18*, 252-258.

Dimitrova,D.S. and Gilbert,D.M. (1999). The spatial position and replication timing of chromosomal domains are both established in early G1 phase. Mol. Cell *4*, 983-993.

Dodge,J.E., Okano,M., Dick,F., Tsujimoto,N., Chen,T.P., Wang,S.M., Ueda,Y., Dyson,N., and Li,E. (2005). Inactivation of Dnmt3b in mouse embryonic fibroblasts results in DNA hypomethylation, chromosomal instability, and spontaneous immortalization. J. Biol. Chem. *280*, 17986-17991.

Dou,Y., Bowen,J., Liu,Y., and Gorovsky,M.A. (2002). Phosphorylation and an ATP-dependent process increase the dynamic exchange of H1 in chromatin. J. Cell Biol. *158*, 1161-1170.

Dousset,T., Wang,C., Verheggen,C., Chen,D., Hernandez-Verdun,D., and Huang,S. (2000). Initiation of nucleolar assembly is independent of RNA polymerase I transcription. Mol. Biol. Cell *11*, 2705-2717.

Dover,J., Schneider,J., Tawiah-Boateng,M.A., Wood,A., Dean,K., Johnston,M., and Shilatifard,A. (2002). Methylation of histone H3 by COMPASS requires ubiquitination of histone H2B by Rad6. J. Biol. Chem. *277*, 28368-28371.

Downs,J.A., Kosmidou,E., Morgan,A., and Jackson,S.P. (2003). Suppression of homologous recombination by the Saccharomyces cerevisiae linker histone. Molecular Cell *11*, 1685-1692.

Drabent,B., Bode,C., and Doenecke,D. (1993). Structure and expression of the mouse testicular H1 histone gene (H1t). Biochim. Biophys. Acta *1216*, 311-313.

Dreesen,T.D., Henikoff,S., and Loughney,K. (1991). A pairing-sensitive element that mediates trans-inactivation is associated with the Drosophila brown gene. Genes Dev. *5*, 331-340.

Dreger M, Bengtsson L, Schoneberg T, Otto H, Hucho F.Nuclear envelope proteomics: novel integral membrane proteins of the inner nuclear membrane.Proc Natl Acad Sci U S A. *98*(21):11943-8

Duggan,M.M. and Thomas,J.O. (2000). Two DNA-binding sites on the globular domain of histone H5 are required for binding to both bulk and 5 S reconstituted nucleosomes. Journal of Molecular Biology *304*, 21-33.

Dundr,M., Phair,R., and Misteli,T. (2000). Dynamics of proteins in the mammalian cell nucleus. Molecular Biology of the Cell *11*, 10A.

Dundr,M. and Misteli,T. (2001). Functional architecture in the cell nucleus. Biochemical Journal *356*, 297-310.

Edelmann,P., Bornfleth,H., Zink,D., Cremer,T., and Cremer,C. (2001). Morphology and dynamics of chromosome territories in living cells. Biochim. Biophys. Acta *1551*, M29-M39.

Eissenberg,J.C. and Elgin,S.C.R. (2000). The HP1 protein family: getting a grip on chromatin. Current Opinion in Genetics & Development *10*, 204-210.

Ellis DJ, Jenkins H, Whitfield WG, Hutchison CJ.1997. GST-lamin fusion proteins act as dominant negative mutants in Xenopus egg extract and reveal the function of the lamina in DNA replication. J Cell Sci *110* (Pt 20):2507-18.

Emmerich,P., Loos,P., Jauch,A., Hopman,A.H., Wiegant,J., Higgins,M.J., White,B.N., van der,P.M., Cremer,C., and Cremer,T. (1989). Double in situ hybridization in combination with digital image analysis: a new approach to study interphase chromosome topography. Exp. Cell Res. *181*, 126-140.

Ernst,P., Hahm,K., Trinh,L., Davis,J.N., Roussel,M.F., Turck,C.W., and Smale,S.T. (1996). A potential role for Elf-1 in terminal transferase gene regulation. Mol. Cell Biol. *16*, 6121-6131.

Espada,J., Ballestar,E., Fraga,M.F., Villar-Garea,A., Juarranz,A., Stockert,J.C., Robertson,K.D., Fuks,F., and Esteller,M. (2004). Human DNA methyltransferase 1 is required for maintenance of the histone H3 modification pattern. J. Biol. Chem. *279*, 37175-37184.

Evangelista,M., Blundell,K., Longtine,M.S., Chow,C.J., Adames,N., Pringle,J.R., Peter,M., and Boone,C. (1997). Bni1p, a yeast formin linking cdc42p and the actin cytoskeleton during polarized morphogenesis. Science *276*, 118-122.

Evangelista,M., Pruyne,D., Amberg,D.C., Boone,C., and Bretscher,A. (2002). Formins direct Arp2/3-independent actin filament assembly to polarize cell growth in yeast. Nat. Cell Biol. *4*, 260-269.

Evans,M.J. and Kaufman,M.H. (1981). Establishment in culture of pluripotential cells from mouse embryos. Nature *292*, 154-156.

Faast,R., Thonglairoam,V., Schulz,T.C., Beall,J., Wells,J.R., Taylor,H., Matthaei,K., Rathjen,P.D., Tremethick,D.J., and Lyons,I. (2001). Histone variant H2A.Z is required for early mammalian development. Curr. Biol. *11*, 1183-1187.

Fairley,E.A., Kendrick-Jones,J., and Ellis,J.A. (1999). The Emery-Dreifuss muscular dystrophy phenotype arises from aberrant targeting and binding of emerin at the inner nuclear membrane. J. Cell Sci. *112 (Pt 15)*, 2571-2582.

Fakan,S. and Nobis,P. (1978). Ultrastructural localization of transcription sites and of RNA distribution during the cell cycle of synchronized CHO cells. Exp. Cell Res. *113*, 327-337.

Fan,J.Y., Rangasamy,D., Luger,K., and Tremethick,D.J. (2004). H2A.Z alters the nucleosome surface to promote HP1 alpha-mediated chromatin fiber folding. Molecular Cell *16*, 655-661.

Fan,Y., Nikitina,T., Morin-Kensicki,E.M., Zhao,J., Magnuson,T.R., Woodcock,C.L., and Skoultchi,A.I. (2003). H1 linker histones are essential for mouse development and affect nucleosome spacing in vivo. Mol. Cell Biol. *23*, 4559-4572.

Faravelli F., NSD1 mutations in Sotos syndrome.Am J Med Genet C Semin Med Genet. 2005 Aug 15;137(1):24-31

Fawcett,D.W. (1966). On the occurrence of a fibrous lamina on the inner aspect of the nuclear envelope in certain cells of vertebrates. Am. J. Anat. *119*, 129-145.

Feng,Q. and Zhang,Y. (2003). The NuRD complex: Linking histone modification to nucleosome remodeling. Protein Complexes That Modify Chromatin *274*, 269-290.

Ferreira,J. and Carmo-Fonseca,M. (1997). Genome replication in early mouse embryos follows a defined temporal and spatial order. J. Cell Sci. *110 (Pt 7)*, 889-897.

Festenstein,R., Sharghi-Namini,S., Fox,M., Roderick,K., Tolaini,M., Norton,T., Saveliev,A., Kioussis,D., and Singh,P. (1999). Heterochromatin protein 1 modifies mammalian PEV in a dose- and chromosomal-context-dependent manner. Nat. Genet. *23*, 457-461.

Festenstein,R., Pagakis,S.N., Hiragami,K., Lyon,D., Verreault,A., Sekkali,B., and Kioussis,D. (2003). Modulation of heterochromatin protein 1 dynamics in primary mammalian cells. Science *299*, 719-721.

Feuerbach,F., Galy,V., Trelles-Sticken,E., Fromont-Racine,M., Jacquier,A., Gilson,E., Olivo-Marin,J.C., Scherthan,H., and Nehrbass,U. (2002). Nuclear architecture and spatial positioning help establish transcriptional states of telomeres in yeast. Nat. Cell Biol. *4*, 214-221.

Finch,J.T. and Klug,A. (1976). Solenoidal model for superstructure in chromatin. Proc. Natl. Acad. Sci. U. S. A *73*, 1897-1901.

Finch,J.T. and Klug,A. (1978). X-ray and electron microscope analyses of crystals of nucleosome cores. Cold Spring Harb. Symp. Quant. Biol. *42 Pt 1*, 1-9.

Finley,M.F., Kulkarni,N., and Huettner,J.E. (1996). Synapse formation and establishment of neuronal polarity by P19 embryonic carcinoma cells and embryonic stem cells. J. Neurosci. *16*, 1056-1065.

Fischle,W., Wang,Y., Jacobs,S.A., Kim,Y., Allis,C.D., and Khorasanizadeh,S. (2003). Molecular basis for the discrimination of repressive methyl-lysine marks in histone H3 by Polycomb and HP1 chromodomains. Genes Dev. *17*, 1870-1881.

Fischle,W., Wang,Y., and Allis,C.D. (2003). Histone and chromatin cross-talk. Curr. Opin. Cell Biol. *15*, 172-183.

Fisher,A.G. and Merkenschlager,M. (2002). Gene silencing, cell fate and nuclear organisation. Curr. Opin. Genet. Dev. *12*, 193-197.

FitzGerald,P.C., Shlyakhtenko,A., Mir,A.A., and Vinson,C. (2004). Clustering of DNA sequences in human promoters. Genome Res. *14*, 1562-1574.

Foecking,M.K. and Hofstetter,H. (1986). Powerful and versatile enhancer-promoter unit for mammalian expression vectors. Gene *45*, 101-105.

Foisner,R. and Gerace,L. (1993). Integral membrane proteins of the nuclear envelope interact with lamins and chromosomes, and binding is modulated by mitotic phosphorylation. Cell *73*, 1267-1279.

Fomproix,N., Gebrane-Younes,J., and Hernandez-Verdun,D. (1998). Effects of anti-fibrillarin antibodies on building of functional nucleoli at the end of mitosis. J. Cell Sci. *111 (Pt 3)*, 359-372.

Forsberg,L.S., Noel,K.D., Box,J., and Carlson,R.W. (2003). Genetic locus and structural characterization of the biochemical defect in the O-antigenic polysaccharide of the symbiotically deficient Rhizobium etli mutant, CE166 - Replacement of N-acetylquinovosamine with its hexosyl-4-ulose precursor. J. Biol. Chem. *278*, 51347-51359.

Fraichard,A., Chassande,O., Bilbaut,G., Dehay,C., Savatier,P., and Samarut,J. (1995). In-Vitro Differentiation of Embryonic Stem-Cells Into Glial-Cells and Functional-Neurons. J. Cell Sci. *108*, 3181-3188.

Francastel,C., Walters,M.C., Groudine,M., and Martin,D.I. (1999). A functional enhancer suppresses silencing of a transgene and prevents its localization close to centrometric heterochromatin. Cell *99*, 259-269.

Francastel,C., Schubeler,D., Martin,D.I., and Groudine,M. (2000). Nuclear compartmentalization and gene activity. Nat. Rev. Mol. Cell Biol. *1*, 137-143.

Francastel,C., Magis,W., and Groudine,M. (2001). Nuclear relocation of a transactivator subunit precedes target gene activation. Proc. Natl. Acad. Sci U. S. A *98*, 12120-12125.

Fricker,M., Hollinshead,M., White,N., and Vaux,D. (1997). Interphase nuclei of many mammalian cell types contain deep, dynamic, tubular membrane-bound invaginations of the nuclear envelope. J. Cell Biol. *136*, 531-544.

Friedrich,G. and Soriano,P. (1991). Promoter traps in embryonic stem cells: a genetic screen to identify and mutate developmental genes in mice. Genes Dev. *5*, 1513-1523.

Friend,C., Scher,W., Holland,J.G., and Sato,T. (1971). Hemoglobin synthesis in murine virus-induced leukemic cells in vitro: stimulation of erythroid differentiation by dimethyl sulfoxide. Proc. Natl. Acad. Sci. U. S. A *68*, 378-382.

Fujimura,F.K., Silbert,P.E., Eckhart,W., and Linney,E. (1981). Polyoma virus infection of retinoic acid-induced differentiated teratocarcinoma cells. J. Virol. *39*, 306-312.

Fujita,N., Watanabe,S., Ichimura,T., Tsuruzoe,S., Shinkai,Y., Tachibana,M., Chiba,T., and Nakao,M. (2003). Methyl-CpG binding domain 1 (MBD1) interacts with the Suv39h1-HP1 heterochromatic complex for DNA methylation-based transcriptional repression. J. Biol. Chem. *278*, 24132-24138.

Fukagawa,T., Nogami,M., Yoshikawa,M., Ikeno,M., Okazaki,T., Takami,Y., Nakayama,T., and Oshimura,M. (2004). Dicer is essential for formation of the heterochromatin structure in vertebrate cells. Nature Cell Biology *6*, 784-791.

Fuks,F., Burgers,W.A., Godin,N., Kasai,M., and Kouzarides,T. (2001). Dnmt3a binds deacetylases and is recruited by a sequence-specific repressor to silence transcription. EMBO J. *20*, 2536-2544.

Fuks,F., Hurd,P.J., Deplus,R., and Kouzarides,T. (2003). The DNA methyltransferases associate with HP1 and the SUV39H1 histone methyltransferase. Nucleic Acids Res. *31*, 2305-2312.

Fuks,F., Hurd,P.J., Wolf,D., Nan,X., Bird,A.P., and Kouzarides,T. (2003). The methyl-CpG-binding protein MeCP2 links DNA methylation to histone methylation. J. Biol. Chem. *278*, 4035-4040.

Furukawa,K., Pante,N., Aebi,U., and Gerace,L. (1995). Cloning of a cDNA for lamina-associated polypeptide 2 (LAP2) and identification of regions that specify targeting to the nuclear envelope. EMBO J. *14*, 1626-1636.

Furukawa K., (1999). LAP2 binding protein 1 (L2BP1/BAF) is a candidate mediator of LAP2-chromatin interaction.J Cell Sci.*112* (Pt 15):2485-92.

Fushimi,K. and Verkman,A.S. (1991). Low viscosity in the aqueous domain of cell cytoplasm measured by picosecond polarization microfluorimetry. J. Cell Biol. *112*, 719-725.

Galy,V., Olivo-Marin,J.C., Scherthan,H., Doye,V., Rascalou,N., and Nehrbass,U. (2000). Nuclear pore complexes in the organization of silent telomeric chromatin. Nature *403*, 108-112.

Gartenberg,M.R., Neumann,F.R., Laroche,T., Blaszczyk,M., and Gasser,S.M. (2004). Sir-mediated repression can occur independently of chromosomal and subnuclear contexts. Cell *119*, 955-967.

Gassmann,M., Donoho,G., and Berg,P. (1995). Maintenance of an extrachromosomal plasmid vector in mouse embryonic stem cells. Proc. Natl. Acad. Sci. U. S. A *92*, 1292-1296.

Gdula,D.A., Gerasimova,T.I., and Corces,V.G. (1996). Genetic and molecular analysis of the gypsy chromatin insulator of Drosophila. Proc. Natl. Acad. Sci. U. S. A *93*, 9378-9383.

Geiman,T.M., Sankpal,U.T., Robertson,A.K., Zhao,Y., Zhao,Y., and Robertson,K.D. (2004). DNMT3B interacts with hSNF2H chromatin remodeling enzyme, HDACs 1 and 2, and components of the histone methylation system. Biochem. Biophys. Res. Commun. *318*, 544-555.

Gemkow,M.J., Verveer,P.J., and Arndt-Jovin,D.J. (1998). Homologous association of the Bithorax-Complex during embryogenesis: consequences for transvection in Drosophila melanogaster. Development *125*, 4541-4552.

Georgopoulos,K., Bigby,M., Wang,J.H., Molnar,A., Wu,P., Winandy,S., and Sharpe,A. (1994). The Ikaros gene is required for the development of all lymphoid lineages. Cell *79*, 143-156.

Gerasimova,T.I. and Corces,V.G. (1996). Boundary and insulator elements in chromosomes. Curr. Opin. Genet. Dev. *6*, 185-192.

Gerasimova,T.I. and Corces,V.G. (1998). Polycomb and trithorax group proteins mediate the function of a chromatin insulator. Cell *92*, 511-521.

Gerasimova,T.I., Byrd,K., and Corces,V.G. (2000). A chromatin insulator determines the nuclear localization of DNA. Mol. Cell *6*, 1025-1035.

Gerlich,D., Beaudouin,J., Kalbfuss,B., Daigle,N., Eils,R., and Ellenberg,J. (2003). Global chromosome positions are transmitted through mitosis in mammalian cells. Cell *112*, 751-764.

Gerlich,D., and Ellenberg,J. (2003). Dynamics of chromosome positioning during the cell cycle.Curr.Opin.Cell.Biol. *15*:664

Geyer,P.K., Green,M.M., and Corces,V.G. (1988). Mutant gene phenotypes mediated by a Drosophila melanogaster retrotransposon require sequences homologous to mammalian enhancers. Proc. Natl. Acad. Sci. U. S. A *85*, 8593-8597.

Geyer,P.K. (1997). The role of insulator elements in defining domains of gene expression. Curr. Opin. Genet. Dev. *7*, 242-248.

Gilbert,N. and Allan,J. (2001). Distinctive higher-order chromatin structure at mammalian centromeres. Proc. Natl. Acad. Sci. U. S. A *98*, 11949-11954.

Gilbert,N., Boyle,S., Sutherland,H., Las Heras,J., Allan,J., Jenuwein,T., and Bickmore,W.A. (2003). Formation of facultative heterochromatin in the absence of HP1. EMBO J. *22*, 5540-5550.

Gilbert,N., Boyle,S., Fiegler,H., Woodfine,K., Carter,N.P., and Bickmore,W.A. (2004). Chromatin architecture of the human genome: gene-rich domains are enriched in open chromatin fibers. Cell *118*, 555-566.

Gilchrist,S., Gilbert,N., Perry,P., and Bickmore,W.A. (2004). Nuclear organization of centromeric domains is not perturbed by inhibition of histone deacetylases. Chromosome. Res. *12*, 505-516.

Goll,M.G. and Bestor,T.H. (2002). Histone modification and replacement in chromatin activation. Genes Dev. *16*, 1739-1742.

Gordon,F., Luger,K., and Hansen,J.C. (2005). The core histone N-terminal tail domains function independently and additively during salt-dependent oligomerization of nucleosomal arrays. J. Biol. Chem.

Gorisch,S.M., Richter,K., Scheuermann,M.O., Herrmann,H., and Lichter,P. (2003). Diffusion-limited compartmentalization of mammalian cell nuclei assessed by microinjected macromolecules. Experimental Cell Research *289*, 282-294.

Gotta,M., Laroche,T., Formenton,A., Maillet,L., Scherthan,H., and Gasser,S.M. (1996). The clustering of telomeres and colocalization with Rap1, Sir3, and Sir4 proteins in wild-type Saccharomyces cerevisiae. J. Cell Biol. *134*, 1349-1363.

Gotta,M. and Gasser,S.M. (1996). Nuclear organization and transcriptional silencing in yeast. Experientia *52*, 1136-1147.

Gowher,H. and Jeltsch,A. (2001). Enzymatic properties of recombinant Dnmt3a DNA methyltransferase from mouse: the enzyme modifies DNA in a non-processive manner and also methylates non-CpG [correction of non-CpA] sites. J. Mol. Biol. *309*, 1201-1208.

Gravel,S., Larrivee,M., Labrecque,P., and Wellinger,R.J. (1998). Yeast Ku as a regulator of chromosomal DNA end structure. Science *280*, 741-744.

Grewal,S.I. and Rice,J.C. (2004). Regulation of heterochromatin by histone methylation and small RNAs. Curr. Opin. Cell Biol. *16*, 230-238.

Grigoryev,S.A., Bednar,J., and Woodcock,C.L. (1999). MENT, a heterochromatin protein that mediates higher order chromatin folding, is a new serpin family member. J. Biol. Chem. *274*, 5626-5636.

Groft,C.M., Uljon,S.N., Wang,R., and Werner,M.H. (1998). Structural homology between the Rap30 DNA-binding domain and linker histone H5: Implications for preinitiation complex assembly. Proceedings of the National Academy of Sciences of the United States of America *95*, 9117-9122.

Grosveld,F., Antoniou,M., Deboer,E., Habets,G., Hurst,J., Kollias,G., Macfarlane,F., and Wrighton,N. (1987). The Regulation of Expression of the Human Beta-Globin Genes. Journal of Cellular Biochemistry 77.

Gruenbaum,Y., Goldman,R.D., Meyuhas,R., Mills,E., Margalit,A., Fridkin,A., Dayani,Y., Prokocimer,M., and Enosh,A. (2003). The nuclear lamina and its functions in the nucleus. Int. Rev. Cytol. *226*, 1-62.

Gruenbaum Y, Margalit A, Goldman RD, Shumaker DK, Wilson KL.The nuclear lamina comes of age.Nat Rev Mol Cell Biol. 2005 Jan;6(1):21-31.

Grune,T., Brzeski,J., Eberharter,A., Clapier,C.R., Corona,D.F.V., Becker,P.B., and Muller,C.W. (2003). Crystal structure and functional analysis of a nucleosome recognition module of the remodeling factor ISWI. Molecular Cell *12*, 449-460.

Grunstein,M. (1997). Histone acetylation in chromatin structure and transcription. Nature *389*, 349-352.

Guacci,V., Hogan,E., and Koshland,D. (1997). Centromere position in budding yeast: evidence for anaphase A. Mol. Biol. Cell *8*, 957-972.

Gunawardena,S. and Rykowski,M.C. (2000). Direct evidence for interphase chromosome movement during the mid-blastula transition in Drosophila. Curr. Biol. *10*, 285-288.

Guo,M., Akiyama,Y., House,M.G., Hooker,C.M., Heath,E., Gabrielson,E., Yang,S.C., Han,Y., Baylin,S.B., Herman,J.G., and Brock,M.V. (2004). Hypermethylation of the GATA genes in lung cancer. Clin. Cancer Res. *10*, 7917-7924.

Guy,J., Hendrich,B., Holmes,M., Martin,J.E., and Bird,A. (2001). A mouse Mecp2-null mutation causes neurological symptoms that mimic Rett syndrome. Nat. Genet. *27*, 322-326.

Habermann, F. A., Cremer, M., Walter, J., Kreth, G., von Hase, J., Bauer, K., Wienberg, J., Cremer, C., Cremer, T., and Solovei, I. Arrangements of macro- and microchromosomes in chicken cells. Chromosome.Res. 9, 569-584. 2001.
Ref Type: Generic

Hagstrom,K., Muller,M., and Schedl,P. (1996). Fab-7 functions as a chromatin domain boundary to ensure proper segment specification by the Drosophila bithorax complex. Genes Dev. *10*, 3202-3215.

Hagstrom,K., Muller,M., and Schedl,P. (1996). Fab-7 functions as a chromatin domain boundary to ensure proper segment specification by the Drosophila bithorax complex. Genes & Development *10*, 3202-3215.

Hahm,K., Ernst,P., Lo,K., Kim,G.S., Turck,C., and Smale,S.T. (1994). The lymphoid transcription factor LyF-1 is encoded by specific, alternatively spliced mRNAs derived from the Ikaros gene. Mol. Cell Biol. *14*, 7111-7123.

Hall,I.M., Noma,K., and Grewal,S.I.S. (2003). RNA interference machinery regulates chromosome dynamics during mitosis and meiosis in fission yeast. Proceedings of the National Academy of Sciences of the United States of America *100*, 193-198.

Hamilton,A.J. and Baulcombe,D.C. (1999). A species of small antisense RNA in posttranscriptional gene silencing in plants. Science *286*, 950-952.

Hannon,G.J. (2002). RNA interference. Nature *418*, 244-251.

Hansen,J.C., Tse,C., and Wolffe,A.P. (1998). Structure and function of the core histone N-termini: more than meets the eye. Biochemistry *37*, 17637-17641.

Hansen,J.C. (2002). Conformational dynamics of the chromatin fiber in solution: determinants, mechanisms, and functions. Annu. Rev. Biophys. Biomol. Struct. *31*, 361-392.

Hansen,R.S., Wijmenga,C., Luo,P., Stanek,A.M., Canfield,T.K., Weemaes,C.M., and Gartler,S.M. (1999). The DNMT3B DNA methyltransferase gene is mutated in the ICF immunodeficiency syndrome. Proc. Natl. Acad. Sci. U. S A *96*, 14412-14417.

Haraguchi,T., Holaska,J.M., Yamane,M., Koujin,T., Hashiguchi,N., Mori,C., Wilson,K.L., and Hiraoka,Y. (2004). Emerin binding to Btf, a death-promoting transcriptional repressor, is disrupted by a missense mutation that causes Emery-Dreifuss muscular dystrophy. Eur. J. Biochem. *271*, 1035-1045.

Harmon,B. and Sedat,J. (2005). Cell-by-cell dissection of gene expression and chromosomal interactions reveals consequences of nuclear reorganization. PLoS. Biol. *3*, e67.

Harvey,A.C. and Downs,J.A. (2004). What functions do linker histones provide? Mol. Microbiol. *53*, 771-775.

Hashimshony,T., Zhang,J., Keshet,I., Bustin,M., and Cedar,H. (2003). The role of DNA methylation in setting up chromatin structure during development. Nat. Genet. *34*, 187-192.

Hassig,C.A. and Schreiber,S.L. (1997). Nuclear histone acetylases and deacetylases and transcriptional regulation: HATs off to HDACs. Curr. Opin. Chem. Biol. *1*, 300-308.

Hassig,C.A., Fleischer,T.C., Billin,A.N., Schreiber,S.L., and Ayer,D.E. (1997). Histone deacetylase activity is required for full transcriptional repression by mSin3A. Cell *89*, 341-347.

Hattori,N., Nishino,K., Ko,Y.G., Hattori,N., Ohgane,J., Tanaka,S., and Shiota,K. (2004). Epigenetic control of mouse Oct-4 gene expression in embryonic stem cells and trophoblast stem cells. J. Biol. Chem. *279*, 17063-17069.

Heard,E., Rougeulle,C., Arnaud,D., Avner,P., Allis,C.D., and Spector,D.L. (2001). Methylation of histone H3 at Lys-9 is an early mark on the X chromosome during X inactivation. Cell *107*, 727-738.

Heard,E. (2005). Delving into the diversity of facultative heterochromatin: the epigenetics of the inactive X chromosome. Curr. Opin. Genet. Dev. *15*, 482-489.

Hecht,A., Laroche,T., Strahl-Bolsinger,S., Gasser,S.M., and Grunstein,M. (1995). Histone H3 and H4 N-termini interact with SIR3 and SIR4 proteins: a molecular model for the formation of heterochromatin in yeast. Cell *80*, 583-592.

Heck,M.M. (1997). Condensins, cohesins, and chromosome architecture: how to make and break a mitotic chromosome. Cell *91*, 5-8.

Hediger,F., Dubrana,K., and Gasser,S.M. (2002). Myosin-like proteins 1 and 2 are not required for silencing or telomere anchoring, but act in the Tel1 pathway of telomere length control. J. Struct. Biol. *140*, 79-91.

Heitlinger E, Peter M, Lustig A, Villiger W, Nigg EA, Aebi U., 1992. The role of the head and tail domain in lamin structure and assembly: analysis of bacterially expressed chicken lamin A and truncated B2 lamins. J Struct Biol *108*(1):74-89.

Hellemans,J., Preobrazhenska,O., Willaert,A., Debeer,P., Verdonk,P.C., Costa,T., Janssens,K., Menten,B., Van Roy,N., Vermeulen,S.J., Savarirayan,R., Van Hul,W., Vanhoenacker,F.,

Huylebroeck,D., De Paepe,A., Naeyaert,J.M., Vandesompele,J., Speleman,F., Verschueren,K., Coucke,P.J., and Mortier,G.R. (2004). Loss-of-function mutations in LEMD3 result in osteopoikilosis, Buschke-Ollendorff syndrome and melorheostosis. Nat. Genet. *36*, 1213-1218.

Hendrich,B. and Bird,A. (1998). Identification and characterization of a family of mammalian methyl-CpG binding proteins. Mol. Cell Biol. *18*, 6538-6547.

Hendrich,B., Hardeland,U., Ng,H.H., Jiricny,J., and Bird,A. (1999). The thymine glycosylase MBD4 can bind to the product of deamination at methylated CpG sites. Nature *401*, 301-304.

Hendzel,M.J., Sun,J.M., Chen,H.Y., Rattner,J.B., and Davie,J.R. (1994). Histone acetyltransferase is associated with the nuclear matrix. J. Biol. Chem. *269*, 22894-22901.

Hendzel,M.J., Lever,M.A., Crawford,E., and Th'Ng,J.P.H. (2004). The C-terminal domain is the primary determinant of histone H1 binding to chromatin in vivo. J. Biol. Chem. *279*, 20028-20034.

Henikoff,S. (1996). Dosage-dependent modification of position-effect variegation in Drosophila. Bioessays *18*, 401-409.

Henikoff,S. and Comai,L. (1998). Trans-sensing effects: the ups and downs of being together. Cell *93*, 329-332.

Hernandez-Munoz,I., Lund,A.H., van der,S.P., Boutsma,E., Muijrers,I., Verhoeven,E., Nusinow,D.A., Panning,B., Marahrens,Y., and van Lohuizen,M. (2005). Stable X chromosome inactivation involves the PRC1 Polycomb complex and requires histone MACROH2A1 and the CULLIN3/SPOP ubiquitin E3 ligase. Proc. Natl. Acad. Sci. U. S A *102*, 7635-7640.

Hernandez-Verdun,D., Roussel,P., and Gebrane-Younes,J. (2002). Emerging concepts of nucleolar assembly. J. Cell Sci. *115*, 2265-2270.

Heslop-Harrison,J.S., Leitch,A.R., Schwarzacher,T., Smith,J.B., Atkinson,M.D., and Bennett,M.D. (1989). The volumes and morphology of human chromosomes in mitotic reconstructions. Hum. Genet. *84*, 27-34.

Hesslein,D.G. and Schatz,D.G. (2001). Factors and forces controlling V(D)J recombination. Adv. Immunol. *78*, 169-232.

Heun,P., Laroche,T., Shimada,K., Furrer,P., and Gasser,S.M. (2001). Chromosome dynamics in the yeast interphase nucleus. Science *294*, 2181-2186.

Hieda,M., Winstanley,H., Maini,P., Iborra,F.J., and Cook,P.R. (2005). Different populations of RNA polymerase II in living mammalian cells. Chromosome Research *13*, 135-144.

Hill,C.S., Rimmer,J.M., Green,B.N., Finch,J.T., and Thomas,J.O. (1991). Histone-DNA interactions and their modulation by phosphorylation of - Ser-Pro-X-Lys/Arg- motifs. EMBO J. *10*, 1939-1948.

Hirschhorn,J.N., Brown,S.A., Clark,C.D., and Winston,F. (1992). Evidence That Snf2/Swi2 and Snf5 Activate Transcription in Yeast by Altering Chromatin Structure. Genes & Development *6*, 2288-2298.

Holaska,J.M., Lee,K.K., Kowalski,A.K., and Wilson,K.L. (2003). Transcriptional repressor germ cell-less (GCL) and barrier to autointegration factor (BAF) compete for binding to emerin in vitro. J. Biol. Chem. *278*, 6969-6975.

Holaska,J.M., Kowalski,A.K., and Wilson,K.L. (2004). Emerin caps the pointed end of actin filaments: evidence for an actin cortical network at the nuclear inner membrane. PLoS. Biol. *2*, E231.

Holmer,L. and Worman,H.J. (2001). Inner nuclear membrane proteins: functions and targeting. Cellular and Molecular Life Sciences *58*, 1741-1747.

Horard,B., Tatout,C., Poux,S., and Pirrotta,V. (2000). Structure of a polycomb response element and in vitro binding of polycomb group complexes containing GAGA factor. Mol. Cell Biol. *20*, 3187-3197.

Horn,P.J. and Peterson,C.L. (2001). The bromodomain: A regulator of ATP-dependent chromatin remodeling? Frontiers in Bioscience *6*, D1019-D1023.

Horn,P.J., Carruthers,L.M., Logie,C., Hill,D.A., Solomon,M.J., Wade,P.A., Imbalzano,A.N., Hansen,J.C., and Peterson,C.L. (2002). Phosphorylation of linker histones regulates ATP-dependent chromatin remodeling enzymes. Nat. Struct. Biol. *9*, 263-267.

Horn,P.J., Carruthers,L.M., Logie,C., Hill,D.A., Solomon,M.J., Wade,P.A., Imbalzano,A.N., Hansen,J.C., and Peterson,C.L. (2002). Phosphorylation of linker histones regulates ATP-dependent chromatin remodeling enzymes. Nat. Struct. Biol. *9*, 263-267.

Houtsmuller,A.B., Rademakers,S., Nigg,A.L., Hoogstraten,D., Hoeijmakers,J.H., and Vermeulen,W. (1999). Action of DNA repair endonuclease ERCC1/XPF in living cells. Science *284*, 958-961.

Hozak,P., Sasseville,A.M., Raymond,Y., and Cook,P.R. (1995). Lamin proteins form an internal nucleoskeleton as well as a peripheral lamina in human cells. J. Cell Sci. *108 (Pt 2)*, 635-644.

Hsu,T.C. (1975). A possible function of constitutive heterochromatin: the bodyguard hypothesis. Genetics *79 Suppl*, 137-150.

Hu,E., Chen,Z., Fredrickson,T., Zhu,Y., Kirkpatrick,R., Zhang,G.F., Johanson,K., Sung,C.M., Liu,R., and Winkler,J. (2000). Cloning and characterization of a novel human class I histone deacetylase that functions as a transcription repressor. J. Biol. Chem. *275*, 15254-15264.

Huang,S., Deerinck,T.J., Ellisman,M.H., and Spector,D.L. (1998). The perinucleolar compartment and transcription. J. Cell Biol. *143*, 35-47.

Iborra,F.J., Pombo,A., Jackson,D.A., and Cook,P.R. (1996). Active RNA polymerases are localized within discrete transcription "factories' in human nuclei. J. Cell Sci. *109 (Pt 6)*, 1427-1436.

Ichimura,T., Watanabe,S., Sakamoto,Y., Aoto,T., Fujita,N., and Nakao,M. (2005). Transcriptional repression and heterochromatin formation by MBD1 and MCAF/AM family proteins. J. Biol. Chem. *280*, 13928-13935.

Ikeno,M., Grimes,B., Okazaki,T., Nakano,M., Saitoh,K., Hoshino,H., Mcgill,N.I., Cooke,H., and Masumoto,H. (1998). Construction of YAC-based mammalian artificial chromosomes. Nature Biotechnology *16*, 431-439.

Inouye,S. and Tsuji,F.I. (1994). Aequorea green fluorescent protein. Expression of the gene and fluorescence characteristics of the recombinant protein. FEBS Lett. *341*, 277-280.

Ishiguro,K. and Sartorelli,A.C. (2004). Activation of transiently transfected reporter genes in 3T3 Swiss cells by the inducers of differentiation/apoptosis--dimethylsulfoxide, hexamethylene bisacetamide and trichostatin A. Eur. J. Biochem. *271*, 2379-2390.

Ishihara,K. and Sasaki,H. (2002). An evolutionarily conserved putative insulator element near the 3' boundary of the imprinted Igf2/H19 domain. Hum. Mol. Genet. *11*, 1627-1636.

Ishii,K., Arib,G., Lin,C., Van Houwe,G., and Laemmli,U.K. (2002). Chromatin boundaries in budding yeast: the nuclear pore connection. Cell *109*, 551-562.

Ivy,J.M., Klar,A.J., and Hicks,J.B. (1986). Cloning and characterization of four SIR genes of Saccharomyces cerevisiae. Mol. Cell Biol. *6*, 688-702.

Jackson,D.A., Hassan,A.B., Errington,R.J., and Cook,P.R. (1993). Visualization of focal sites of transcription within human nuclei. EMBO J. *12*, 1059-1065.

Jackson,D.A. and Pombo,A. (1998). Replicon clusters are stable units of chromosome structure: evidence that nuclear organization contributes to the efficient activation and propagation of S phase in human cells. J. Cell Biol. *140*, 1285-1295.

Jackson,D.A., Iborra,F.J., Manders,E.M., and Cook,P.R. (1998). Numbers and organization of RNA polymerases, nascent transcripts, and transcription units in HeLa nuclei. Mol. Biol. Cell *9*, 1523-1536.

Jackson,J.P., Lindroth,A.M., Cao,X., and Jacobsen,S.E. (2002). Control of CpNpG DNA methylation by the KRYPTONITE histone H3 methyltransferase. Nature *416*, 556-560.

Jackson,J.P., Lindroth,A.M., Cao,X., and Jacobsen,S.E. (2002). Control of CpNpG DNA methylation by the KRYPTONITE histone H3 methyltransferase. Nature *416*, 556-560.

Jackson,M., Krassowska,A., Gilbert,N., Chevassut,T., Forrester,L., Ansell,J., and Ramsahoye,B. (2004). Severe global DNA hypomethylation blocks differentiation and induces histone hyperacetylation in embryonic stem cells. Mol. Cell Biol. *24*, 8862-8871.

Jacobs,S.A., Taverna,S.D., Zhang,Y., Briggs,S.D., Li,J., Eissenberg,J.C., Allis,C.D., and Khorasanizadeh,S. (2001). Specificity of the HP1 chromo domain for the methylated N-terminus of histone H3. EMBO J. *20*, 5232-5241.

Jacobs,S.A., Taverna,S.D., Zhang,Y., Briggs,S.D., Li,J., Eissenberg,J.C., Allis,C.D., and Khorasanizadeh,S. (2001). Specificity of the HP1 chromo domain for the methylated N-terminus of histone H3. EMBO J. *20*, 5232-5241.

James,T.C., Eissenberg,J.C., Craig,C., Dietrich,V., Hobson,A., and Elgin,S.C. (1989). Distribution patterns of HP1, a heterochromatin-associated nonhistone chromosomal protein of Drosophila. Eur. J. Cell Biol. *50*, 170-180.

Janicki,S.M., Tsukamoto,T., Salghetti,S.E., Tansey,W.P., Sachidanandam,R., Prasanth,K.V., Ried,T., Shav-Tal,Y., Bertrand,E., Singer,R.H., and Spector,D.L. (2004). From silencing to gene expression: Real-time analysis in single cells. Cell *116*, 683-698.

Jeddeloh,J.A., Stokes,T.L., and Richards,E.J. (1999). Maintenance of genomic methylation requires a SWI2/SNF2-like protein. Nat. Genet. *22*, 94-97.

Jenuwein,T., Forrester,W.C., Fernandez-Herrero,L.A., Laible,G., Dull,M., and Grosschedl,R. (1997). Extension of chromatin accessibility by nuclear matrix attachment regions. Nature *385*, 269-272.

Jenuwein,T. and Allis,C.D. (2001). Translating the histone code. Science *293*, 1074-1080.

Jenuwein,T. (2001). Re-SET-ting heterochromatin by histone methyltransferases. Trends Cell Biol. *11*, 266-273.

Jeong,S. and Stein,A. (1994). Micrococcal nuclease digestion of nuclei reveals extended nucleosome ladders having anomalous DNA lengths for chromatin assembled on non-replicating plasmids in transfected cells. Nucleic Acids Res. *22*, 370-375.

Jeppesen,P. and Turner,B.M. (1993). The inactive X chromosome in female mammals is distinguished by a lack of histone H4 acetylation, a cytogenetic marker for gene expression. Cell *74*, 281-289.

Jimenez-Garcia,L.F., Segura-Valdez,M.L., Ochs,R.L., Rothblum,L.I., Hannan,R., and Spector,D.L. (1994). Nucleologenesis: U3 snRNA-containing prenucleolar bodies move to sites of active pre-rRNA transcription after mitosis. Mol. Biol. Cell *5*, 955-966.

Jin,Y., Jin,C., Wennerberg,J., Mertens,F., and Hoglund,M. (1998). Cytogenetic and fluorescence in situ hybridization characterization of chromosome 1 rearrangements in head and neck carcinomas delineate a target region for deletions within 1p11-1p13. Cancer Res. *58*, 5859-5865.

Jones,P.A. and Takai,D. (2001). The role of DNA methylation in mammalian epigenetics. Science *293*, 1068-1070.

Jones,P.L., Veenstra,G.J., Wade,P.A., Vermaak,D., Kass,S.U., Landsberger,N., Strouboulis,J., and Wolffe,A.P. (1998). Methylated DNA and MeCP2 recruit histone deacetylase to repress transcription. Nat. Genet. *19*, 187-191.

Joseph,A., Mitchell,A.R., and Miller,O.J. (1989). The organization of the mouse satellite DNA at centromeres. Exp. Cell Res. *183*, 494-500.

Kambach,C., Walke,S., and Nagai,K. (1999). Structure and assembly of the spliceosomal small nuclear ribonucleoprotein particles. Curr. Opin. Struct. Biol. *9*, 222-230.

Karymov,M.A., Tomschik,M., Leuba,S.H., Caiafa,P., and Zlatanova,J. (2001). DNA methylation-dependent chromatin fiber compaction in vivo and in vitro: requirement for linker histone. FASEB J. *15*, 2631-2641.

Kato,N. and Lam,E. (2001). Detection of chromosomes tagged with green fluorescent protein in live Arabidopsis thaliana plants. Genome Biol. *2*, RESEARCH0045.

Kato,N. and Lam,E. (2003). Chromatin of endoreduplicated pavement cells has greater range of movement than that of diploid guard cells in Arabidopsis thaliana. J. Cell Sci. *116*, 2195-2201.

Kawasaki,H., Taira,K., and Yokoyama,K. (2000). Histone acetyltransferase (HAT) activity of ATF-2 is necessary for the CRE-dependent transcription. Nucleic Acids Symp. Ser. 259-260.

Kawasaki,H., Schiltz,L., Chiu,R., Itakura,K., Taira,K., Nakatani,Y., and Yokoyama,K.K. (2000). ATF-2 has intrinsic histone acetyltransferase activity which is modulated by phosphorylation. Nature *405*, 195-200.

Keller,G.M. (1995). In vitro Differentiation of Embryonic Stem Cells. Curr. Opin. Cell Biol. *7*, 862-869.

Kelley,D.E., Stokes,D.G., and Perry,R.P. (1999). CHD1 interacts with SSRP1 and depends on both its chromodomain and its ATPase/helicase-like domain for proper association with chromatin. Chromosoma *108*, 10-25.

Kellum,R. and Schedl,P. (1991). A position-effect assay for boundaries of higher order chromosomal domains. Cell *64*, 941-950.

Khavari,P.A., Peterson,C.L., Tamkun,J.W., Mendel,D.B., and Crabtree,G.R. (1993). Brg1 Contains A Conserved Domain of the Swi2/Snf2 Family Necessary for Normal Mitotic Growth and Transcription. Nature *366*, 170-174.

Kim,S.H., McQueen,P.G., Lichtman,M.K., Shevach,E.M., Parada,L.A., and Misteli,T. (2004). Spatial genome organization during T-cell differentiation. Cytogenet. Genome Res. *105*, 292-301.

Kim,S.H., Kang,Y.K., Koo,D.B., Kang,M.J., Moon,S.J., Lee,K.K., and Han,Y.M. (2004). Differential DNA methylation reprogramming of various repetitive sequences in mouse preimplantation embryos. Biochem. Biophys. Res. Commun. *324*, 58-63.

Kim,Y. and Clark,D.J. (2002). SWI/SNF-dependent long-range remodeling of yeast HIS3 chromatin. Proc. Natl. Acad. Sci. U. S. A *99*, 15381-15386.

Kimura,H. and Cook,P.R. (2001). Kinetics of core histones in living human cells: Little exchange of H3 and H4 and some rapid exchange of H2B. JCB *153*, 1341-1353.

Kimura,H., Nakamura,T., Ogawa,T., Tanaka,S., and Shiota,K. (2003). Transcription of mouse DNA methyltransferase 1 (Dnmt1) is regulated by both E2F-Rb-HDAC-dependent and -independent pathways. Nucleic Acids Res. *31*, 3101-3113.

Kimura,H. and Shiota,K. (2003). Methyl-CpG-binding protein, MeCP2, is a target molecule for maintenance DNA methyltransferase, Dnmt1. J. Biol. Chem. *278*, 4806-4812.

Kipling,D., Ackford,H.E., Taylor,B.A., and Cooke,H.J. (1991). Mouse minor satellite DNA genetically maps to the centromere and is physically linked to the proximal telomere. Genomics *11*, 235-241.

Kipling,D., Wilson,H.E., Mitchell,A.R., Taylor,B.A., and Cooke,H.J. (1994). Mouse centromere mapping using oligonucleotide probes that detect variants of the minor satellite. Chromosoma *103*, 46-55.

Klar,A.J., Strathern,J.N., and Hicks,J.B. (1981). A position-effect control for gene transposition: state of expression of yeast mating-type genes affects their ability to switch. Cell *25*, 517-524.

Klar,A.J., Strathern,J.N., Broach,J.R., and Hicks,J.B. (1981). Regulation of transcription in expressed and unexpressed mating type cassettes of yeast. Nature *289*, 239-244.

Klein,F., Laroche,T., Cardenas,M.E., Hofmann,J.F., Schweizer,D., and Gasser,S.M. (1992). Localization of RAP1 and topoisomerase II in nuclei and meiotic chromosomes of yeast. J. Cell Biol. *117*, 935-948.

Klose RJ, Sarraf SA, Schmiedeberg L, McDermott SM, Stancheva I, Bird AP.DNA binding selectivity of MeCP2 due to a requirement for A/T sequences adjacent to methyl-CpG. Mol Cell. 2005 Sep 2;19(5)

Knoepfler,P.S. and Eisenman,R.N. (1999). Sin meets NuRD and other tails of repression. Cell *99*, 447-450.

Kobayashi,J., Tauchi,H., Sakamoto,S., Nakamura,A., Morishima,K., Matsuura,S., Kobayashi,T., Tamai,K., Tanimoto,K., and Komatsu,K. (2002). NBS1 localizes to gamma-H2AX foci through interaction with the FHA/BRCT domain. Curr. Biol. *12*, 1846-1851.

Kohlmaier,A., Savarese,F., Lachner,M., Martens,J., Jenuwein,T., and Wutz,A. (2004). A chromosomal memory triggered by Xist regulates histone methylation in X inactivation. PLoS. Biol. *2*, E171.

Konishi,A., Shimizu,S., Hirota,J., Takao,T., Fan,Y.H., Matsuoka,Y., Zhang,L.L., Yoneda,Y., Fujii,Y., Skouitchi,A.I., and Tsujimoto,Y. (2003). Involvement of histone H1.2 in apoptosis induced by DNA double-strand breaks. Cell *114*, 673-688.

Kornberg,R.D. (1974). Chromatin structure: a repeating unit of histones and DNA. Science *184*, 868-871.

Kosak,S.T. and Groudine,M. (2002). The undiscovered country: chromosome territories and the organization of transcription. Dev. Cell *2*, 690-692.

Kosak,S.T., Skok,J.A., Medina,K.L., Riblet,R., Le Beau,M.M., Fisher,A.G., and Singh,H. (2002). Subnuclear compartmentalization of immunoglobulin loci during lymphocyte development. Science *296*, 158-162.

Kourmouli,N., Theodoropoulos,P.A., Dialynas,G., Bakou,A., Politou,A.S., Cowell,I.G., Singh,P.B., and Georgatos,S.D. (2000). Dynamic associations of heterochromatin protein 1 with the nuclear envelope. EMBO J. *19*, 6558-6568.

Kourmouli,N., Jeppesen,P., Mahadevhaiah,S., Burgoyne,P., Wu,R., Gilbert,D.M., Bongiorni,S., Prantera,G., Fanti,L., Pimpinelli,S., Shi,W., Fundele,R., and Singh,P.B. (2004). Heterochromatin and tri-methylated lysine 20 of histone H4 in animals. J. Cell Sci. *117*, 2491-2501.

Koutzamani,E., Loborg,H., Sarg,B., Lindner,H.H., and Rundquist,I. (2002). Linker histone subtype composition and affinity for chromatin in situ in nucleated mature erythrocytes. J. Biol. Chem. *277*, 44688-44694.

Kozubek,S., Lukasova,E., Jirsova,P., Koutna,I., Kozubek,M., Ganova,A., Bartova,E., Falk,M., and Pasekova,R. (2002). 3D Structure of the human genome: order in randomness. Chromosoma *111*, 321-331.

Kramer,A. (1993). Mammalian protein factors involved in nuclear pre-mRNA splicing. Mol. Biol. Rep. *18*, 93-98.

Kraus,W.L. and Wong,J. (2002). Nuclear receptor-dependent transcription with chromatin. Is it all about enzymes? Eur. J. Biochem. *269*, 2275-2283.

Krebs,J.E., Kuo,M.H., Allis,C.D., and Peterson,C.L. (1999). Cell cycle-regulated histone acetylation required for expression of the yeast HO gene. Genes & Development *13*, 1412-1421.

Krogan,N.J., Dover,J., Wood,A., Schneider,J., Heidt,J., Boateng,M.A., Dean,K., Ryan,O.W., Golshani,A., Johnston,M., Greenblatt,J.F., and Shilatifard,A. (2003). The Paf1 complex is required for histone h3 methylation by COMPASS and Dot1p: Linking transcriptional elongation to histone methylation. Molecular Cell *11*, 721-729.

Kukimoto,I., Elderkin,S., Grimaldi,M., Oelgeschlager,T., and Varga-Weisz,P.D. (2004). The histone-fold protein complex CHRAC-15/17 enhances nucleosome sliding and assembly mediated by ACF. Molecular Cell *13*, 265-277.

Kumaran,R.I., Muralikrishna,B., and Parnaik,V.K. (2002). Lamin A/C speckles mediate spatial organization of splicing factor compartments and RNA polymerase II transcription. J. Cell Biol. *159*, 783-793.

Kuo,M.H. and Allis,C.D. (1998). Roles of histone acetyltransferases and deacetylases in gene regulation. Bioessays *20*, 615-626.

Kurdistani,S.K. and Grunstein,M. (2003). Histone acetylation and deacetylation in yeast. Nat. Rev. Mol. Cell Biol. *4*, 276-284.

Kurdistani,S.K. and Grunstein,M. (2003). In vivo protein-protein and protein-DNA crosslinking for genomewide binding microarray. Methods *31*, 90-95.

Kurdistani,S.K., Tavazoie,S., and Grunstein,M. (2004). Mapping global histone acetylation patterns to gene expression. Cell *117*, 721-733.

Kuroda,M., Tanabe,H., Yoshida,K., Oikawa,K., Saito,A., Kiyuna,T., Mizusawa,H., and Mukai,K. (2004). Alteration of chromosome positioning during adipocyte differentiation. J. Cell Sci. *117*, 5897-5903.

Kurz,A., Lampel,S., Nickolenko,J.E., Bradl,J., Benner,A., Zirbel,R.M., Cremer,T., and Lichter,P. (1996). Active and inactive genes localize preferentially in the periphery of chromosome territories. J. Cell Biol. *135*, 1195-1205.

Kustatscher,G., Hothorn,M., Pugieux,C., Scheffzek,K., and Ladurner,A.G. (2005). Splicing regulates NAD metabolite binding to histone macroH2A. Nat. Struct. Mol. Biol. *12*, 624-625.

Kuzmichev,A., Jenuwein,T., Tempst,P., and Reinberg,D. (2004). Different EZH2-containing complexes target methylation of histone H1 or nucleosomal histone H3. Mol. Cell *14*, 183-193.

Lachner,M., O'Carroll,N., Rea,S., Mechtler,K., and Jenuwein,T. (2001). Methylation of histone H3 lysine 9 creates a binding site for HP1 proteins. Nature *410*, 116-120.

Laherty,C.D., Yang,W.M., Sun,J.M., Davie,J.R., Seto,E., and Eisenman,R.N. (1997). Histone deacetylases associated with the mSin3 corepressor mediate mad transcriptional repression. Cell *89*, 349-356.

Langst,G. and Becker,P.B. (2001). ISWI induces nucleosome sliding on nicked DNA. Molecular Cell *8*, 1085-1092.

Laroche,T., Martin,S.G., Gotta,M., Gorham,H.C., Pryde,F.E., Louis,E.J., and Gasser,S.M. (1998). Mutation of yeast Ku genes disrupts the subnuclear organization of telomeres. Curr. Biol. *8*, 653-656.

Lattanzi,G., Cenni,V., Marmiroli,S., Capanni,C., Mattioli,E., Merlini,L., Squarzoni,S., and Maraldi,N.M. (2003). Association of emerin with nuclear and cytoplasmic actin is regulated in differentiating myoblasts. Biochemical and Biophysical Research Communications *303*, 764-770.

Lawrence,J.B., Singer,R.H., Villnave,C.A., Stein,J.L., and Stein,G.S. (1988). Intracellular distribution of histone mRNAs in human fibroblasts studied by in situ hybridization. Proc. Natl. Acad. Sci. U. S. A *85*, 463-467.

Lechardeur,D., Sohn,K.J., Haardt,M., Joshi,P.B., Monck,M., Graham,R.W., Beatty,B., Squire,J., O'Brodovich,H., and Lukacs,G.L. (1999). Metabolic instability of plasmid DNA in the cytosol: a potential barrier to gene transfer. Gene Ther. *6*, 482-497.

Lee,G.R., Spilianakis,C.G., and Flavell,R.A. (2005). Hypersensitive site 7 of the T(H)2 locus control region is essential for expressing T(H)2 cytokine genes and for long-range intrachromosomal interactions. Nature Immunology *6*, 42-48.

Lee,J.H., Hart,S.R., and Skalnik,D.G. (2004). Histone deacetylase activity is required for embryonic stem cell differentiation. Genesis. *38*, 32-38.

Lee,J.T. and Jaenisch,R. (1997). Long-range cis effects of ectopic X-inactivation centres on a mouse autosome. Nature *386*, 275-279.

Lee,J.T. and Lu,N. (1999). Targeted mutagenesis of Tsix leads to nonrandom X inactivation. Cell *99*, 47-57.

Lee,J.T., Lu,N., and Han,Y. (1999). Genetic analysis of the mouse X inactivation center defines an 80-kb multifunction domain. Proc. Natl. Acad. Sci. U. S A *96*, 3836-3841.

Lee,K.K., Haraguchi,T., Lee,R.S., Koujin,T., Hiraoka,Y., and Wilson,K.L. (2001). Distinct functional domains in emerin bind lamin A and DNA-bridging protein BAF. J. Cell Sci. *114*, 4567-4573.

Lee,K.K. and Wilson,K.L. (2004). All in the family: evidence for four new LEM-domain proteins Lem2 (NET-25), Lem3, Lem4 and Lem5 in the human genome. Symp. Soc. Exp. Biol. 329-339.

Lehner,C.F., Stick,R., Eppenberger,H.M., and Nigg,E.A. (1987). Differential expression of nuclear lamin proteins during chicken development. J. Cell Biol. *105*, 577-587.

Lehnertz,B., Ueda,Y., Derijck,A.A., Braunschweig,U., Perez-Burgos,L., Kubicek,S., Chen,T., Li,E., Jenuwein,T., and Peters,A.H. (2003). Suv39h-mediated histone H3 lysine 9 methylation directs DNA methylation to major satellite repeats at pericentric heterochromatin. Curr. Biol. *13*, 1192-1200.

Leitch,A.R., Mosgoller,W., Schwarzacher,T., Bennett,M.D., and Heslop-Harrison,J.S. (1990). Genomic in situ hybridization to sectioned nuclei shows chromosome domains in grass hybrids. J. Cell Sci. *95 (Pt 3)*, 335-341.

Leonhardt,H., Page,A.W., Weier,H.U., and Bestor,T.H. (1992). A targeting sequence directs DNA methyltransferase to sites of DNA replication in mammalian nuclei. Cell *71*, 865-873.

Lever,M.A., Th'Ng,J.P.H., Sun,X.J., and Hendzel,M.J. (2000). Rapid exchange of histone H1.1 on chromatin in living human cells. Nature *408*, 873-876.

Levine,A., Yeivin,A., Ben Asher,E., Aloni,Y., and Razin,A. (1993). Histone H1-mediated inhibition of transcription initiation of methylated templates in vitro. J. Biol. Chem. *268*, 21754-21759.

Lewis,J.D., Meehan,R.R., Henzel,W.J., Maurer-Fogy,I., Jeppesen,P., Klein,F., and Bird,A. (1992). Purification, sequence, and cellular localization of a novel chromosomal protein that binds to methylated DNA. Cell *69*, 905-914.

Li,A., Eirin-Lopez,J.M., and Ausio,J. (2005). H2AX: tailoring histone H2A for chromatin-dependent genomic integrity. Biochem. Cell Biol. *83*, 505-515.

Li,E. (1999). The mojo of methylation. Nat. Genet. *23*, 5-6.

Li,M., Pevny,L., Lovell-Badge,R., and Smith,A. (1998). Generation of purified neural precursors from embryonic stem cells by lineage selection. Curr. Biol. *8*, 971-974.

Li,Q.L., Peterson,K.R., Fang,X.D., and Stamatoyannopoulos,G. (2002). Locus control regions. Blood *100*, 3077-3086.

Li,X., Zhao,X., Fang,Y., Jiang,X., Duong,T., Fan,C., Huang,C.C., and Kain,S.R. (1998). Generation of destabilized green fluorescent protein as a transcription reporter. J. Biol. Chem. *273*, 34970-34975.

Lichter,P., Cremer,T., Borden,J., Manuelidis,L., and Ward,D.C. (1988). Delineation of individual human chromosomes in metaphase and interphase cells by in situ suppression hybridization using recombinant DNA libraries. Hum. Genet. *80*, 224-234.

Lin,F., Blake,D.L., Callebaut,I., Skerjanc,I.S., Holmer,L., McBurney,M.W., Paulin-Levasseur,M., and Worman,H.J. (2000). MAN1, an inner nuclear membrane protein that shares the LEM domain with lamina-associated polypeptide 2 and emerin. J. Biol. Chem. *275*, 4840-4847.

Lin,F., Morrison,J.M., Wu,W., and Worman,H.J. (2005). MAN1, an integral protein of the inner nuclear membrane, binds Smad2 and Smad3 and antagonizes transforming growth factor-beta signaling. Hum. Mol. Genet. *14*, 437-445.

Linder,P., Lasko,P.F., Ashburner,M., Leroy,P., Nielsen,P.J., Nishi,K., Schnier,J., and Slonimski,P.P. (1989). Birth of the D-E-A-D box. Nature *337*, 121-122.

Lippincott-Schwartz,J. and Patterson,G.H. (2003). Development and use of fluorescent protein markers in living cells. Science *300*, 87-91.

Lippincott-Schwartz J, Altan-Bonnet N, Patterson GH.Photobleaching and photoactivation: following protein dynamics in living cells. Nat Cell Biol. 2003 Sep;Suppl:S7-14.

Liu,J., Prunuske,A.J., Fager,A.M., and Ullman,K.S. (2003). The COPI complex functions in nuclear envelope breakdown and is recruited by the nucleoporin Nup153. Dev. Cell *5*, 487-498.

Liu,J., Lee,K.K., Segura-Totten,M., Neufeld,E., Wilson,K.L., and Gruenbaum,Y. (2003). MAN1 and emerin have overlapping function(s) essential for chromosome segregation and cell division in Caenorhabditis elegans. Proc. Natl. Acad. Sci. U. S A *100*, 4598-4603.

Liu,X.L., Shen,Y., Chen,E.J., and Zhai,Z.H. (2000). Nuclear assembly of purified Crythecodinium cohnii chromosomes in cell-free extracts of Xenopus laevis eggs. Cell Res. *10*, 127-137.

Lo,W.S., Duggan,L., Tolga,N.C., Emre, Belotserkovskya,R., Lane,W.S., Shiekhattar,R., and Berger,S.L. (2001). Snf1--a histone kinase that works in concert with the histone acetyltransferase Gcn5 to regulate transcription. Science *293*, 1142-1146.

Loidl,J., Jin,Q.W., and Jantsch,M. (1998). Meiotic pairing and segregation of translocation quadrivalents in yeast. Chromosoma *107*, 247-254.

Lopez-Soler,R.I., Moir,R.D., Spann,T.P., Stick,R., and Goldman,R.D. (2001). A role for nuclear lamins in nuclear envelope assembly. J. Cell Biol. *154*, 61-70.

Luger,K., Mader,A.W., Richmond,R.K., Sargent,D.F., and Richmond,T.J. (1997). Crystal structure of the nucleosome core particle at 2.8 A resolution. Nature *389*, 251-260.

Luger,K. and Richmond,T.J. (1998). The histone tails of the nucleosome. Curr. Opin. Genet. Dev. *8*, 140-146.

Lund,A.H. and van Lohuizen,M. (2004). Polycomb complexes and silencing mechansims. Curr. Opin. Cell Biol. *16*, 239-246.

Lundgren,M., Chow,C.M., Sabbattini,P., Georgiou,A., Minaee,S., and Dillon,N. (2000). Transcription factor dosage affects changes in higher order chromatin structure associated with activation of a heterochromatic gene. Cell *103*, 733-743.

Lupton,S.D., Brunton,L.L., Kalberg,V.A., and Overell,R.W. (1991). Dominant positive and negative selection using a hygromycin phosphotransferase-thymidine kinase fusion gene. Mol. Cell Biol. *11*, 3374-3378.

Ma,Y., Jacobs,S.B., Jackson-Grusby,L., Mastrangelo,M.A., Torres-Betancourt,J.A., Jaenisch,R., and Rasmussen,T.P. (2005). DNA CpG hypomethylation induces heterochromatin reorganization involving the histone variant macroH2A. J. Cell Sci. *118*, 1607-1616.

Mahadevan,L.C., Willis,A.C., and Barratt,M.J. (1991). Rapid histone H3 phosphorylation in response to growth factors, phorbol esters, okadaic acid, and protein synthesis inhibitors. Cell *65*, 775-783.

Mahy, N. L., Bickmore, W. A., Tumbar, T., and Belmont, A. S. Linking large-scale chromatin structure with nuclear function. Chromatin Structure and Gene Expression Edited by Elgin, S.C.R and Workman, J.L, 300-321. 2000.
Ref Type: Generic

Mahy,N.L., Perry,P.E., and Bickmore,W.A. (2002). Gene density and transcription influence the localization of chromatin outside of chromosome territories detectable by FISH. J. Cell Biol. *159*, 753-763.

Mahy,N.L., Perry,P.E., Gilchrist,S., Baldock,R.A., and Bickmore,W.A. (2002). Spatial organization of active and inactive genes and noncoding DNA within chromosome territories. J. Cell Biol. *157*, 579-589.

Maillet,L., Boscheron,C., Gotta,M., Marcand,S., Gilson,E., and Gasser,S.M. (1996). Evidence for silencing compartments within the yeast nucleus: a role for telomere proximity and Sir protein concentration in silencer-mediated repression. Genes Dev. *10*, 1796-1811.

Maison,C., Bailly,D., Peters,A.H.F.M., Quivy,J.P., Roche,D., Taddei,A., Lachner,M., Jenuwein,T., and Almouzni,G. (2002). Higher-order structure in pericentric heterochromatin involves a distinct pattern of histone modification and an RNA component. Nat. Genet. *30*, 329-334.

Malagnac,F., Bartee,L., and Bender,J. (2002). An Arabidopsis SET domain protein required for maintenance but not establishment of DNA methylation. EMBO J. *21*, 6842-6852.

Manilal,S., Nguyen,T.M., Sewry,C.A., and Morris,G.E. (1996). The Emery-Dreifuss muscular dystrophy protein, emerin, is a nuclear membrane protein. Hum. Mol. Genet. *5*, 801-808.

Manuelidis,L. (1985). Individual interphase chromosome domains revealed by in situ hybridization. Hum. Genet. *71*, 288-293.

Manuelidis,L. (1990). A view of interphase chromosomes. Science *250*, 1533-1540.

Manz,J., Denis,K., Witte,O., Brinster,R., and Storb,U. (1988). Feedback inhibition of immunoglobulin gene rearrangement by membrane mu, but not by secreted mu heavy chains. J. Exp. Med. *168*, 1363-1381.

Maraldi,N.M., Squarzoni,S., Sabatelli,P., Capanni,C., Mattioli,E., Ognibene,A., and Lattanzi,G. (2005). Laminopathies: involvement of structural nuclear proteins in the pathogenesis of an increasing number of human diseases. J. Cell Physiol *203*, 319-327.

Marcand,S., Buck,S.W., Moretti,P., Gilson,E., and Shore,D. (1996). Silencing of genes at nontelomeric sites in yeast is controlled by sequestration of silencing factors at telomeres by Rap 1 protein. Genes Dev. *10*, 1297-1309.

Maresca,T.J., Freedman,B.S., and Heald,R. (2005). Histone H1 is essential for mitotic chromosome architecture and segregation in Xenopus laevis egg extracts. J. Cell Biol. *169*, 859-869.

Marks,P.A., Rifkind,R.A., Richon,V.M., and Breslow,R. (2001). Inhibitors of histone deacetylase are potentially effective anticancer agents. Clin. Cancer Res. *7*, 759-760.

Marshall,W.F., Dernburg,A.F., Harmon,B., Agard,D.A., and Sedat,J.W. (1996). Specific interactions of chromatin with the nuclear envelope: positional determination within the nucleus in Drosophila melanogaster. Mol. Biol. Cell *7*, 825-842.

Marshall,W.F., Dernburg,A.F., Harmon,B., Agard,D.A., and Sedat,J.W. (1996). Specific interactions of chromatin with the nuclear envelope: Positional determination within the nucleus in Drosophila melanogaster. Molecular Biology of the Cell *7*, 825-842.

Marshall,W.F., Straight,A., Marko,J.F., Swedlow,J., Dernburg,A., Belmont,A., Murray,A.W., Agard,D.A., and Sedat,J.W. (1997). Interphase chromosomes undergo constrained diffusional motion in living cells. Curr. Biol. *7*, 930-939.

Marshall,W.F., Fung,J.C., and Sedat,J.W. (1997). Deconstructing the nucleus: global architecture from local interactions. Curr. Opin. Genet. Dev. *7*, 259-263.

Martens,J.A. and Winston,F. (2003). Recent advances in understanding chromatin remodeling by Swi/Snf complexes. Current Opinion in Genetics & Development *13*, 136-142.

Martens,J.H., Verlaan,M., Kalkhoven,E., Dorsman,J.C., and Zantema,A. (2002). Scaffold/matrix attachment region elements interact with a p300-scaffold attachment factor A complex and are bound by acetylated nucleosomes. Mol. Cell Biol. *22*, 2598-2606.

Martens,J.H., O'Sullivan,R.J., Braunschweig,U., Opravil,S., Radolf,M., Steinlein,P., and Jenuwein,T. (2005). The profile of repeat-associated histone lysine methylation states in the mouse epigenome. EMBO J. *24*, 800-812.

Matin MM, Walsh JR, Gokhale PJ, Draper JS, Bahrami AR, Morton I, Moore HD, Andrews PW. (2004). Specific knockdown of Oct4 and beta2-microglobulin expression by RNA interference in human embryonic stem cells and embryonic carcinoma cells.Stem Cells *22(5)*:659-68.

Mazda,O., Satoh,E., Yasutomi,K., and Imanishi,J. (1997). Extremely efficient gene transfection into lympho-hematopoietic cell lines by Epstein-Barr virus-based vectors. J. Immunol. Methods *204*, 143-151.

McArthur,M. and Thomas,J.O. (1996). A preference of histone H1 for methylated DNA. EMBO J. *15*, 1705-1714.

McGhee,J.D., Nickol,J.M., Felsenfeld,G., and Rau,D.C. (1983). Histone hyperacetylation has little effect on the higher order folding of chromatin. Nucleic Acids Res. *11*, 4065-4075.

McGhee,J.D., Nickol,J.M., Felsenfeld,G., and Rau,D.C. (1983). Higher order structure of chromatin: orientation of nucleosomes within the 30 nm chromatin solenoid is independent of species and spacer length. Cell *33*, 831-841.

Mckay,D.B. and Steitz,T.A. (1981). Structure of Catabolite Gene Activator Protein at 2.9 A Resolution Suggests Binding to Left-Handed B-Dna. Nature *290*, 744-749.

Mearini,G., Nielsen,P.E., and Fackelmayer,F.O. (2004). Localization and dynamics of small circular DNA in live mammalian nuclei. Nucleic Acids Res. *32*, 2642-2651.

Meehan,R., Lewis,J., Cross,S., Nan,X., Jeppesen,P., and Bird,A. (1992). Transcriptional repression by methylation of CpG. J. Cell Sci. *Supplement 16*, 9-14.

Meehan,R.R., Lewis,J.D., McKay,S., Kleiner,E.L., and Bird,A.P. (1989). Identification of a mammalian protein that binds specifically to DNA containing methylated CpGs. Cell *58*, 499-507.

Meersseman,G., Pennings,S., and Bradbury,E.M. (1991). Chromatosome positioning on assembled long chromatin. Linker histones affect nucleosome placement on 5 S rDNA. J. Mol. Biol. *220*, 89-100.

Meijsing,S.H. and Ehrenhofer-Murray,A.E. (2001). The silencing complex SAS-I links histone acetylation to the assembly of repressed chromatin by CAF-I and Asf1 in Saccharomyces cerevisiae. Genes Dev. *15*, 3169-3182.

Mermoud,J.E., Tassin,A.M., Pehrson,J.R., and Brockdorff,N. (2001). Centrosomal association of histone macroH2A1.2 in embryonic stem cells and somatic cells. Experimental Cell Research *268*, 245-251.

Metzger,E., Wissmann,M., Yin,N., Muller,J.M., Schneider,R., Peters,A.H., Gunther,T., Buettner,R., and Schule,R. (2005). LSD1 demethylates repressive histone marks to promote androgen-receptor-dependent transcription. Nature.

Miao,F. and Natarajan,R. (2005). Mapping global histone methylation patterns in the coding regions of human genes. Mol. Cell Biol. *25*, 4650-4661.

Mihaly,J., Hogga,I., Gausz,J., Gyurkovics,H., and Karch,F. (1997). In situ dissection of the Fab-7 region of the bithorax complex into a chromatin domain boundary and a Polycomb-response element. Development *124*, 1809-1820.

Miller,J.H. (1980). Genetic analysis of the lac repressor. Curr. Top. Microbiol. Immunol. *90*, 1-18.

Minc,E., Courvalin,J.C., and Buendia,B. (2000). HP1gamma associates with euchromatin and heterochromatin in mammalian nuclei and chromosomes. Cytogenet. Cell Genet. *90*, 279-284.

Mintz,P.J., Patterson,S.D., Neuwald,A.F., Spahr,C.S., and Spector,D.L. (1999). Purification and biochemical characterization of interchromatin granule clusters. EMBO J. *18*, 4308-4320.

Mirkovitch,J., Mirault,M.E., and Laemmli,U.K. (1984). Organization of the higher-order chromatin loop: specific DNA attachment sites on nuclear scaffold. Cell *39*, 223-232.

Mirkovitch,J., Gasser,S.M., and Laemmli,U.K. (1987). Relation of chromosome structure and gene expression. Philos. Trans. R. Soc. Lond B Biol. Sci. *317*, 563-574.

Misteli,T., Gunjan,A., Hock,R., Bustin,M., and Brown,D.T. (2000). Dynamic binding of histone H1 to chromatin in living cells. Nature *408*, 877-881.

Mitra,S., Sen,D., and Crothers,D.M. (1984). Orientation of nucleosomes and linker DNA in calf thymus chromatin determined by photochemical dichroism. Nature *308*, 247-250.

Mizuguchi,G., Shen,X., Landry,J., Wu,W.H., Sen,S., and Wu,C. (2004). ATP-driven exchange of histone H2AZ variant catalyzed by SWR1 chromatin remodeling complex. Science *303*, 343-348.

Mizuguchi,G., Shen,X., Landry,J., Wu,W.H., Sen,S., and Wu,C. (2004). ATP-driven exchange of histone H2AZ variant catalyzed by SWR1 chromatin remodeling complex. Science *303*, 343-348.

Moir,R.D., Yoon,M., Khuon,S., and Goldman,R.D. (2000). Nuclear lamins A and B1: Different pathways of assembly during nuclear envelope formation in living cells. JCB *151*, 1155-1168.

Molnar,A. and Georgopoulos,K. (1994). The Ikaros gene encodes a family of functionally diverse zinc finger DNA-binding proteins. Mol. Cell Biol. *14*, 8292-8303.

Montgomery,N.D., Yee,D., Chen,A., Kalantry,S., Chamberlain,S.J., Otte,A.P., and Magnuson,T. (2005). The murine polycomb group protein Eed is required for global histone H3 lysine-27 methylation. Curr. Biol. *15*, 942-947.

Moore,S.C., Jason,L., and Ausio,J. (2002). The elusive structural role of ubiquitinated histones. Biochem. Cell Biol. *80*, 311-319.

Mounkes,L., Kozlov,S., Burke,B., and Stewart,C.L. (2003). The laminopathies: nuclear structure meets disease. Curr. Opin. Genet. Dev. *13*, 223-230.

Mounkes,L., Kozlov,S., Burke,B., and Stewart,C.L. (2003). The laminopathies: nuclear structure meets disease. Curr. Opin. Genet. Dev. *13*, 223-230.

Muchardt,C. and Yaniv,M. (1993). A Human Homolog of Saccharomyces-Cerevisiae Snf2/Swi2 and Drosophila-Brm Genes Potentiates Transcriptional Activation by the Glucocorticoid Receptor. EMBO J. *12*, 4279-4290.

Muchardt,C., Sardet,C., Bourachot,B., Onufryk,C., and Yaniv,M. (1995). A Human Protein with Homology to Saccharomyces-Cerevisiae Snf5 Interacts with the Potential Helicase Hbrm. Nucleic Acids Res. *23*, 1127-1132.

Muchardt,C., Guilleme,M., Seeler,J.S., Trouche,D., Dejean,A., and Yaniv,M. (2002). Coordinated methyl and RNA binding is required for heterochromatin localization of mammalian HP1alpha. EMBO Rep. *3*, 975-981.

Muller,J., Hart,C.M., Francis,N.J., Vargas,M.L., Sengupta,A., Wild,B., Miller,E.L., O'Connor,M.B., Kingston,R.E., and Simon,J.A. (2002). Histone methyltransferase activity of a Drosophila polycomb group repressor complex. Cell *111*, 197-208.

Muller,W.G., Walker,D., Hager,G.L., and McNally,J.G. (2001). Large-scale chromatin decondensation and recondensation regulated by transcription from a natural promoter. J. Cell Biol. *154*, 33-48.

Nagano,A., Koga,R., Ogawa,M., Kurano,Y., Kawada,J., Okada,R., Hayashi,Y.K., Tsukahara,T., and Arahata,K. (1996). Emerin deficiency at the nuclear membrane in patients with Emery-Dreifuss muscular dystrophy. Nat. Genet. *12*, 254-259.

Nagele,R., Freeman,T., McMorrow,L., and Lee,H.Y. (1995). Precise spatial positioning of chromosomes during prometaphase: evidence for chromosomal order. Science *270*, 1831-1835.

Nagy,A., Gocza,E., Diaz,E.M., Prideaux,V.R., Ivanyi,E., Markkula,M., and Rossant,J. (1990). Embryonic Stem-Cells Alone Are Able to Support Fetal Development in the Mouse. Development *110*, 815.

Nagy,A., Rossant,J., Nagy,R., Abramownewerly,W., and Roder,J.C. (1993). Derivation Of Completely Cell Culture-Derived Mice From Early-Passage Embryonic Stem-Cells. Proc. Natl. Acad. Sci. U. S. A. *90*, 8424-8428.

Nagy,L., Kao,H.Y., Chakravarti,D., Lin,R.J., Hassig,C.A., Ayer,D.E., Schreiber,S.L., and Evans,R.M. (1997). Nuclear receptor repression mediated by a complex containing SMRT, mSin3A, and histone deacetylase. Cell *89*, 373-380.

Nakayama,J., Rice,J.C., Strahl,B.D., Allis,C.D., and Grewal,S.I. (2001). Role of histone H3 lysine 9 methylation in epigenetic control of heterochromatin assembly. Science *292*, 110-113.

Nakielny,S. and Dreyfuss,G. (1999). Transport of proteins and RNAs in and out of the nucleus. Cell *99*, 677-690.

Nan,X., Tate,P., Li,E., and Bird,A. (1996). DNA methylation specifies chromosomal localization of MeCP2. Mol. Cell Biol. *16*, 414-421.

Nan,X., Ng,H.H., Johnson,C.A., Laherty,C.D., Turner,B.M., Eisenman,R.N., and Bird,A. (1998). Transcriptional repression by the methyl-CpG-binding protein MeCP2 involves a histone deacetylase complex. Nature *393*, 386-389.

Narlikar,G.J., Phelan,M.L., and Kingston,R.E. (2001). Generation and interconversion of multiple distinct nucleosomal states as a mechanism for catalyzing chromatin fluidity. Molecular Cell *8*, 1219-1230.

Narlikar,G.J., Fan,H.Y., and Kingston,R.E. (2002). Cooperation between complexes that regulate chromatin structure and transcription. Cell *108*, 475-487.

Neal,K.C., Pannuti,A., Smith,E.R., and Lucchesi,J.C. (2000). A new human member of the MYST family of histone acetyl transferases with high sequence similarity to Drosophila MOF. Biochim. Biophys. Acta *1490*, 170-174.

Neigeborn,L. and Carlson,M. (1984). Genes Affecting the Regulation of Suc2 Gene-Expression by Glucose Repression in Saccharomyces-Cerevisiae. Genetics *108*, 845-858.

Nelson,W.G., Pienta,K.J., Barrack,E.R., and Coffey,D.S. (1986). The role of the nuclear matrix in the organization and function of DNA. Annu. Rev. Biophys. Biophys. Chem. *15*, 457-475.

Neri,L.M., Raymond,Y., Giordano,A., Capitani,S., and Martelli,A.M. (1999). Lamin A is part of the internal nucleoskeleton of human erythroleukemia cells. J. Cell Physiol *178*, 284-295.

Neumann,B., Kubicka,P., and Barlow,D.P. (1995). Characteristics of imprinted genes. Nat. Genet. *9*, 12-13.

Ng,H.H., Zhang,Y., Hendrich,B., Johnson,C.A., Turner,B.M., Erdjument-Bromage,H., Tempst,P., Reinberg,D., and Bird,A. (1999). MBD2 is a transcriptional repressor belonging to the MeCP1 histone deacetylase complex. Nat. Genet. *23*, 58-61.

Ng,H.H. and Bird,A. (2000). Histone deacetylases: silencers for hire. Trends Biochem. Sci. *25*, 121-126.

Ng,J., Hart,C.M., Morgan,K., and Simon,J.A. (2000). A Drosophila ESC-E(Z) protein complex is distinct from other polycomb group complexes and contains covalently modified ESC. Molecular and Cellular Biology *20*, 3069-3078.

Nichols,J., Zevnik,B., Anastassiadis,K., Niwa,H., Klewe-Nebenius,D., Chambers,I., Scholer,H., and Smith,A. (1998). Formation of Pluripotent Stem Cells in the Mammalian Embryo Depends on the POU Transcription Factor Oct-4. Cell *95*, 379-391.

Nickerson,J. (2001). Experimental observations of a nuclear matrix. J. Cell Sci. *114*, 463-474.

Nielsen,A.L., Oulad-Abdelghani,M., Ortiz,J.A., Remboutsika,E., Chambon,P., and Losson,R. (2001). Heterochromatin formation in mammalian cells: interaction between histones and HP1 proteins. Mol. Cell *7*, 729-739.

Nili,E., Cojocaru,G.S., Kalma,Y., Ginsberg,D., Copeland,N.G., Gilbert,D.J., Jenkns,N.A., Berger,R., Shaklai,S., Amariglio,N., Brok-Simoni,F., Simon,A.J., and Rechavi,G. (2001). Nuclear membrane protein LAP2 beta mediates transcriptional repression alone and together with its binding partner GCL (germ-cell-less). J. Cell Sci. *114*, 3297-3307.

Nishioka,K., Chuikov,S., Sarma,K., Erdjument-Bromage,H., Allis,C.D., Tempst,P., and Reinberg,D. (2002). Set9, a novel histone H3 methyltransferase that facilitates transcription by precluding histone tail modifications required for heterochromatin formation. Genes & Development *16*, 479-489.

Nogami,M., Nogami,O., Kagotani,K., Okumura,M., Taguchi,H., Ikemura,T., and Okumura,K. (2000). Intranuclear arrangement of human chromosome 12 correlates to large- scale replication domains. Chromosoma *108* , 514-522.

Nogami,M., Kohda,A., Taguchi,H., Nakao,M., Ikemura,T., and Okumura,K. (2000). Relative locations of the centromere and imprinted SNRPN gene within chromosome 15 territories during the cell cycle in HL60 cells. J. Cell Sci *113 (Pt 12)*, 2157-2165.

Nussenzweig,M.C., Shaw,A.C., Sinn,E., Danner,D.B., Holmes,K.L., Morse,H.C., III, and Leder,P. (1987). Allelic exclusion in transgenic mice that express the membrane form of immunoglobulin mu. Science *236*, 816-819.

O'Carroll,D., Erhardt,S., Pagani,M., Barton,S.C., Surani,M.A., and Jenuwein,T. (2001). The Polycomb-group gene Ezh2 is required for early mouse development. Molecular and Cellular Biology *21*, 4330-4336.

O'Neill,L.P., Randall,T.E., Lavender,J., Spotswood,H.T., Lee,J.T., and Turner,B.M. (2003). X-linked genes in female embryonic stem cells carry an epigenetic mark prior to the onset of X inactivation. Hum. Mol. Genet. *12*, 1783-1790.

Ochs,R.L., Lischwe,M.A., Spohn,W.H., and Busch,H. (1985). Fibrillarin: a new protein of the nucleolus identified by autoimmune sera. Biol. Cell *54*, 123-133.

Ogawa,H., Ishiguro,K., Gaubatz,S., Livingston,D.M., and Nakatani,Y. (2002). A complex with chromatin modifiers that occupies E2F- and Myc-responsive genes in G0 cells. Science *296*, 1132-1136.

Ogryzko,V.V., Hirai,T.H., Russanova,V.R., Barbie,D.A., and Howard,B.H. (1996). Human fibroblast commitment to a senescence-like state in response to histone deacetylase inhibitors is cell cycle dependent. Mol. Cell Biol. *16*, 5210-5218.

Okano,M., Xie,S., and Li,E. (1998). Dnmt2 is not required for de novo and maintenance methylation of viral DNA in embryonic stem cells. Nucleic Acids Res. *26*, 2536-2540.

Olins,A.L. and Olins,D.E. (1974). Spheroid chromatin units (v bodies). Science *183*, 330-332.

Oliva,R., Bazett-Jones,D.P., Locklear,L., and Dixon,G.H. (1990). Histone hyperacetylation can induce unfolding of the nucleosome core particle. Nucleic Acids Res. *18*, 2739-2747.

Orlando,V. (2003). Polycomb, epigenomes, and control of cell identity. Cell *112*, 599-606.

Osada,S., Ohmori,S.Y., and Taira,M. (2003). XMAN1, an inner nuclear membrane protein, antagonizes BMP signaling by interacting with Smad1 in Xenopus embryos. Development *130*, 1783-1794.

Osborne,C.S., Chakalova,L., Brown,K.E., Carter,D., Horton,A., Debrand,E., Goyenechea,B., Mitchell,J.A., Lopes,S., Reik,W., and Fraser,P. (2004). Active genes dynamically colocalize to shared sites of ongoing transcription. Nat. Genet. *36*, 1065-1071.

Osley,M.A. (2004). H2B ubiquitylation: the end is in sight. Biochim. Biophys. Acta *1677*, 74-78.

Palazzo,A.F., Cook,T.A., Alberts,A.S., and Gundersen,G.G. (2001). mDia mediates Rho-regulated formation and orientation of stable microtubules. Nat. Cell Biol. *3*, 723-729.

Palladino,F., Laroche,T., Gilson,E., Axelrod,A., Pillus,L., and Gasser,S.M. (1993). SIR3 and SIR4 proteins are required for the positioning and integrity of yeast telomeres. Cell *75*, 543-555.

Pan,D., Estevez-Salmeron,L.D., Stroschein,S.L., Zhu,X., He,J., Zhou,S., and Luo,K. (2005). The integral inner nuclear membrane protein MAN1 physically interacts with the R-Smad proteins to repress signaling by the transforming growth factor-{beta} superfamily of cytokines. J. Biol. Chem. *280*, 15992-16001.

Parada,L.A., Roix,J.J., and Misteli,T. (2003). An uncertainty principle in chromosome positioning. Trends Cell Biol. *13*, 393-396.

Parada,L.A., McQueen,P.G., and Misteli,T. (2004). Tissue-specific spatial organization of genomes. Genome Biol. *5*, R44.

Pardoll,D.M. and Vogelstein,B. (1980). Sequence analysis of nuclear matrix associated DNA from rat liver. Exp. Cell Res. *128* , 466-470.

Paulson,J.R. and Laemmli,U.K. (1977). The structure of histone-depleted metaphase chromosomes. Cell *12*, 817-828.

Pederson,T. (2000). Half a century of "the nuclear matrix". Mol. Biol. Cell *11*, 799-805.

Pederson,T. (2000). Diffusional protein transport within the nucleus: a message in the medium. Nat. Cell Biol. *2*, E73-E74.

Pederson,T. (2002). Dynamics and genome-centricity of interchromatin domains in the nucleus. Nat. Cell Biol. *4*, E287-E291.

Pederson,T. and Aebi,U. (2002). Actin in the nucleus: what form and what for? Journal of Structural Biology *140*, 3-9.

Peifer,M. and Bender,W. (1988). Sequences of the gypsy transposon of Drosophila necessary for its effects on adjacent genes. Proc. Natl. Acad. Sci. U. S. A *85*, 9650-9654.

Peters,A.H., Mermoud,J.E., O'Carroll,D., Pagani,M., Schweizer,D., Brockdorff,N., and Jenuwein,T. (2002). Histone H3 lysine 9 methylation is an epigenetic imprint of facultative heterochromatin. Nat. Genet. *30*, 77-80.

Peters,A.H., Kubicek,S., Mechtler,K., O'Sullivan,R.J., Derijck,A.A., Perez-Burgos,L., Kohlmaier,A., Opravil,S., Tachibana,M., Shinkai,Y., Martens,J.H., and Jenuwein,T. (2003). Partitioning and plasticity of repressive histone methylation states in mammalian chromatin. Mol. Cell *12*, 1577-1589.

Peters,A.H.F.M., O'Carroll,D., Scherthan,H., Mechtler,K., Sauer,S., Schofer,C., Weipoltshammer,K., Pagani,M., Lachner,M., Kohlmaier,A., Opravil,S., Doyle,M., Sibilia,M., and Jenuwein,T. (2001). Loss of the Suv39h histone methyltransferases impairs mammalian heterochromatin and genome stability. Cell *107*, 323-337.

Peterson,C., Kordich,J., Milligan,L., Bodor,E., Siner,A., Nagy,K., and Paquin,C.E. (2000). Mutations in RAD3, MSH2, and RAD52 affect the rate of gene amplification in the yeast Saccharomyces cerevisiae. Environ. Mol. Mutagen. *36*, 325-334.

Phair,R.D. and Misteli,T. (2000). High mobility of proteins in the mammalian cell nucleus. Nature *404*, 604-+.

Phair,R.D. and Misteli,T. (2001). Kinetic modelling approaches to in vivo imaging. Nature Reviews Molecular Cell Biology *2*, 898-907.

Phair,R.D., Scaffidi,P., Elbi,C., Vecerova,J., Dey,A., Ozato,K., Brown,D.T., Hager,G., Bustin,M., and Misteli,T. (2004). Global nature of dynamic protein-chromatin interactions in vivo: three-dimensional genome scanning and dynamic interaction networks of chromatin proteins. Mol. Cell Biol. *24*, 6393-6402.

Pietras,D.F., Bennett,K.L., Siracusa,L.D., Woodworth-Gutai,M., Chapman,V.M., Gross,K.W., Kane-Haas,C., and Hastie,N.D. (1983). Construction of a small Mus musculus repetitive DNA library: identification of a new satellite sequence in Mus musculus. Nucleic Acids Res. *11*, 6965-6983.

Pinkel,D., Landegent,J., Collins,C., Fuscoe,J., Segraves,R., Lucas,J., and Gray,J. (1988). Fluorescence in situ hybridization with human chromosome-specific libraries: detection of trisomy 21 and translocations of chromosome 4. Proc. Natl. Acad. Sci. U. S. A *85*, 9138-9142.

Pirrotta,V. (1999). Polycomb silencing and the maintenance of stable chromatin states. Results Probl. Cell Differ. *25*, 205-228.

Platani,M., Goldberg,I., Swedlow,J.R., and Lamond,A.I. (2000). In vivo analysis of Cajal body movement, separation, and joining in live human cells. J. Cell Biol. *151*, 1561-1574.

Platani,M., Goldberg,I., Lamond,A.I., and Swedlow,J.R. (2002). Cajal Body dynamics and association with chromatin are ATP-dependent. Nature Cell Biology *4*, 502-508.

Plath,K., Fang,J., Mlynarczyk-Evans,S.K., Cao,R., Worringer,K.A., Wang,H., de la Cruz,C.C., Otte,A.P., Panning,B., and Zhang,Y. (2003). Role of histone H3 lysine 27 methylation in X inactivation. Science *300*, 131-135.

Plath,K., Talbot,D., Hamer,K.M., Otte,A.P., Yang,T.P., Jaenisch,R., and Panning,B. (2004). Developmentally regulated alterations in Polycomb repressive complex 1 proteins on the inactive X chromosome. J. Cell Biol. *167*, 1025-1035.

Polach,K.J., Lowary,P.T., and Widom,J. (2000). Effects of core histone tail domains on the equilibrium constants for dynamic DNA site accessibility in nucleosomes. J. Mol. Biol. *298*, 211-223.

Polioudaki,H., Kourmouli,N., Drosou,V., Bakou,A., Theodoropoulos,P.A., Singh,P.B., Giannakouros,T., and Georgatos,S.D. (2001). Histones H3/H4 form a tight complex with the inner nuclear membrane protein LBR and heterochromatin protein 1. EMBO Rep. *2*, 920-925.

Pollard,H., Toumaniantz,G., Amos,J.L., Avet-Loiseau,H., Guihard,G., Behr,J.P., and Escande,D. (2001). Ca2+-sensitive cytosolic nucleases prevent efficient delivery to the nucleus of injected plasmids. J. Gene Med. *3*, 153-164.

Pombo,A., Jones,E., Iborra,F.J., Kimura,H., Sugaya,K., Cook,P.R., and Jackson,D.A. (2000). Specialized transcription factories within mammalian nuclei. Crit Rev. Eukaryot. Gene Expr. *10*, 21-29.

Ponger,L., Duret,L., and Mouchiroud,D. (2001). Determinants of CpG islands: expression in early embryo and isochore structure. Genome Res. *11*, 1854-1860.

Poot,R.A., Dellaire,G., Hulsmann,B.B., Grimaldi,M.A., Corona,D.F.V., Becker,P.B., Bickmore,W.A., and Varga-Weisz,P.D. (2000). HuCHRAC, a human ISWI chromatin remodelling complex contains hACF1 and two novel histone-fold proteins. EMBO J. *19*, 3377-3387.

Popp,S., Scholl,H.P., Loos,P., Jauch,A., Stelzer,E., Cremer,C., and Cremer,T. (1990). Distribution of chromosome 18 and X centric heterochromatin in the interphase nucleus of cultured human cells. Exp. Cell Res. *189*, 1-12.

Popp,S., Jauch,A., Schindler,D., Speicher,M.R., Lengauer,C., Donis-Keller,H., Riethman,H.C., and Cremer,T. (1993). A strategy for the characterization of minute chromosome rearrangements using multiple color fluorescence in situ hybridization with chromosome-specific DNA libraries and YAC clones. Hum. Genet. *92*, 527-532.

Poux,S., Kostic,C., and Pirrotta,V. (1996). Hunchback-independent silencing of late Ubx enhancers by a Polycomb Group Response Element. EMBO J. *15*, 4713-4722.

Pradhan,S., Bacolla,A., Wells,R.D., and Roberts,R.J. (1999). Recombinant human DNA (cytosine-5) methyltransferase. I. Expression, purification, and comparison of de novo and maintenance methylation. J. Biol. Chem. *274*, 33002-33010.

Prasher,D.C., Eckenrode,V.K., Ward,W.W., Prendergast,F.G., and Cormier,M.J. (1992). Primary structure of the Aequorea victoria green-fluorescent protein. Gene *111*, 229-233.

PRESCOTT,D.M. and BENDER,M.A. (1962). Synthesis of RNA and protein during mitosis in mammalian tissue culture cells. Exp. Cell Res. *26*, 260-268.

Qian,H., Sheetz,M.P., and Elson,E.L. (1991). Single particle tracking. Analysis of diffusion and flow in two-dimensional systems. Biophys. J. *60*, 910-921.

Rajewsky,K. (1996). Clonal selection and learning in the antibody system. Nature *381*, 751-758.

Rangasamy,D., Berven,L., Ridgway,P., and Tremethick,D.J. (2003). Pericentric heterochromatin becomes enriched with H2A.Z during early mammalian development. EMBO J. *22*, 1599-1607.

Rangasamy,D., Greaves,I., and Tremethick,D.J. (2004). RNA interference demonstrates a novel role for H2A.Z in chromosome segregation. Nat. Struct. Mol. Biol. *11*, 650-655.

Rappold,G.A., Cremer,T., Hager,H.D., Davies,K.E., Muller,C.R., and Yang,T. (1984). Sex chromosome positions in human interphase nuclei as studied by in situ hybridization with chromosome specific DNA probes. Hum. Genet. *67*, 317-325.

Rasmussen,T.P., Mastrangelo,M.A., Eden,A., Pehrson,J.R., and Jaenisch,R. (2000). Dynamic relocalization of histone MacroH2A1 from centrosomes to inactive X chromosomes during X inactivation. JCB *150*, 1189-1198.

Rattner,J.B., Kingwell,B.G., and Fritzler,M.J. (1988). Detection of distinct structural domains within the primary constriction using autoantibodies. Chromosoma *96*, 360-367.

Razin,A. and Cedar,H. (1993). DNA methylation and embryogenesis. EXS *64*, 343-357.

Razin,S.V., Gromova,I.I., and Iarovaia,O.V. (1995). Specificity and functional significance of DNA interaction with the nuclear matrix: new approaches to clarify the old questions. Int. Rev. Cytol. *162B*, 405-448.

Rea,S., Eisenhaber,F., O'Carroll,D., Strahl,B.D., Sun,Z.W., Schmid,M., Opravil,S., Mechtler,K., Ponting,C.P., Allis,C.D., and Jenuwein,T. (2000). Regulation of chromatin structure by site-specific histone H3 methyltransferases. Nature *406*, 593-599.

Redon,C., Pilch,D., Rogakou,E., Sedelnikova,O., Newrock,K., and Bonner,W. (2002). Histone H2A variants H2AX and H2AZ. Curr. Opin. Genet. Dev. *12*, 162-169.

Reed,R. (1996). Initial splice-site recognition and pairing during pre-mRNA splicing. Curr. Opin. Genet. Dev. *6*, 215-220.

Reed,K.C., Mann,D.A. (1985). Rapid transfer of DNA from agarose gels to nylon membranes. Nucleic Acids Res. *13*, 7207-7221.

Reeves,R., Gorman,C.M., and Howard,B. (1985). Minichromosome assembly of non-integrated plasmid DNA transfected into mammalian cells. Nucleic Acids Res. *13*, 3599-3615.

Reyes,J.C., Muchardt,C., and Yaniv,M. (1997). Components of the human SWI/SNF complex are enriched in active chromatin and are associated with the nuclear matrix. J. Cell Biol. *137*, 263-274.

Rice,J.C., Briggs,S.D., Ueberheide,B., Barber,C.M., Shabanowitz,J., Hunt,D.F., Shinkai,Y., and Allis,C.D. (2003). Histone methyltransferases direct different degrees of methylation to define distinct chromatin domains. Mol. Cell *12*, 1591-1598.

Richards,E.J. and Elgin,S.C. (2002). Epigenetic codes for heterochromatin formation and silencing: rounding up the usual suspects. Cell *108*, 489-500.

Rine,J. and Herskowitz,I. (1987). Four genes responsible for a position effect on expression from HML and HMR in Saccharomyces cerevisiae. Genetics *116*, 9-22.

Ringrose,L., Ehret,H., and Paro,R. (2004). Distinct contributions of histone H3 lysine 9 and 27 methylation to locus-specific stability of Polycomb complexes. Molecular Cell *16*, 641-653.

Rober,R.A., Weber,K., and Osborn,M. (1989). Differential timing of nuclear lamin A/C expression in the various organs of the mouse embryo and the young animal: a developmental study. Development *105*, 365-378.

Robert,F., Pokholok,D.K., Hannett,N.M., Rinaldi,N.J., Chandy,M., Rolfe,A., Workman,J.L., Gifford,D.K., and Young,R.A. (2004). Global position and recruitment of HATs and HDACs in the yeast genome. Mol. Cell *16*, 199-209.

Robertson,E., Bradley,A., Kuehn,M., and Evans,M. (1986). Germ-line transmission of genes introduced into cultured pluripotential cells by retroviral vector. Nature *323*, 445-448.

Robinett,C.C., Straight,A., Li,G., Willhelm,C., Sudlow,G., Murray,A., and Belmont,A.S. (1996). In vivo localization of DNA sequences and visualization of large-scale chromatin organization using lac operator/repressor recognition. J. Cell Biol. *135*, 1685-1700.

Robyr,D., Suka,Y., Xenarios,I., Kurdistani,S.K., Wang,A., Suka,N., and Grunstein,M. (2002). Microarray deacetylation maps determine genome-wide functions for yeast histone deacetylases. Cell *109*, 437-446.

Robyr,D. and Grunstein,M. (2003). Genomewide histone acetylation microarrays. Methods *31*, 83-89.
Roelfsema JH, White SJ, Ariyurek Y, Bartholdi D, Niedrist D, Papadia F, Bacino CA, den Dunnen JT, van Ommen GJ, Breuning MH, Hennekam RC, Peters DJ.Genetic heterogeneity in Rubinstein-Taybi syndrome: mutations in both the CBP and EP300 genes cause disease.Am J Hum Genet. 2005 76(4):572-80.

Rogers,S., Wells,R., and Rechsteiner,M. (1986). Amino acid sequences common to rapidly degraded proteins: the PEST hypothesis. Science *234*, 364-368.

Roh,T.Y., Ngau,W.C., Cui,K., Landsman,D., and Zhao,K. (2004). High-resolution genome-wide mapping of histone modifications. Nat. Biotechnol. *22*, 1013-1016.

Roix,J.J., McQueen,P.G., Munson,P.J., Parada,L.A., and Misteli,T. (2003). Spatial proximity of translocation-prone gene loci in human lymphomas. Nat. Genet. *34*, 287-291.

Roldan,E., Fuxa,M., Chong,W., Martinez,D., Novatchkova,M., Busslinger,M., and Skok,J.A. (2005). Locus 'decontraction' and centromeric recruitment contribute to allelic exclusion of the immunoglobulin heavy-chain gene. Nat. Immunol. *6*, 31-41.

Rolink,A.G., Melchers,F., and Andersson,J. (1999). The transition from immature to mature B cells. Curr. Top. Microbiol. Immunol. *246*, 39-43.

Rosner,M.H., Vigano,M.A., Ozato,K., Timmons,P.M., Poirier,F., Rigby,P.W., and Staudt,L.M. (1990). A POU-domain transcription factor in early stem cells and germ cells of the mammalian embryo. Nature *345*, 686-692.

Rougeulle,C., Chaumeil,J., Sarma,K., Allis,C.D., Reinberg,D., Avner,P., and Heard,E. (2004). Differential histone H3 Lys-9 and Lys-27 methylation profiles on the X chromosome. Mol. Cell Biol. *24*, 5475-5484.

Rountree,M.R., Bachman,K.E., Herman,J.G., and Baylin,S.B. (2001). DNA methylation, chromatin inheritance, and cancer. Oncogene *20*, 3156-3165.

Roy,R., Meier,B., McAinsh,A.D., Feldmann,H.M., and Jackson,S.P. (2004). Separation-of-function mutants of yeast Ku80 reveal a Yku80p-Sir4p interaction involved in telomeric silencing. J. Biol. Chem. *279*, 86-94.

Ruggero,D., Wang,Z.G., and Pandolfi,P.P. (2000). The puzzling multiple lives of PML and its role in the genesis of cancer. Bioessays *22*, 827-835.

Rusche,L.N., Kirchmaier,A.L., and Rine,J. (2003). The establishment, inheritance, and function of silenced chromatin in Saccharomyces cerevisiae. Annu. Rev. Biochem. *72*, 481-516.

Sabbattini,P., Lundgren,M., Georgiou,A., Chow,C., Warnes,G., and Dillon,N. (2001). Binding of Ikaros to the lambda5 promoter silences transcription through a mechanism that does not require heterochromatin formation. EMBO J. *20*, 2812-2822.

Sadoni,N., Langer,S., Fauth,C., Bernardi,G., Cremer,T., Turner,B.M., and Zink,D. (1999). Nuclear organization of mammalian genomes. Polar chromosome territories build up functionally distinct higher order compartments. J. Cell Biol. *146*, 1211-1226.

Sagot,I., Rodal,A.A., Moseley,J., Goode,B.L., and Pellman,D. (2002). An actin nucleation mechanism mediated by Bni1 and profilin. Nat. Cell Biol. *4*, 626-631.

Saitoh,N., Bell,A.C., Recillas-Targa,F., West,A.G., Simpson,M., Pikaart,M., and Felsenfeld,G. (2000). Structural and functional conservation at the boundaries of the chicken beta-globin domain. EMBO J. *19* , 2315-2322.

Sambrook, J. and and Russell, D. W. Molecular Cloning. Irwin, N. and Janssen K. A laboratory manual. [3rd Edition]. 2001. Cold Spring Harbor Laboratory Press.

Santoro,R., Li,J.W., and Grummt,I. (2002). The nucleolar remodeling complex NoRC mediates heterochromatin formation and silencing of ribosomal gene transcription. Nat. Genet. *32*, 393-396.

Santos-Rosa,H., Schneider,R., Bannister,A.J., Sherriff,J., Bernstein,B.E., Emre,N.C., Schreiber,S.L., Mellor,J., and Kouzarides,T. (2002). Active genes are tri-methylated at K4 of histone H3. Nature *419*, 407-411.

Santoso,B., Ortiz,B.D., and Winoto,A. (2000). Control of organ-specific demethylation by an element of the T-cell receptor-alpha locus control region. J. Biol. Chem. *275*, 1952-1958.

Sarraf,S.A. and Stancheva,I. (2004). Methyl-CpG binding protein MBD1 couples histone H3 methylation at lysine 9 by SETDB1 to DNA replication and chromatin assembly. Mol. Cell *15*, 595-605.

Saunders,W.S., Cooke,C.A., and Earnshaw,W.C. (1991). Compartmentalization within the nucleus: discovery of a novel subnuclear region. J. Cell Biol. *115*, 919-931.

Saurin,A.J., Shao,Z.H., Erdjument-Bromage,H., Tempst,P., and Kingston,R.E. (2001). A Drosophila Polycomb group complex includes Zeste and dTAFII proteins. Nature *412*, 655-660.

Saurin,A.J., Shao,Z.H., Erdjument-Bromage,H., Tempst,P., and Kingston,R.E. (2001). A Drosophila Polycomb group complex includes Zeste and dTAFII proteins. Nature *412*, 655-660.

Sawado,T., Igarashi,K., and Groudine,M. (2001). Activation of beta-major globin gene transcription is associated with recruitment of NF-E2 to the beta-globin LCR and gene promoter. Proc. Natl. Acad. Sci. U. S. A *98*, 10226-10231.

Schalch,T., Duda,S., Sargent,D.F., and Richmond,T.J. (2005). X-ray structure of a tetranucleosome and its implications for the chromatin fibre. Nature *436*, 138-141.

Schardin,M., Cremer,T., Hager,H.D., and Lang,M. (1985). Specific staining of human chromosomes in Chinese hamster x man hybrid cell lines demonstrates interphase chromosome territories. Hum. Genet. *71*, 281-287.

Schatz,D.G., Oettinger,M.A., and Baltimore,D. (1989). The V(D)J recombination activating gene, RAG-1. Cell *59*, 1035-1048.

Scheer,U., Thiry,M., and Goessens,G. (1993). Structure, function and assembly of the nucleolus. Trends Cell Biol. *3*, 236-241.

Schirmer,E.C., Guan,T., and Gerace,L. (2001). Involvement of the lamin rod domain in heterotypic lamin interactions important for nuclear organization. J. Cell Biol. *153*, 479-489.

Schirmer,E.C., Florens,L., Guan,T., Yates,J.R., III, and Gerace,L. (2003). Nuclear membrane proteins with potential disease links found by subtractive proteomics. Science *301*, 1380-1382.

Schirmer EC, Gerace L.The nuclear membrane proteome: extending the envelope.
Trends Biochem Sci. 2005 Aug 24;

Schmid,M., Haaf,T., and Grunert,D. (1984). 5-Azacytidine-Induced Undercondensations in Human-Chromosomes. Human Genetics *67*, 257-263.

Schmiedeberg,L., Weisshart,K., Diekmann,S., Hoerste,G.M.Z., and Hemmerich,P. (2004). High- and low-mobility populations of HP1 in heterochromatin of mammalian cells. Molecular Biology of the Cell *15*, 2819-2833.

Scholer,H.R., Dressler,G.R., Balling,R., Rohdewohld,H., and Gruss,P. (1990). Oct-4: a germline-specific transcription factor mapping to the mouse t- complex. EMBO J. *9*, 2185-2195.

Schotta,G., Lachner,M., Sarma,K., Ebert,A., Sengupta,R., Reuter,G., Reinberg,D., and Jenuwein,T. (2004). A silencing pathway to induce H3-K9 and H4-K20 trimethylation at constitutive heterochromatin. Genes Dev. *18*, 1251-1262.

Schramke,V. and Allshire,R. (2004). Those interfering little RNAs! Silencing and eliminating chromatin. Current Opinion in Genetics & Development *14*, 174-180.

Schreiber,S.L. and Bernstein,B.E. (2002). Signaling network model of chromatin. Cell *111*, 771-778.

Schubeler,D., Francastel,C., Cimbora,D.M., Reik,A., Martin,D.I., and Groudine,M. (2000). Nuclear localization and histone acetylation: a pathway for chromatin opening and transcriptional activation of the human beta-globin locus. Genes Dev. *14*, 940-950.

Schubeler,D., MacAlpine,D.M., Scalzo,D., Wirbelauer,C., Kooperberg,C., van Leeuwen,F., Gottschling,D.E., O'Neill,L.P., Turner,B.M., Delrow,J., Bell,S.P., and Groudine,M. (2004). The histone modification pattern of active genes revealed through genome-wide chromatin analysis of a higher eukaryote. Genes Dev. *18*, 1263-1271.

Schug,J., Schuller,W.P., Kappen,C., Salbaum,J.M., Bucan,M., and Stoeckert,C.J., Jr. (2005). Promoter features related to tissue specificity as measured by Shannon entropy. Genome Biol. *6*, R33.

Schultz,C.L., Elenich,L.A., and Dunnick,W.A. (1991). Nuclear-Protein Binding to Octamer Motifs in the Immunoglobulin Gamma-1 Switch Region. International Immunology *3*, 109-116.

Schultz,D.C., Ayyanathan,K., Negorev,D., Maul,G.G., and Rauscher,F.J., III (2002). SETDB1: a novel KAP-1-associated histone H3, lysine 9-specific methyltransferase that contributes to HP1-mediated silencing of euchromatic genes by KRAB zinc-finger proteins. Genes Dev. *16*, 919-932.

Schwartz,B.E. and Ahmad,K. (2005). Transcriptional activation triggers deposition and removal of the histone variant H3.3. Genes & Development *19*, 804-814.

Schwarzacher,T. and Heslop-Harrison,J.S. (1994). Direct fluorochrome-labeled DNA probes for direct fluorescent in situ hybridization to chromosomes. Methods Mol. Biol. *28*, 167-176.

Sedat,J. and Manuelidis,L. (1978). A direct approach to the structure of eukaryotic chromosomes. Cold Spring Harb. Symp. Quant. Biol. *42 Pt 1*, 331-350.

Seeler,J.S. and Dejean,A. (1999). The PML nuclear bodies: actors or extras? Current Opinion in Genetics & Development *9*, 362-367.

Seksek,O., Biwersi,J., and Verkman,A.S. (1997). Translational diffusion of macromolecule-sized solutes in cytoplasm and nucleus. J. Cell Biol. *138*, 131-142.

Sewalt,R.G.A.B., Gunster,M.J., Van der Vlag,J., Satijn,D.P.E., and Otte,A.P. (1999). C-terminal binding protein is a transcriptional repressor that interacts with a specific class of vertebrate polycomb proteins. Molecular and Cellular Biology *19*, 777-787.

Shao,Z.H., Raible,F., Mollaaghababa,R., Guyon,J.R., Wu,C.T., Bender,W., and Kingston,R.E. (1999). Stabilization of chromatin structure by PRC1, a polycomb complex. Cell *98*, 37-46.

Shelby,R.D., Hahn,K.M., and Sullivan,K.F. (1996). Dynamic elastic behavior of alpha-satellite DNA domains visualized in situ in living human cells. J. Cell Biol. *135*, 545-557.

Shen,C.H., Leblanc,B.P., Alfieri,J.A., and Clark,D.J. (2001). Remodeling of yeast CUP1 chromatin involves activator-dependent repositioning of nucleosomes over the entire gene and flanking sequences. Mol. Cell Biol. *21*, 534-547.

Shen,X., Yu,L., Weir,J.W., and Gorovsky,M.A. (1995). Linker histones are not essential and affect chromatin condensation in vivo. Cell *82*, 47-56.

Shen,X., Mizuguchi,G., Hamiche,A., and Wu,C. (2000). A chromatin remodelling complex involved in transcription and DNA processing. Nature *406*, 541-544.

Shi,Y., Lan,F., Matson,C., Mulligan,P., Whetstine,J.R., Cole,P.A., Casero,R.A., and Shi,Y. (2004). Histone demethylation mediated by the nuclear amine oxidase homolog LSD1. Cell *119*, 941-953.

Shopland,L.S. and Lawrence,J.B. (2000). Seeking common ground in nuclear complexity. J. Cell Biol. *150*, F1-F4.

Shopland,L.S., Johnson,C.V., Byron,M., McNeil,J., and Lawrence,J.B. (2003). Clustering of multiple specific genes and gene-rich R-bands around SC-35 domains: evidence for local euchromatic neighborhoods. JCB *162*, 981-990.

Shumaker,D.K., Lee,K.K., Tanhehco,Y.C., Craigie,R., and Wilson,K.L. (2001). LAP2 binds to BAF.DNA complexes: requirement for the LEM domain and modulation by variable regions. EMBO J. *20*, 1754-1764.

Sigrist,C.J. and Pirrotta,V. (1997). Chromatin insulator elements block the silencing of a target gene by the Drosophila polycomb response element (PRE) but allow trans interactions between PREs on different chromosomes. Genetics *147*, 209-221.

Silva,J., Mak,W., Zvetkova,I., Appanah,R., Nesterova,T.B., Webster,Z., Peters,A.H., Jenuwein,T., Otte,A.P., and Brockdorff,N. (2003). Establishment of histone h3 methylation on the inactive X chromosome requires transient recruitment of Eed-Enx1 polycomb group complexes. Dev. Cell *4*, 481-495.

Singh,P.B. and Georgatos,S.D. (2002). HP1: facts, open questions, and speculation. J. Struct. Biol. *140*, 10-16.

Skarnes,W.C., Moss,J.E., Hurtley,S.M., and Beddington,R.S. (1995). Capturing genes encoding membrane and secreted proteins important for mouse development. Proc. Natl. Acad. Sci. U. S. A *92*, 6592-6596.

Skok,J.A., Brown,K.E., Azuara,V., Caparros,M.L., Baxter,J., Takacs,K., Dillon,N., Gray,D., Perry,R.P., Merkenschlager,M., and Fisher,A.G. (2001). Nonequivalent nuclear location of immunoglobulin alleles in B lymphocytes. Nat. Immunol. *2*, 848-854.

Sleutels,F., Zwart,R., and Barlow,D.P. (2002). The non-coding Air RNA is required for silencing autosomal imprinted genes. Nature *415*, 810-813.

Smith,A.G., Heath,J.K., Donaldson,D.D., Wong,G.G., Moreau,J., Stahl,M., and Rogers,D. (1988). Inhibition of Pluripotential Embryonic Stem-Cell Differentiation By Purified Polypeptides. Nature *336*, 688-690.

Smith,K.P., Moen,P.T., Wydner,K.L., Coleman,J.R., and Lawrence,J.B. (1999). Processing of endogenous pre-mRNAs in association with SC-35 domains is gene specific. JCB *144*, 617-629.

Smith,M.M. (2002). Centromeres and variant histones: what, where, when and why? Curr. Opin. Cell Biol. *14*, 279-285.

Snaar,S., Wiesmeijer,K., Jochemsen,A.G., Tanke,H.J., and Dirks,R.W. (2000). Mutational analysis of fibrillarin and its mobility in living human cells. J. Cell Biol. *151*, 653-662.

Somech,R., Shaklai,S., Geller,O., Amariglio,N., Simon,A.J., Rechavi,G., and Gal-Yam,E.N. (2005). The nuclear-envelope protein and transcriptional repressor LAP2{beta} interacts with HDAC3 at the nuclear periphery, and induces histone H4 deacetylation. J. Cell Sci. *118*, 4017-4025.

Soppe,W.J., Jasencakova,Z., Houben,A., Kakutani,T., Meister,A., Huang,M.S., Jacobsen,S.E., Schubert,I., and Fransz,P.F. (2002). DNA methylation controls histone H3 lysine 9 methylation and heterochromatin assembly in Arabidopsis. EMBO J. *21*, 6549-6559.

Spann,T.P., Moir,R.D., Goldman,A.E., Stick,R., and Goldman,R.D. (1997). Disruption of nuclear lamin organization alters the distribution of replication factors and inhibits DNA synthesis. J. Cell Biol. *136*, 1201-1212.

Spann,T.P., Goldman,A.E., Wang,C., Huang,S., and Goldman,R.D. (2002). Alteration of nuclear lamin organization inhibits RNA polymerase II-dependent transcription. J. Cell Biol. *156*, 603-608.

Spector,D.L. (1990). Higher order nuclear organization: three-dimensional distribution of small nuclear ribonucleoprotein particles [published erratum appears in Proc Natl Acad Sci U S A 1990 Mar;87(6):2384]. Proc. Natl. Acad. Sci. U. S. A *87*, 147-151.

Spector,D.L. (2003). The dynamics of chromosome organization and gene regulation. Annu. Rev. Biochem. *72*, 573-608.

Spilianakis CG, Lalioti MD, Town T, Lee GR, Flavell RA. (2005). Interchromosomal associations between alternatively expressed loci. Nature *435(7042)*:637-45.

Stadler,S., Schnapp,V., Mayer,R., Stein,S., Cremer,C., Bonifer,C., Cremer,T., and Dietzel,S. (2004). The architecture of chicken chromosome territories changes during differentiation. BMC. Cell Biol. *5*, 44.

Starr,D.A., Hermann,G.J., Malone,C.J., Fixsen,W., Priess,J.R., Horvitz,H.R., and Han,M. (2001). unc-83 encodes a novel component of the nuclear envelope and is essential for proper nuclear migration. Development *128*, 5039-5050.

Starr,D.A. and Han,M. (2002). Role of ANC-1 in tethering nuclei to the actin cytoskeleton. Science *298*, 406-409.

Sterner,D.E. and Berger,S.L. (2000). Acetylation of histones and transcription-related factors. Microbiol. Mol. Biol. Rev. *64*, 435-459.

Stick,R. and Hausen,P. (1985). Changes in the nuclear lamina composition during early development of Xenopus laevis. Cell *41* , 191-200.

Stief,A., Winter,D.M., Stratling,W.H., and Sippel,A.E. (1989). A nuclear DNA attachment element mediates elevated and position-independent gene activity. Nature *341*, 343-345.

Strahl,B.D. and Allis,C.D. (2000). The language of covalent histone modifications. Nature *403*, 41-45.

Strahl,B.D., Grant,P.A., Briggs,S.D., Sun,Z.W., Bone,J.R., Caldwell,J.A., Mollah,S., Cook,R.G., Shabanowitz,J., Hunt,D.F., and Allis,C.D. (2002). Set2 is a nucleosomal histone H3-selective methyltransferase that mediates transcriptional repression. Mol. Cell Biol. *22*, 1298-1306.

Straight,A.F., Belmont,A.S., Robinett,C.C., and Murray,A.W. (1996). GFP tagging of budding yeast chromosomes reveals that protein-protein interactions can mediate sister chromatid cohesion. Curr. Biol. *6*, 1599-1608.

Strelkov SV, Schumacher J, Burkhard P, Aebi U, Herrmann H, 2004.Crystal structure of the human lamin A coil 2B dimer: implications for the head-to-tail association of nuclear lamins.J Mol Biol *29*;343(4):1067-80.

Strickland S, Mahdavi V (1978). The induction of differentiation in teratocarcinoma stem cells by retinoic acid. Cell. *15*, 393-403.

Strohner,R., Nemeth,A., Jansa,P., Hofmann-Rohrer,U., Santoro,R., Langst,G., and Grummt,I. (2001). NoRC - a novel member of mammalian ISWI-containing chromatin remodeling machines. EMBO J. *20*, 4892-4900.

Strohner,R., Nemeth,A., Nightingale,K.P., Grummt,I., Becker,P.B., and Langst,G. (2004). Recruitment of the nucleolar remodeling complex NoRC establishes ribosomal DNA silencing in chromatin. Molecular and Cellular Biology *24*, 1791-1798.

Struhl,K. (1998). Histone acetylation and transcriptional regulatory mechanisms. Genes Dev. *12*, 599-606.

Strutt,H. and Paro,R. (1997). The polycomb group protein complex of Drosophila melanogaster has different compositions at different target genes. Mol. Cell Biol. *17*, 6773-6783.

Stuurman,N., Heins,S., and Aebi,U. (1998). Nuclear lamins: their structure, assembly, and interactions. J. Struct. Biol. *122* , 42-66.

Su,R.C., Brown,K.E., Saaber,S., Fisher,A.G., Merkenschlager,M., and Smale,S.T. (2004). Dynamic assembly of silent chromatin during thymocyte maturation. Nat. Genet. *36*, 502-506.

Suau,P., Bradbury,E.M., and Baldwin,J.P. (1979). Higher-order structures of chromatin in solution. Eur. J. Biochem. *97*, 593-602.

Sugita,K., Yoshida,H., Matsumoto,M., and Matsutani,S. (1992). A novel compound, depudecin, induces production of transformation to the flat phenotype of NIH3T3 cells transformed by ras-oncogene. Biochem. Biophys. Res. Commun. *182*, 379-387.

Sullivan,G.J., Bridger,J.M., Cuthbert,A.P., Newbold,R.F., Bickmore,W.A., and McStay,B. (2001). Human acrocentric chromosomes with transcriptionally silent nucleolar organizer regions associate with nucleoli. EMBO J. *20*, 2867-2874.

Sullivan,K.F., Hechenberger,M., and Masri,K. (1994). Human CENP-A contains a histone H3 related histone fold domain that is required for targeting to the centromere. J. Cell Biol. *127*, 581-592.

Sun,F.L. and Elgin,S.C. (1999). Putting boundaries on silence. Cell *99*, 459-462.

Sun,H.B. and Yokota,H. (1999). Correlated positioning of homologous chromosomes in daughter fibroblast cells. Chromosome. Res. *7*, 603-610.

Sun,H.B., Shen,J., and Yokota,H. (2000). Size-dependent positioning of human chromosomes in interphase nuclei. Biophys. J. *79*, 184-190.

Sutherland,H.G., Mumford,G.K., Newton,K., Ford,L.V., Farrall,R., Dellaire,G., Caceres,J.F., and Bickmore,W.A. (2001). Large-scale identification of mammalian proteins localized to nuclear sub-compartments. Hum. Mol. Genet. *10*, 1995-2011.

Tachibana,M., Sugimoto,K., Fukushima,T., and Shinkai,Y. (2001). Set domain-containing protein, G9a, is a novel lysine-preferring mammalian histone methyltransferase with hyperactivity and specific selectivity to lysines 9 and 27 of histone H3. J. Biol. Chem. *276*, 25309-25317.

Tachibana,M., Sugimoto,K., Nozaki,M., Ueda,J., Ohta,T., Ohki,M., Fukuda,M., Takeda,N., Niida,H., Kato,H., and Shinkai,Y. (2002). G9a histone methyltransferase plays a dominant role in euchromatic histone H3 lysine 9 methylation and is essential for early embryogenesis. Genes Dev. *16*, 1779-1791.

Taddei,A., Roche,D., Sibarita,J.B., Turner,B.M., and Almouzni,G. (1999). Duplication and maintenance of heterochromatin domains. J. Cell Biol. *147*, 1153-1166.

Taddei,A., Maison,C., Roche,D., and Almouzni,G. (2001). Reversible disruption of pericentric heterochromatin and centromere function by inhibiting deacetylases. Nat. Cell Biol. *3*, 114-120.

Taddei,A., Hediger,F., Neumann,F.R., Bauer,C., and Gasser,S.M. (2004). Separation of silencing from perinuclear anchoring functions in yeast Ku80, Sir4 and Esc1 proteins. EMBO J. *23*, 1301-1312.

Taddei,A. and Gasser,S.M. (2004). Multiple pathways for telomere tethering: functional implications of subnuclear position for heterochromatin formation. Biochim. Biophys. Acta *1677*, 120-128.

Taddei,A., Gartenberg,M.R., Neumann,F.R., Hediger,F., and Gasser,S.M. (2005). Multiple pathways tether telomeres and silent chromatin at the nuclear periphery: functional implications for sir-mediated repression. Novartis. Found. Symp. *264*, 140-156.

Tajbakhsh,J., Luz,H., Bornfleth,H., Lampel,S., Cremer,C., and Lichter,P. (2000). Spatial distribution of GC- and AT-rich DNA sequences within human chromosome territories. Exp. Cell Res. *255*, 229-237.

Takami,Y. and Nakayama,T. (2000). N-terminal region, C-terminal region, nuclear export signal, and deacetylation activity of histone deacetylase-3 are essential for the viability of the DT40 chicken B cell line. J. Biol. Chem. *275*, 16191-16201.

Talbert,P.B., LeCiel,C.D., and Henikoff,S. (1994). Modification of the Drosophila heterochromatic mutation brownDominant by linkage alterations. Genetics *136*, 559-571.

Talbert,P.B. and Henikoff,S. (2000). A reexamination of spreading of position-effect variegation in the white-roughest region of Drosophila melanogaster. Genetics *154*, 259-272.

Tamaru,H. and Selker,E.U. (2001). A histone H3 methyltransferase controls DNA methylation in Neurospora crassa. Nature *414*, 277-283.

Tanabe,H., Muller,S., Neusser,M., von Hase,J., Calcagno,E., Cremer,M., Solovei,I., Cremer,C., and Cremer,T. (2002). Evolutionary conservation of chromosome territory arrangements in cell nuclei from higher primates. Proc. Natl. Acad. Sci. U. S. A *99*, 4424-4429.

Tanabe,H., Habermann,F.A., Solovei,I., Cremer,M., and Cremer,T. (2002). Non-random radial arrangements of interphase chromosome territories: evolutionary considerations and functional implications. Mutat. Res. *504*, 37-45.

Tanabe,H., Kupper,K., Ishida,T., Neusser,M., and Mizusawa,H. (2005). Inter- and intra-specific gene-density-correlated radial chromosome territory arrangements are conserved in Old World monkeys. Cytogenet. Genome Res. *108*, 255-261.

Tanaka,T.S., Kunath,T., Kimber,W.L., Jaradat,S.A., Stagg,C.A., Usuda,M., Yokota,T., Niwa,H., Rossant,J., and Ko,M.S. (2002). Gene expression profiling of embryo-derived stem cells reveals candidate genes associated with pluripotency and lineage specificity. Genome Res. *12*, 1921-1928.

Tariq,M., Saze,H., Probst,A.V., Lichota,J., Habu,Y., and Paszkowski,J. (2003). Erasure of CpG methylation in Arabidopsis alters patterns of histone H3 methylation in heterochromatin. Proc. Natl. Acad. Sci. U. S. A *100*, 8823-8827.

Tate,P., Lee,M., Tweedie,S., Skarnes,W.C., and Bickmore,W.A. (1998). Capturing novel mouse genes encoding chromosomal and other nuclear proteins. J. Cell Sci. *111 (Pt 17)*, 2575-2585.

Taunton,J., Hassig,C.A., and Schreiber,S.L. (1996). A mammalian histone deacetylase related to the yeast transcriptional regulator Rpd3p. Science *272*, 408-411.

Tazi,J. and Bird,A. (1990). Alternative chromatin structure at CpG islands. Cell *60*, 909-920.

Tham,W.H., Wyithe,J.S., Ko,F.P., Silver,P.A., and Zakian,V.A. (2001). Localization of yeast telomeres to the nuclear periphery is separable from transcriptional repression and telomere stability functions. Mol. Cell *8*, 189-199.

Thoma,F., Koller,T., and Klug,A. (1979). Involvement of histone H1 in the organization of the nucleosome and of the salt-dependent superstructures of chromatin. J. Cell Biol. *83*, 403-427.

Thomsen,D.R., Stenberg,R.M., Goins,W.F., and Stinski,M.F. (1984). Promoter-regulatory region of the major immediate early gene of human cytomegalovirus. Proc. Natl. Acad. Sci. U. S. A *81*, 659-663.

Tie,F., Furuyama,T., Prasad-Sinha,J., Jane,E., and Harte,P.J. (2001). The Drosophila Polycomb Group proteins ESC and E(Z) are present in a complex containing the histone-binding protein p55 and the histone deacetylase RPD3. Development *128*, 275-286.

Tolhuis,B., Palstra,R.J., Splinter,E., Grosveld,F., and de Laat,W. (2002). Looping and interaction between hypersensitive sites in the active beta-globin locus. Mol. Cell *10*, 1453-1465.

Tomschik,M., Karymov,M.A., Zlatanova,J., and Leuba,S.H. (2001). The archaeal histone-fold protein HMf organizes DNA into bona fide chromatin fibers. Structure *9*, 1201-1211.

Tong,J.K., Hassig,C.A., Schnitzler,G.R., Kingston,R.E., and Schreiber,S.L. (1998). Chromatin deacetylation by an ATP-dependent nucleosome remodelling complex. Nature *395*, 917-921.

Tran,H.G., Steger,D.J., Iyer,V.R., and Johnson,A.D. (2000). The chrome domain protein Chd1p from budding yeast is an ATP-dependent chromatin-modifying factor. EMBO J. *19*, 2323-2331.

Tsiftsoglou,A.S. and Wong,W. (1985). Molecular and cellular mechanisms of leukemic hemopoietic cell differentiation: an analysis of the Friend system. Anticancer Res. *5*, 81-99.

Tumbar,T. and Belmont,A.S. (2001). Interphase movements of a DNA chromosome region modulated by VP16 transcriptional activator. Nature Cell Biology *3*, 134-139.

Turner,B.M. (1991). Histone acetylation and control of gene expression. J. Cell Sci. *99 (Pt 1)*, 13-20.

Vakoc,C.R., Mandat,S.A., Olenchock,B.A., and Blobel,G.A. (2005). Histone H3 lysine 9 methylation and HP1gamma are associated with transcription elongation through mammalian chromatin. Mol. Cell *19*, 381-391.

Van der Vlag,J. and Otte,A.P. (1999). Transcriptional repression mediated by the human polycomb-group protein EED involves histone deacetylation. Nat. Genet. *23*, 474-478.

van Leeuwen,F., Gafken,P.R., and Gottschling,D.E. (2002). Dot1p modulates silencing in yeast by methylation of the nucleosome core. Cell *109*, 745-756.

Vaughan,A., Alvarez-Reyes,M., Bridger,J.M., Broers,J.L., Ramaekers,F.C., Wehnert,M., Morris,G.E., Whitfield,W.G.F., and Hutchison,C.J. (2001). Both emerin and lamin C depend on lamin A for localization at the nuclear envelope. J. Cell Sci. *114*, 2577-2590.

Vazquez,J., Belmont,A.S., and Sedat,J.W. (2001). Multiple regimes of constrained chromosome motion are regulated in the interphase Drosophila nucleus. Curr. Biol. *11*, 1227-1239.

Vazquez,J., Belmont,A.S., and Sedat,J.W. (2002). The dynamics of homologous chromosome pairing during male Drosophila meiosis. Curr. Biol. *12*, 1473-1483.

Vecerova,J., Koberna,K., Malinsky,J., Soutoglou,E., Sullivan,T., Stewart,C.L., Raska,I., and Misteli,T. (2004). Formation of nuclear splicing factor compartments is independent of lamins A/C. Mol. Biol. Cell *15*, 4904-4910.

Verdel,A., Jia,S.T., Gerber,S., Sugiyama,T., Gygi,S., Grewal,S.I.S., and Moazed,D. (2004). RNAi-mediated targeting of heterochromatin by the RITS complex. Science *303*, 672-676.

Verschure,P.J., van,D.K., I, Manders,E.M., and van Driel,R. (1999). Spatial relationship between transcription sites and chromosome territories. J. Cell Biol. *147*, 13-24.

Verschure,P.J., van,D.K., I, Manders,E.M., Hoogstraten,D., Houtsmuller,A.B., and van Driel,R. (2003). Condensed chromatin domains in the mammalian nucleus are accessible to large macromolecules. EMBO Rep. *4*, 861-866.

Vignali,M., Steger,D.J., Neely,K.E., and Workman,J.L. (2000). Distribution of acetylated histones resulting from Gal4-VP16 recruitment of SAGA and NuA4 complexes. EMBO J. *19*, 2629-2640.

Visser,A.E., Eils,R., Jauch,A., Little,G., Bakker,P.J., Cremer,T., and Aten,J.A. (1998). Spatial distributions of early and late replicating chromatin in interphase chromosome territories. Exp. Cell Res. *243*, 398-407.

Visser,A.E. and Aten,J.A. (1999). Chromosomes as well as chromosomal subdomains constitute distinct units in interphase nuclei. J. Cell Sci. *112 (Pt 19)*, 3353-3360.

Volpe,T., Schramke,V., Hamilton,G.L., White,S.A., Teng,G., Martienssen,R.A., and Allshire,R.C. (2003). RNA interference is required for normal centromere function in fission yeast. Chromosome Research *11*, 137-146.

Volpe,T.A., Kidner,C., Hall,I.M., Teng,G., Grewal,S.I.S., and Martienssen,R.A. (2002). Regulation of heterochromatic silencing and histone H3 lysine-9 methylation by RNAi. Science *297*, 1833-1837.

Volpi,E.V., Chevret,E., Jones,T., Vatcheva,R., Williamson,J., Beck,S., Campbell,R.D., Goldsworthy,M., Powis,S.H., Ragoussis,J., Trowsdale,J., and Sheer,D. (2000). Large-scale chromatin organization of the major histocompatibility complex and other regions of human chromosome 6 and its response to interferon in interphase nuclei. J. Cell Sci. *113 (Pt 9)*, 1565-1576.

Wade,P.A., Gegonne,A., Jones,P.L., Ballestar,E., Aubry,F., and Wolffe,A.P. (1999). Mi-2 complex couples DNA methylation to chromatin remodelling and histone deacetylation. Nat. Genet. *23*, 62-66.

Wakimoto,B.T. (1998). Beyond the nucleosome: Epigenetic aspects of position-effect variegation in Drosophila. Cell *93*, 321-324.

Walter,J., Schermelleh,L., Cremer,M., Tashiro,S., and Cremer,T. (2003). Chromosome order in HeLa cells changes during mitosis and early G1, but is stably maintained during subsequent interphase stages. J. Cell Biol. *160*, 685-697.

Wang,A., Kurdistani,S.K., and Grunstein,M. (2002). Requirement of Hos2 histone deacetylase for gene activity in yeast. Science *298*, 1412-1414.

Wang,H., Huang,Z.Q., Xia,L., Feng,Q., Erdjument-Bromage,H., Strahl,B.D., Briggs,S.D., Allis,C.D., Wong,J., Tempst,P., and Zhang,Y. (2001). Methylation of histone H4 at arginine 3 facilitating transcriptional activation by nuclear hormone receptor. Science *293*, 853-857.

Wang,H., An,W., Cao,R., Xia,L., Erdjument-Bromage,H., Chatton,B., Tempst,P., Roeder,R.G., and Zhang,Y. (2003). mAM facilitates conversion by ESET of dimethyl to trimethyl lysine 9 of histone H3 to cause transcriptional repression. Mol. Cell *12*, 475-487.

Wang,J., Shiels,C., Sasieni,P., Wu,P.J., Islam,S.A., Freemont,P.S., and Sheer,D. (2004). Promyelocytic leukemia nuclear bodies associate with transcriptionally active genomic regions. JCB *164*, 515-526.

Wang,Y., Wysocka,J., Sayegh,J., Lee,Y.H., Perlin,J.R., Leonelli,L., Sonbuchner,L.S., McDonald,C.H., Cook,R.G., Dou,Y., Roeder,R.G., Clarke,S., Stallcup,M.R., Allis,C.D., and Coonrod,S.A. (2004). Human PAD4 regulates histone arginine methylation levels via demethylimination. Science *306*, 279-283.

Wang,Z.F., Sirotkin,A.M., Buchold,G.M., Skoultchi,A.I., and Marzluff,W.F. (1997). The mouse histone H1 genes: gene organization and differential regulation. J. Mol. Biol. *271*, 124-138.

Wansink,D.G., Schul,W., van,D.K., I, van Steensel,B., van Driel,R., and de Jong,L. (1993). Fluorescent labeling of nascent RNA reveals transcription by RNA polymerase II in domains scattered throughout the nucleus. J. Cell Biol. *122*, 283-293.

Wansink,D.G., Manders,E.E., van,D.K., I, Aten,J.A., van Driel,R., and de Jong,L. (1994). RNA polymerase II transcription is concentrated outside replication domains throughout S-phase. J. Cell Sci. *107 (Pt 6)*, 1449-1456.

Wansink,D.G., Sibon,O.C., Cremers,F.F., van Driel,R., and de Jong,L. (1996). Ultrastructural localization of active genes in nuclei of A431 cells. J. Cell Biochem. *62*, 10-18.

Warner,J.R. (1989). Synthesis of ribosomes in Saccharomyces cerevisiae. Microbiol. Rev. *53*, 256-271.

Warner,J.R. (1990). The nucleolus and ribosome formation. Curr. Opin. Cell Biol. *2*, 521-527.

Wasserman,S. (1998). FH proteins as cytoskeletal organizers. Trends Cell Biol. *8*, 111-115.

Watanabe,S., Ichimura,T., Fujita,N., Tsuruzoe,S., Ohki,I., Shirakawa,M., Kawasuji,M., and Nakao,M. (2003). Methylated DNA-binding domain 1 and methylpurine-DNA glycosylase link transcriptional repression and DNA repair in chromatin. Proc. Natl. Acad. Sci. U. S. A *100*, 12859-12864.

Waterham,H.R., Koster,J., Mooyer,P., Noort,G.G., Kelley,R.I., Wilcox,W.R., Wanders,R.J., Hennekam,R.C., and Oosterwijk,J.C. (2003). Autosomal recessive HEM/Greenberg skeletal dysplasia is caused by 3 beta-hydroxysterol delta 14-reductase deficiency due to mutations in the lamin B receptor gene. Am. J. Hum. Genet. *72*, 1013-1017.

Weierich,C., Brero,A., Stein,S., von Hase,J., Cremer,C., Cremer,T., and Solovei,I. (2003). Three-dimensional arrangements of centromeres and telomeres in nuclei of human and murine lymphocytes. Chromosome. Res. *11*, 485-502.

Weintraub,M. (1994). Histamine H-1 Antagonists. New England Journal of Medicine *331*, 1019.

Weis,K., Rambaud,S., Lavau,C., Jansen,J., Carvalho,T., Carmo-Fonseca,M., Lamond,A., and Dejean,A. (1994). Retinoic acid regulates aberrant nuclear localization of PML-RAR alpha in acute promyelocytic leukemia cells. Cell *76*, 345-356.

West,A.G., Gaszner,M., and Felsenfeld,G. (2002). Insulators: many functions, many mechanisms. Genes & Development *16*, 271-288.

West,M.H. and Bonner,W.M. (1980). Histone 2B can be modified by the attachment of ubiquitin. Nucleic Acids Res. *8*, 4671-4680.

Widom,J. and Klug,A. (1985). Structure of the 300A chromatin filament: X-ray diffraction from oriented samples. Cell *43*, 207-213.

Wielckens,K., Schmidt,A., George,E., Bredehorst,R., and Hilz,H. (1982). DNA fragmentation and NAD depletion. Their relation to the turnover of endogenous mono(ADP-ribosyl) and poly(ADP-ribosyl) proteins. J. Biol. Chem. *257*, 12872-12877.

Wierzbicki,A.T. and Jerzmanowski,A. (2005). Suppression of histone H1 genes in Arabidopsis results in heritable developmental defects and stochastic changes in DNA methylation. Genetics *169*, 997-1008.

Williams,R.R. and Fisher,A.G. (2003). Chromosomes, positions please! Nat. Cell Biol. *5*, 388-390.

Wirbelauer,C., Bell,O., and Schubeler,D. (2005). Variant histone H3.3 is deposited at sites of nucleosomal displacement throughout transcribed genes while active histone modifications show a promoter-proximal bias. Genes Dev. *19*, 1761-1766.

Wiren,M., Silverstein,R.A., Sinha,I., Walfridsson,J., Lee,H.M., Laurenson,P., Pillus,L., Robyr,D., Grunstein,M., and Ekwall,K. (2005). Genomewide analysis of nucleosome density histone acetylation and HDAC function in fission yeast. EMBO J. *24*, 2906-2918.

Wolffe,A.P., Khochbin,S., and Dimitrov,S. (1997). What do linker histones do in chromatin? Bioessays *19*, 249-255.

Wolffe,A.P. and Hayes,J.J. (1999). Chromatin disruption and modification. Nucleic Acids Res. *27*, 711-720.

Wong,A.K. and Rattner,J.B. (1988). Sequence organization and cytological localization of the minor satellite of mouse. Nucleic Acids Res. *16*, 11645-11661.

Wong,A.K., Biddle,F.G., and Rattner,J.B. (1990). The chromosomal distribution of the major and minor satellite is not conserved in the genus Mus. Chromosoma *99*, 190-195.

Wong,J., Patterton,D., Imhof,A., Guschin,D., Shi,Y.B., and Wolffe,A.P. (1998). Distinct requirements for chromatin assembly in transcriptional repression by thyroid hormone receptor and histone deacetylase. EMBO J. *17*, 520-534.

Woodcock,C.L., Frado,L.L., and Rattner,J.B. (1984). The higher-order structure of chromatin: evidence for a helical ribbon arrangement. J. Cell Biol. *99*, 42-52.

Woodcock,C.L. and Dimitrov,S. (2001). Higher-order structure of chromatin and chromosomes. Curr. Opin. Genet. Dev. *11*, 130-135.

Worcel,A. (1978). Molecular architecture of the chromatin fiber. Cold Spring Harb. Symp. Quant. Biol. *42 Pt 1*, 313-324.

Worman,H.J. and Courvalin,J.C. (2004). How do mutations in lamins A and C cause disease? J. Clin. Invest *113*, 349-351.

Wu,J., Carmen,A.A., Kobayashi,R., Suka,N., and Grunstein,M. (2001). HDA2 and HDA3 are related proteins that interact with and are essential for the activity of the yeast histone deacetylase HDA1. Proc. Natl. Acad. Sci. U. S. A *98*, 4391-4396.

Wydner,K.L., McNeil,J.A., Lin,F., Worman,H.J., and Lawrence,J.B. (1996). Chromosomal assignment of human nuclear envelope protein genes LMNA, LMNB1, and LBR by fluorescence in situ hybridization. Genomics *32*, 474-478.

Xu,G.L., Bestor,T.H., Bourc'his,D., Hsieh,C.L., Tommerup,N., Bugge,M., Hulten,M., Qu,X., Russo,J.J., and Viegas-Pequignot,E. (1999). Chromosome instability and immunodeficiency syndrome caused by mutations in a DNA methyltransferase gene. Nature *402*, 187-191.

Xu,Q.H., Li,M., Adams,J., and Cai,H.N. (2004). Nuclear location of a chromatin insulator in Drosophila melanogaster. J. Cell Sci. *117*, 1025-1032.

Yamamoto,K., Sonoda,M., Inokuchi,J., Shirasawa,S., and Sasazuki,T. (2004). Polycomb group suppressor of zeste 12 links heterochromatin protein 1 alpha and enhancer of zeste 2. J. Biol. Chem. *279*, 401-406.

Yang,L., Mei,Q., Zielinska-Kwiatkowska,A., Matsui,Y., Blackburn,M.L., Benedetti,D., Krumm,A.A., Taborsky,G.J., Jr., and Chansky,H.A. (2003). An ERG (ets-related gene)-associated histone methyltransferase interacts with histone deacetylases 1/2 and transcription co-repressors mSin3A/B. Biochem. J. *369*, 651-657.

Ye,Q. and Worman,H.J. (1996). Interaction between an integral protein of the nuclear envelope inner membrane and human chromodomain proteins homologous to Drosophila HP1. J. Biol. Chem. *271*, 14653-14656.

Ye,Q., Callebaut,I., Courvalin,J.C., and Worman,H.J. (1996). Structure-function analysis of the binding of chromosomal HP1 proteins to the nucleoplasmic domain of inner nuclear membrane protein LBR. Molecular Biology of the Cell *7*, 548.

Ying,Q.L., Stavridis,M., Griffiths,D., Li,M., and Smith,A. (2003). Conversion of embryonic stem cells into neuroectodermal precursors in adherent monoculture. Nat. Biotechnol. *21*, 183-186.

Yoshida,M., Kijima,M., Akita,M., and Beppu,T. (1990). Potent and specific inhibition of mammalian histone deacetylase both in vivo and in vitro by trichostatin A. J. Biol. Chem. *265*, 17174-17179.

Yu,X. and Gabriel,A. (2003). Ku-dependent and Ku-independent end-joining pathways lead to chromosomal rearrangements during double-strand break repair in Saccharomyces cerevisiae. Genetics *163*, 843-856.

Yusufzai,T.M., Tagami,H., Nakatani,Y., and Felsenfeld,G. (2004). CTCF tethers an insulator to subnuclear sites, suggesting shared insulator mechanisms across species. Mol. Cell *13*, 291-298.

Zastrow,M.S., Vlcek,S., and Wilson,K.L. (2004). Proteins that bind A-type lamins: integrating isolated clues. J. Cell Sci. *117*, 979-987.

Zentgraf,H. and Franke,W.W. (1984). Differences of supranucleosomal organization in different kinds of chromatin: cell type-specific globular subunits containing different numbers of nucleosomes. J. Cell Biol. *99*, 272-286.

Zhang,C.C. and Bienz,M. (1992). Segmental determination in Drosophila conferred by hunchback (hb), a repressor of the homeotic gene Ultrabithorax (Ubx). Proc. Natl. Acad. Sci. U. S. A *89*, 7511-7515.

Zhang,Y., Iratni,R., Erdjument-Bromage,H., Tempst,P., and Reinberg,D. (1997). Histone deacetylases and SAP18, a novel polypeptide, are components of a human Sin3 complex. Cell *89*, 357-364.

Zhang,Y., Ng,H.H., Erdjument-Bromage,H., Tempst,P., Bird,A., and Reinberg,D. (1999). Analysis of the NuRD subunits reveals a histone deacetylase core complex and a connection with DNA methylation. Genes Dev. *13*, 1924-1935.

Zhang,Y. and Reinberg,D. (2001). Transcription regulation by histone methylation: interplay between different covalent modifications of the core histone tails. Genes Dev. *15*, 2343-2360.

Zhang,Y. and Dufau,M.L. (2002). Silencing of transcription of the human luteinizing hormone receptor gene by histone deacetylase-mSin3A complex. J. Biol. Chem. *277*, 33431-33438.

Zhao,K., Hart,C.M., and Laemmli,U.K. (1995). Visualization of chromosomal domains with boundary element-associated factor BEAF-32. Cell *81*, 879-889.

Zhao,K., Harel,A., Stuurman,N., Guedalia,D., and Gruenbaum,Y. (1996). Binding of matrix attachment regions to nuclear lamin is mediated by the rod domain and depends on the lamin polymerization state. FEBS Lett. *380*, 161-164.

Zheng,R.L., Ghirlando,R., Lee,M.S., Mizuuchi,K., Krause,M., and Craigie,R. (2000). Barrier-to-autointegration factor (BAF) bridges DNA in a discrete, higher-order nucleoprotein complex. Proceedings of the National Academy of Sciences of the United States of America *97*, 8997-+.

Zimber,A., Nguyen,Q.D., and Gespach,C. (2004). Nuclear bodies and compartments: functional roles and cellular signalling in health and disease. Cell Signal. *16*, 1085-1104.

Zink,D. and Cremer,T. (1998). Cell nucleus: chromosome dynamics in nuclei of living cells. Curr. Biol. *8*, R321-R324.

Zink,D., Cremer,T., Saffrich,R., Fischer,R., Trendelenburg,M.F., Ansorge,W., and Stelzer,E.H. (1998). Structure and dynamics of human interphase chromosome territories in vivo. Hum. Genet. *102*, 241-251.

Zink,D., Bornfleth,H., Visser,A., Cremer,C., and Cremer,T. (1999). Organization of early and late replicating DNA in human chromosome territories. Exp. Cell Res. *247*, 176-188.

Zink,D., Amaral,M.D., Englmann,A., Lang,S., Clarke,L.A., Rudolph,C., Alt,F., Luther,K., Braz,C., Sadoni,N., Rosenecker,J., and Schindelhauer,D. (2004). Transcription-dependent spatial arrangements of CFTR and adjacent genes in human cell nuclei. J. Cell Biol. *166*, 815-825.

Zirbel,R.M., Mathieu,U.R., Kurz,A., Cremer,T., and Lichter,P. (1993). Evidence for a nuclear compartment of transcription and splicing located at chromosome domain boundaries. Chromosome.Res. *1*, 93-106.

Zlatanova,J. and van Holde,K. (1998). Linker histones versus HMG1/2: a struggle for dominance? Bioessays *20*, 584-588.

Zorn,C., Cremer,C., Cremer,T., and Zimmer,J. (1979). Unscheduled DNA synthesis after partial UV irradiation of the cell nucleus. Distribution in interphase and metaphase. Exp. Cell Res. *124*, 111-119.

APPENDIX 1

CONSTRUCTION OF VECTORS

A.1 pGTXN6

To insert a Lac array into pGT1, a linker sequence containing XhoI and NotI restriction sites was inserted into the HindIII site of pGT1 to create the plasmid, pGTXN. This HindIII site was previously used to linearise the plasmid for transfection since it is well away from the splice acceptor and β–geo (figure A.1.a). XhoI and NotI sites are not present anywhere else in pGT1XN making them unique sites to linearise the vector for transfection. The XhoI and NotI sites were also used to ligate in 16 copies of LacO seqeuence to make the plasmid pGTXN6. This LacO array was taken from the plasmid, pJRC35, previously constructed in the lab (figure A.1.b) (Chubb et al.., 2002).

A.2 pCAGASIZ73/74

To clone the anchor transcript (myc-tag-NLS-LacI- emerin/LAP2β) into the pCAGASIZ backbone, the emerin anchor was cloned first and this then used to subsequently clone the LAP2β anchor. Initially the alkaline phosphatase was cut out of the pCAGASIZ vector using NotI and XhoI restriction sites and the vector religated. This new vector, pCAGASIZXN, and the pJRC73 vector were then digested with XhoI and ClaI. The emerin fragment, and the pCAGASIZXN backbone fragment were isolated from the other digestion products by gel electrophoresis and ligated together to create pCAGASIZ73 (figure A.2.a). The LAP2β anchor was cloned into pCAGASIZ73 by digestion of the backbone by ClaI. The linearised vector then had its 3' recessed ends filled in with Kleenow, before digestion with MluI. The LAP2β fragment from pJRC74 was then obtained by digestion with MluI and SmaI and ligated into the pCAGASIZ73 backbone (figure A.2.b). Both vectors were sequenced before transfection.

A.3 pd1EGFP-N1-Lac

The EGFP encoding region of pd1EGFP-N1 was ligated into pJRC49 which contains a 128mer Lac operator array to create the plasmid pd1EGFP-N1-Lac (figure A.3). To do this, pd1EGFP-N1 was digested with the enzyme AflII, and the 3' recessed ends filled in Kleenow. A second digest with the restriction enzymes StuI and AlwN1 then created an EGFP encoding DNA fragment 2.2kb in length which was isolated from the other digest products by gel electrophoresis. pJRC49 was prepared for ligation to the EGFP fragment by digestion with the restriction enzymes SapI and AlwN1. A 9kb fragment containing the Lac operator array and Amp gene was gel purified and ligated to the d1EGFP fragment from pd1EGFP-N1.

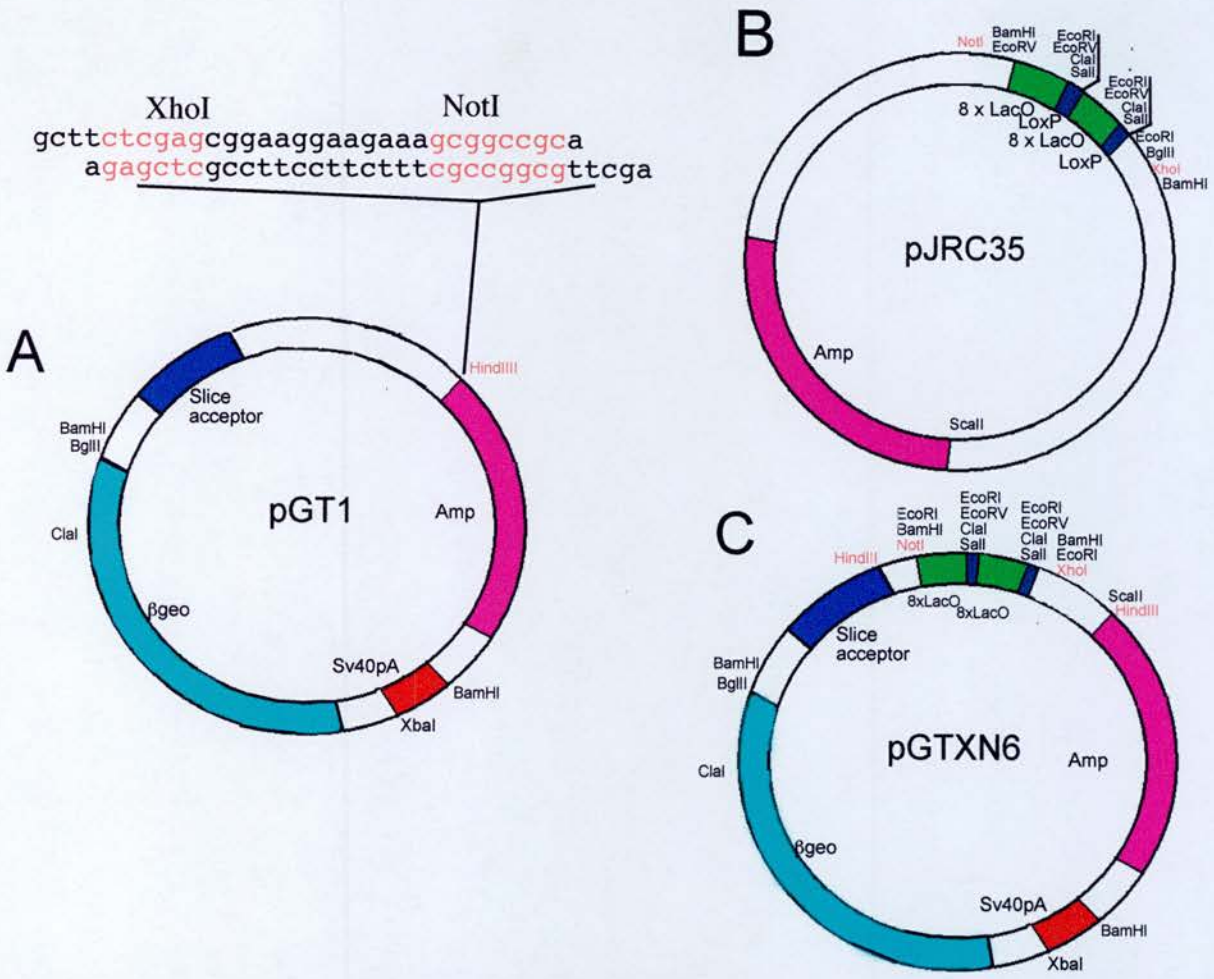

Figure A.1: Creation of the vector pGTXN6, used to put Lac operator arrays into active genes. A) The original pGT1 vector (Sutherland et al., 2001) and the linker sequence added to pGT1 via the Hind III site. This contained NotI and XhoI sites, not present elsewhere in pGT1.B) The Lac operator array from pJRC35 was digested out using NotI and XhoI sites. This was then ligated into pGT1 which had also been disgested with XhoI and NotI via the linker sequence, to create pGTXN6 (C).

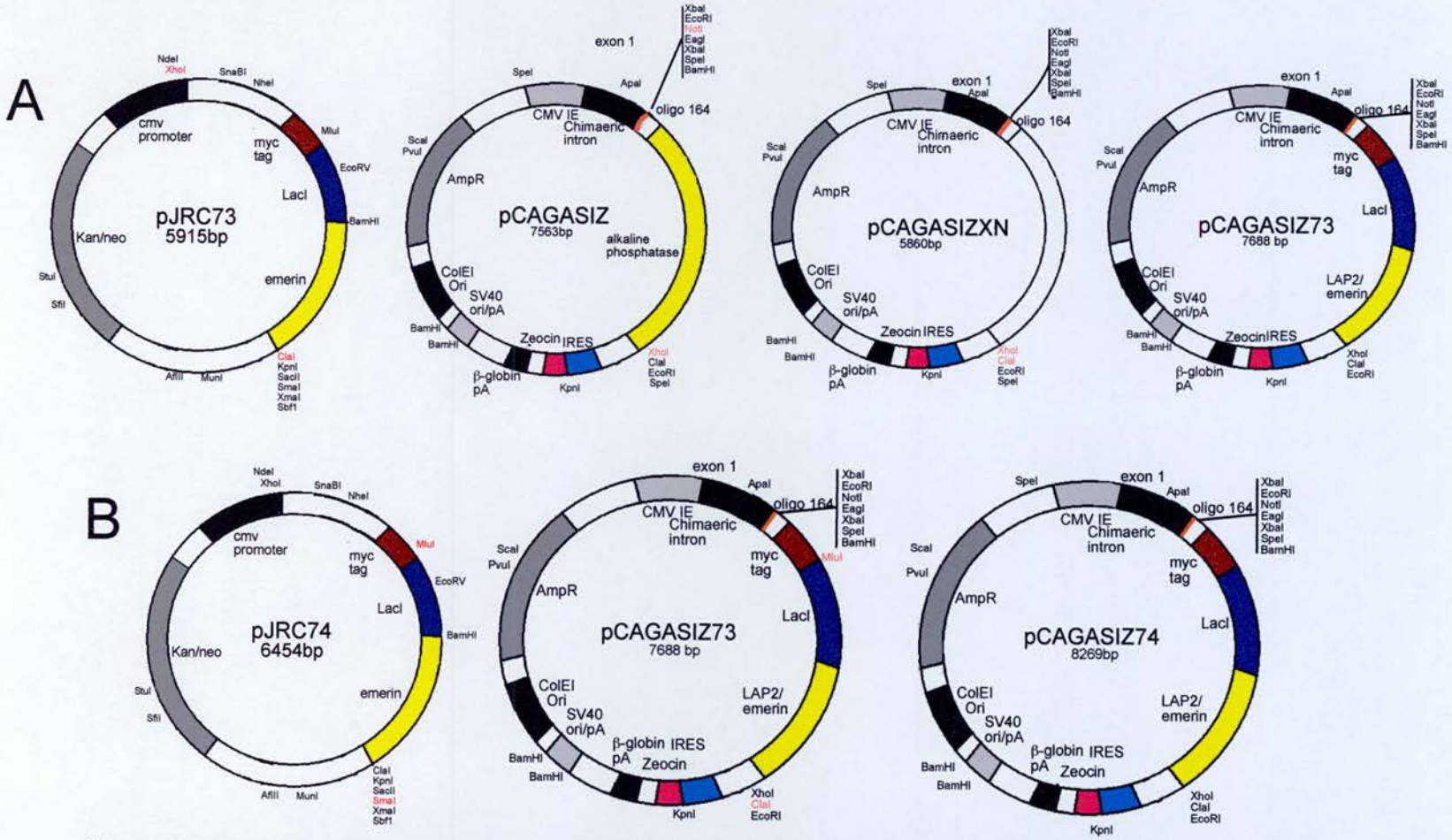

Figure A.2: Plasmids encoding anchoring proteins. A) the original plasmid pCAGASIZ was disgested via XhoI and NotI and religated to remove the alkaline phosphatase transcript. The second plasmid pCAGASIZXN was then digested via XhoI and ClaI as was pJRC73. The appropriate fragments from both vectors were then ligated together to make pCAGASIZ73, encoding the emerin anchor. B)To create pCAGASIZ74, pCAGASIZ73 was digested via ClaI, and MluI and pJRC74 via SmaI and MluI. The appropriate fragments were then ligated to create pCAGASIZ74. All sites used in cloning are shown in red.

Figure A.3: Vectors used to investigate the effect of nuclear position on gene regulation A) Schematics of the original pd1EGFP-N1 vector and the reporter vector pd1EGFP-N1-Lac containing a Lac operator array with 128 copies of the LacO sequence and t he transgene pd1EGFP-N1.Restriction digest sites in red were those used to clone pd1EGFP-N1 into the Lac Array plasmid, to create pd1EGFP-N1Lac.

APPENDIX 2

The radial position of chromatin is not inherited through mitosis but is established *de novo* in early G1

Current Biology, Vol. 14, 166–172, January 20, 2004, ©2004 Elsevier Science Ltd. All rights reserved. DOI 10.1016/j.cub.2003.12.024

The Radial Positioning of Chromatin Is Not Inherited through Mitosis but Is Established De Novo in Early G1

Inga Thomson,[1] Susan Gilchrist,[1]
Wendy A. Bickmore,[1,*] and Jonathan R. Chubb[1,2]
[1]Medical Research Council
Human Genetics Unit
Edinburgh EH4 2XU
United Kingdom

Summary

The organization of chromatin in the nucleus is nonrandom. Different genomic regions tend to reside in preferred nuclear locations, relative to radial position and nuclear compartments. Several lines of evidence support a role for chromatin localization in the regulation of gene expression [1–3]. Therefore, a key problem is how the organization of chromatin is established and maintained in dividing cell populations. There is controversy about the extent to which chromatin organization is inherited from mother to daughter nucleus [4–8]. We have used time-lapse microscopy to track specific human loci after exit from mitosis. In comparison to later stages of interphase, we detect increased chromatin mobility during the first 2 hr of G1, and during this period association of loci with nuclear compartments is both gained and lost. Although chromatin in daughter nuclei has a rough symmetry in its spatial distribution, we show, for the first time, that the association of loci with nuclear compartments displays significant asymmetry between daughter nuclei and therefore cannot be inherited from the mother nucleus. We conclude that the organization of chromatin in the nucleus is not passed down precisely from one cell to its descendents but is more plastic and becomes refined during early G1.

Results and Discussion

Enhanced Chromatin Motion in the Nuclei of Early G1 Human Cells

An important question in nuclear structure is how the interphase organization of chromatin is established. On one hand, chromosome position could be accurately inherited from the mother nucleus via the congression of chromosomes onto the metaphase plate and their ordered separation at anaphase. At the other extreme, chromosome order could be scrambled from one cell generation to the next, but the distinctive organization of chromosomes within the nucleus (i.e., their radial organization and/or association with nuclear compartments) could be reestablished de novo at the beginning of each cell cycle. Somewhere in between these two extremes, mitosis could preserve some, but not all, aspects of chromosome position, with chromatin repositioning also occurring in G1. Recent studies [4, 5] have addressed this problem by the labeling of large chromatin domains, but they arrive at different conclusions [reviewed in 6–8,]. By photobleaching GFP variant-tagged histone H2B in chromatin at prophase at different angles relative to the plane of chromosome separation, Gerlich et al. [5] present data displaying conservation of bleach patterns into daughter nuclei and conclude that chromosome architecture is not randomized during mitosis. In contrast, Walter et al. [4] show some dispersal of labeled regions and reorganization of chromatin domains as cells proceed from G2 through mitosis and into G1.

Neither study assessed the inheritance of chromatin position relative to radial position or nuclear compartments (such as the nucleolus and the nuclear periphery) linked to the control of gene expression. Addressing this problem requires knowledge of the identity of the labeled chromatin. We have therefore approached this question by tracking the dynamics and spatial distribution of defined GFP-tagged loci from the completion of mitosis into newly forming daughter nuclei. We used human cell lines with lacO arrays inserted into cytologically determined genomic integration sites with different subnuclear distributions (Table S1 in the Supplemental Data available with this article online). The loci were visualized in living cells by expression of a GFP-LacI-NLS fusion protein [9]. We identified mitotic cells by their rounded morphology and by the redistribution of the background GFP-LacI-NLS staining to the entire cell in the absence of a nuclear membrane. The metaphase-anaphase transition is evidenced by the separation of tagged loci on sister chromatids (t = 0 in Figure 1). The start of G1 in daughter nuclei is indicated by the reconcentration of GFP-LacI-NLS into nuclei as the nuclear membrane is reformed (t = 10 in Figure 1). We quantified chromatin motion by measuring the distance (d) between the tagged loci every 10 min over a 2 hr period (Figure 2), the change in distance between each frame ($d - d_{t-1}$), and the change in distance over a time period relative to t = 0 (Δd) [9–11] (Table 1). Chromatin motion was mostly limited to small regions of the nuclear volume (the longest axis of interphase nuclei of 5p14 cells ranges from 15 to 25 μm) during early G1, indicating that the position of a locus is already considerably constrained as soon as the nuclear envelope is reformed.

The inter-locus distance (d) was often similar, but not identical, between daughter nuclei. The average value of d over the 2 hr time period was 5.1 and 7.6 μm for the 5p14 and 11q13 loci, respectively (n = 5 mitoses, 10 daughter nuclei), whereas the mean difference in the value of d between daughter nuclei at any time point was only 1.5 and 1.4 μm, respectively (standard deviations = 1.2 and 1.1 μm). This suggests that some organization of chromatin on the metaphase plate, when the sister chromatids were last close to each other, has been transmitted to daughter nuclei. However, we clearly see nonsymmetrical dynamic behavior of loci in early G1 daughter nuclei (e.g., 5p14 in Figure 2B). Also, the average and maximum values of both $d - d_{t-1}$ and

*Correspondence: w.bickmore@hgu.mrc.ac.uk
[2]Present address: Department of Anatomy and Structural Biology, Albert Einstein College of Medicine, 1300 Morris Park Avenue, The Bronx, New York 10461.

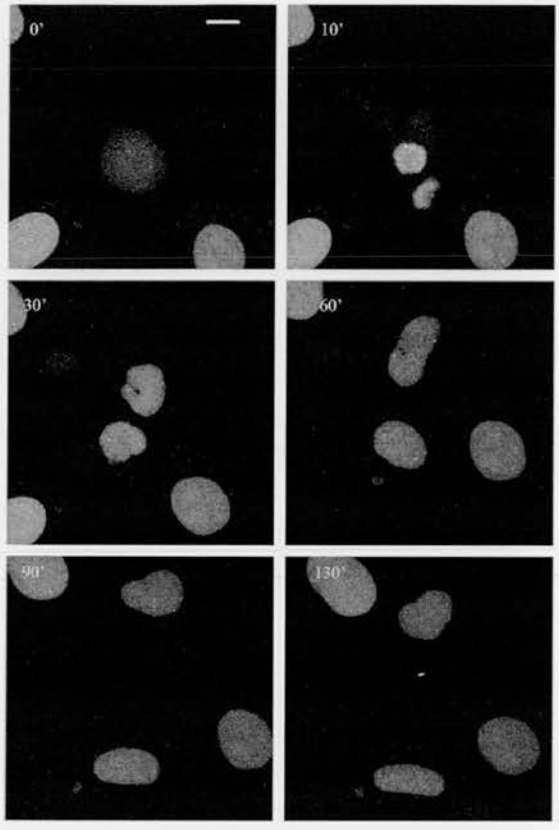

Figure 1. Tracking the Motion of Defined Loci during Early G1

Mitotic cells were identified by the dispersal of the GFP-LacI-NLS fusion throughout the entire cell volume in the absence of the nuclear envelope (0' frame). Confocal z stacks were captured at 10 min intervals for a 2 hr period after the completion of mitosis and are shown flattened to allow simultaneous visualization of all spots. Considerable changes in the distances separating the tagged loci in the newly formed daughter nuclei occur over time. Note the relative lack of chromatin motion in an interphase cell that has not just exited mitosis (top left) The scale bar represents 10 μm.

Δd during early G1 are larger than those detected at other stages of interphase (Figure 2 and Table 1). Our observations are consistent with other reports of enhanced motion of centromeres [12] and photobleached chromatin domains [4] during early G1.

It is unclear which events of G1 are responsible for the enhanced mobility. We found an approximately similar range of motion for the tagged 11q13 locus in early G1 cells that had exited mitosis in the presence of the transcriptional inhibitor 5,6-dichloro-D-ribofuranosylbenzimidazole (DRB) (Figure 2B). Therefore, chromatin motion in early G1 cells is not simply due to the recommencement of transcription after mitosis. In some cases, large increases in distance in early G1 may be due to nuclear morphogenesis [7]. For example, the increasing distance between the tagged loci in the bottom daughter nucleus of Figure 1A clearly parallels the expansion and elongation of this nucleus along the same axis. The other daughter nucleus goes through a similar process of expansion and elongation, but in this case, the two loci are not aligned along the axis of elongation, and the increase in distance between the spots is not so great. However, we do not detect a general increase in the distances separating loci in all early G1 nuclei over time, as would be expected if chromatin movements were just a passive consequence of nuclear expansion. Decreases in the distances between tagged loci are also visible during this period (Figure 2B). As we demonstrate below, regardless of the driving force for chromatin motion, active remodeling of chromatin position relative to nuclear compartments is occurring during early G1.

Interactions with Nuclear Compartments Are Established De Novo in Early G1

Individual lacO-tagged loci are restricted in their access to the total nuclear volume after chromosome separation, yet they display enhanced mobility that persists for at least 1–2 hr into G1 (Figures 1 and 2). To what extent do these factors contribute to positioning of loci relative to nuclear compartments? FISH studies have indicated nuclear repositioning of late replicating origins and human chromosome 18 to the nuclear periphery during early G1 [13, 14]. In addition, transient movements of a lacO array away from the nuclear periphery during early G1 have been observed [15, 16]. In living cells, photobleaching studies have not considered the distribution of specific chromosome regions relative to the nucleolus, nuclear envelope, or other nuclear compartments [4, 5]. We addressed this issue by looking at the acquisition of nuclear position for specific loci in early G1 daughter cells. The tagged 5p14 locus frequently locates in the nuclear interior but can also be found at the nuclear edge (Table S1). This could reflect different populations of cells with different, but heritable, locus radial position, or it could reflect stochastic repositioning of the locus after cell division. In the former case, both daughter nuclei should show similar locus radial position relative to the nuclear periphery; in the latter case, they need not. Our data support the latter conclusion. Figure 3A shows a z stack through two daughter 5p14 nuclei, taken 110 min after the completion of mitosis. In the left nucleus, both loci are far (>1 μm) from any nuclear edge (visible in the 1.0 and 2.0 μm z slices). In contrast, both loci in the right nucleus are more peripheral. The locus in the 4.0 μm z slice is visually inseparable from the edge of the nucleus, as defined by the background GFP-LacI-NLS signals. The other locus (6.0 μm z slice) is very close to, but not quite in contact with, the top of the nucleus (7.0 μm slice). Therefore, these two daughter nuclei have asymmetric radial organization of this locus. Of the mitoses studied for the 5p14 cell line, two out of five movies displayed asymmetry between daughters.

These observations were reproduced for another locus. Tagged 19q12 also distributes between nuclear domains. It is most often seen adjacent to the nucleolus but can also be found at the nuclear periphery (Table S1). Analysis of fixed two-cell clones of the 19q12 cell line reveals many daughter cells with nonidentical distributions of the locus with respect to these nuclear com-

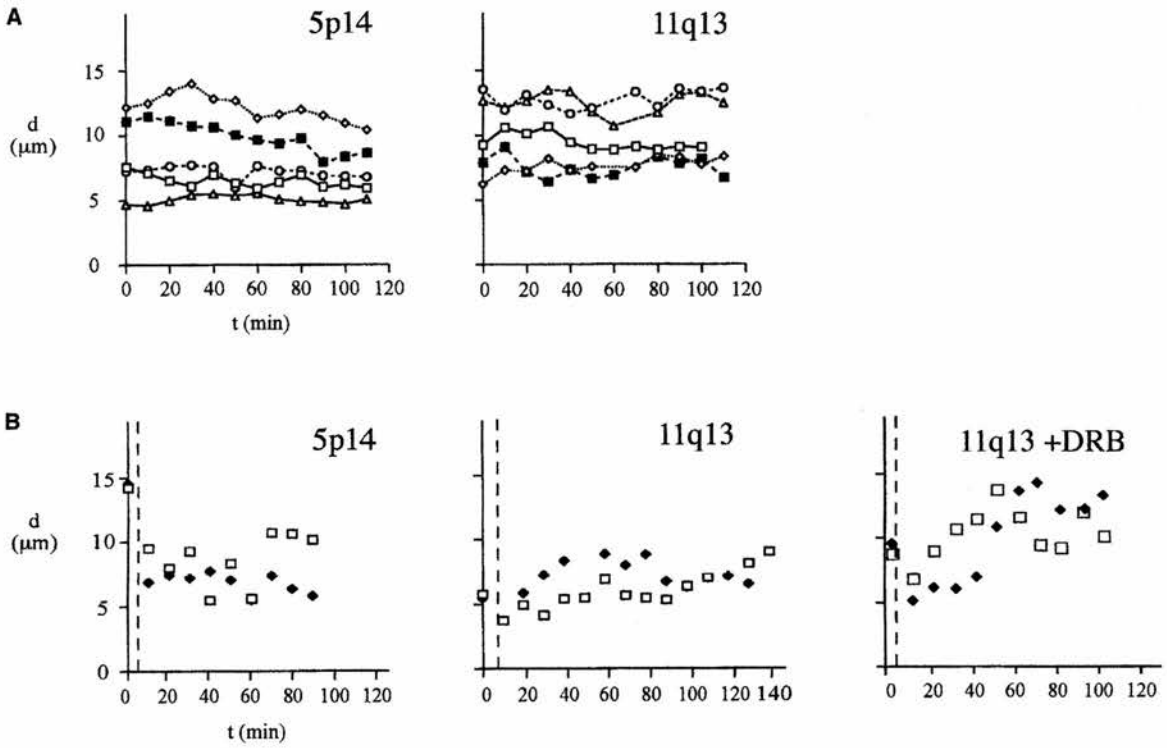

Figure 2. Long-Range Motion of Human Chromatin during Interphase and Early G1

(A) 3D distance (d) in μm between two spots for the 11q13 and 5p14 loci was measured at 10 min intervals over a 2 hr period, for five interphase nuclei each.

(B) d between two spots in both early G1 daughters (squares or diamonds) of a single mitotic cell after mitosis. Data for an example of the 5p14- and 11q13-tagged loci and for 11q13 cells treated with 50 μg/ml DRB are shown. A dashed line represents the metaphase-anaphase transition. Complete data are summarized in Table 1.

partments. In Figure 3B the locus in one daughter cell (left) is associated with the nuclear envelope. In its sibling cell, the locus is associated with the nucleolus. We extended these observations to a larger sample of fixed 5p14 and 19q12 two-cell clones (Figure 3C). A high frequency of differently organized daughters was seen for both loci. There is no statistically significant inheritance, from mother to daughter cells, of the association of the 19q12-tagged locus with nuclear compartments (Figure 3D). For the null hypothesis of no inheritance of nuclear position, the probability of a locus associating with a particular compartment is directly related to the population frequency of this association and is independent of the behavior of its sister locus in the other cell of the clone pair. The population frequencies for 19q12 association with the nuclear periphery, nucleolus, or nucleoplasm were 0.35, 0.46, and 0.19, respectively (See Table S1). Expected (E) values for the frequency of particular

Table 1. Parameters of Chromatin Dynamics in the Cell Cycle

		$d - d_{t-1}$ (μm)		Δd (μm) over a 2 hr Period		
Cell Line	Stage	Mean	Max	Mean	Median	Max
5p14	interphase	0.46	1.83	2.28	1.72	3.57
	early G1	1.17	5.07	3.87	3.86	5.39
11q13	interphase	0.73	1.94	2.30	2.24	2.78
	early G1	0.82	4.34	5.25	3.19	16.45
	G1 + DRB	1.35	6.20	6.16	6.27	8.90

Mean and maximum change in distance between frames ($d - d_{t-1}$) taken every 10 min, and the mean, median, and maximum range of motion (Δd), over a 2 hr observation period, for tagged loci in cells that are in interphase (n = 5 cells per locus) and for cells that have just exited from mitosis (early G1; n = 5 mitoses per locus, i.e., 10 G1 nuclei). 11q13 cells were also examined in the presence of the transcriptional inhibitor DRB.

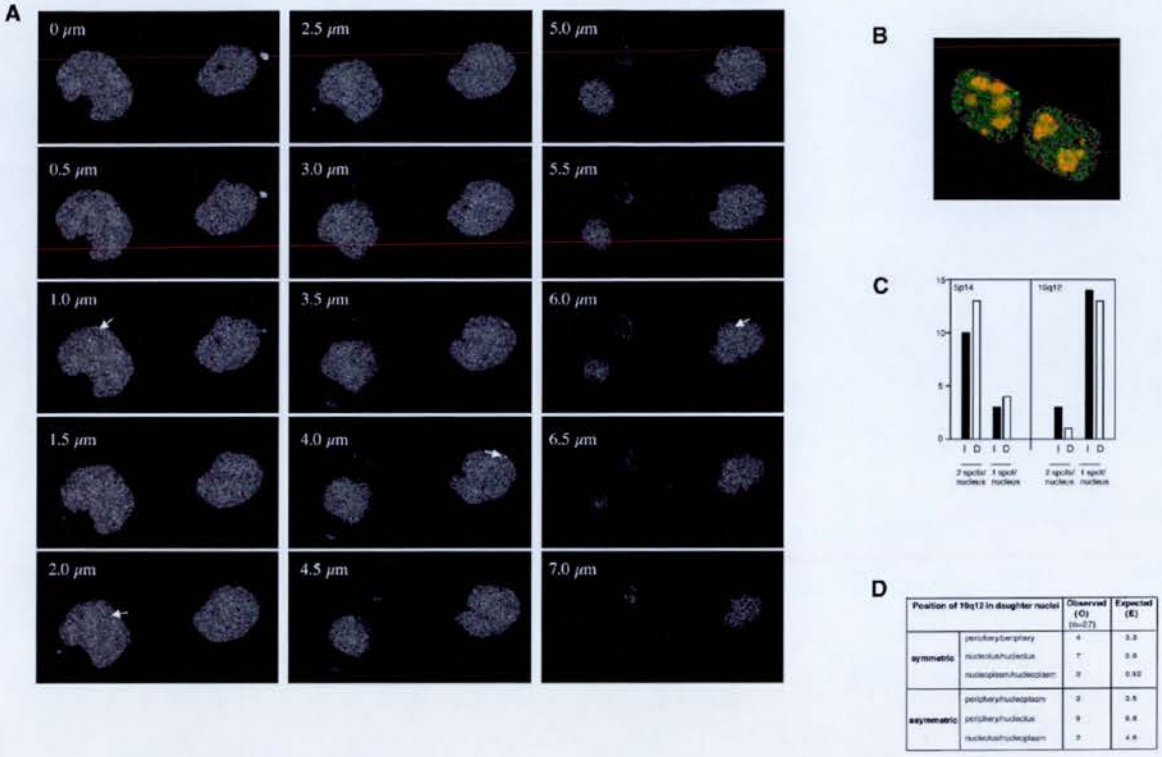

Figure 3. Asymmetry of Locus Position and Association with Nuclear Compartments in Daughter Nuclei

(A) 0.5 μm interval confocal sections through daughter nuclei tagged at 5p14 from a z stack taken 110 min after the completion of mitosis. Analysis of previous stacks indicated the GFP spot positions had been stable for 30 min. In the left nucleus, both spots are internal (arrowed in the 1 and 2 μm sections). In the right nucleus, one spot abuts the nuclear edge (4 μm), and the other (6 μm) is close to, but not at, the upper surface of the nucleus. The scale bar represents 10 μm.

(B) Confocal slice of a two-cell clone of the 19q12-tagged cell line. The lacO-tagged locus is visible in both cells (green dot). Nucleoli are detected by immunofluorescence with antibody recognizing pKi67 (red).

(C) Proportions of two-cell clones (with either 1 or 2 tagged loci/cell) whose daughter cells have identical (I) or different (D) positions of loci relative to nuclear compartments.

(D) Statistical analysis of the 19q12 one spot data from (C). There were three symmetric and three asymmetric expected combinations of locus-nuclear compartment association. The observed (O) patterns of association are compared with those predicted (E) from the incidence of locus association with the nuclear periphery, nucleolus, or the nucleoplasm within the population of cells (see Experimental Procedures).

combinations of locus association in sister cells were then generated from these data (see Experimental Procedures) and compared to the observed frequencies (O) (Figure 3D). This gives a χ^2 value of 7.2 for 5 degrees of freedom and corresponds to $p = 0.2–0.3$; therefore, we cannot refute the null hypothesis. The validity of the null hypothesis is clearly apparent from the raw observed data because the most frequent observation (9 out of 27 clones) was where 19q12 was nucleolar in one daughter and peripheral in the other. This is not compatible with the inheritance of chromatin organization, with respect to nuclear compartments, from a mother nucleus to both daughter nuclei.

The observed asymmetry of daughter nuclei and the enhanced mobility of chromatin in early G1 indicates that loci can form, and lose, associations with nuclear substructures in daughter nuclei independently of their position in the mother nucleus. For example, Figure 4A shows confocal sections taken at 10 min intervals after the completion of mitosis in a 5p14-tagged nucleus. This nucleus is the right-hand nucleus from Figure 3A. At the earliest time point after nuclear membrane reformation, the locus is in the nuclear interior. As the nucleus begins to expand and flatten, the locus remains at least 2 μm from the nearest nuclear edge (20 to 40 min time points), but by 70 min it has moved to the nuclear periphery, where it persists for the remainder of the movie. Hence, association with the nuclear envelope develops over the course of G1 and is not set up immediately after nuclear envelope formation.

The converse situation, in which a locus moves away from the nuclear periphery to an internal position in early G1, can also be seen. Figure 4B shows z stacks of a nucleus from the 11q13 cell line at 10 min intervals shortly after mitosis. In the first two frames, 10–20 min after the completion of mitosis, the locus is located in the nuclear interior. By 40 min after mitosis, it is associated with the edge of the nucleus before it moves back

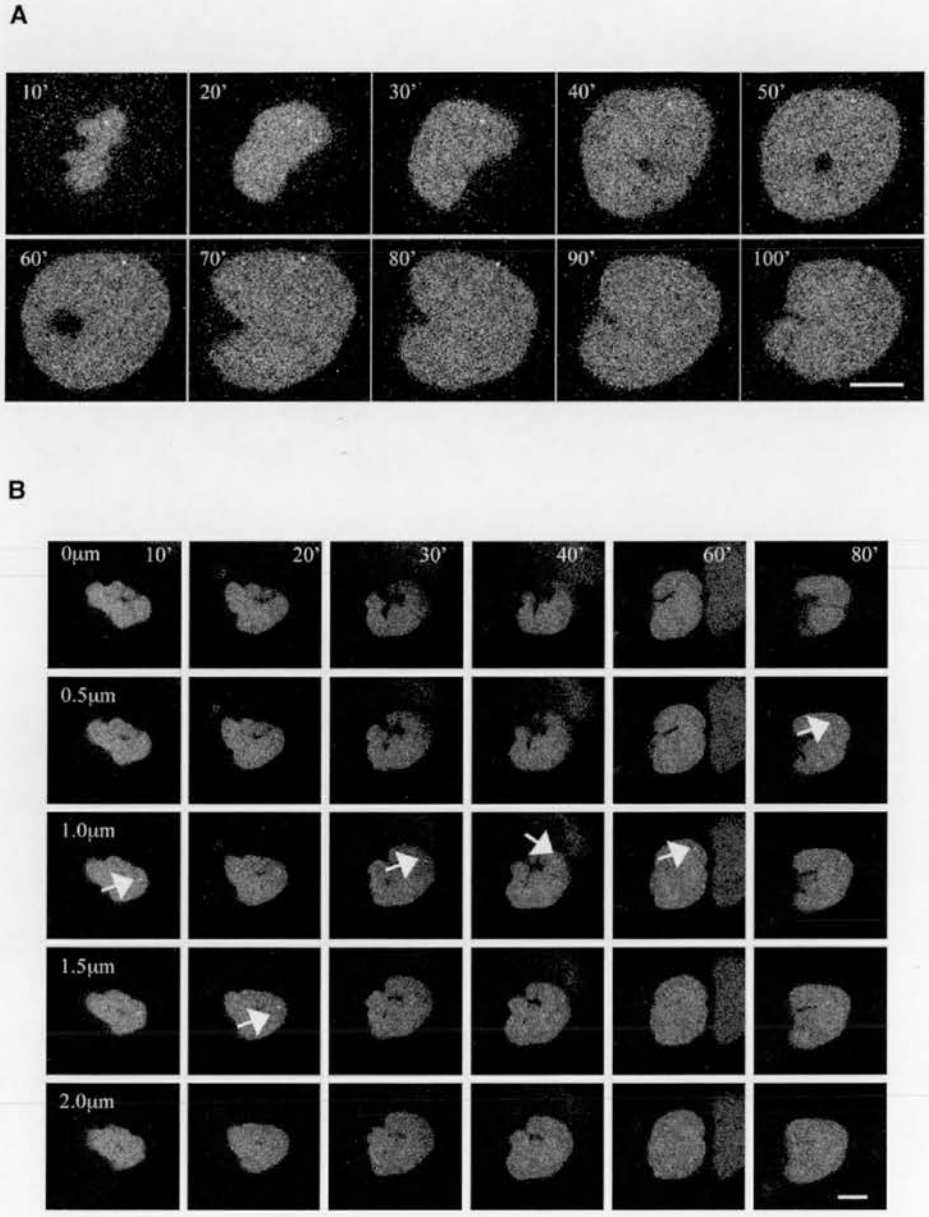

Figure 4. Changing Associations with the Nuclear Periphery in early G1

(A) Progressive establishment of peripheral localization for a 5p14-tagged locus during G1. Each frame is a z slice, captured at 10 min intervals after the metaphase-anaphase transition. Association of the locus with the nuclear lamina is not established until the 70 min frame and then persists for the remaining 40 min duration of the movie. The scale bar represents 10 μm.

(B) z stacks through an 11q13-tagged nucleus at 10 min intervals after mitosis. At the earliest time (10 min), the locus (arrowed) is located within the nucleoplasm (1 μm section). By the 40 min frame, the locus is at the nuclear edge but then moves back into the nuclear interior, where it persists for an additional 20 min. The scale bar represents 5 μm.

to the nuclear interior for the rest of the observation period.

Conclusions

The question of whether chromosome position in the nucleus can be transmitted to daughter nuclei through an open mitosis is important for understanding whether nuclear organization can contribute some form of cellular memory or epigenetic information. After analyzing the motion of specific loci in human cells in the period immediately after exit from mitosis, we conclude that the position of chromatin relative to the nuclear architecture—for example, the nuclear periphery—is not directly inherited through mitosis into daughter nuclei. Although

the gross nuclear position of a locus can be restricted by its position on the metaphase plate, and the angular relation between chromosomes transmitted, subsequent chromatin movements in early G1 allow for substantial repositioning of loci within the nucleus relative to nuclear compartments.

Experimental Procedures

Cell Lines

The HT1080 cell lines with lacO arrays integrated into the G-band at 5p14 have been described previously [9]. The present study also makes use of newly characterized lacO integrant lines, where the insertion has occurred in the R-band at 11q13 and the pericentromeric region at 19q12 (Table S1).

Visualizing Chromatin Motion in Live HT-1080 Cells

Live cell analysis was performed with the Bioptechs Delta T open dish system (Bioptechs Inc., PA) mounted on the stage of a Zeiss LSM510 confocal microscope. Cells were cultured to approximately 80% confluency in medium buffered by the addition of 25 mM HEPES (pH 7). The confocal was operated with version 3.0 LSM software.

Throughout the course of image capture, a large number of mitotic cells could be seen in the chamber. An additional indicator of cell health is the retention of polarized cell morphology, and images were only collected for as long as the cells retained this morphology. To follow the behavior of chromatin through mitosis and early G1 in GFP-LacI clones, we used the 488 nm laser line with 75% laser power, 6% transmission, and a pinhole of 1 AU. Mitotic cells were identified by their rounded morphology and absence of a nuclear envelope, revealed by the distribution of GFP-LacI-NLS throughout the entire cell (Figure 1). Approximately 80% of these cells divided within 1 hr of viewing. We captured 60 z slices per time point, with a scan time of 1.5 s, a z-interval of 0.5 μm, and a between-stack interval of 10 min. The position of a GFP-LacI spot was defined as the brightest pixel. Three-dimensional distances between spots were calculated from $d = \sqrt{(x^2 + y^2 + z^2)}$. The change in distance between spots between successive frames is represented by $d - d_{t-1}$, and the change in distance between spots over a time period relative to $t = 0$ is Δd [9].

Immunofluorescence

The subnuclear position of GFP-tagged loci was assessed by visual inspection of confocal images of cells fixed in 4% paraformaldehyde (pFa). Association with nucleoli was determined relative to staining with an antibody recognizing pKi67 [9]. The distribution of loci relative to nuclear compartments in two-cell clones was analyzed via the method of Walter et al. [4]. Cells were seeded on coverslips at very low density. More than 95% of cells were alone and well isolated 3 hr after seeding. The cells were fixed and processed for immunofluorescence 24 hr later, at which point they were mostly in well-isolated pairs. As a further confirmation that cell pairs were derived from a single mother cell, we used the following criteria: (1) cell pairs should have a similar nuclear size; HT-1080s are heterogeneous in nuclear size as a result of their tendency for aneuploidy; (2) cell pairs should have a similar level of GFP-LacI-NLS signal because expression variegates after a few days culture without selection; (3) no other cells should be within 500 μm; (4) cell pairs should have the same number of GFP spots. According to criteria 1–3, all cell pairs obeyed this rule. Because HT-1080s display limited motility and usually form well-defined colonies at low density, most of the cell pairs also retained some form of cell-cell contact. Residual cytokinetic structures were frequently visible.

Statistical Analysis

To calculate expected (E) numbers of 19q12 loci associated with nuclear compartments in 2 cell pairs, we classed each cell as having one of three possible positions for the locus: peripheral (p), nucleolar (n), and nucleoplasmic (i). The null hypothesis was no inheritance of position, and therefore the observed distributions in 2 cell clones should reflect only the population frequencies of p, n, and i (19/54, 25/54, and 10/54, respectively). Nine possible outcomes of clone pair combinations can arise. These are (1) p/p, p/n, p/i, (2) n/p, n/n, n/i, and (3) i/p, i/n, i/i. The expected frequency of each combination is calculated by multiplying the observed population frequencies together, and E values are generated by multiplying the expected frequencies by 54, the population size. After we pooled like combinations (e.g., p/n and n/p), we tabulated the E values and compared them to the observed values (O) by using a χ^2 test (Figure 3B). $\chi^2 = \Sigma(O - E)^2/E = 7.2$, $p_{\nu=5} > 0.2$.

Supplemental Data

A supplemental table is available with this article online at http://www.current-biology.com/cgi/content/full/14/2/166/DC1/.

Acknowledgments

I.T. and S.G. are in receipt of PhD studentships from the Medical Research Council, United Kingdom. W.A.B. is a Centennial fellow of the James S. McDonnell foundation. J.R.C. is in receipt of a Medical Research Council Research Training Fellowship.

Received: September 8, 2003
Revised: October 27, 2003
Accepted: November 12, 2003
Published: January 20, 2004

References

1. Csink, A.K., and Henikoff, S. (1996). Genetic modification of heterochromatic association and nuclear organization in Drosophila. Nature *381*, 529–531.
2. Brown, K.E., Guest, S.S., Smale, S.T., Hahm, K., Merkenschlager, M., and Fisher, A.G. (1997). Association of transcriptionally silent genes with Ikaros complexes at centromeric heterochromatin. Cell *91*, 845–854.
3. Andrulis, E.D., Neiman, A.M., Zappulla, D.C., and Sternglanz, R. (1998). Perinuclear localization of chromatin facilitates transcriptional silencing. Nature *394*, 592–595.
4. Walter, J., Schermelleh, L., Cremer, M., Tashiro, S., and Cremer, T. (2003). Chromosome order in HeLa cells changes during mitosis and early G1, but is stably maintained during subsequent interphase stages. J. Cell Biol. *160*, 685–697.
5. Gerlich, D., Beaudouin, J., Kalbfuss, B., Daigle, N., Eils, R., and Ellenberg, J. (2003). Global chromosome positions are transmitted through mitosis in mammalian cells. Cell *112*, 751–764.
6. Bickmore, W.A., and Chubb, J.R. (2003). Chromosome position: Now where was I? Curr. Biol. *13*, R357–R359.
7. Williams, R.R., and Fisher, A.G. (2003). Chromosomes, positions please! Nat. Cell Biol. *5*, 388–390.
8. Parada, L.A., Roix, J.L., and Misteli, T. (2003). An uncertainty principle in chromosome positioning. Trends Cell Biol. *13*, 393–396.
9. Chubb, J.R., Boyle, S., Perry, P., and Bickmore, W.A. (2002). Chromatin motion is constrained by association with nuclear compartments in human cells. Curr. Biol. *12*, 439–445.
10. Marshall, W.F., Straight, A., Marko, J.F., Swedlow, J., Dernburg, A., Belmont, A., Murray, A.W., Agard, D.A., and Sedat, J.W. (1997). Interphase chromosomes undergo constrained diffusional motion in living cells. Curr. Biol. *7*, 930–939.
11. Vazquez, J., Belmont, A., and S.and Sedat, J.W. (2001). Multiple regimes of constrained chromosome motion are regulated in the interphase Drosophila nucleus. Curr. Biol. *11*, 1227–1239.
12. Shelby, R.D., Hahn, K.M., and Sullivan, K.F. (1996). Dynamic elastic behavior of alpha-satellite DNA domains visualized in situ in living human cells. J. Cell Biol. *135*, 545–557.
13. Dimitrova, D.S., and Gilbert, D.M. (1999). The spatial position and timing of chromosomal domains are both established in early G1 phase. Mol. Cell *4*, 983–993.

14. Bridger, J.M., Boyle, S., Kill, I.R., and Bickmore, W.A. (2000). Remodelling of nuclear architecture in quiescent and senescent human fibroblasts. Curr. Biol. *10*, 149–152.
15. Li, G., Sudlow, G., and Belmont, A.S. (1998). Interphase cell cycle dynamics of a late-replicating, heterochromatic homogenously staining region: precise choreography of condensation/decondensation and nuclear positioning. J. Cell Biol. *140*, 975–989.
16. Tumbar, T., and Belmont, A.S. (2001). Interphase movements of a DNA chromosome region modulated by VP16 transcriptional activator. Nat. Cell Biol. *2*, 134–139.

The Radial Positioning of Chromatin Is Not Inherited through Mitosis but Is Established De Novo in Early G1

Inga Thomson, Susan Gilchrist,
Wendy A. Bickmore, and Jonathan R. Chubb

Table S1. Characteristics of LacO-Tagged Loci

		Percent Association with Nuclear Compartments		
Locus	Insertion Site	Nucleoplasm	Nucleolus	Periphery
5p14	G-band	52.5	7.5	40
11q13	R-band	85	3.5	11.5
19q12	pericentromeric	10.5	50	39.5

The cytogenetic position of lacO integration was determined by FISH [15]. The localization of tagged loci within the nucleus was established by inspection of confocal images ($n > 26$ cells).